STORE OPERATED Ca^{2+} CHANNELS IN LIVER CELLS: REGULATION BY BILE ACIDS AND A SUB-REGION OF THE ENDOPLASMIC RETICULUM

A thesis submitted in fulfillment of
the requirements for the
degree of:

Doctor of Philosophy

by

Joel Castro Kraftchenko
Microbiology (Hons.)

Department of Medical Biochemistry
School of Medicine, Faculty of Health Sciences
Flinders University

August 2008

TABLE OF CONTENTS

LIST OF FIGURES

SUMMARY

Cholestasis is an important liver pathology. During cholestasis bile acids accumulate in the bile canaliculus affecting hepatocyte viability. The actions of bile acids require changes in the release of Ca^{2+} from intracellular stores and in Ca^{2+} entry. The target(s) of the Ca^{2+} entry pathway affected by bile acids is, however, not known. The overall objective of the work described in this thesis was to elucidate the target(s) and mechanism(s) of bile acids-induced modulation of hepatocytes calcium homeostasis.

First, it was shown that a 12 h pre-incubation with cholestatic bile acids (to mimic cholestasis conditions) induced the inhibition of Ca^{2+} entry through store-operated Ca^{2+} channels (SOCs), while the addition of choleretic bile acids to the incubation medium caused the reversible activation of Ca^{2+} entry through SOCs. Moreover, it was shown that incubation of liver cells with choleretic bile acids counteracts the inhibition of Ca^{2+} entry caused by pre-incubation with cholestatic bile acids. Thus, it was concluded that SOCs are the target of bile acids action in liver cells.

Surprisingly, despite the effect of choleretic bile acids in activating SOCs, the Ca^{2+} dye fura-2 failed to detect choleretic bile acid-induced Ca^{2+} release from intracellular stores in the absence of extracellular Ca^{2+}. However, under the same conditions, when the sub-plasma membrane Ca^{2+} levels were measured using FFP-18 Ca^{2+} dye, choleretic bile acid induced a transient increase in FFP-18 fluorescence. This evidence suggested that choleretic bile acids-induced activation of Ca^{2+} entry through SOCs, involving the release of Ca^{2+} from a region of the endoplasmic reticulum (ER) located in the vicinity of the plasma membrane.

To explore the possible requirement of a small sub-region of the ER in SOCs activation, TRPV1 channels ectopically expressed in the ER, were used as an alternative approach. Using this strategy it was demonstrated that TRPV1 agonists mediated the release of Ca^{2+} from the bulk of the ER (detected by cytoplasmic fura-2 but not by sub-plasma membrane FFP-18) but failed to activate SOCs in liver cells. This represents additional evidence for the suggested role of a small sub-region of the ER in the activation of SOCs.

Finally, the effect of either choleretic bile acid taurodeoxycholate (TDCA) or TRPV1 agonists, on the distribution of the ER calcium sensor stromal interaction molecule 1 (STIM1) (required for SOCs activation) was investigated. It was observed that TDCA caused the reversible redistribution of STIM1 into punctate aggregates within the ER sub-region in the vicinity of the plasma membrane, similar to that induced by the ER (Ca^{2+}+Mg^{2+}) ATPase pump inhibitor, thapsigargin. TRPV1 agonists however, do not induce the redistribution of STIM1 proteins in the majority of cells expressing TRPV1.

In summary, the work described in this thesis indicates that the main type of plasma membrane Ca^{2+} channel, inhibited by cholestatic bile acids and activated by choleretic bile acids, is the hepatocyte SOC. Additionally, this work provides evidence that bile acids activated SOCs by a mechanism that involves the release of Ca^{2+} from- and the STIM1 redistribution within- a small sub-region of the ER located in the vecinity of the plasma membrane.

DECLARATION

I certify that this thesis does not incorporate without acknowledgment any material previously submitted for a degree or diploma in any university; and that to the best of my knowledge and belief it does not contain any material previously published or written by another person except where due reference is made in the text.

Joel Castro Kraftchenko

ACKNOWLEDGEMENTS

I would like to give my sincere thanks to my chief supervisor Dr. Greg Barritt, for the opportunity of undertaking my Ph.D. in his laboratory and for the continuing support, guidance, encouragement and dedication he has given me throughout this "journey". I am also grateful to my co-supervisors Simon Brookes and Grigori Rychkov, especially to Grigori for his helpful comments and guidance during my Ph.D.

I would also like to give thanks for the help given in the de-convolution analysis of the confocal images by Ian Gibbins and Jennifer Clarke and in the isolation of rat hepatocytes by my lab colleagues Yabin Zhou and Rachael Hughes. Thanks as well to them, and the rest of my lab members, for their support, good times and friendship. I would like to thank the fantastic "troop" of friends from the "Centro de Estudios Científicos" in Chile, especially to Felipe Barros, for their support in my overseas field trip and for his guidance throughout my scientific career.

My profound gratitude to the Government of Australia for the opportunity of doing my Ph.D. studies, through the financial assistance of the "International Postgraduate Research Scholarship" (IPRS) award. In addition, I would like to thank Flinders University and FMC for their financial support of the Overseas Field Trip; and to the Higher Degree Administration Office and ISSU personal, for all their assistance.

I would like to thank my family and my exceptional partner for their unending help, their energies, trust, emotional support and their unconditional love. THANKS!

Finally, for the love and inspiration that day after day my daughter, Antonia Castro, gives to my life, it is to her that I dedicate this thesis.

ABBREVIATIONS

$[Ca^{2+}]_{cyt}$	Cytoplasmic free Ca^{2+} concentration
$(Ca^{2+})_{SPM}$	Sub-plasma membrane Ca^{2+} levels
$(Ca^{2+}{}_{ext})$	Extracellular Ca^{2+}
CA	Cholic acid
CRAC	Ca^{2+} Release-Activated Ca^{2+} Channel
DBHQ	Di-*tert*-butylhydroquinone
DMEM	Dulbecco's Modified Eagles Medium
DMSO	Dimethylsulfoside
EGTA	Ethylene Glycol-bis(b-aminoethyl ether)-*N,N,N´N´*-Tetraacetic Acid
ER	Endoplasmic reticulum
FBS	Fetal bovine serum
FCCP	Carbonylcyanide-p-trifluoromethoxyphenylhydrazone
Gd^{3+}	Gadolinium
GFP	Green Fluorescent Protein
I_{crac}	Ca^{2+} Release-Activated Ca^{2+} Current
IP_3	Inositol 1,4,5-trisphosphate
IP_3Rs	Inositol 1,4,5-trisphosphate receptors
KRH	Krebs-Ringer-HEPES buffer
La^{3+}	Lanthanum
LCA	Lithocholic acid
PBS	Phosphate Buffered Saline
PM	Plasma membrane
PMCA	Plasma Membrane (Ca^{2+} + Mg^{2+}) ATP-ases pump

ROI	Regions of interest
RR	Ruthenium red
RTX	Resiniferatoxin
SERCA	Endoplasmic Reticulum (Ca^{2+} + Mg^{2+}) ATP-ase pump
SOCs	Store-Operated Ca^{2+} channels
STIM1	Stromal Interaction Molecule 1
TCA	Taurocholic acid
TDCA	Taurodeoxycholic acid
Tg	Thapsigargin
TLCA	Taurolithocholic acid
TMRM	Tetramethyl Rhodamine Methyl ester
TPEN	*N*,*N*,*N*',*N*'-tetrakis(2-pyridylmethyl) ethylene diamine
TRPV1	Transient Receptor Potential cation channel, subfamily V, member 1
TUDCA	Tauroursodeoxycholic acid
UDCA	Ursodeoxycholic
YFP	Yelow Fluorescent Protein
2-APB	2-aminoethoxydiphenylborane

CHAPTER I: INTRODUCTION

The work undertaken in this thesis investigates the effects of bile acids on the regulation of Store-Operated Ca^{2+} Channels (SOCs) in liver cells. Additionally, the role of the endoplasmic reticulum in the activation of SOCs will also be examined. Therefore this introductory chapter will cover: (i) the liver role, physiology and structure, including cellular organisation and function; as well as the causes and consequences of the pathological condition, cholestasis; (ii) the regulation of Ca^{2+} homeostasis in liver cells, including the different Ca^{2+} permeable channels presents in the plasma membrane; (iii) the physiological relevance, properties and activation mechanism of one of these Ca^{2+} permeable channels, called the store-operated Ca^{2+} channels (SOCs); (iv) finally, some facts about the role of the endoplasmic reticulum, in the activation of SOCs, will be presented.

1.1 Liver physiology and effects of bile acids accumulation during liver cholestasis

1.1.1. Roles of the liver in whole body homeostasis

The liver plays a central role in the metabolism, detoxification, and overall regulation of the body homeostasis. During fetal development, the liver is the primary organ of hematopoiesis and is required for the maintenance of normal bone marrow formation. The liver is involve in the efficient uptake of amino acids, carbohydrates, lipids and vitamins and their subsequent storage, metabolic conversion and release into the blood and bile. Additionally, the liver performs

several roles in carbohydrate metabolism, including: (i) the synthesis of glucose from certain amino acids, lactate or glycerol (Gluconeogenesis); (ii) the breakdown of glycogen into glucose (Glycogenolysis); (iii) the formation of glycogen from glucose (Glycogenesis); and (iv) the breakdown of insulin and other hormones. The liver also performs several roles in lipid metabolism including cholesterol synthesis and triglycerides production.

This organ is responsible of the synthesis and trans-cellular movement of bile acids, bile fluid, and the synthesis and secretion of proteins (Leite and Nathanson, 2001; Boyer, 2002b). Additionally, the liver is the hepatic bio-transformation of hydrophobic substances into water-soluble derivates that can be excreted into bile or urine (Leite and Nathanson, 2001). The liver breaks down toxic substances and most medicinal products. Furthermore, the large vascular capacity of the liver operates as a reservoir of blood volume in the circulation (Miayai, 1991). The liver's function also influences the central nervous system, endocrine organs and the immune system (Leite and Nathanson, 2001).

In human, the liver is among the few internal organs capable of regenerating lost tissue; as little as 25% of intact liver can regenerate into a whole liver again. There is no artificial organ, or device, capable of emulating all the functions of the liver.

1.1.2. The structure of the structure

The liver is the largest glandular organ of the body, constituting approximately 2% to 5% of the body weight. According to the "functional vascular anatomy" the liver is divided into VIII segments with independent afferent and efferent blood supplies. The caudate segment (segment I) is considered autonomous and the remaining segments are named clockwise from II to VIII (Dawson and Tan, 1992). The

"classical anatomy" divides the organ in four lobes, according to the peritoneal attachments and surface fissures of the liver (Fig. 1.1 A, a). Within each liver lobe, the tissue (liver parenchyma) is arranged into hexagonal-shaped lobules each comprised of a central vein surrounded by six portal triads (Fig. 1.1 A, b) (Young and J.W, 2000; Mohammed and Khokha, 2005). Each portal triad is comprised of a hepatic vein, hepatic artery and bile duct (Fig. 1.1 A, c).

The predominant cell in the liver is the hepatocyte (parenchymal cell) which represents ~ 70% of all cells in the liver (Dawson and Tan, 1992; Boyer, 2002b; Mohammed and Khokha, 2005). Endothelial cells, biliary epithelial cells (cholangiocytes), hepatic stellate cells, Kupffer cells (macrophages) and oval cells, also play important roles in the liver. Hepatocytes, often considered as specialised epithelial cells, are organised in single-cell plates (Fig. 1.1 B). The hepatocyte plates are perfused by blood from the gut (hepatic portal vein) and heart (hepatic artery), which drains into the central vein (Fig. 1.1 B). The bile canaliculi (surrounded by the adjacent membranes of two hepatocyte lines) collects bile fluid from each hepatocyte and moves this fluid to the bile duct (Figs. 1.1 A and 1.2).

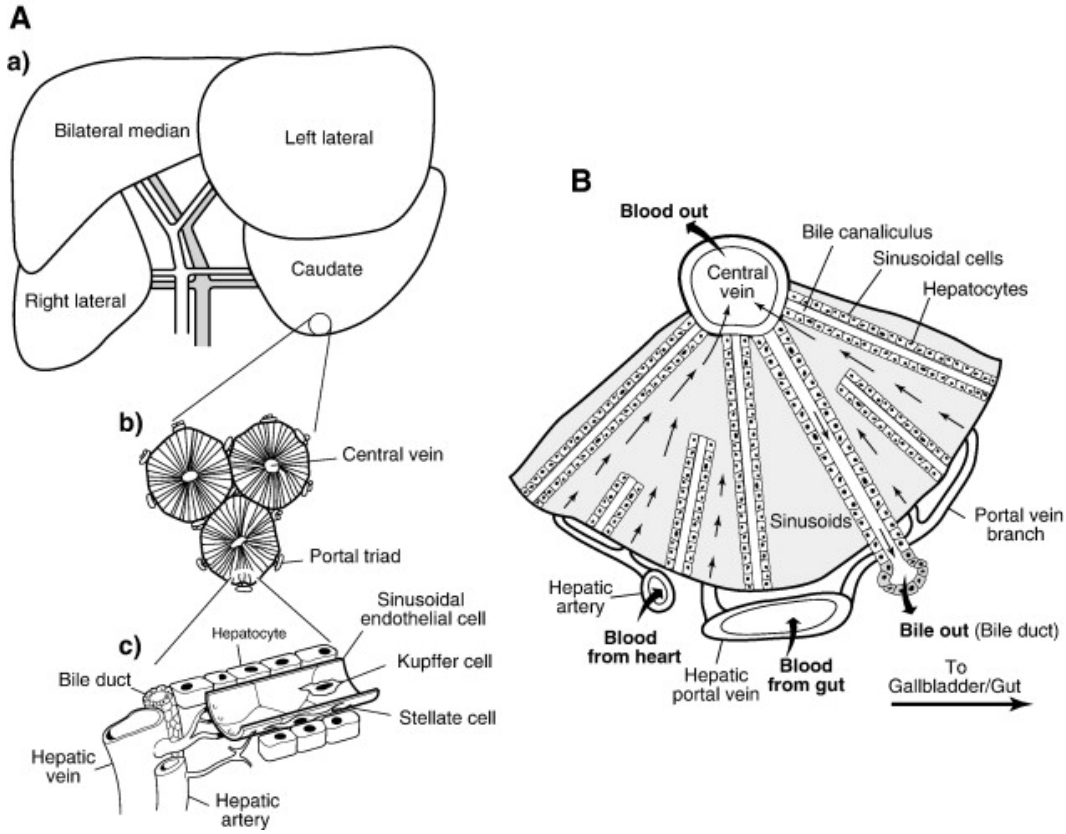

Fig. 1.1. Liver anatomy and hepatocytes organisation. (A) Drawing of the major lobes of rat liver (a), the relationship between the central vein and portal triads (b), and the arrangement of the hepatic vein, hepatic artery, bile duct, hepatocyte plate and sinusoidal space (c), is presented. (B) A schematic drawing of the hepatocyte plates showing the direction of blood flow from the hepatic portal vein and hepatic artery to the central vein, and the direction of bile flow through the bile canaliculus. This figure is adopted from (Barritt *et al.*, 2008).

Consistent with the complex function and architecture of the liver, hepatocytes are highly differentiated cells exhibiting spatial polarisation and a characteristic intracellular organization (Berry *et al.*, 1991; Hubbard *et al.*, 1994; Zegers and Hoekstra, 1998; Boyer, 2002b; Wakabayashi *et al.*, 2006). Some features of the spatial polarity of hepatocytes are schematically shown in Fig. 1.2. The plasma membrane (PM) of each hepatocyte is differentiated into the sinusoidal (basal), contiguous (lateral), and canalicular (apical domains) domains. The sinusoidal domain, facing the blood circulation, comprises more than 70% of the surface area, contains many receptors, transport systems and ion channels, which facilitate exchange of nutrients and other solutes between hepatocytes and the systemic circulation. The lateral domain is mainly involved in intracellular communications through cell adhesion molecules and intracellular junctions such as tight junctions, desmosomes, and gap junctions. Gap junctions permit the movement of molecules between adjacent hepatocytes (Berry *et al.*, 1991; Hubbard *et al.*, 1994; Zegers and Hoekstra, 1998; Boyer, 2002b; Wakabayashi *et al.*, 2006). The canalicular domain (formed by the facing plasma membrane of two adjacent hepatocytes), is separated from the sinusoidal and lateral domains by tight junctions. It has been described that the canalicular domain is involved in the secretion of bile acids and polymeric immunoglobulin A into the bile; the unique excretory products of hepatocytes (Nathanson and Boyer, 1991). The trafficking of proteins and vesicles through the hepatocyte cytoplasmic space is critical for the maintenance of hepatocyte spatial polarity and for many hepatocyte functions (Zegers and Hoekstra, 1998; Wakabayashi *et al.*, 2006).

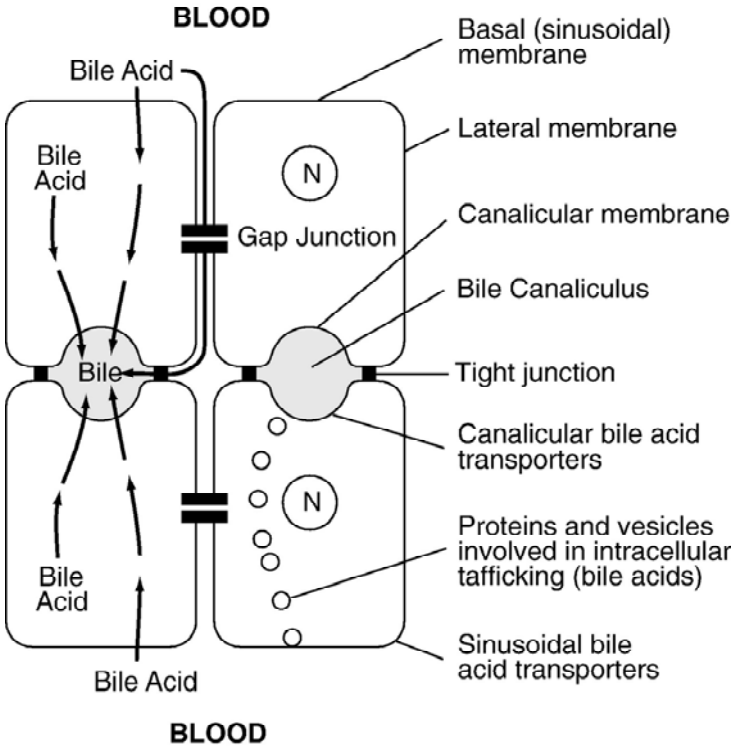

Fig. 1.2. Schematic representation of the hepatocyte spatial polarity. The scheme shows the different hepatocytes domains and the pathways of bile acid movement and vesicle trafficking in hepatocytes within the hepatocyte plate. This figure is adapted from (Barritt *et al.*, 2008).

As shown in Fig. 1.3, hepatocytes are enriched in rough and smooth endoplasmic reticulum (ER). This comprises an extensive array of interconnecting membranes that exhibit remarkable spatial extensions forming cisternae and tubules and has continuity with the nuclear envelope (Wang *et al.*, 2000). The ER is the largest compartment in hepatocytes, its surface area is ~ 38 times that of the PM and constitutes ~ 15% of the total cellular volume (Lippincoott-Schwartz, 1994). As described below, this intracellular organelle is one of the focal points of this thesis.

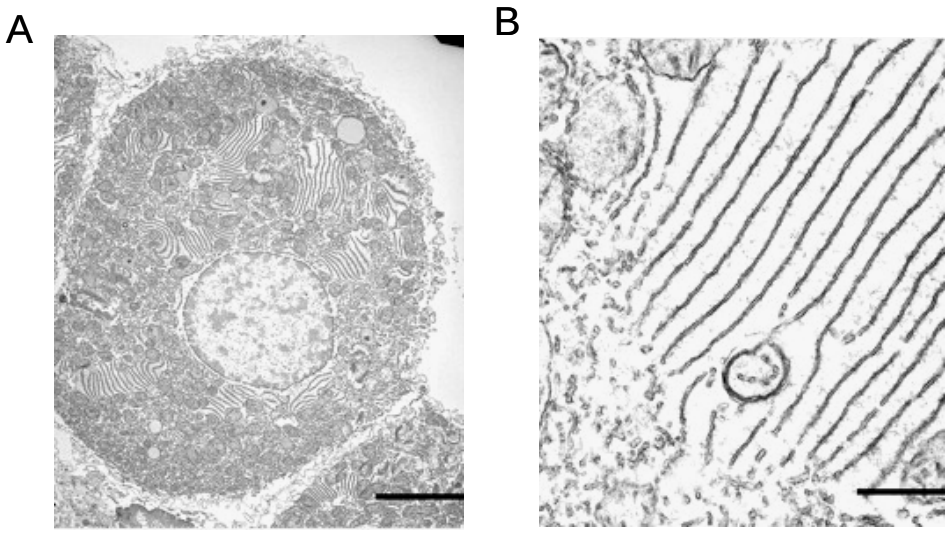

Fig. 1.3. Electron micrographs of hepatocytes. Panel A shows electron micrographs of whole hepatocytes showing different intracellular organelles. Panel B shows a zoom image of an intracellular region showing in fine detail the structure of the endoplasmic reticulum. Scale bars are 5 μm This figure is adapted from (Wang *et al.*, 2000).

1.1.3. Cholestasis and the consequences of bile acid accumulation in liver

Cholestasis is an important liver pathology, which can lead to primary sclerosis and liver failure (Boyer, 2002a; Maddrey, 2002; O'Leary and Pratt, 2007). Cholestasis arises from hepatocyte dysfunction or intrahepatic or extrahepatic biliary obstruction leading to impaired movement of bile along the biliary duct tree and impaired secretion of the components of bile fluid into the bile canaliculus. Cholestasis has many causes including primary sclerosing cholangitis, primary biliary cirrhosis, liver disorders associated with liver injury, and genetic abnormalities in hepatocyte bile acid transporters. Additionally, cholestasis is associated with decreases in the expression and/or activity of hepatocyte bile acid transporters (Boyer, 2001).

In cholestasis, conjugated and unconjugated bile acids accumulate in hepatocytes and the blood (Boyer, 2001). Hepatocytes play a central role in the synthesis of bile acids and in the movement of bile acids from the portal blood to the gallbladder and intestine. Bile acids are transported from the blood across the basal (sinusoidal) and basolateral membranes of hepatocytes, through the cytoplasmic space, and then across the canalicular membrane into the bile canaliculus.

Bile acids can be classified according their hydrophobicity, the more hydrophobic bile acids (such as taurolithocholic (TLCA), lithocholic (LCA), cholic (CA) and taurocholic (TCA) acids), are called cholestatic bile acids; while the less hydrophobic bile acids (such as taurodeoxycholic (TDCA), tauroursodeoxycholic (TUDCA) and ursodeoxycholic (UDCA) acids), are called choleretic bile acids.

It has been shown that cholestatic bile acids induce bile flow inhibition (Boyer, 2002a). Additionally, it has been reported that cholestatic bile acids induce liver injury, leading to apoptosis and necrosis of hepatocytes (Chieco *et al.*, 1997; Benz *et*

al., 1998; Sodeman *et al.*, 2000; Higuchi and Gores, 2003; Higuchi *et al.*, 2003; Borgognone *et al.*, 2005). In addition, it has been shown that cholestatic bile acids induce mitochondrial depolarisation (Rolo *et al.*, 2000; Huang *et al.*, 2003; Criddle *et al.*, 2004; Voronina *et al.*, 2004).

In contrast with the deleterious effects of cholestatic bile acids, it has been described that choleretic bile acids enhance bile flow (Boyer, 2002a). Furthermore, it has been reported that choleretic bile acids TUDCA and UDCA have been used at pharmacological doses to treat cholestasis (Bouchard *et al.*, 1993; Jacquemin *et al.*, 1993; Azer *et al.*, 1995; van de Meeberg *et al.*, 1996; Kinbara *et al.*, 1997; Poupon *et al.*, 1997; Beuers *et al.*, 1998; Ono *et al.*, 1998; Fabris *et al.*, 1999; Pares *et al.*, 2000; Lazaridis *et al.*, 2001).

Central to the physiological, pathological, and pharmacological actions of bile acids on hepatocytes are the bile acid-induced changes in the cytoplasmic free Ca^{2+} concentration ($[Ca^{2+}]_{cyt}$). The results of experiments conducted with hepatocytes and hepatocyte cell lines have shown that bile acids increase $[Ca^{2+}]_{cyt}$ (Combettes *et al.*, 1988b; Combettes *et al.*, 1990; Beuers *et al.*, 1993a; Bouscarel *et al.*, 1993), release Ca^{2+} from intracellular stores (Combettes *et al.*, 1988b, a; Beuers *et al.*, 1993a) and induce Ca^{2+} entry into hepatocytes (Beuers et al., 1993a; Beuers *et al.*, 1993b). It has been shown that while cholestatic bile acid TLCA inhibits Ca^{2+} entry (Combettes *et al.*, 1990; Beuers *et al.*, 1993a; Beuers *et al.*, 1999), choleretic bile acid (TUDCA) stimulates bile flow probably by activating Ca^{2+} entry and increasing hepatocyte $[Ca^{2+}]_{cyt}$ (Combettes *et al.*, 1988b; Beuers *et al.*, 1993a; Beuers *et al.*, 1993b; Bouscarel *et al.*, 1993). This, in turn, may activate Ca^{2+}-dependent myosin light chain kinase and the polymerisation of F-actin, and enhance contraction of the bile canaliculus (Watanabe and Phillips, 1984).

Little is known about the Ca^{2+} regulation pathways modulated by bile acids in liver cells. The next section will present some information about the regulation of Ca^{2+} homeostasis in liver cells.

1.2 Regulation of calcium homeostasis in liver cells

1.2.1. General features

An increase in cytoplasmic Ca^{2+} concentration ($[Ca^{2+}]_{cyt}$) is a ubiquitous signalling messenger that regulates a broad spectrum of distinct cellular processes (Berridge, 1993; Carafoli, 2002; Parekh and Putney, 2005). In hepatocyte, $[Ca^{2+}]_{cyt}$ regulates glucose and fatty acid metabolism, bile acid secretion, protein synthesis and secretion, the movement of lysosomes and other vesicles, the cell cycle and cell proliferation, as well as apoptosis and necrosis (Leite and Nathanson, 2001; Boyer, 2002b; Enfissi *et al.*, 2004; Dixon *et al.*, 2005; Nieuwenhuijs *et al.*, 2006; O'Brien *et al.*, 2007).

An increase in cytoplasmic Ca^{2+} concentration can occur in one of two ways: through the release of Ca^{2+} from intracellular stores; or by Ca^{2+} entry across the plasma membrane. In Fig. 1.4 the different entities that contribute to the cellular cytoplasmic Ca^{2+} concentration are schematically shown.

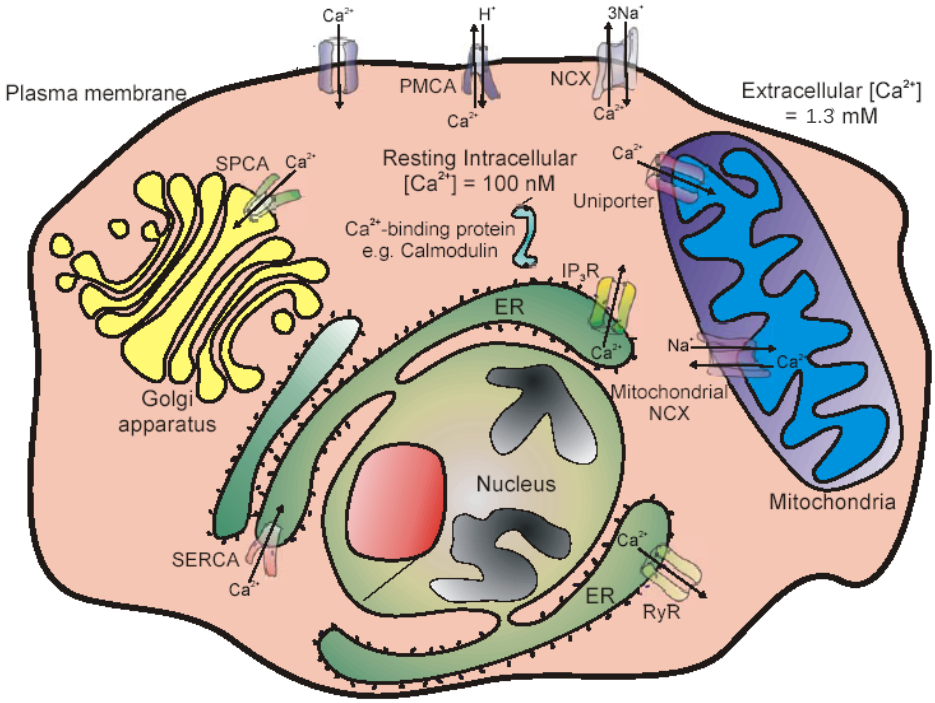

Fig. 1.4. Intracellular Ca^{2+} regulation. The plasma membrane Ca^{2+} entry channels, the Ca^{2+} extrusion across the plasma membrane mediated by the plasma membrane (Ca^{2+} + Mg^{2+})ATP-ases (PMCA), and by the Na^{+}-Ca^{2+} exchanger (NCX). Ca^{2+} uptake by the ER is mediated by the ER (Ca^{2+} + Mg^{2+})ATP-ase (SERCA) and Ca^{2+} outflow from the ER by IP_3 and ryanodine receptors (RyR). Ca^{2+} uptake by mitochondria is mediated by an electrogenic Ca^{2+} uni-porter and Ca^{2+} outflow by Na^{+}/Ca^{2+} and H^{+}/Ca^{2+} anti-porters. Golgi also possess IP_3R and (Ca^{2+} + Mg^{2+})ATP-ase (SPCA). Numerous Ca^{2+} binding proteins are present in the cytoplasmic space and in organelles.

1.2.2. Role of intracellular stores in the regulation $[Ca^{2+}]_{cyt}$

The resting level of Ca^{2+} in the cytoplasmic space of non-excitable cells is ~ 100nM. As showed in Fig 1.4, there are several intracellular organelles such as endoplasmic reticulum, mitochondria, Golgi apparatus, lysosomes, nuclear envelope (contiguous with the ER), and possibly secretory granules, which contributes to regulated $[Ca^{2+}]_{cyt}$ (Prakriya and Lewis, 2001; Sorrentino and Rizzuto, 2001).

Among the different intracellular stores mentioned above, the endoplasmic reticulum (ER) plays a central role in the regulation of $[Ca^{2+}]_{cyt}$. Studies with hepatocytes have shown that Ca^{2+} can be released from the ER by types 1 and 2 inositol 1,4,5-trisphosphate receptors (IP_3R), (Wojcikiewicz, 1995; Hirata *et al.*, 2002) and from ryanodine receptors (Pierobon *et al.*, 2006). However, the uptake of Ca^{2+} by the ER is mediated by the ER $(Ca^{2+} + Mg^{2+})$ATP-ase pump (SERCA).

It has been described that the release of Ca^{2+} from the ER is involved in different cellular process, such as: hormone-induced Ca^{2+} oscillations (Woods *et al.*, 1986, 1987; Rooney *et al.*, 1989, 1990; Thomas *et al.*, 1991); vesicle trafficking (Gorelick and Shugrue, 2001); release of stress signals (Kaufman, 1999); regulation of cholesterol metabolism (Brown and Goldstein, 1999), and apoptosis (Ferri and Kroemer, 2001). The release of Ca^{2+} from intracellular stores (ER) is transient event. This is in part due to Ca^{2+}- and/or ligand-dependent inactivation of the release channels themselves; as well as due to the clearance of Ca^{2+} from the cytoplasmic space by re-sequestration into the ER (by the action of SERCA pumps) and into other organelles, particularly mitochondria (Barritt *et al.*, 2000; Gaspers and Thomas, 2005; Delgado-Coello *et al.*, 2006). Additionally, Ca^{2+} can be actively extruded from the cell by plasma membrane $(Ca^{2+} + Mg^{2+})$ATP-ases (PMCA) (Howard *et al.*, 1994;

Delgado-Coello *et al.*, 2003) and Na^{+}/Ca^{2+} exchangers (Studer and Borle, 1992; Gasbarrini *et al.*, 1993; Delgado-Coello *et al.*, 2006).

1.2.3. Ca^{2+} entry across the plasma membrane

1.2.3.1 Gradient of Ca^{2+} in the cells

As illustrated in Fig 1.4, the extracellular free Ca^{2+} concentration in the physiological range is ~ 1.3mM (reviewed in (Clapham, 1995)). Considering the low levels of cytoplasmic Ca^{2+} (100nM), the gradient for Ca^{2+} across the plasma membrane represents a difference in concentration of 10,000-fold. Additionally, the resting membrane potential of non-excitable cells is ~ -70mV. Despite this huge electrochemical driving force (in favour of Ca^{2+} entry), resting cells generally have low membrane permeability to Ca^{2+}. However, modest increases in the membrane permeability result in large Ca^{2+} entry, due to the Ca^{2+} electrochemical driving force. An increase in membrane permeability to Ca^{2+} can be produced by the opening of Ca^{2+}-permeable ion channels in the plasma membrane.

1.2.3.2 Ca^{2+}-permeable channels in liver cells

A variety of different Ca^{2+}-permeable channels have been found to coexist in the plasma membrane of liver cells. They are described as follows:

- Receptor-operated channels (reviewed in (Barritt, 1999; Barritt *et al.*, 2008)): these channels open as result of the binding of an agonist (such as hormones or other agonists) to its receptor. In this case, the receptor protein is separate from the channel protein. The binding of the agonist to its receptor in the extracellular space, either activates the channel directly or generates an intracellular messenger which binds to a region on the cytoplasmic domain of the channel, leading to activation of the channel.

- Ligand-gated channels ((Capiod, 1998) and reviewed in (Barritt, 1999; Barritt *et al.*, 2008)): these channels are activated directly by the binding of an external ligand to the channel proteins that contain both, the binding site for the ligand and the pore of the ion channel. They are non-selective cation channels, which, under physiological conditions, admit considerable amounts of Na^+ as well as Ca^{2+}.

- Stretch-activated Ca^{2+}-permeable channels (Bear, 1990; Bear and Li, 1991; Barros *et al.*, 2001): these channels open by transduction of mechanical forces (*eg*., plasma membrane stretch induced by increases in cellular volume).

- Store-operated Ca^{2+} channels (Rychkov *et al.*, 2001; Litjens *et al.*, 2004): these channels open in response to a decrease in the endoplasmic reticulum Ca^{2+} concentrations. They are high selective for Ca^{2+} and their main function is the replenishment of the ER Ca^{2+} levels. Moreover, it has been suggested that SOCs are the main Ca^{2+} entry pathway activated by hormones and growth factors in hepatocytes (Rychkov *et al.*, 2001; Rychkov *et al.*, 2005). This channel will be the focus of attention in the next section.

1.3 Store-operated Ca^{2+} channels (SOCs)

The concept of store-operated Ca^{2+} entry arose from the work of Putney and colleagues (Putney, 1986). They concluded that the decrease of Ca^{2+} from intracellular stores (the ER) trigged by receptor agonists, could initiate the activation of Ca^{2+} entry through the plasma membrane. Such a phenomenon was subsequently described to be a ubiquitous pathway of Ca^{2+} entry, apparently existing in all eukaryotes from yeast (Locke *et al.*, 2000) to humans (Partiseti *et al.*, 1994).

1.3.1. Physiological significance of Ca^{2+} entry through SOCs

It has been described that SOCs appears to be important for a wide range of biological processes such as: gene transcription, cell proliferation, exocytosis, secretion, chemotaxis, fertilization, among others (Fanger *et al.*, 1995; Artalejo *et al.*, 1998; Fomina and Nowycky, 1999; Saunders *et al.*, 2002; Sweeney *et al.*, 2002; Ishikawa *et al.*, 2003; Yoshida *et al.*, 2003). Additionally, it has been proposed that Ca^{2+} entry through SOCs is required for the maintenance of bile flow in rats. The mechanism proposed by which SOCs could regulated the bile flow is by contributing to the increase in the hepatocyte $[Ca^{2+}]_{cyt}$ that initiates contraction of the bile canaliculus (Gregory *et al.*, 2004a).

At the cellular level, when Ca^{2+} is released from intracellular stores, store-operated calcium entry is required as described below:

- During transient stimulation, for example occurring with cholinergic neurotransmission, Ca^{2+} entry through SOCs, replenishes rapidly the intracellular Ca^{2+} stores, leaving the cells ready for subsequent stimulations.

- Store-operated calcium entry provides a way for inducing sustained elevation in $[Ca^{2+}]_{cyt}$. For example, in the maintenance of smooth muscle tone, a sustained $[Ca^{2+}]_{cyt}$ elevation is needed. This cannot be achieved without a calcium entry mechanism, because intracellular stores contain a finite amount of Ca^{2+} to provide an elevated $[Ca^{2+}]_{cyt}$ for only few minutes.

- Finally, SOCs are described to be involved during the Ca^{2+} oscillations response. In this case, store-operated Ca^{2+} entry provides the refilling of intracellular Ca^{2+} stores, to maintain the amplitude of each intracellular Ca^{2+} spike. In the absence of Ca^{2+} entry the spike height would gradually diminish. Previous studies, with

primary cultured rat hepatocytes, demonstrated that Ca^{2+} entry through SOCs were required to maintained the oscillatory response of hormone-induced Ca^{2+} oscillations (Gregory and Barritt, 2003).

Additionally, it has been found, that Ca^{2+} entry through SOCs is involved in the regulation of several enzymes; such is the case of adenylate cyclase (Cooper *et al.*, 1998; Fagan *et al.*, 1998; Gu and Cooper, 2000) and endothelial nitric-oxide synthase (Lin *et al.*, 2000). SOCs activation may also be important for the remodelling of plasma membrane such as phosphatidyl serine externalisation, which is one of the early characteristics of cells undergoing apoptosis (Martinez *et al.*, 1999; Kunzelmann-Marche *et al.*, 2001).

1.3.2. Approaches to activate SOCs

Under physiological conditions, SOCs are activated by Ca^{2+} release from the endoplasmic reticulum induced by an increase in the levels of inositol 1,4,5-trisphosphate (IP_3), produced through receptor stimulation, or other Ca^{2+}-releasing signals (reviewed in (Parekh and Penner, 1997; Parekh and Putney, 2005)). Additionally, SOCs can be activated by any method that induces the decrease of Ca^{2+} in the ER such as:

- By addition of sarcoplasmic/endoplasmic reticulum Ca^{2+}-ATPase (SERCA) inhibitors like thapsigargin and di-*tert*-butylhydroquinone (DBHQ). The inhibition of the SERCA pump would impede the active endoplasmic reticulum Ca^{2+} refilling; hence would causing the depletion of the ER Ca^{2+} content (Hoth and Penner, 1992; Parekh and Penner, 1995, 1997; Hofer *et al.*, 1998; Lewis, 1999).

- By cytoplasmic IP_3 elevation via dialysis of the cytoplasm with IP_3 (Putney, 1986; Hoth and Penner, 1992; Parekh and Penner, 1997; Rychkov *et al.*, 2001). Usually

the IP_3 addition is combined with cytoplasmic Ca^{2+} chelation induced with high concentrations of Ethylene Glycol-bis(b-aminoethyl ether)-*N,N,N´N´*-Tetraacetic Acid (EGTA). This compound chelates the Ca^{2+} that leaks from the stores and hence prevents store refilling.

- By diminishing the free intraluminal Ca^{2+} concentration in the ER via loading the cells with membrane-permeable metal Ca^{2+} chelators like *N,N,N',N'*-tetrakis(2-pyridylmethyl) ethylene diamine (TPEN) (Hofer *et al.*, 1998; Chan *et al.*, 2004); or by addition of Ca^{2+} ionophore ionomycin, which permeabilise the ER membrane (Morgan and Jacob, 1994).

1.3.3. Mechanism of activation of SOCs

1.3.3.1 Molecular identities of the ER Ca^{2+} sensor and the PM Ca^{2+} permeable channel

The molecular identity of the ER Ca^{2+} sensor that detects the decrease in ER Ca^{2+}, and the Ca^{2+}-permeable channel (SOCs) that consequently opens at the PM, remained elusive for almost 20 years. Recent studies have shown that Orai1 proteins constitute the pore of SOCs; while Stromal Interaction Molecule 1 (STIM1) proteins constitute the "Ca^{2+} sensor", which detects the decrease in Ca^{2+} in the ER and communicates this information to Orai1 in the plasma membrane (Liou *et al.*, 2005; Roos *et al.*, 2005; Zhang *et al.*, 2005; Feske *et al.*, 2006; Mercer *et al.*, 2006; Peinelt *et al.*, 2006; Prakriya *et al.*, 2006; Soboloff *et al.*, 2006b; Spassova *et al.*, 2006; Vig *et al.*, 2006; Yeromin *et al.*, 2006; Zhang *et al.*, 2006).

STIM1 is a protein with only one transmembrane domain and no known catalytic activity. The N-terminal region of STIM1 (within the ER lumen) includes a sterile α-motif (SAM), which often mediate oligomerization, and most importantly, a single EF-hand that binds Ca^{2+} (Williams *et al.*, 2001) **(**Fig. 1.5). Orai1 is a protein with

four membrane-spanning regions (M1–M4); it is incorporated into the PM with its M3–M4 loop in the extracellular space (Prakriya *et al.*, 2006) and its N and C termini in the cytoplasmic space (Feske *et al.*, 2006; Vig *et al.*, 2006) **(**Fig. 1.5). Orai1 mRNA is widely expressed (Feske *et al.*, 2006) and its function conserved across diverse species. The M1-M2 loop of the Orai1 channel is the region involved in the ion selectivity and Gd^{3+} inhibition (Yeromin *et al.*, 2006). Both proteins contain cytoplasmic proline-rich regions (Fig. 1.5, S/P) and coiled-coil domains (Fig. 1.5, CC), each of which could mediate protein–protein interactions (reviewed in (Taylor, 2006)).

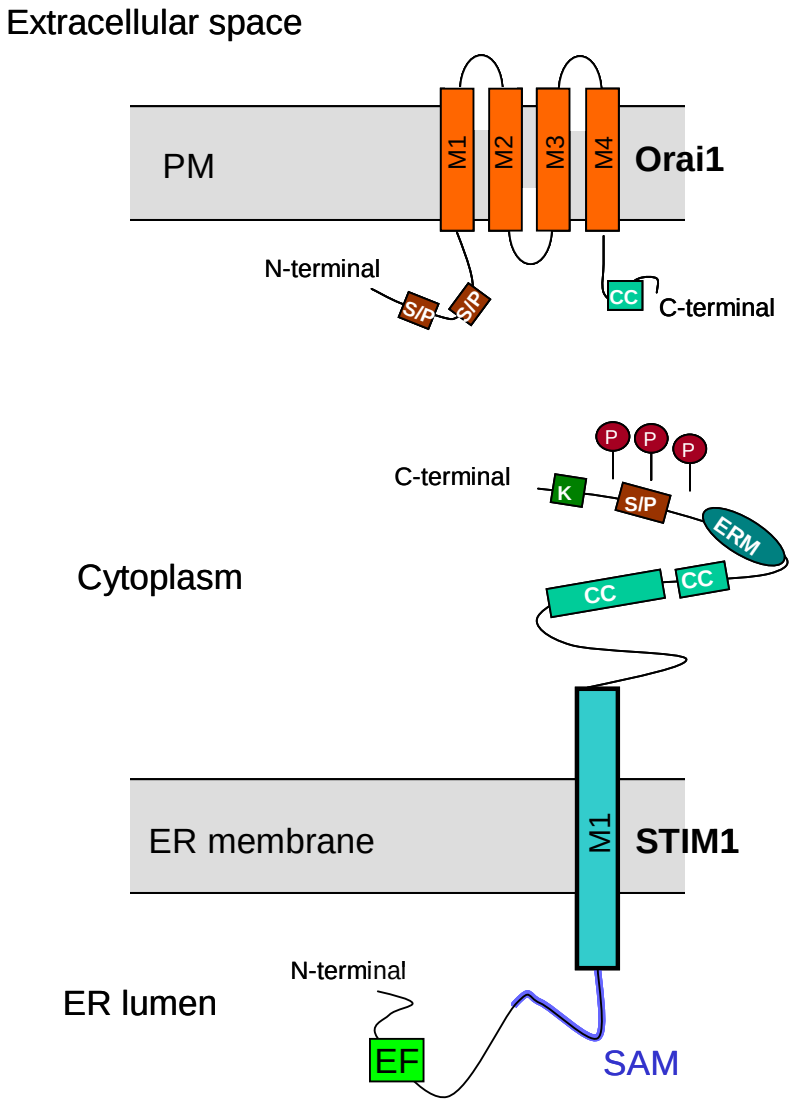

Fig. 1.5. Expected topology of STIM1 and Orai 1 proteins. STIM1 is localized primarily in the ER membrane. The organization of the major predicted domains is shown, including an unpaired EF hand and sterile-α motif (SAM) domains on the luminal side. In the cytoplasmic space side, overlapping coiled-coil (CC) and ezrin-radixin-moesin (ERM) domains, and serine-proline-rich (S/P), which includes many phosphorylation sites (P), and lysine-rich (K) domains, are shown. Orai1 located at the PM has four membrane-spanning regions and intracellular N and C terminal.

1.3.3.2 Mechanism of activation of SOCs

It has been suggested that the mechanism of activation of SOCs (Orai1) involves the sequence of events schematically shown in Fig. 1.6. These are described as follows: In resting cells with the Ca^{2+} stores full (Fig. 1.6 A), STIM1 and Orai1 are homogeneously dispersed throughout the ER and plasma membrane, respectively. When Ca^{2+} is released from the ER, the EF-hand portion of STIM1 proteins sense the decrease of Ca^{2+} inside the ER. As a consequence, STIM1 aggregates at locations where the ER is located in the vecinity of the plasma membrane ('junctional ER') (blue arrows); additionally the ER increases the number of these close contacts with the plasma membrane (red arrow) (Wu *et al.*, 2006). Moreover, Orai1 moves within the PM (green arrows) and concentrates above STIM1 aggregates. Finally, after this sequence of events, Orai1 opens allowing Ca^{2+} entry into the cytoplasmic space (Fig. 1.6 C). Subsequently, the SERCA pumps restore the ER Ca^{2+} content (Fig. 1.6 C). (Liou *et al.*, 2005; Zhang *et al.*, 2005; Baba *et al.*, 2006; Mercer *et al.*, 2006; Wu *et al.*, 2006; Xu *et al.*, 2006; Liou *et al.*, 2007; Ong *et al.*, 2007a).

It has been reported that, the peripheral ER membrane frequently comes within 8–20 nm of the PM, with which it appears to form ‘junctions’. These junctions have being reported in liver cells (Guillemette *et al.*, 1988; Rossier *et al.*, 1991) and other cellular types such as excitable cells (Henkart *et al.*, 1976; Watanabe and Burnstock, 1976; Chadborn *et al.*, 2002) and yeast (Pichler *et al.*, 2001). The idea that the close relationship between the ER and the PM is required, for the activation of SOCs, has previously been suggested (Patterson *et al.*, 1999; Yao *et al.*, 1999; Rosado *et al.*, 2000; Wang *et al.*, 2000; Venkatachalam *et al.*, 2002).

Furthermore, it has been demonstrated that STIM1 redistribution is necessary for SOCs activation in lymphocytes, mast cells and other cell types (Liou *et al.*, 2005; Zhang *et al.*, 2005; Baba *et al.*, 2006; Luik *et al.*, 2006; Mercer *et al.*, 2006; Soboloff *et al.*, 2006a; Wu *et al.*, 2006; Xu *et al.*, 2006), including liver cells (Litjens *et al.*, 2007). Additionally, two independent groups have indicated that mutations within the putative pore regions of Orai1 change the biophysical properties of SOC (Prakriya *et al.*, 2006; Yeromin *et al.*, 2006).

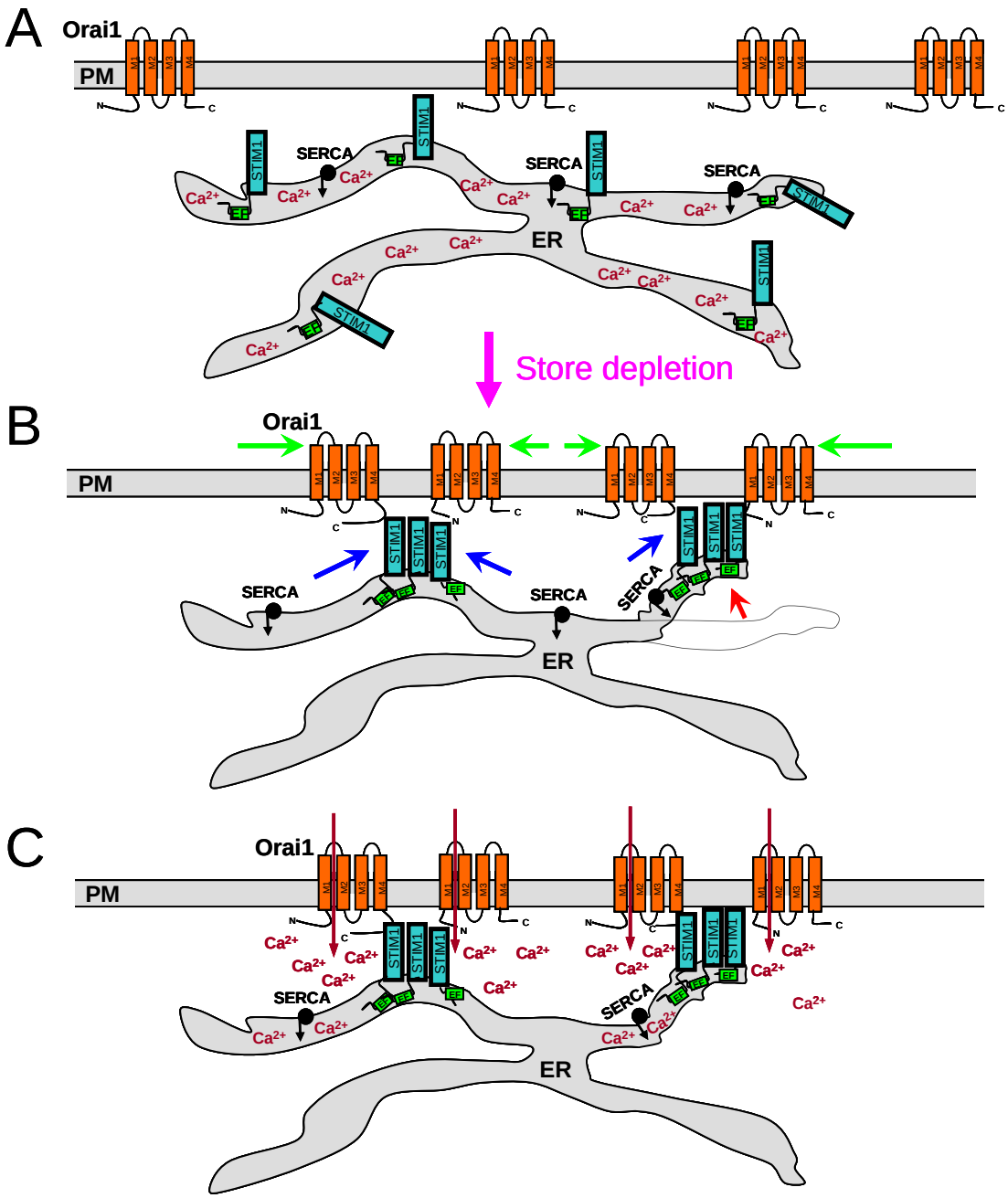

Fig. 1.6. Proposed model for the mechanism of activation of SOCs. Ca^{2+} depletion of the ER induced the redistribution of homogeneously distributed STIM1 proteins (**A**) into punctate aggregates within the ER (**B**, blue arrows). This redistribution occurs in ER regions located in close apposition to the plasma membrane and induces the activation of SOCs (CRAC). Additionally, Orai1 channels moves within the PM (**B**, green arrows) towards the STIM1 aggregates. (**C**) Once Orai1 channels at the PM activates, Ca^{2+} entry into the cytoplasmic space and the ER SERCA pumps replenish the ER Ca^{2+} content.

1.3.4. Measurement of Ca^{2+} entry through SOCs

1.3.4.1 The use of fluorescent Ca^{2+} dyes to measure Ca^{2+} entry through SOCs

A valuable and important tool for the study of SOCs activation is the use of fluorescent Ca^{2+} dyes (like fura-2). Using this method, Ca^{2+} entry can be measured; additionally Ca^{2+} release from the intracellular stores (ER) can be determined, a key step in the activation of SOCs.

Roger Y. Tsien designed the first calcium-binding indicator, called "quin2" (Tsien, 1980, 1981). The measurement of Ca^{2+} using calcium indicators is a non-invasive method in which the cells are loaded with the dye in its acetoxymethylester form. Once the dye is inside the cell, cytoplasmic esterases cleave off the ester groups and the dye remains free in the cytoplasmic space, where reports the changes in calcium concentration with great sensitivity. Nevertheless this method has some particularities as below discussed:

The Ca^{2+} dyes (like fura-2) measure the changes in the cytoplasmic Ca^{2+} concentration, which is not an accurate indication of Ca^{2+} entry across the plasma membrane. The concentration of cytoplasmic Ca^{2+} is a balance between Ca^{2+} entry and Ca^{2+} removal from the cytoplasmic space; so if Ca^{2+} entry stays constant, the net size of the cytoplasmic signal could be underestimated, because of the active removal of Ca^{2+} from the cytoplasmic space.

Additionally, in experiments conducted with Ca^{2+} dyes, the membrane potential is not controlled. SOCs are considered voltage-independent channels in the sense that they are not gated by membrane voltage changes (Hoth and Penner, 1993; Zweifach and Lewis, 1993). Depolarisation of the plasma membrane could inhibit Ca^{2+} entry by reducing the driving force for Ca^{2+} entry (Kagaya *et al.*, 2002), whereas

hyperpolarisation can reduce the size of the SOCs current, at least in RBL-1 cells (Bakowski and Parekh, 2000, 2002). Although, it is has been reported that the effect of any altered membrane potential on Ca^{2+} entry through SOCs is likely to be small (Parekh and Putney, 2005).

Finally, it is possible that the protocol used to activate SOCs, activates in addition, another Ca^{2+}-permeable channel. In this case the resulting increases in $[Ca^{2+}]_{cyt}$ would not be through SOCs channels exclusively. It has been described that thapsigargin-induced Ca^{2+} release can activate the Ca^{2+}/calmodulin-dependent protein kinase. Once active, this kinase can phosphorylate (activate) Ca^{2+}-dependent channels located at the plasma membrane (Braun and Schulman, 1995).

1.3.4.2 The use of electrophysiology to measure Ca^{2+} entry through SOCs

The other method to measure the Ca^{2+} entry through SOCs is the use of electrophysiology patch-clamp techniques to monitor the store-operated Ca^{2+} current. This technique was invented by Erwin Neher and Bert Sakmann (Neher and Sakmann, 1976). For this method, an electrode is introduced into a tiny glass pipette (filled with a saline controlled solution), which is placed against the cell membrane. The movement of ions in or out of the ion channels located in the plasma membrane can be detected by this electrode, which transmits the signal to an amplifier.

The key problem of this technique is presented by the dialysis of the cytoplasmic space via the patch pipette. Because of this, cytoplasmic factors diffuse into the pipette and are hence lost from the cell, moreover, isolation of SOCs currents requires inhibition of other currents, and hence, the ionic composition of the pipette solution is non-physiological. Finally, in some cell types, the store-operated currents

are very small, limiting the measurement of direct currents (Parekh and Putney, 2005).

Using the patch clamp electrophysiological technique in mast cells, the Ca^{2+} current induced by intracellular stores depletion was identified. The current was named Ca^{2+} Release-Activated Ca^{2+} Current (I_{crac}) and the channel responsible was called Ca^{2+} Release-Activated Ca^{2+} Channel (CRAC) (Hoth and Penner, 1992). I_{CRAC} is not the only store-operated current but remains the most used model for studying store-operated entry.

The combination of both techniques (fluorescent Ca^{2+} dyes and electrophysiology) it is considered the best strategy to study the activation of SOCs. Previous evidence obtained from our group (using patch clamp recording and fura-2 to measure $[Ca^{2+}]_{cyt}$) indicates that there is only one type of SOC in liver cells; which has a high selectivity for Ca^{2+} and its properties are essentially indistinguishable from those of Ca^{2+} release-activated Ca^{2+} channels (Rychkov *et al.*, 2001; Rychkov *et al.*, 2005).

The experiments performed and described in this thesis were done using fura-2, however a series of patch clamp complementary experiments (used in the discussion of this thesis), were undertaken in parallel by our collaborators.

1.3.5. Ca^{2+} feed back and pharmacological inhibition of SOCs

1.3.5.1. Ca^{2+} feed back inhibition of SOCs

When SOCs opens, the Ca^{2+} entry through the channel creates a micro-domain of elevated Ca^{2+} in the vicinity of each open channel, which causes the inactivation of SOCs (Hoth and Penner, 1993; Zweifach and Lewis, 1995; Fierro and Parekh, 1999). However, it has been demonstrated that, under physiological conditions, the

polarised mitochondria located below the plasma membrane can buffer the Ca^{2+} entry through SOCs. This bypasses SOCs inhibition caused by Ca^{2+} accumulation at the channel mouth, resulting in a sustained Ca^{2+} entry through SOCs. Accordingly, it has been reported that mitochondrial depolarisation inhibits Ca^{2+} entry through CRAC channels in lymphocytes and mast cells (Gilabert and Parekh, 2000b; Hoth *et al.*, 2000; Gilabert *et al.*, 2001; Glitsch *et al.*, 2002a; Malli *et al.*, 2003; Montalvo *et al.*, 2006).

1.3.5.2. Pharmacological inhibition of SOCs

Ca^{2+} entry through SOCs can be pharmacologically inhibited by addition of trivalent cations like Lanthanum (La^{3+}) and Gadolinium (Gd^{3+}) into the incubation medium. These compounds are particularly effective, blocking SOCs fully in the low micromolar concentration range (Hoth and Penner, 1993). In experiments employing fluorescent dyes to study Ca^{2+} entry through SOCs, Gd^{3+} is often used (Parekh and Putney, 2005).

Another pharmacological agent used to inhibit store-operated Ca^{2+} entry is 2-aminoethoxydiphenylborane (2-APB). 2-APB was first described as a membrane-permeable inhibitor of IP_3 receptor function, which rapidly inhibited thapsigargin-induced Ca^{2+} entry (Ma *et al.*, 2000). Electrophysiological experiments subsequently confirmed that 2-APB inhibited I_{CRAC} activation (Bakowski *et al.*, 2001; Prakriya and Lewis, 2001; Voets *et al.*, 2001). The inhibition of SOCs caused by 2-APB appears to be on an external site of the channel (Bakowski *et al.*, 2001; Prakriya and Lewis, 2001).

1.4 Role of an endoplasmic reticulum sub-region in the activation of SOCs

1.4.1. Role of the ER in the activation of SOCs

As mentioned in Sections 1.3.1 and 1.3.2, the decrease in Ca^{2+} in the ER is required for the activation of SOCs. However, it is not clearly established whether this involves the whole of the ER or only a small region. There are some studies that suggested that Ca^{2+} can freely move through the ER and that the whole of the ER is involved in the activation of SOCs (Mogami *et al.*, 1997; Subramanian and Meyer, 1997; Hofer *et al.*, 1998; Park *et al.*, 2000; Sedova *et al.*, 2000). Nevertheless, growing evidence indicates that functional compartmentalisation exists within the reticulum such that it's Ca^{2+}-releasing capabilities are not homogeneously distributed throughout the organelle (Pozzan *et al.*, 1994). In this respect, the results of some studies suggest that only a small component of the ER is required for activation of SOCs (Parekh and Penner, 1997; Hartmann and Verkhratsky, 1998; Huang and Putney, 1998; Gregory *et al.*, 1999; Parekh and Putney, 2005; Ong *et al.*, 2007b); accordingly, it has been suggested that Ca^{2+} movement through the ER is restricted (Golovina and Blaustein, 1997; Horne and Meyer, 1997).

1.4.1.1 Role of the ER sub-region in the activation of SOCs in non-liver cell types

The following points take into account the reported evidence from different experimental approaches, which suggest that only a sub-region of the ER is required for the activation of SOCs in non-liver cell types:

- In other study with NIH 3T3 cells, the treatment with phorbol esters, reduced the total Ca^{2+} content of the ER by ~ 50% (via activation of protein kinase C). However, this depletion of Ca^{2+} did not activate entry, nor did it affect the ability

of thapsigargin to activate entry when the remaining stores were emptied (Ribeiro and Putney, 1996).

- In a recent study, the abilities of two concentrations of thapsigargin (1.0nM and 1.0μM) were used to release Ca^{2+} from the ER and activate Ca^{2+} entry in human salivary gland cells (Ong *et al.*, 2007b). In that study it was observed that the addition of 1nM thapsigargin, despite the reduced capacity of Ca^{2+} release from the ER, was able to induce the complete activation of SOCs to the same extent as that of 1μM. In addition it was demonstrated that both concentrations of thapsigargin were able to induce the redistribution of STIM1 in a region of the ER located close to the PM.

- The results of experiments conducted with DT40B lymphocytes and ectopically-expressed STIM1-GFP indicate that while the bulk of STIM1 is located in the ER, some is localised in a sub-compartment, possibly comprised of mobile vesicles. When Ca^{2+} stores are depleted these vesicles accumulate just below the plasma membrane and are associated with SOCs activation (Baba et al., 2006).

- In another study, Liou et al (Liou et al., 2007), using TIRF microscopy combined with confocal microscopy, showed that upon Ca^{2+} release from the ER, STIM1 redistributes in a region of the ER located at 2 μm plasma membrane. Suggesting that region is the relevant component of the ER in the activation of SOCs.

- Recent studies using fluorescence quenching and electron microscopy have identified that after the redistribution of STMI1 within the ER, the distance of STIM1 from the plasma membrane was calculated to be ~ 6 nm. This ER-PM junction is the site of STIM1-Orai1 interactions (Varnai *et al.*, 2007).

- Finally, there is some evidence that SOCs can not be activated by the release of Ca^{2+} from the ER induced by activation of ectopically expressed Transient Receptor Potential cation channel, subfamily V, member 1 (TRPV1) in the ER (Turner *et al.*, 2003; Wisnoskey *et al.*, 2003).

1.4.1.2 Role of the ER sub-region in the activation of SOCs in liver cell

Evidence has been presented, which suggest that a small sub-region of the ER, enriched in type 1 IP_3Rs, is required for SOC activation in liver cells. It was observed that the microinjection of rat hepatocytes with adenophostin A (which has high affinity for IP_3Rs), induced the near-maximal activation of Ca^{2+} entry, with little detectable release of Ca^{2+} from intracellular stores (Gregory *et al.*, 1999). Additionally, when rat hepatocytes were microinjected with the monoclonal anti-type 1 IP_3R antibody (to inhibit Ca^{2+} release mediated by type 1 IP_3R), the addition of hormone or thapsigargin, despite causing normal release of Ca^{2+} from intracellular stores, failed to fully activate Ca^{2+} entry through SOCs (Gregory *et al.*, 1999).

In another study using microinjection of IP_3 analogues, it was found that the IP_3 analogue selective for IP_3R type 1, was more efficient in activating SOCs than the IP_3 analogue selective for IP_3R type 2 (Gregory *et al.*, 2004b). Moreover, it was found that type 1 IP_3R was located throughout most regions of the ER with some concentrated very close to the plasma membrane (Rossier *et al.*, 1991; Lievremont *et al.*, 1994; Lievremont *et al.*, 1996; Hirata *et al.*, 2002; Gregory *et al.*, 2004b; Hernandez *et al.*, 2007).

1.4.2. Use of TRPV1 to investigate the involvement of an small region of the ER in the activation of SOCs

The TRPV1 channel (Transient Receptor Potential cation channel, subfamily V, member 1) was first cloned by Julius and co-workers in 1997 (Caterina *et al.*, 1997).

TRPV1 is a nonselective ligand-gated cation channel that can be activated by a wide variety of exogenous and endogenous stimuli, including heat greater than 43°C, low pH, anandamide, N-vanillilnonamide, capsaicin and resiniferatoxin (RTX) (reviewed in (Szallasi and Blumberg, 1999)). TRPV1 receptors are found in the central and peripheral nervous systems and are involved in the transmission and modulation of pain (Huang *et al.*, 2002; Cui *et al.*, 2006).

Several studies have shown that TRPV1 is localised at the plasma membrane and at intracellular membranes. Moreover it has been shown that the activation of TRPV1, in addition to promoting Ca^{2+} entry across the plasma membrane, releases Ca^{2+} from intracellular stores (Olah *et al.*, 2001; Liu *et al.*, 2003; Marshall *et al.*, 2003; Turner *et al.*, 2003; Wisnoskey *et al.*, 2003; Karai *et al.*, 2004; Vos *et al.*, 2006; Thomas *et al.*, 2007). In the work performed by Turner and collaborators, the membrane-permeable agonist capsaicin, was used to activate intracellular TRPV1 channels expressed in RBL cells. In that work it was found that capsaicin released Ca^{2+} from intracellular stores that were contained within the total IP_3-sensitive stores. However, the release of the Ca^{2+} from the capsaicin-sensitive Ca^{2+} store failed to activate I_{CRAC} (Turner *et al.*, 2003). Using a similar approach, in insect Sf 9 and HEK-293 cells, and using fura-2 to monitor Ca^{2+} and Ba^{2+}, it was observed that in TRPV1-expressing cells, capsaicin was able to trigger both Ca^{2+} release and Ba^{2+} entry. However, in contrast to the store-operated pathway, capsaicin-induced Ba^{2+} entry was insensitive to La^{3+} and 2-APB. Moreover, these authors found that the capsaicin- and thapsigargin-sensitive stores overlapped considerably. Despite the considerable overlap, thapsigargin, but not TRPV1 agonists, was capable of activating store-operated Ca^{2+} entry. (Wisnoskey *et al.*, 2003). These two separated works may represent additional evidence for the idea that the component of the ER responsible

for signalling to store-operated channels is specialized and distinct from the bulk of the ER.

1.4.3. Use of FFP-18 Ca^{2+} dye to measure changes in Ca^{2+} levels at the vicinity of the plasma membrane

As mentioned above (section 1.4.1), the ER sub-region suggested to be responsible for the activation of SOCs, is located in the vicinity of the plasma membrane. Thus, measurements of Ca^{2+} changes restricted to that region represent key information to understand the role of the ER on the activation of SOCs.

The Ca^{2+} dye FFP-18, is a lipophilic analogue of fura-2 (Vorndran *et al.*, 1995), which has been successfully used to monitor rapid changes in the sub-plasma membrane Ca^{2+} levels ($(Ca^{2+})_{SPM}$) in a variety of cells types (Etter et al., 1994; Etter et al., 1996; Davies and Hallett, 1998; Graier et al., 1998; Chadborn et al., 2002). FFP-18-AM incorporates into the plasma membrane and reorientates (by slow "flip-flop" diffusion) to the inner face of the plasma membrane where cytoplasmic esterases cleave off the ester groups. The Ca^{2+} sensitive FFP-18 acid generated on the inner face of the plasma membrane is unable to diffuse back. It has a 12-carbon hydrophobic tail that partitions into the cell membrane and a positively charged piperazine moiety that aids in binding to membrane phospholipids and thereby prevents the Ca^{2+}-binding portion of the dye from being pulled out of the plasma membrane (Etter *et al.*, 1996).

As mentioned above, the peripheral ER membrane frequently comes within few nanometers of the PM ('ER-PM junctions'). It is suggested that the diffusion of ions from the 'bulk' of the cytoplasm to the 'ER-PM junctions' could be markedly restricted (van Breemen *et al.*, 1995; Delmas and Brown, 2002; Golovina, 2005). Consequently, some studies reported that FFP-18 monitors changes in $(Ca^{2+})_{SPM}$

rather than the bulk of the cytoplasmic space ($[Ca^{2+}]_{cyt}$) (Davies *et al.*, 1997; Paltauf-Doburzynska *et al.*, 1998; Chadborn *et al.*, 2002).

One of those studies (Paltauf-Doburzynska *et al.*, 1998), describes the inability of the cytoplasmic Ca^{2+} dye fura-2 (distributed it in the bulk of the cytoplasm) to detected the Ca^{2+} release induced by ryanodine, in endothelial cells (in spite of the existence of ryanodine receptors in this cellular type). The lack of fura-2 detection was attributed to the active extrusion of the Ca^{2+} released by the plasma membrane Na^{+}-Ca^{2+} exchange; hence, in cells in which the Na^{+}-Ca^{2+} exchange was inhibited, fura-2 could effectively detect the ryanodine induced Ca^{2+} release. Moreover, when FFP-18 (distributed beneath the plasma membrane) was employed to measured $(Ca^{2+})_{SPM}$ changes, the addition of ryanodine caused a detectable Ca^{2+} release (Paltauf-Doburzynska *et al.*, 1998).

In this thesis, the Ca^{2+} dye FFP-18 is used, to estimate the changes in Ca^{2+} levels beneath the plasma membrane. This, together with the measurement of $[Ca^{2+}]_{cyt}$ reported by fura-2, offers a significant approach to understand the spatial location of the ER sub-region involved in the activation of SOCs.

1.5 Aims of the present study

The overall aims for this study are to investigate the effects and mechanism(s) of bile acids on SOCs activity, and to evaluate the role of the ER in the activation of SOCs in liver cells. The specific aims are as follows:

1- Evaluate the effects of cholestatic and choleretic bile acids on SOCs.

2- Test the ability of choleretic bile acids to counteract the effects induced by cholestatic bile acids.

3- Characterise the mechanism(s) of action of cholestatic and choleretic bile acids-mediated effects on SOCs.

4- Test if all the ER is required for the activation of SOCs in liver cells.

5- Evaluate the distribution and requirement of STIM1 proteins in bile acid-mediated SOC regulation.

CHAPTER II: GENERAL MATERIALS AND METHODS

2.1 Materials

Collagenase (Type IV) was obtained from Worthington Biochemical Corporation; fura-2, Calcium Green 5N and FFP-18 (in their acetoxymethylester form), Tetramethyl rhodamine methyl ester (TMRM), Dulbecco's Modified Eagles Medium (DMEM), F-12 (Ham) nutrient mixture (F-12), Opti-MEM medium, Bodipy TR-X Tg, goat anti-mouse Alexa-Fluor 488 antibody, goat anti-rabbit Alexa-Fluor 647 antibody, chicken anti-rabbit Alexa-Fluor 594 antibody, pluronic acid F-127 and Library Efficiency DH5α^{TM} competent cells were purchase from Invitrogen (Mt Waverley, Victoria Australia); ruthenium red (RR), ionomycin, digitonin, bile acids, Ethylene Glycol-bis(b-aminoethyl ether)-*N,N,N´N´*-Tetraacetic Acid (EGTA), carbonylcyanide-p-trifluoromethoxyphenylhydrazone (FCCP) and 2-aminoethyl diphenylborate (2-APB) from Sigma-Aldrich (Castle Hill, N.S.W., Australia); thapsigargin, 2,5-di-(tert-butyl)-1,4-benzohydro-quinone (DBHQ) and goat anti-rabbit Cy5 labelled polyclonal antibody from Sapphire Bioscience (Redfern, N.S.W., Australia); mouse anti-GOK STIM1 monoclonal antibody from BD Biosciences Pharmingen (San Jose, CA, USA); capsaicin, resiniferatoxin (RTX), and N-vanillylnonamide from Alexis Biochemical Co (Lausem Switzerland); FuGENE 6 from Roche Pharmaceutical (Nutley, NJ, USA); HiperFect from QIAGEN Pty Ltd. (Doncaster VIC., Australia); the pDsRed2-ER and pEYFP-ER plasmids from

Clontech (Mountain View, CA, USA); and glass coverslips from Menzel-Glaser (GmgH, Braunschweig, Germany); IMMU-Mount medium was purchased from Theomo Shandon (Pittsburg, PA, USA). The GFP-STIM1 plasmid, in which cDNA encoding Green Fluorescent Protein (GFP) is located immediately downstream of the predicted signal sequence of the STIM1 gene and inserted into the pApuro expression vector (GFP-STIM1/pApuro) (Baba *et al.*, 2006) was kindly provided by Dr T Kurosaki, RIKEN Research Centre for Allergy and Immunology, Kanagwa, Japan. Ad-Track-CMV-TRPV1, prepared by ligating DNA encoding TRPV1, cloned from mouse nodose ganglia, into the Ad-Track-CMV plasmid, was kindly provided by Drs Lei Zhang and S Brookes, Department of Physiology, Flinders University, Adelaide. The Cherry-STIM1 plasmid (HRP-STIM1), constructed by inserting mCherry after the signal sequence of hSTIM1 then inserting this construct into HRP (Luik *et al.*, 2006), was kindly provided by Dr Rich Lewis, Stanford University, Ca, USA. The YFP-TRPV1 plasmid, constructed by inserting Yellow Fluorescent Protein (YFP) into the Xba1 and Apa I sites of pcDNA3 vector (invitrogen) followed by C-terminal fusion of rat TRPV1 with the FLAG epitope of the YFP for which the stop codons were replaced by in –frame XbaI restriction sites by PCR-mediated mutagenesis and subsequent subcloning into pcDNA3-YFP types (Turner *et al.*, 2003; Wisnoskey *et al.*, 2003; Hellwig *et al.*, 2005),was kindly provided by Dr Michael Schaefer, Charite University, Berlin, Germany. Concentrated stocks (250-1000 times working solution) were prepared from solid chemicals, by dissolved in double deionised water (DDI H_20), dimethylsulfoside (DMSO) or ethanol as appropriate, then diluted with the respective solution as required.

2.2 Cell culture

2.2.1. H4-IIE rat cell line culture

H4-IIE rat liver cells (ATCC CRL 1548) (Darlington, 1987) were cultured in 75mm sterile flask in DMEM, supplemented with 10% (v/v) fetal bovine serum (FBS), penicillin (100 U/ml), streptomycin (0.1 mg/mL) and 10mM HEPES in 5% (v/v) CO_2 (pH 7.4) at 37°C. Once a week the cells were subcultured to another flask and/or individual 35mm sterile Petri dishes containing No. 1 glass coverslips. The coverslips (12, 22 and 30mm diameter for immunofluorescence, calcium imaging and confocal imaging experiments, respectively), were previously sterilised by immersion into 100% ethanol and subsequently flamed. After 48 h the medium was replaced for fresh medium (DMEM medium was used for no longer than 1 month and was stored at 4^0C). The cell subculture was performed by washing cells 3 times with Phosphate Buffered Saline (PBS) followed by addition of 1mL of the mix trypsin 0.25% plus EDTA 1mM, and left for 2-4 min at 37^0C to de-attach the cells. Once the cells were de-attached, 9mL of DMEM medium was added and the cells were resuspended by pipetting up and down. Finally, 3mL of that suspension was transferred to another flask to which 10mL of fresh DMEM medium was added. The cells were used for 25-30 passages in order to preserver the morphological/functional characteristics of the cellular line. The PBS solution contained (mM): NaCl, 136; KCl, 4.7; KH_2PO_4, 1.3; Na_2HPO_4, 3.2; adjusted to pH 7.4 with NaOH.

2.2.2. Isolation and culture of rat hepatocytes

Hepatocytes were isolated from rat liver by perfusion with collagenase, as described previously (Aromataris *et al.*, 2006). Hepatocytes were plated on 35mm sterile Petri dishes containing No. 1 glass coverslips pre-treated with concentrated HCl to

facilitate their attachment. The hepatocytes were plated for 4 hours in 5% (v/v) CO_2 (pH 7.4) at 37^0C in "attachment medium" (see below). After this period, the "attachment medium" was replaced for "growing medium" (see below) and then cultured for 24-72 h in 5% (v/v) CO_2 (pH 7.4) at 37^0C. Animals received humane care, and the experimental protocols were conducted according to the criteria outlined in the "Australian Code of Practice for the Care and Use of Animals for Scientific Purposes" (National Health and Medical Research Council of Australia). The Animal Welfare Committee approval number is 165/02 (i).

Attachment medium: DMEM/F12 supplemented with 10% (v/v) fetal bovine serum plus penicillin/streptomycin and HEPES plus dexamethasone and insulin 100nM. Growing medium: DMEM/F12 supplemented with 10% (v/v) fetal bovine serum, penicillin/streptomycin and HEPES.

2.3 Measurement of Ca^{2+} in the cytoplasm, beneath the plasma membrane and endoplasmic reticulum using fluorescence dyes

2.3.1. Loading of liver cells with fura-2, FFP-18 and Calcium Green 5N

Cells attached to 22mm No. 1 glass coverslips were incubated with 5 μM of fura-2, FFP-18 or Calcium Green 5N in the acetoxymethylester (AM) form in Krebs-Ringer-HEPES buffer (KRH) containing 0.02% (v/v) pluronic acid for the incubation periods indicated below. After the loading period, the cells were washed twice with KRH and then incubated for a further 30 min at room temperature to allow de-esterification of the acetoxymethylester by intracellular esterases. The Krebs-Ringer-Hepes solution contained (mM): NaCl, 136; KCl, 4.7; $CaCl_2$, 1.3; $MgCl_2$, 1.25; glucose, 10; and HEPES, 10; adjusted to pH 7.4 with NaOH.

Fura-2 and Calcium Green 5N were loaded for 30 min at room temperature in H4-IIE cells, while rat hepatocytes were loaded with fura-2 for 1 h at 37^0C.

FFP-18 loading was carried out for 90 min at room temperature in Krebs-Ringer-HEPES buffer containing 0.02% (v/v) pluronic acid supplemented with 10% BSA. FFP-18 Ca^{2+} dye is derived from fura-2. FFP-18-AM incorporates into the plasma membrane and reorientates (by slow "flip-flop" diffusion) to the inner face of the plasma membrane where cytosolic esterases cleave off the ester groups. Because the "flip-flop" process is slow compared to diffusion of other dyes like fura-2, loading the cells with FFP-18 takes longer than fura-2 and Calcium Green 5N ((Davies *et al.*, 1997; Golovina, 2005)).

2.3.2. Measurement of cytoplasmic fura-2, sub-plasma membrane FFP-18 and endoplasmic reticulum Calcium Green 5N fluorescence in liver cells

After the loading period, cells were placed in an open working chamber containing KRH buffer, for the measurement of the respective dyes fluorescence. Fura-2, FFP-18 or Calcium Green 5N fluorescence were measured with a Nikon TE300 Eclipse inverted microscope in conjunction with a Sutter DG-4/OF wavelength switcher at room temperature, in the presence of the indicated concentrations of $CaCl_2$ (zero mM Ca^{2+} was achieved by prepared a KRH buffer without any Ca^{2+} addition plus 0.5mM EGTA in order to chelated any Ca^{2+} traces). An Omega XF04 filter set was used for fura-2 and FFP-18. The band pass emission Endow GFP filter block was used for Calcium Green (Chroma Technology Corp., Rockingham, VT., USA). Fluorescence measurements were performed over a given experimental period, using ratiometric acquisition of fura-2 and FFP-18 fluorescence, under alternating excitation wavelengths of 340 nm and 380 nm. The fluorescence emission was measured at a wavelength of 510 nm. For Calcium Green 5N the excitation wavelength was 470/40

nm with emission wavelength of 525-550 nm and a 495 LP dichroic mirror. The images were acquired every 20 seconds (unless indicated otherwise) using a 40x objective. The time course of the changes in the fluorescence emissions was measured with the Photonic Science ISIS-3 ICCD camera controlled by a computer running UIC MetaFluor software (Molecular Devices Co., Downingtown, PA., USA). The fluorescence of fura-2, FFP-18 or Calcium Green 5N were acquired by selecting regions of interest (ROI) at the cytoplasmic, plasma membrane or endoplasmic reticulum regions, respectively. Background noise was automatically subtracted to each individual ROI by setting a reference ROI in a region without of cells. Only those cells with homogeneous fluorescence and with a range of fluorescence intensity below the saturation set point of the camera were chosen for experiments. In this manner, normally 15-20 out of 30 cells in a field were selected. In control experiments the fluorescence of non-loaded cells (autofluorescence) was estimated to be less than 5% of that of the dye-loaded cells under the above settings.

To test the specificity of the FFP-18 Ca^{2+} dye, to measured Ca^{2+} levels exclusively from sub-plasma membrane locations, a separate group of control experiments were performed. For this, the fluorescence from extracellular facing FFP-18 was quenched by the addition of Ni^{2+} (1mM). The remaining FFP-18 fluorescence signal corresponds to the inner face of the plasma membrane (Pettit and Hallett, 1995; Davies *et al.*, 1997; Golovina and Blaustein, 1997; Davies and Hallett, 1998; Golovina, 2005). Using this approach, the proportion of the FFP-18 dye distributed beneath the plasma membrane was estimated to be more than 95%.

Experimental agents were added directly to the working chamber and mixed twice by gently drawing buffer into the pipette tip and expelling back into the chamber.

All the fluorescence changes inside the ROI were automatically analysed with the MetaFluor software and stored as a Microsoft Excel files for further analysis. Finally, all the graphs were created by GraphPad prism software (GraphPad Software, Inc., San Diego, CA., USA). The results of the individual experiments are expressed as means ± SEM (between 10 and 20 cells for each experiment as indicated in the figure legends).

2.3.3. Conversion of fura-2 fluorescence ratio to cytoplasmic Ca^{2+} concentration ($[Ca^{2+}]_{cyt}$)

Values of fura-2 fluorescence ratio (340 nm/380 nm) were converted to cytoplasmic calcium concentration ($[Ca^{2+}]_{cyt}$) using the equation (shown below) and dissociation constant (K_d) derived by Grynkiewicz et al (1985) (Grynkiewicz *et al.*, 1985). The values for the equation were determined in the calibration experiment, as illustrated in Fig. 2.1.

Briefly, cells loaded with fura-2 in the presence of KRH buffer containing 5mM $CaCl_2$, were exposed to the Ca^{2+} ionophore, ionomycin (10μM) to allow the equilibrium of cytoplasmic Ca^{2+} with extracellular Ca^{2+} to be achieved. The values of fluorescence obtained at 380 nm represent fura-2 emission fluorescence when fully bound to Ca^{2+} ($F_{380\ bound}$). Once the new plateau was established, Ca^{2+} was chelated by replacing the previous buffer (KRH buffer containing 5mM $CaCl_2$) for a mix of 0.15 M Tris buffer plus 20mM EGTA at pH 8.7. The values of fluorescence obtained at 380 nm represent fura-2 emission fluorescence when completely unbound to Ca^{2+} ($F_{380\ unbound}$) (Fig 2.1 A).

After the calibration assay, the ratio of 340 nm/380 nm fluorescence was calculated. The maximum and minimum ratios (R_{max} and R_{min}), were obtained after ionomycin

and EGTA addition respectively (Fig. 2.1 B). The K_d for binding of fura-2 to Ca^{2+} is 224nM and the equation used to convert fura-2 fluorescence ratio to $[Ca^{2+}]_{cyt}$ is:

$$[Ca^{2+}]_{cyt} = K_d \frac{F_{380unbound}}{F_{380bound}} X \frac{r - R_{min}}{R_{max} - r}$$

"r" is the ratio at any given time.

Using this equation, the subsequent experiments undertaken with fura-2, were converted to $[Ca^{2+}]_{cyt}$ in order to compare quantitatively the change in cytoplasmic Ca^{2+} levels.

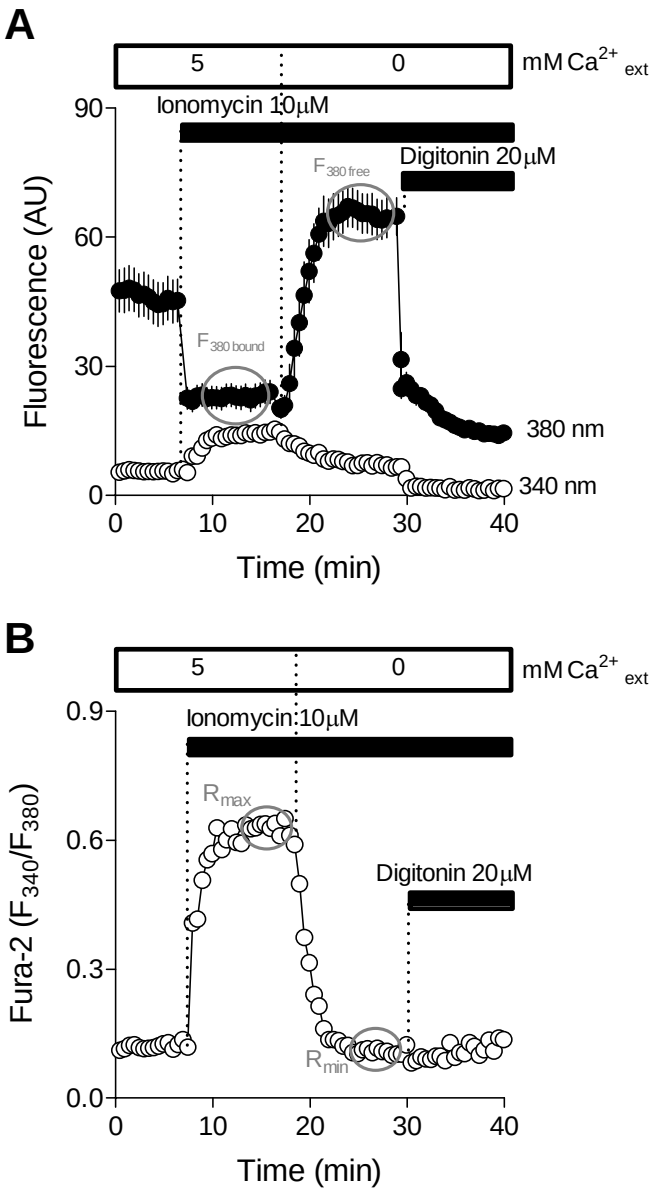

Fig. 2.1. Experimental protocol used to convert fura-2 fluorescence to cytoplasmic Ca^{2+} concentration. Representatives traces (averaged for 15-20 cells on a coverslip) are presented, showing the changes in the fluorescence at 340 and 380 nm (A) or 340/380 ratio (B) of fura-2 induced by ionomycin 10µM in the presence of 5 or 0 mM Ca^{2+}_{ext} (as indicated by the horizontal bar) followed by the cellular lysis and consequent fura-2 washing out from the cytoplasmic space induced by digitonin.

2.3.4. Quantification of Ca^{2+} release from the intracellular calcium stores and Ca^{2+} entry across the plasma membrane

To study quantitatively the amount of the agonist-induced Ca^{2+} release from intracellular stores and Ca^{2+} entry across the plasma membrane, a so-called "Ca^{2+}-add back" protocol was used. The "Ca^{2+}-add back" protocol is illustrated in Fig. 2.2 and was performed as follows. Agonist (thapsigargin in this particular case) was added to cells in the absence of extracellular Ca^{2+} (Ca^{2+}_{ext}) inducing Ca^{2+} release from intracellular stores. After the $[Ca^{2+}]_{cyt}$ returned to the basal levels, Ca^{2+}_{ext} was added back to the medium, causing a second increase in $[Ca^{2+}]_{cyt}$ until a new plateau was reached. This second increase in $[Ca^{2+}]_{cyt}$ corresponds to Ca^{2+} entry across the plasma membrane (through the channel activated by the agonist added).

A representative graph showing changes in $[Ca^{2+}]_{cyt}$, resulting from the release of Ca^{2+} from the endoplasmic reticulum and subsequent Ca^{2+} entry is illustrated in Fig. 2.2. The amounts of Ca^{2+} released were determined by measuring the height of the peak of the agonist-induced increase in $[Ca^{2+}]_{cyt}$. The initial rate of Ca^{2+} entry was determined by linear regression. In order to get an adequate amount of data in the linear area of the curve (for the linear regression analysis), the frequency of the image acquisition was increased by 4 times (every 5 seconds). Values of the peak of Ca^{2+} entry observed after Ca^{2+}_{ext} addition were determined by calculating the difference between the maximum $[Ca^{2+}]_{cyt}$ observed after Ca^{2+}_{ext} addition and the value of $[Ca^{2+}]_{cyt}$ obtained immediately before Ca^{2+}_{ext} addition.

The experiment shown in Fig. 2.2 represents the protocol used in this study to induce the activation of the Store-Operated Ca^{2+} Channels (SOCs). It is well documented that SOCs can be activated pharmacologically by inhibiting the ER (Ca^{2+} + Mg^{2+})

ATPase (SERCA) with DBHQ and thapsigargin (Parekh and Penner, 1997; Lewis, 1999).

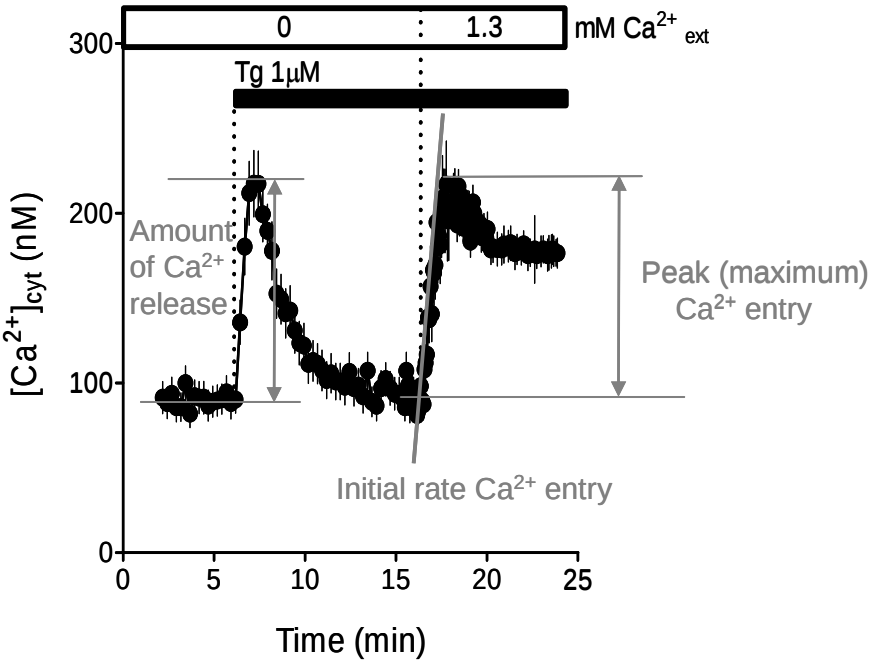

Fig. 2.2. "Ca^{2+}-add back" protocol to quantify the amount of Ca^{2+} release from intracellular stores and Ca^{2+} entry through SOCs at the plasma membrane. A representative trace (averaged for 18 cells on a coverslip) is presented, showing the changes in $[Ca^{2+}]_{cyt}$ resulting from the release of Ca^{2+}, by thapsigargin in the absence of Ca^{2+}_{ext}, from thapsigargin-sensitive stores (endoplasmic reticulum) and Ca^{2+} entry (through SOCs) by subsequently Ca^{2+} re-addition into the medium. The quantitation of Ca^{2+} release and entry is described in Section 2.3.4.

2.4 Measurement of mitochondrial potential using TMRM

Mitochondrial membrane potential was measured using tetramethylrhodamine methyl ester (TMRM). TMRM is a cationic dye that crosses lipid membranes with ease but remains in the aqueous phase, distributing in intracellular compartments according to their membrane potential, following the Nerst equation. H4-IIE cells were loaded with 100nM TMRM by incubation at room temperature for up to 10 min, this concentration does not affect mitochondrial function (Scaduto and Grotyohann, 1999). TMRM fluorescence was measured using a Leica SP5 confocal microscope imaged at 541 nm excitation and 560-615 nm emission wavelengths. Peripheral mitochondria were highly mobile, which precluded reliable measurement of individual organelles. Two to five clusters of approximately 20 organelles in the perinuclear region were averaged for every cell.

2.5 Ectopic expression of proteins by DNA plasmid transfection

2.5.1. Plasmid amplification by bacterial transformation

The Ad-Track-CMV-TRPV1, YFP-TRPV1 and Cherry-STIM1 plasmids were separately inserted into "Library Efficiency DH5α^{TM}" competent bacteria by ice/heat shock incubation following the instruction of the manufacturer. After the bacteria transformation with each individual plasmid, 1:10 dilutions of the transformed cells were spread on LB agar plates (which contains ampicillin 100μg/mL in order to allow the growth of the transformed bacteria only). After overnight incubation at 37^0C, 2-3 colonies were separately picked and placed in sterile containers with 10mL LB medium plus ampicillin 100μg/mL at 37^0C for 8 hours, shaking at 300rpm. Then 1 to 1.5mL of each bacterial solution were inoculated into separate Erlenmeyer

containing 100mL LB medium plus ampicillin 100μg/mL for an overnight growth at 37^0C, shaking at 300rpm. After this 7mL of each individual bacterial suspension, corresponding to an individual colony, was mixed with 3mL of glycerol 50% solution (made in distilled water) and then frozen at - 80^0C in 1mL aliquots. These aliquots were labelled with the name of the colony they originated from. The rest of the bacterial suspension was used for the plasmid purification. The LB medium contained (grams): Tryptone, 10; Yeast extract, 5; NaCl 10; adjusted to pH 7.0 with NaOH. The LB agar plates were prepared by adding 1.5% agar to the LB medium, then mixing, autoclaving and finally placing 15mL into 10cm sterile plates.

2.5.2. Plasmid purification from transformed bacteria

The DNA plasmids were extracted individually from the large scale bacterial-contained plasmid suspension by a "DNA purification assay", using QIAfilter Maxi Kit. This Kit is based on a modified alkaline lysis procedure, followed by the binding of DNA to an anion-exchange resin under appropriate low-salt and pH conditions (QIAGEN Pty Ltd., Doncaster VIC., Australia). The pure DNA plasmids obtained were redissolved in 200-300μL of Tris-Cl pH 8.5 (prepared with RNA-ase free distilled water). The concentration of DNA present was then determined by UV spectrophotometry analysis. For this, DNA aliquots were diluted into Tris-Cl, pH 7.0 buffer (prepared with RNA-ase free distillate water) and read in a Shimadzu Spectrophotometer (Shimadzu Scientific Instrument Pty. Ltd Waverly, Victoria, Australia) at an absorbance wavelength of 260 nm, to determine the DNA concentration through the following equation:

$$\mathbf{[DNA] = Absorbance_{260nm} \times Dilution\ factor \times 50\mu g/mL}$$

Where: 1 unit of DNA at 260nm is = 50μg/mL.

The concentration of DNA obtained (yield) for the plasmids Ad-Track-CMV-TRPV1, YFP-TRPV1 and Cherry-STIM1 were 0.9, 1.2 and 1.15μg/μL, respectively.

2.5.3. Plasmid DNA analyses by restriction enzyme assay, followed by agarose gel electrophoresis

After obtaining pure plasmid DNA, a "restriction enzyme analysis" was performed, for each of the plasmids individually, to verify they correspond to the correct plasmid they were originally amplified from. This assay is based on size estimation of the DNA fragments, originated by specific cuts into plasmid DNA by selected enzymes: BamH1 or EcoR1 (for Ad-Track-CMV-TRPV1 plasmid); a mix of Hind-III and Xab-I (for YFP-TRPV1 plasmid); and Kpn1 (for Cherry-STIM1 plasmid). The restriction enzyme analyses were performed with 1μL of the selected enzymes; which were incubated for 1 h, at 37^0C, with 0.5μg of the cDNA plasmid. In order to determine the size of the DNA fragments obtained by the restriction enzymes assay, the samples were loaded into agarose gel and an electrophoresis performed. The agarose gel was prepared with agarose (electrophoresis grade) at different percentages (0.7, 1.1 and 1.3 % agarose gel for Ad-Track-CMV-TRPV1, YFP-TRPV1 and Chery-STIM1 plasmids, respectively) in TBE buffer, melted in the microwave and subsequently cooled to 55^0C in a water bath. The TBE buffer contained (mM): Tris-base. 89; Boric acid, 89; EDTA 2; adjusted to pH 8.0 with NaOH. Once the mix reached ~ 55^0C, it was placed into the gel casting platform (in which the gel comb was previously positioned). After 40 min (to allow the complete solidification of the gel), the gel comb was removed and the gel casting platform (containing the gel) was placed into the electrophoresis chamber with the adequate voltage setting (80, 60 and 70V for Ad-Track-CMV-TRPV1, YFP-TRPV1 and Chery-STIM1 plasmids, respectively). Then the samples from the restriction enzyme assay, were loaded in

separate lanes and electrophoreses performed for 60min (for Ad-Track-CMV-TRPV1), and 90min (for YFP-TRPV1 and Chery-STIM1 plasmids). After this, the gel was stained for 20 min with ethidium bromide (0.5μg/mL), and de-staining for 30 min in H_2O. An image of the gel was subsequently captured with an Amershan Pharmacia Biotech UV trans-illuminator operated by Image Master UDS-Cl software (GE Healthcare Bio-Sciences Pty. Ltd., Rydalmere, N.S.W., Australia). The sizes of the DNA fragments, from the different plasmids used in this study, were then determined by comparing them to the size of commercially available DNA fragments marker SPP1-DNA/EcoR1.

A representative image of three gels, showing the cDNA fragments (bands) obtained from the restriction enzyme assays of the plasmids Ad-Track-CMV-TRPV1, YFP-TRPV1 and Chery-STIM1, are illustrated below in Fig. 2.3, 2.4 and 2.5, respectively.

As shown in Fig. 2.3 the size of the Ad-Track-CMV-TRPV1 DNA fragments obtained from the restriction enzyme analysis (BamH1 or EcoR1), match the expected DNA fragment sizes, confirming the pure-DNA solution obtained above corresponds to the Ad-Track-CMV-TRPV1 plasmid. The expected size of Ad-Track-CMV-TRPV1 DNA fragments are: 2.9 and 9.1 Kb for the cuts originated by EcoR1 and 1.0, 5.5 and 5.6 Kb for the cuts originated by BamH1.

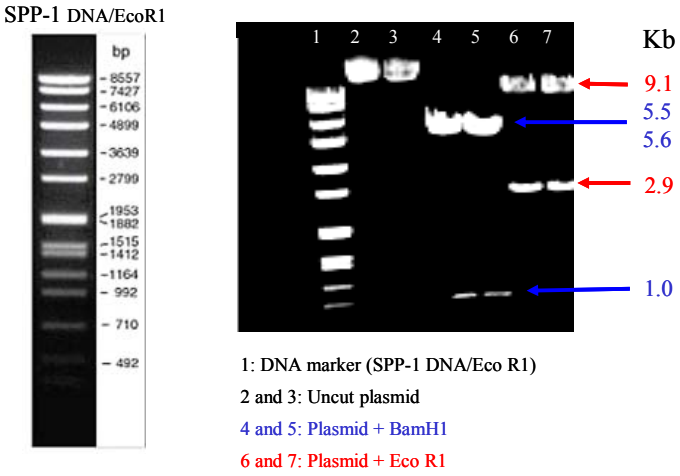

Fig. 2.3. Gel electrophoresis of Ad-Track-CMV-TRPV1 DNA fragments obtained after restriction enzyme analysis. The samples obtained from the restriction enzyme analysis of Ad-Track-CMV-TRPV1 plasmid performed with BamH1 or Eco R1, were loaded into a 0.7% agarose gel and an electrophoresis was performed at 80V for 60 min. The image on the right illustrated the size (Kb) of the fragments obtained by the respective enzyme cuts per duplicate plus the un-cut plasmid (at the top). The size of the fragments originated by BamH1 or Eco R1 (estimated by comparison with the commercial DNA marker SPP-1 DNA/Eco R1 (left panel)), correspond to 5.5-5.6 and 1.0 Kb and 9.1 and 2.9 Kb respectively.

As shown in Fig. 2.4, the size of the YFP-TRPV1 DNA fragments obtained from the restriction enzyme analysis (Hind-III / Xab-I), match the expected DNA fragment sizes, confirming the pure-DNA solution obtained above corresponds to the YFP-TRPV1 plasmid. The expected size for YFP-TRPV1 DNA fragments originated by the mix of Hind-III and Xab-I are approximately: 0.8, 2.5 and 6.2 Kb (corresponding to the YFP sequence, the TRPV1 portion and the pcDNA3 vector, respectively).

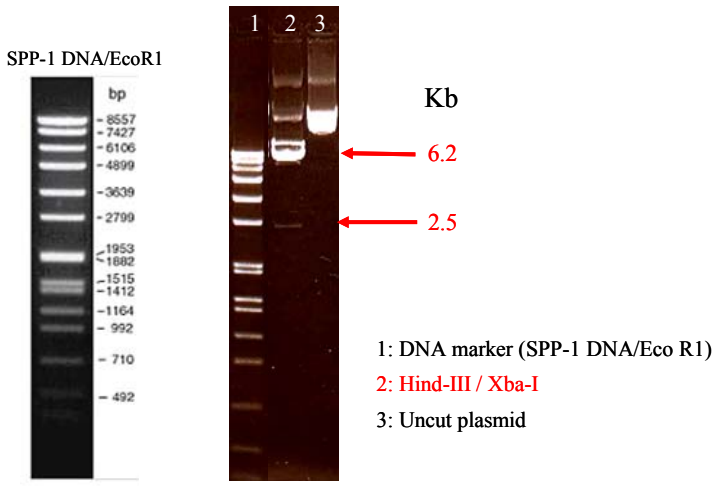

Fig. 2.4. Gel electrophoresis of YFP-TRPV1 DNA fragments obtained after restriction enzyme analysis. The samples obtained from the restriction enzyme analysis of YFP-TRPV1 plasmid performed with Hind-III plus Kba-I, were loaded into a 1.1% agarose gel and an electrophoresis was performed at 60V for 90 min. The image on the right illustrated the size (Kb) of the fragments obtained by the respective enzyme cuts plus the un-cut plasmid (at the top). The size of the fragments originated by Hind-III plus Kba-I (estimated by comparison with the commercial DNA marker SPP-1 DNA/Eco R1 (left panel)), correspond to 6.2 and 2.5 Kb.

As is shown in Fig. 2.5, the size of the Cherry-STIM1 fragments obtained from the restriction enzyme analysis (Kpn1), match the expected DNA fragment sizes, confirming the pure-DNA solution obtained above corresponds to the Cherry-STIM1 plasmid. The uncut Cherry-STIM1 plasmid has the total size of 8.773 Kb. The expected sizes for cuts originated by Kpn1 are: 0.719 Kb from Cherry sequence and 8.054 Kb from the rest of the plasmid.

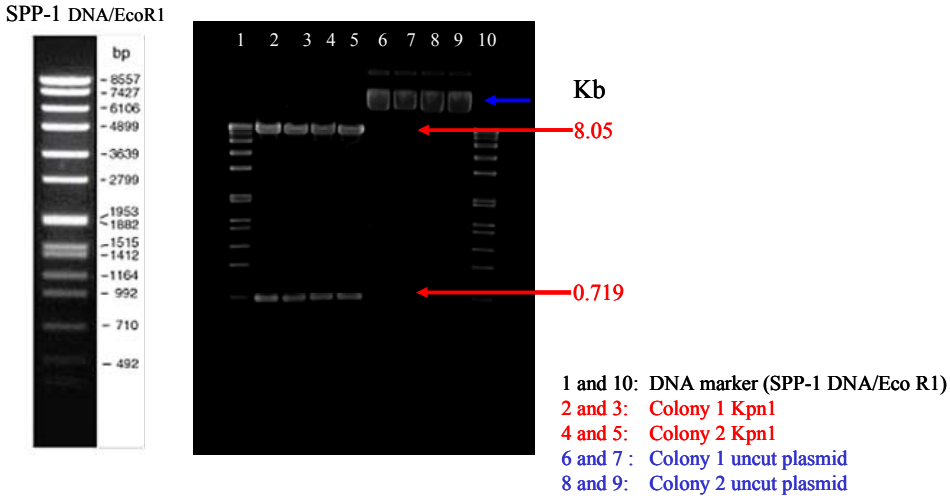

Fig. 2.5. Gel electrophoresis of Cherry-STIM1 DNA fragments obtained after restriction enzyme analysis. The samples obtained from the restriction enzyme analysis from two colonies of the Cherry-STIM1 plasmid performed with Kpn1, were loaded into a 1.3% agarose gel and an electrophoresis was performed at 70V for 90 min. The image on the right illustrated the size (Kb) of the fragments obtained by the respective enzyme cuts per duplicate plus the uncut plasmid (at the top). The size of the fragments originated by Kpn1 (estimated by comparison with the commercial DNA marker SPP-1 DNA/Eco R1 (left panel)), correspond approximately to 8.05 and 0.719 Kb.

2.5.4. Cellular transfection

H4-IIE cells were transfected with 1-3μg of the plasmids used in this study (Ad-Track-CMV-TRPV1; Ad-Track-CMV; YFP-TRPV1; pDesRed2-ER; pEYFP-ER Cherry-STIM1 and GFP-STIM1/pApuro) using the lipidic reagent FuGENE 6, according to the manufacturers instructions. For the transfection a "transfection cocktail" was prepared by mixing 15μL of FuGENE 6 with 150μL Opti-MEM medium (antibiotic and serum free) placed into an eppendorf tube and incubated for 5 min. After this, the plasmid was added, mixed and incubated for another 30 min. Simultaneously, H4-IIE cells growing in a 75 mm culture flask (≈ 90% confluence) were subcultured by adding 1mL of trypsin 0.25% plus EDTA 1mM and then resuspended in 9mL DMEM medium. 250μL of this cell suspension was placed in a Flacon tube containing 40mL of PBS in order to wash out any remaining trypsin/EDTA. Then the cells were pelleted down for 1 ½ min at 1500rpm, the supernatant discarded, and 1mL of normal DMEM added to resuspend the cells. After the 30 min incubation for the "transfection cocktail" was concluded, the "transfection cocktail" was added in a drop fashion to the cell suspension and then mixed by pipetting up and down. After this, 70μL of the DNA/cells mix was placed at the centre of sterile coverslips (previously positioned into sterile 35 mm Petri dishes). The petri dishes were then placed into the incubator at 5% (v/v) CO_2 and 37^0C. Four hours later, 1mL of warm DMEM medium was added to each petri dish and the cells were incubated for 48-72 h before the use.

For selected experiments (control transfected cells), control transfections were performed, for which a similar protocol was used but the "transfection cocktail" was prepared without DNA.

For cells transfected with the Ad-Track-CMV-TRPV1 plasmid (1 μg), the transfection efficiency (proportion of cells expressing TRPV1) was approximately 10%, while for cells transfected with 3 μg of either GFP-STIM1/pApuro or Cherry-STIM1 plasmids, the transfection efficiency (proportion of cells expressing STIM1) was approximately 30%.

For immunofluorescence assays (described below), H4-IIE cells attached to 12 mm glass coverslips were co-transfected with 3 μg of both, pDsRed2-ER and Ad-Track-CMV-TRPV1 plasmids. For co-localisation assays (described below), H4-IIE cells attached to 30 mm glass coverslips were co-transfected with 3 μg of both YFP-TRPV1 and pDsRed2-ER plasmids; or 3 μg of both Cherry-STIM1 and pEYFP-STIM1 plasmids; or 3 μg of both GFP-STIM1/pApuro and pDsRed2-ER plasmids.

The Biosafety Committee approval number for the research involving DNA technology is NLDR 1335/2004.

2.6 Transfection with siRNA to knockdown STIM1 expression

H4-IIE cells were transfected with 125nM custom siRNA, targeted against STIM1 and control siRNA, using HiperFect, according to the manufacturer's instructions. For the transfection, a "transfection cocktail" was prepared by mixing 7.5μL of HiperFect transfection reagent plus 6.6 μL of the siRNA (20μM) with 43.4 μL Opti-MEM medium (antibiotic and serum free) in an eppendorf. The mix was incubated for 10 min. Simultaneously, H4-IIE cells growing in a 75 mm culture flask (≈ 90% confluence) were de-attached by adding 1mL of trypsin 0.25% plus EDTA 1mM and then resuspended in 9mL DMEM medium (antibiotic free). 100μL of this cell suspension was placed in a Falcon tube containing 40mL of PBS in order to wash out

any remaining trypsin/EDTA. Then the cells were pelleted down for 1 ½ min at 1500 rpm, the supernatant discarded, and 1mL of DMEM (antibiotic free) added to resuspend the cells. After the 10 min incubation for the siRNA/transfection mix concluded, the "transfection cocktail" was added in a drop fashion to the cell suspension, and then mixed by pipetting up and down. After this 500μL of the siRNA/cells mix was placed at the centre of sterile coverslips (previously positioned into sterile 35mm Petri dishes). The petri dishes were then placed into the incubator at 5% (v/v) CO_2 and 37^0C. Four hours later, 500μL of warm DMEM medium (antibiotic free) was added to each petri dish and the cells incubated for 72 h before use.

Note: The RNA sense sequence used in this study of` rat STIM1 was 5'-AGCUGCGUGACGAGAUCdTdT-3' and RNA sense sequence of the negative control was 5'-UUCUCCGAACGUGUCACGUdTdT-3'. The negative control siRNA has no significant sequence homology to any known rat gene.

2.7 Visualisation of TRPV1 and STIM1 proteins by confocal microscopy

2.7.1. TRPV1 and STIM1 detection by immunofluorescence

To visualise the distribution of ectopically expressed TRPV1 proteins, an immunofluorescence assay was performed. For this, H4-IIE cells (attached to 12 mm glass coverslips) were fixed for 15 min in 4% (v/v) paraformaldehyde in PBS and permeabilised with 0.2% (v/v) Triton X-100 in PBS at room temperature. Fixed cells were blocked for 2 h in 10% (v/v) fetal bovine serum, in PBS at room temperature; and subsequently washed and incubated overnight at 4^0C with a polyclonal anti-TRPV1 antibody raised in rabbits (1/1000) in 1% (v/v) fetal bovine serum diluted in

PBS. The cells were then washed in PBS, and incubated with Alexa-Fluor 647 labelled polyclonal anti-rabbit antibody made in goat (1/1000) for 2 h at room temperature. Finally, the cells were washed 5 times with PBS and mounted on glass slides in IMMU-Mount medium. The fluorescence of Alexa-Fluor 647 was measured using a Leica SP5 laser-scanning confocal microscope, the excitation/emission wavelengths were 633/675-750 nm.

The cells used for this assay, were expressing ectopically TRPV1 proteins, which were identified by the presence of GFP fluorescent protein (present in the Ad-Track-CMV-TRPV1 plasmid) at excitation/emission wavelengths 488/500-550 nm. The Ad-Track-CMV-TRPV1 plasmid expresses TRPV1 and GFP as separate proteins, each under the control of the CMV promoter, Fig. 2.3 right panel.

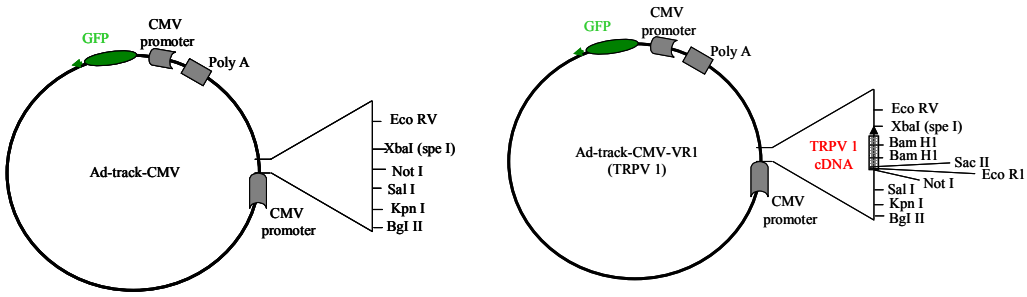

Fig. 2.6. Ad-Track-CMV and Ad-Track-CMV-TRPV1 plasmids maps. The right panel represent the plasmid map encoding TRPV1 cDNA which was sub-cloned into Ad-Track-CMV plasmid (left panel) as an Xba I / Not I fragment. The TRPV1 cDNA region is under the control of the CMV promoter. In addition to the cDNA encoding TRPV1, both Ad-Track-CMV and Ad-Track-CMV-TRPV1 plasmids has incorporated the cDNA encoding for the GFP protein, which, as well, is under the control of the CMV promoter. The sites of cut for different restriction enzymes are schematically represented.

To visualise the distribution of endogenously expressed STIM1, an immunofluorescence assay was performed. For this, H4-IIE cells (attached to 12 mm glass coverslips) were washed 3 times with PBS and then fixed in 3% (v/v) paraformaldehyde at room temperature, for 10 min. The fixed cells were washed 5 times with 100mM glycine in PBS, and permeabilised with 0.1% (v/v) saponin in PBS for 10 min at room temperature. Cells were washed 5 times in PBS, and then blocked with blocking buffer (gelatine 0.2% (w/v) plus TWEEN 0.1% (w/v) in PBS) for 30 min at room temperature. After this, the cells were incubated for 3 hours with the monoclonal mouse anti-GOK/STIM1 (1:100 dilutions in blocking buffer). Subsequently, the cells were washed 5 times with blocking buffer and incubated for 1 hour with Alexa-Fluor 488-conjugated goat anti-mouse IgG (1:500 dilutions in blocking buffer). Finally, the cells were washed 5 times with PBS and the coverslips mounted on slides in IMMU-Mount medium. The fluorescence was imaged at excitation/emission wavelengths 488/500-550 nm using Leica SP5 scanning confocal microscope.

In both immunofluorescence assays mentioned above (against TRPV1 and STIM1 proteins), control samples were prepared by omitting the primary antibodies. The images of those control samples consistently showed low fluorescence (due to non-specific binding of the secondary antibody), compared with samples containing both primary and secondary antibodies. The fluorescence of control samples was set to zero by adjusting the gain of the confocal microscope detector, until no fluorescence could be detected. These confocal settings were used to image the subsequent samples, containing both primary and secondary antibodies.

2.7.2. Visualisation of ectopically expressed YFP-TRPV1, GFP-STIM1 and Cherry-STIM1 in living cells using confocal microscopy

Ectopically expressed TRPV1-YFP proteins were imaged at 514 nm excitation/520-550 nm emission by Leica SP5 scanning confocal microscope. Ectopically expressed GFP-STIM1 and Cherry-STIM1 proteins were imaged at 488/500-550 nm or 561/600-650 nm excitation/emission, respectively, using a Leica SP5 scanning confocal microscope.

2.8 Co-localisation of TRPV1 or STIM1 proteins with endoplasmic reticulum markers

2.8.1. Co-localisation of ectopically expressed TRPV1 proteins with the ER markers pDsRed2-ER and BODIPY TR-X Tg

To determine whether the ectopically expressed TRPV1 proteins were expressed in the endoplasmic reticulum, a co-localisation study was performed in cells co-transfected with both Ad-Track-CMV-TRPV1 and pDsRed2-ER plasmids, followed by immunofluorescence against TRPV1. The resultant fluorescent proteins were simultaneously imaged by a Leica SP5 scanning confocal microscope with excitation/emission wavelengths: 561/600-640 nm for DsRed2 and 633/675-750 nm for Alexa-Fluor 647. The cells imaged, ectopically expressed TRPV1 proteins, which were identified by the presence of GFP fluorescent protein (present in the Ad-Track-CMV-TRPV1 plasmid).

Alternatively, cells were co-transfected with both YFP-TRPV1 and pDsRed2-ER plasmids and the resultant fluorescent proteins were simultaneous imaged in living cells, by a Leica SP5 scanning confocal microscope with excitation/emission wavelengths of 561/600-650 nm for DsRed2 and 514/520-550 nm for YFP.

In a separate group of experiments H4-IIE cells were ectopically transfected with YFP-TRPV1 plasmid. After 48 h the cells were loaded for 10 min at room temperature with 1μM of membrane-permeant dye, BODIPY TR-X Tg methyl ester (which distributes throughout the thapsigargin binding sites (at the ER) in live cells). After the incubation period, the dye was washed out and the resultant fluorescent proteins simultaneously imaged, by a Leica SP5 scanning confocal microscope with excitation/emission wavelengths of 561/600-650 nm for BODIPY TR-X and 514/520-550 nm for YFP.

2.8.2. De-convolution of confocal images

For the further resolution of the co-localisation images, a de-convolution analysis of the YFP-TRPV1, pDsRed2-ER and BODIPY TR-X Tg confocal images, was performed. A series of images (4-9 in total) of the cellular Z plane were captured by confocal microscope using the 63x water immersion objective (1.2 numeric aperture). The sizes of the images were (μm): 0.045, 0.045 and 0.200 in X, Y and Z axis, respectively. The images were imported into the AutoDeblur 7.5 software (Auto Quant Imaging, Inc. Watervliet, N.Y., USA) and a "3D blind de-convolution" analysis performed.

2.8.3. Co-localisation of endogenous STIM1 with the ER marker pDsRed2-ER

To determine whether endogenous intracellular STIM1 proteins were expressed in the endoplasmic reticulum, a co-localisation study was performed between the ectopically expressed ER marker pDsRed2-ER and the endogenous expressed STIM1 (assessed by immunofluorescence). The resultant fluorescent proteins were simultaneously imaged by a Leica SP5 scanning confocal microscope with

excitation/emission wavelengths of 561/600-650 nm for DsRed2 and 488/500-550 nm for Alexa-Fluor 488.

2.8.4. Co-localisation of ectopically expressed STIM1 with the ER markers pEYFP-ER and pDsRed2-ER

To determine whether ectopically expressed STIM1 proteins were expressed in the endoplasmic reticulum, two different co-localisation studies were performed. For this, co-transfections between Cherry-STIM1 and pEYFP-ER plasmids and GFP-STIM1 and pDsRed2-ER plasmids were performed. The resultant fluorescent proteins were simultaneously imaged by a Leica SP5 scanning confocal microscope with excitation/emission wavelengths of 561/600-650 nm for Cherry or DsRed2 and 514/520-550 nm for YFP.

2.9 Statistical analysis

All data were entered into a standard spread sheet (Excel 2003, Microsoft Co) and the statistical significance of two groups was compare using Student's t-test (unpaired and two tailed). The statistical significance between multiple groups was compare using ANOVA followed by the Bonferroni *post hoc* test (SPSS 12.0.1 software (SPSS inc., Chicago, IL., USA)). Unless indicated otherwise, the data are expressed as Means ± Standard Error of the Mean (S.E.M) with "n" as the number of independent experiments. Differences between means were considered significant at $P \leq 0.05$.

CHAPTER III: ROLE OF BILE ACIDS IN LIVER CELLS CALCIUM HOMEOSTASIS

3.1 Introduction

Cholestasis is a significant contributor to liver pathology and can lead to primary sclerosis and liver failure. Cholestasis arises from hepatocyte dysfunction or intrahepatic or extrahepatic biliary obstruction, leading to impaired movement of bile along the biliary duct tree and impaired secretion of the components of bile fluid into the bile canaliculus. It has been shown that during cholestasis, conjugated and un-conjugated bile acids accumulate in the blood, hepatocytes, and possibly also in the bile cannaliculus; leading to hepatocyte injury, apoptosis and necrosis (Lee and Boyer, 2000; Jansen *et al.*, 2001; Bohan and Boyer, 2002; Boyer, 2002a; Elferink and Groen, 2002; Maddrey, 2002; Pauli-Magnus *et al.*, 2005).

It has been reported that these effects of bile acids involve changes in $[Ca^{2+}]_{cyt}$. While the effect of bile acids on the release of Ca^{2+} from intracellular stores in hepatocytes (Combettes *et al.*, 1990; Beuers *et al.*, 1993a) and other cell types (Gerasimenko *et al.*, 2006) have been reasonably well described, little is known about the Ca^{2+} entry pathways modulated by bile acids.

The main Ca^{2+} entry pathway activated by hormones and growth factors in hepatocytes is the Ca^{2+}-selective store-operated Ca^{2+} channel (SOC) (Rychkov *et al.*, 2001; Rychkov *et al.*, 2005) located in the plasma membrane. Previous studies have

provided evidence that Ca^{2+} entry through SOCs is required for normal bile flow, most likely by contributing to the increase in $[Ca^{2+}]_{cyt}$ that initiates contraction of the bile canaliculus (Gregory *et al.*, 2004a).

Considering the evidence above, the general aim of the experiments described in this chapter was to evaluate the effects of bile acids on the activity of SOCs in liver cells. This chapter describes the inhibition and activation of Ca^{2+} entry through SOCs respectively, caused by cholestatic and choleretic bile acids, in H4-IIE rat liver cell line and primary cultured rat hepatocytes. It is demonstrated that inhibition of SOCs caused by cholestatic bile acids involves mitochondrial depolarisation; while activation of SOCs induced by choleretic bile acids, involves the release of Ca^{2+} from a region of the endoplasmic reticulum located in the vicinity of the plasma membrane.

3.2 Results

3.2.1. Effects of cholestatic bile acids on SOCs

To mimic the effects of the *in vivo* accumulation of bile acids during cholestasis, H4-IIE liver cells were pre-incubated for 12 h with either LCA or CA cholestatic bile acids. Subsequently, the changes in $[Ca^{2+}]_{cyt}$ induced by addition of the SERCA inhibitor DBHQ, was measured and compared in cholestatic bile acids treated and un-treated cells.

As shown in Fig 3.1 A (top panel), in H4-IIE cells incubated in the absence of Ca^{2+}_{ext}, the addition of the SERCA inhibitor DBHQ induced a transient increase in $[Ca^{2+}]_{cyt}$ (representing Ca^{2+} release from intracellular stores). Additionally, the addition of Ca^{2+}_{ext} back to the incubation medium caused a large increase in $[Ca^{2+}]_{cyt}$ (representing Ca^{2+} entry through SOCs activated by DBHQ (Rychkov *et al.*, 2001)). However, in H4-IIE cells pre-incubated for 12 h with the cholestatic bile acids LCA (middle panel) or CA (bottom panel); the magnitude of DBHQ-induced Ca^{2+} release from intracellular stores and Ca^{2+} entry was greatly reduced in comparison to control cells. The values of both the DBHQ-induced Ca^{2+} release and the DBHQ-induced Ca^{2+} entry through SOCs (calculated using the "Ca^{2+}-add back" protocol), are respectively illustrated in Fig. 3.1 B and C. These results suggest in H4-IIE liver cells cholestatic bile acids inhibit Ca^{2+} entry through SOCs and indicate that pre-incubation with LCA or CA leads to a depletion of Ca^{2+} from intracellular stores.

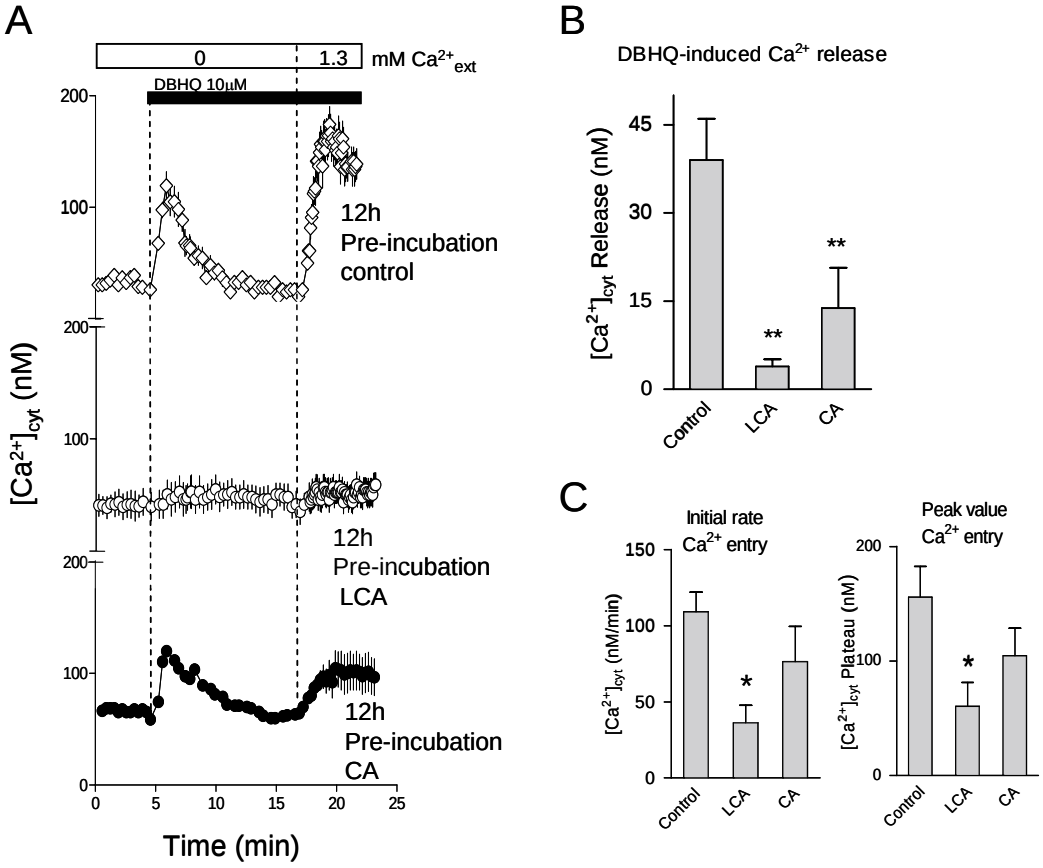

Fig. 3.1. Cholestatic bile acid LCA overnight pre-incubation, inhibit DBHQ-induced Ca^{2+} release from intracellular stores and Ca^{2+} entry through SOCs in H4-IIE liver cells. (**A**) The addition of the SERCA inhibitor DBHQ (10µM) to H4-IIE cells loaded with fura-2, in the absence of Ca^{2+}_{ext}, induces the release of Ca^{2+} from intracellular stores. When Ca^{2+} was added back to the bath a DBHQ-dependent increase in $[Ca^{2+}]_{cyt}$ was observed. Both, the DBHQ-induced Ca^{2+} release and Ca^{2+} entry, were diminished in cells pre-treated for 12 h with 50µM of cholestatic bile acids LCA or CA. $[Ca^{2+}]_{cyt}$ was measured as a function of time in H4-IIE cells loaded with fura-2, as described in Section 2.3. The additions to the bath are indicated by the horizontal bars. Each data point is the mean ± SEM of the values of $[Ca^{2+}]_{cyt}$ obtained for 10 - 20 cells. (**B**) Amounts of Ca^{2+} released (peak height) by DBHQ in the presence and absence of LCA or CA. (**C**) Initial rates of Ca^{2+} entry and peak (maximum) values of $[Ca^{2+}]_{cyt}$ following Ca^{2+}_{ext} addition, determined as described in Section 2.3.4. The values are the means ± SEM of 6 - 7 experiments similar to the one shown in panel **A**. In **B** and **C**, degrees of significance between LCA and the control and CA and the control, determined using ANOVA followed by Bonferroni *post hoc* test, are * $P<0.05$ and **, $P<0.01$.

In rat hepatocytes in primary culture, cholestatic bile acids also inhibited Ca^{2+} entry through SOCs when pre-incubated with the cells for 12 h. Cholestatic bile acids LCA and CA inhibited both the initial rate and peak maximum of Ca^{2+} entry through SOCs (Fig. 3.2 A and C). These decreases in the rate and peak maximum of Ca^{2+} entry were associated with a substantial reduction in the DBHQ-induced release of Ca^{2+} from intracellular stores (Fig. 3.2 A and B).

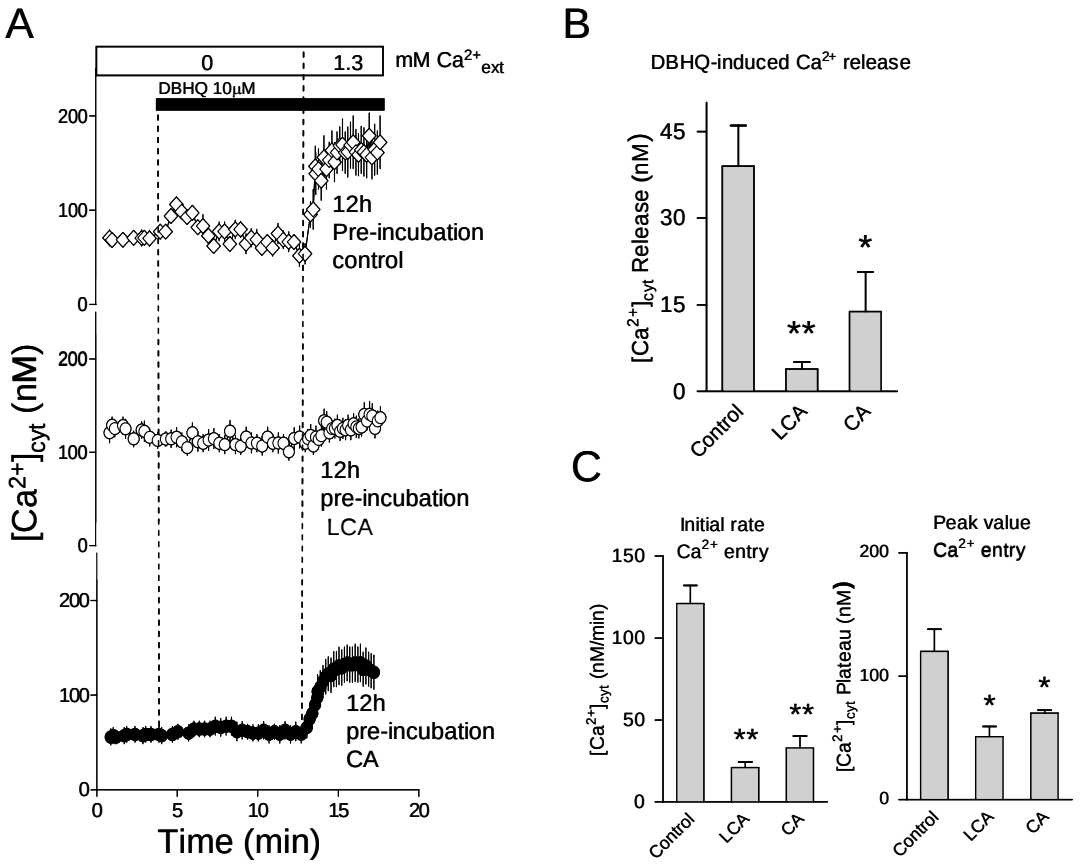

Fig. 3.2. Cholestatic bile acid LCA overnight pre-incubation, inhibit Ca^{2+} entry through SOCs activated by thapsigargin in rat hepatocytes. (**A**) The addition of the SERCA inhibitor DBHQ (10µM) to rat hepatocytes loaded with fura-2, in the absence of Ca^{2+}_{ext}, induces the release of Ca^{2+} from intracellular stores. When Ca^{2+} was added back to the bath a DBHQ-dependent increase in $[Ca^{2+}]_{cyt}$ was observed. Both, the DBHQ-induced Ca^{2+} release and Ca^{2+} entry, were diminished in cells pre-treated for 12 h with 50µM of cholestatic bile acids LCA or CA. $[Ca^{2+}]_{cyt}$ was measured as a function of time in rat hepatocytes loaded with fura-2, as described in Section 2.3. The additions to the bath are indicated by the horizontal bars. Each data point is the mean ± SEM of the values of $[Ca^{2+}]_{cyt}$ obtained for 10 - 20 cells. (**B**) Amounts of Ca^{2+} released (peak height) by DBHQ in the presence and absence of LCA or CA. (**C**) Initial rates of Ca^{2+} entry and peak (maximum) values of $[Ca^{2+}]_{cyt}$ following Ca^{2+}_{ext} addition, determined as described in Section 2.3.4. The values are the means ± SEM of 3 - 4 experiments similar to the one shown in panel **A**. In **B** and **C**, degrees of significance between LCA and the control and CA and the control, determined using ANOVA followed by Bonferroni *post hoc* test, are * $P<0.05$ and **, $P<0.01$.

3.2.2. Pre-incubation with cholestatic LCA bile acid induces mitochondrial membrane depolarisation in H4-IIE cells

It has been demonstrated that cholestatic bile acids can induce mitochondrial membrane depolarisation (Rolo *et al*., 2000; Huang *et al*., 2003; Criddle *et al*., 2004; Voronina *et al*., 2004). Additionally, it has been suggested that polarised mitochondria located below the plasma membrane play an important role in maintaining the sustained Ca^{2+} entry through SOCs (Gilabert and Parekh, 2000b; Hoth *et al.*, 2000; Gilabert *et al.*, 2001; Glitsch *et al.*, 2002a; Malli *et al.*, 2003; Montalvo *et al.*, 2006). Hence, the effect of LCA on mitochondrial membrane potential was evaluated in H4-IIE cells using TMRM.

TMRM is a cationic lipophilic dye, which distributes into the negatively charged mitochondria according to the Nerst equilibrium. The mitochondria membrane potential is normally -120mV. In order to make a semi-quantitative estimation of the mitochondrial membrane potential, the mitochondrial un-coupler FCCP was added (to induce mitochondrial depolarisation) to cells loaded with TMRM. The magnitude of the TMRM dye released by FCCP, is directly representative of the mitochondrial membrane potential of the cells analysed (Castro *et al*., 2004).

In cells pre-incubated for 12 h with LCA, the initial measured values of mitochondrial TMRM fluorescence was less than that in control cells (Fig. 3.3 A and B (LCA)). Additionally, FCCP induced a substantial decrease in mitochondrial TMRM fluorescence in control cells (Fig. 3.3 A, and B (control)). However, in LCA-treated cells, FCCP only induced a minor decrease in mitochondrial TMRM fluorescence (Fig. 3.3 A and B (LCA)). These results indicate that pre-treatment with LCA caused a substantial mitochondrial depolarisation.

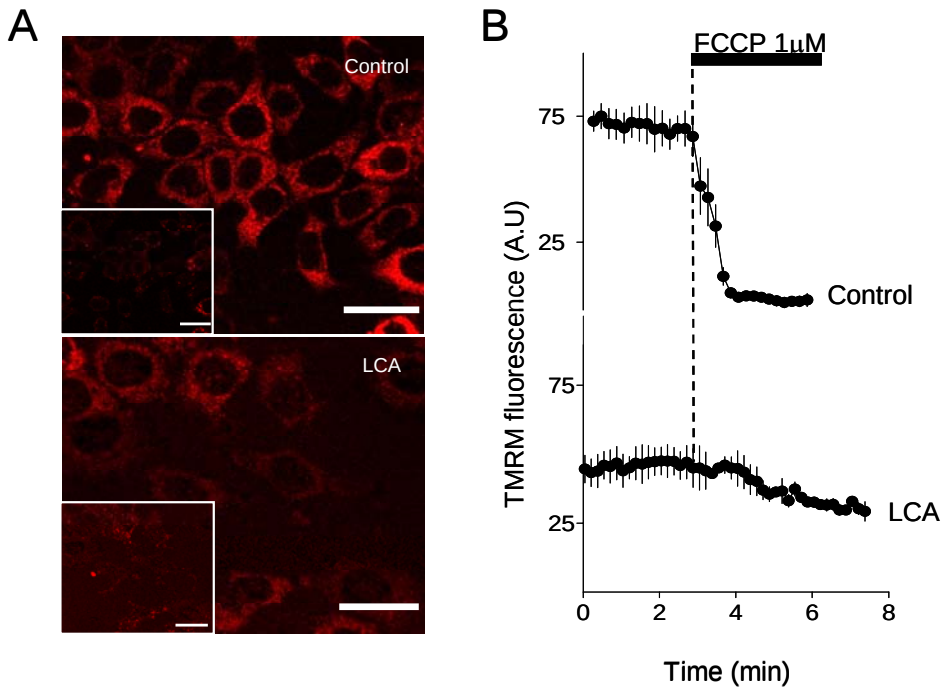

Fig. 3.3. Cholestatic bile acid LCA overnight pre-incubation, induce mitochondrial membrane depolarisation. (**A**) Representative images of H4-IIE cells showing mitochondrial TMRM fluorescence before the addition of FCCP (1µM) and at the end of the incubation with FCCP (inserts), in control cells and cells pre-incubated for 12 h with 50µM LCA. The scale bars represent 25µm. (**B**) Plots of TMRM fluorescence as a function of time in control cells and cells pre-incubated with LCA. Mitochondrial membrane potential was measured using TMRM as described in Section 2.4. The additions to the bath are indicated by the horizontal bars. The data are from a representative experiment in which the fluorescence of 10 - 20 cells was measured. The results shown are representative of those obtained in 4 similar experiments.

To test if mitochondrial depolarisation, induced by LCA, could be responsible for cholestatic bile acid-induced inhibition of Ca^{2+} entry through SOCs (observed in Fig. 3.1), the effect of the mitochondrial un-coupler FCCP on Ca^{2+} entry through SOCs was then investigated in H4-IIE liver cells loaded with fura-2.

As is illustrated in Fig 3.4 A, in control H4-IIE cells, the addition of the SERCA inhibitor thapsigargin (Tg) induced the release of Ca^{2+} from ER (in the absence of Ca^{2+}_{ext}) and activated Ca^{2+} entry through SOCs once Ca^{2+} is added back to the incubation medium. However, as shown in Fig. 3.4 B, addition of FCCP (in the presence of 1.3mM Ca^{2+}_{ext}) caused an increase in $[Ca^{2+}]_{cyt}$ and substantially reduced the thapsigargin-induced Ca^{2+} release from intracellular stores (in the absence Ca^{2+}_{ext}). Moreover, the presence of FCCP completely inhibited the thapsigargin-induced Ca^{2+} entry through SOCs, observed when Ca^{2+}_{ext} is added back to the incubation medium (Fig. 3.4 B cf Fig. 3.4 A). These results suggest that polarised mitochondria may be required to maintain the Ca^{2+} entry through SOCs in liver cells.

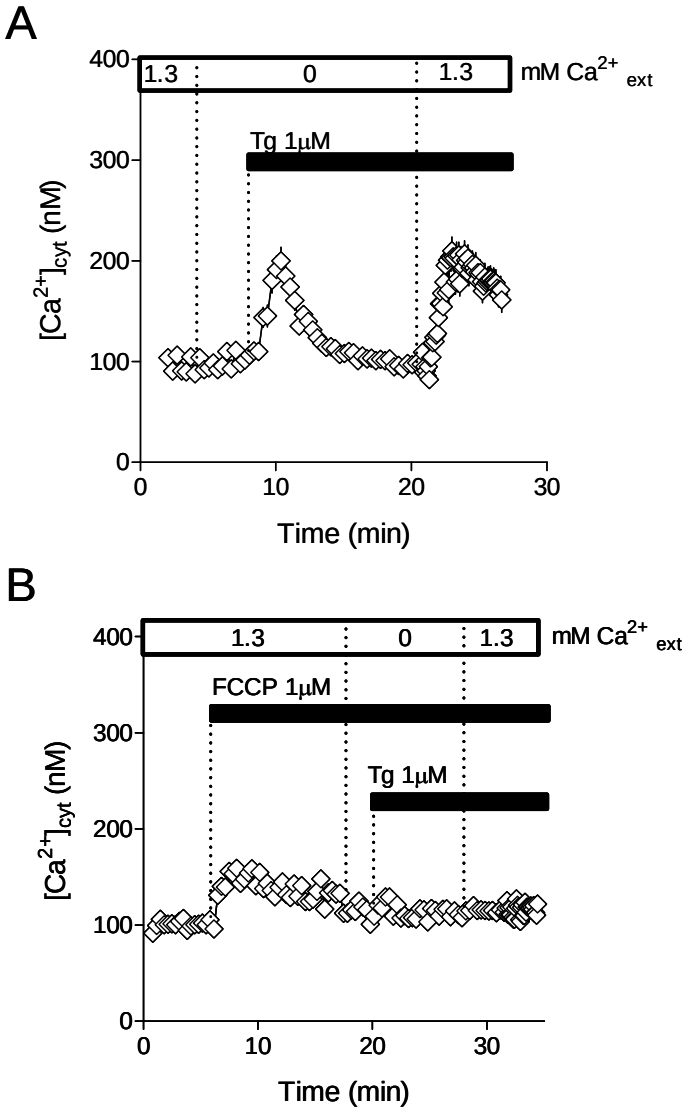

Fig. 3.4. In H4-IIE cells with depolarised mitochondria, thapsigargin failed in activates SOCs. (**A**) Fura-2 loaded H4-IIE cells were exposed to the SERCA inhibitor Tg (1μM) in the absence of Ca^{2+}_{ext}. When Ca^{2+} was added back to the bath the typical Tg-dependent increase in $[Ca^{2+}]_{cyt}$ originated by the Ca^{2+} entry through SOCs was observed. (**B**) The Tg-induced Ca^{2+} entry through SOCs, observed in **A**, was abolished in cells previously treated with the mitochondrial un-coupler FCCP (1μM). $[Ca^{2+}]_{cyt}$ was measured as a function of time in H4-IIE cells loaded with fura-2, as described in Section 2.3. The additions to the bath are indicated by the horizontal bars. The data in **A** and **B** are from a representative experiment in which the fluorescence of 10 - 20 cells was measured. The results shown are representative of those obtained in 4 similar experiments.

3.2.3. The choleretic bile acid TDCA rescues inhibition of SOCs and mitochondrial depolarisation caused by LCA pre-incubation

Choleretic bile acids, like TUDCA and UDCA, have been used at pharmacological doses to treat cholestasis (Bouchard *et al.*, 1993; Jacquemin *et al.*, 1993; Azer *et al.*, 1995; van de Meeberg *et al.*, 1996; Kinbara *et al.*, 1997; Poupon *et al.*, 1997; Beuers *et al.*, 1998; Ono *et al.*, 1998; Fabris *et al.*, 1999; Pares *et al.*, 2000; Lazaridis *et al.*, 2001). It has been shown in rat models of cholestasis, that treatment with choleretic bile acids can stimulate bile flow (Ishizaki *et al.*, 2001). In addition, there is evidence to suggest that choleretic bile acid (TUDCA) may enhance bile flow by activating Ca^{2+} entry and increasing hepatocyte $[Ca^{2+}]_{cyt}$ (Combettes *et al.*, 1988b; Beuers *et al.*, 1993a; Beuers *et al.*, 1993b; Bouscarel *et al.*, 1993).

Considering this evidence, the ability of choleretic bile acid TDCA to counteract the inhibition of Ca^{2+} entry through SOCs, caused by a 12 h pre-incubation with cholestatic bile acid LCA, was tested.

Fig. 3.5 A (right panel), shows the characteristic changes in $[Ca^{2+}{}_{cyt}]$ induced by thapsigargin (Ca^{2+} release from intracellular stores and Ca^{2+} entry through SOCs), measured in H4-IIE cells using the "Ca^{2+}-add back" assay. Pre-incubation for 12 h with the cholestatic bile acid LCA caused a substantial reduction in the thapsigargin-induced Ca^{2+} entry through SOCs (Fig. 3.5 A, middle panel and B). However, when TDCA was pre-incubated together with LCA, the thapsigargin-induced Ca^{2+} entry through SOCs was significantly recovered (Fig. 3.5 A, right panel and B). Nevertheless, the inhibition of thapsigargin-induced intracellular Ca^{2+} release, caused by LCA, could not be reverted by the pre-incubation with TDCA (Fig. 3.5 A). In addition to this, when the TDCA was added to cells already pre-incubated for 12 h with LCA, a substantial increase in $[Ca^{2+}]_{cyt}$ was observed (Fig. 3.5 C). All these

results suggest that choleretic bile acid TDCA can counteract the inhibition of Ca^{2+} entry through SOCs caused by pre-incubation with cholestatic bile acid LCA.

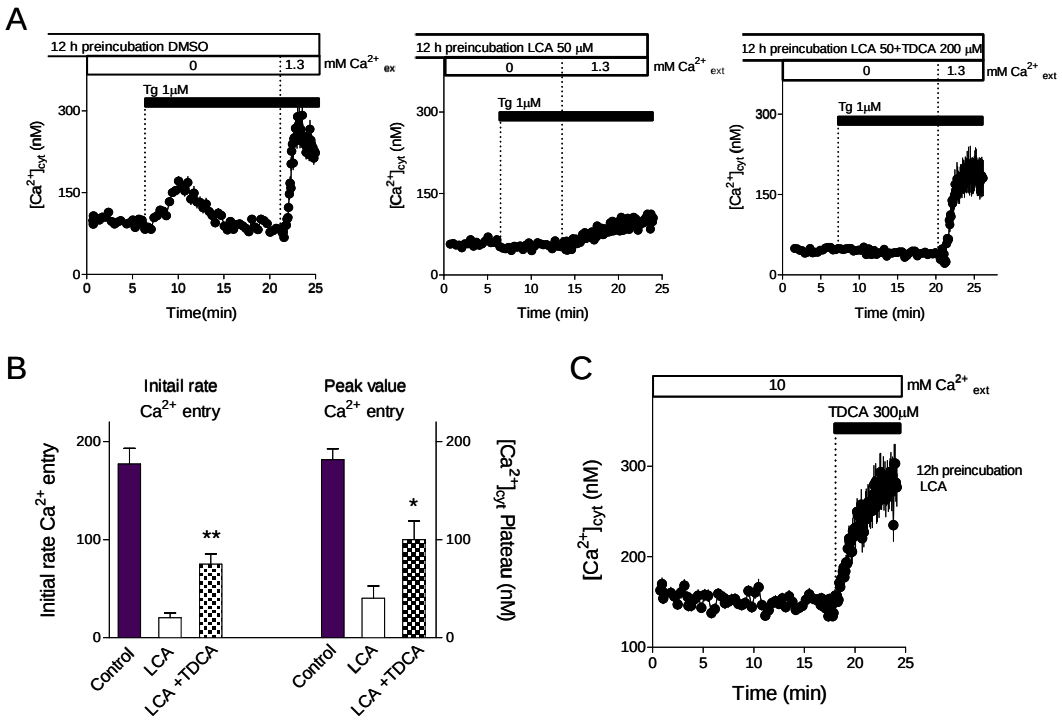

Fig. 3.5. Choleretic bile salt TDCA, counteract the inhibition of SOCs caused by 12 h pre-incubation with cholestatic bile salt LCA. (**A**) Fura-2 loaded H4-IIE cells were exposed to SERCA inhibitor thapsigargin (1µM) in the absence of Ca^{2+}_{ext}. When Ca^{2+}_{ext} was added back to the bath the typical increase in $[Ca^{2+}]_{cyt}$ was abolished in cells pre-incubated for 12 h with 50µM LCA but not in cells pre-incubated for 12 h with 50µM LCA plus 200µM TDCA. $[Ca^{2+}]_{cyt}$ was measured as a function of time in H4-IIE cells loaded with fura-2, as described in Section 2.3. The additions to the bath are indicated by the horizontal bars. Each data point is the mean $\pm$ SEM of the values of $[Ca^{2+}]_{cyt}$ obtained for 10 - 20 cells. (**B**) Initial rates of Ca^{2+} entry and peak (maximum) values of $[Ca^{2+}]_{cyt}$ following Ca^{2+}_{ext} re-addition, were determined as described in Section 2.3.4. The degrees of significance for comparison of the values obtained for LCA plus TDCA with those obtained for LCA alone determined using Student's t-test for unpaired samples are * $P < 0.05$ and ** $P < 0.01$. The values are the means $\pm$ SEM of 5 - 6 experiments similar to the one shown in panel **A**. (**C**) In the presence of 10mM Ca^{2+}_{ext}, the addition of TDCA (300µM) induces an increase in $[Ca^{2+}]_{cyt}$ in cells pre-incubated for 12 h with the cholestatic bile acid LCA. The result in **C** is from a representative experiment, of those obtained in 3 similar experiments, in which the fluorescence of 18 cells was measured.

Since the above results suggest that inhibition of SOCs, induced by 12 h pre-incubation with LCA is due, in part, to a reduction of the mitochondrial membrane potential; the ability of choleretic bile acid TDCA to counteract the effect of LCA-induced mitochondrial depolarisation, was evaluated in H4-IIE cells using TMRM.

As shown in Fig. 3.6, the initial measured values of TMRM fluorescence in cells pre-incubated for 12 h with both LCA plus TDCA was greater than that of cells treated with LCA alone (Fig. 3.6 A and B). In addition, in cells treated with LCA plus TDCA, FCCP caused a substantial decrease in the initial measured values of TMRM fluorescence compared with the FCCP-induced decrease in TMRM fluorescence of cells pre-incubated with LCA alone (Fig. 3.6). These results indicate that choleretic bile acid TDCA is able to prevent mitochondrial membrane depolarisation induced by cholestatic bile acid LCA.

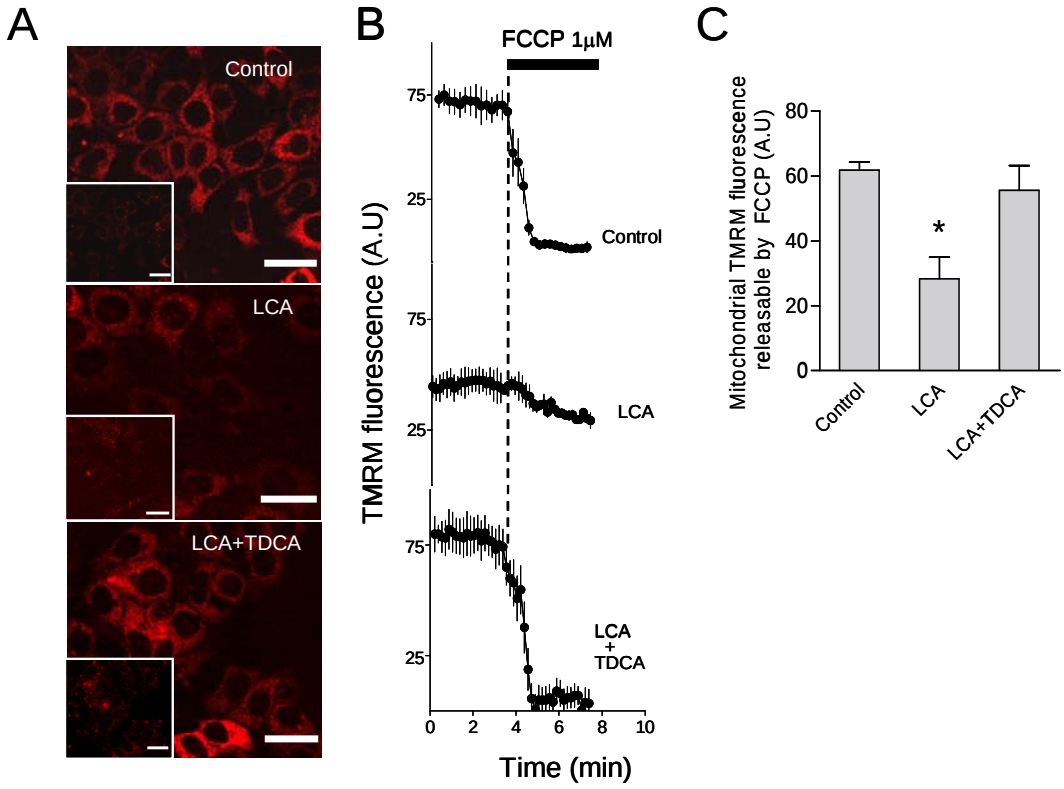

Fig. 3.6. Pre-treatment with choleretic bile salt TDCA, is associated with the recovery of mitochondrial depolarisation caused by 12 h pre-incubation with cholestatic bile salt LCA. (**A**) Representative images of H4-IIE cells showing mitochondrial TMRM fluorescence before and after (inserts) the addition of FCCP (1µM) for control cells, cells pre-incubated for 12 h with 50µM LCA, and for cells incubated for 12 h with 50µM LCA plus 200µM TDC. The scale bars represent 25µm. (**B**) Plots of TMRM fluorescence as a function of time for control cells and cells pre-incubated with LCA or LCA plus TDCA. The data are from a representative experiment in which the fluorescence of 10 - 20 cells was measured. (**C**) The decrease in TMRM fluorescence induced by addition of FCCP, between control and LCA plus TDCA treated cells is similar and approximately the double amount of the one in cells treated with LCA. The data are the means $\pm$ SEM of 5 - 6 experiments similar to those shown in (**B**). The degrees of significance between control and LCA or between LCA and LCA plus TDCA, determined using ANOVA followed by Bonferroni *post hoc* test, are ** $P < 0.01$. Mitochondrial membrane potential was measured using TMRM as described in Section 2.4. The additions to the bath are indicated by the horizontal bars.

3.2.4. Choleretic bile acid TDCA activates Ca^{2+} entry through SOCs in H4-IIE liver cells and rat hepatocytes

Considering the evidence presented that, choleretic bile acid TDCA can rescue the cholestatic bile acid-induced inhibition of Ca^{2+} entry through SOCs; the possible effect of choleretic bile acids on the activation of SOCs in H4-IIE liver cells, was investigated.

As shown in Fig. 3.7 A, when TDCA was added to H4-IIE cells in the presence of 1.3mM Ca^{2+}_{ext} there was no increase in $[Ca^{2+}]_{cyt}$, but when Ca^{2+}_{ext} was increased to 10mM, a substantial increase in $[Ca^{2+}]_{cyt}$ was observed. When $[Ca^{2+}]_{ext}$ was reduced from 10mM to zero, the increases in $[Ca^{2+}]_{cyt}$ induced by TDCA decreased to the basal level. The ability of TDCA to increase $[Ca^{2+}]_{cyt}$, at 10mM Ca^{2+}_{ext}, was retained when TDCA was washed out and then re-introduced to the incubation medium in the presence of 10mM Ca^{2+}_{ext}. As illustrated in Fig. 3.7 A insert, increases in the extracellular Ca^{2+} concentration from 1.3 to 10mM are not responsible for changes in $[Ca^{2+}]_{cyt}$.

In addition, as is shown in Fig. 3.7 B, the choleretic bile acid TDCA was able to induce increases in $[Ca^{2+}]_{cyt}$ at 2.4mM Ca^{2+}_{ext}.

Based on the above results and considering that in the patch clamp experiments (directed to investigate the effects of bile acids on SOCs activation) conducted in parallel by our collaborators Edoardo C. Aromataris and Grigori Y. Rychkov (Aromataris *et al.*, 2008), where performed in 10mM Ca^{2+}_{ext}; future experiments of the effect of TDCA on inducing Ca^{2+} entry, were performed with 10mM of Ca^{2+}_{ext}.

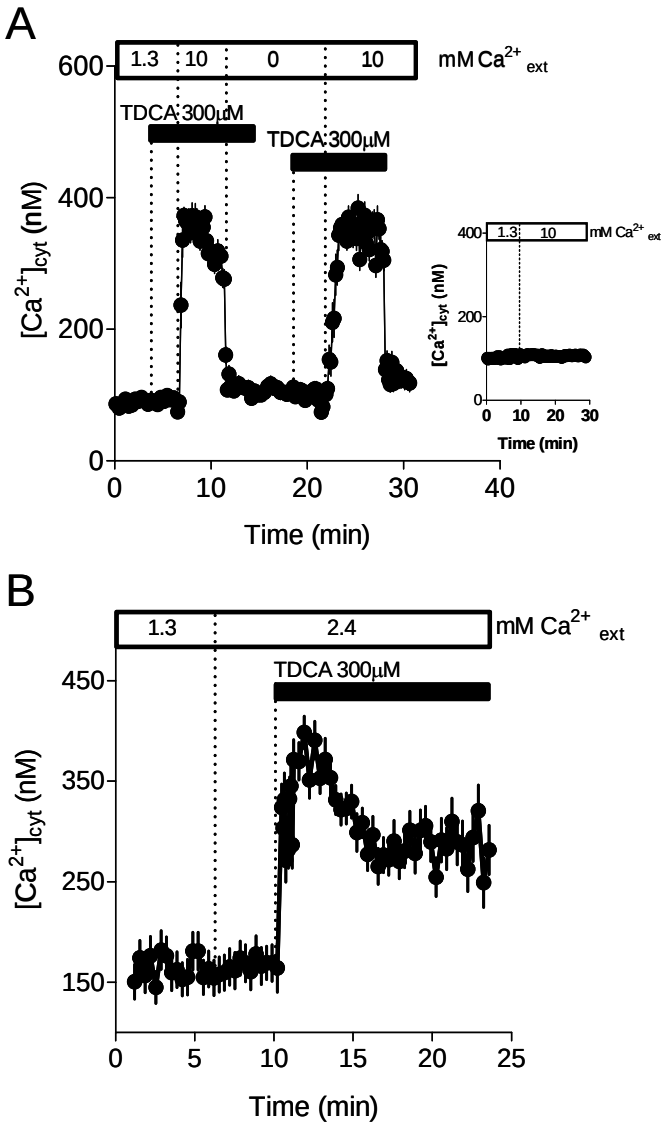

Fig. 3.7. Choleretic bile salt TDCA induces a reversible Ca^{2+} entry in H4-IIE liver cells. (**A**) TDCA induces an increase in $[Ca^{2+}]_{cyt}$ in the presence of 10mM Ca^{2+}_{ext}. The TDCA-induced increase in $[Ca^{2+}]_{cyt}$ is abolished when $[Ca^{2+}]_{ext}$ is reduced to zero in the presence of TDCA. A second addition of TDCA increases $[Ca^{2+}]_{cyt}$ in the presence of 10mM $[Ca^{2+}]_{ext}$. This increase in $[Ca^{2+}]_{cyt}$ is abolished when TDCA is removed from the extracellular medium (in the presence of 10mM Ca^{2+}_{ext}). The insert shows that the change in $[Ca^{2+}]_{ext}$ does not induce any change in $[Ca^{2+}]_{cyt}$ *per se* (**B**) TDCA induces an increase in $[Ca^{2+}]_{cyt}$ in the presence of 2.4mM Ca^{2+}_{ext}. The measurement of $[Ca^{2+}]_{cyt}$ as a function of time in cells loaded with fura-2 was conducted as described in Section 2.3. The additions to the bath are indicated by the horizontal bars. The results shown in **A** and **B** are from a representative experiment, of those obtained in 3 similar experiments, in which the fluorescence of 10-20 cells was measured.

To investigate whether the TDCA-induced increase in $[Ca^{2+}]_{cyt}$ observed at 10mM Ca^{2+}_{ext} takes place through the SOCs, gadolinium (an inhibitor of SOCs (Broad *et al.*, 1999)), was added after TDCA-induced increase in $[Ca^{2+}]_{cyt}$ had reached maximum levels.

As shown in Fig. 3.8, the TDCA-induced increase in $[Ca^{2+}]_{cyt}$ was substantially reduced to near basal values by addition of 10μM gadolinium (Gd^{3+}). Since concentrations of Gd^{3+} within this range have been shown to inhibit Ca^{2+}-entry through SOCs in a hepatocyte cell line (Auld *et al.*, 2000; Rychkov *et al.*, 2001; Rychkov *et al.*, 2005), this result provides some evidence that the Ca^{2+} entry pathway activated by TDCA is the hepatocyte SOC channel.

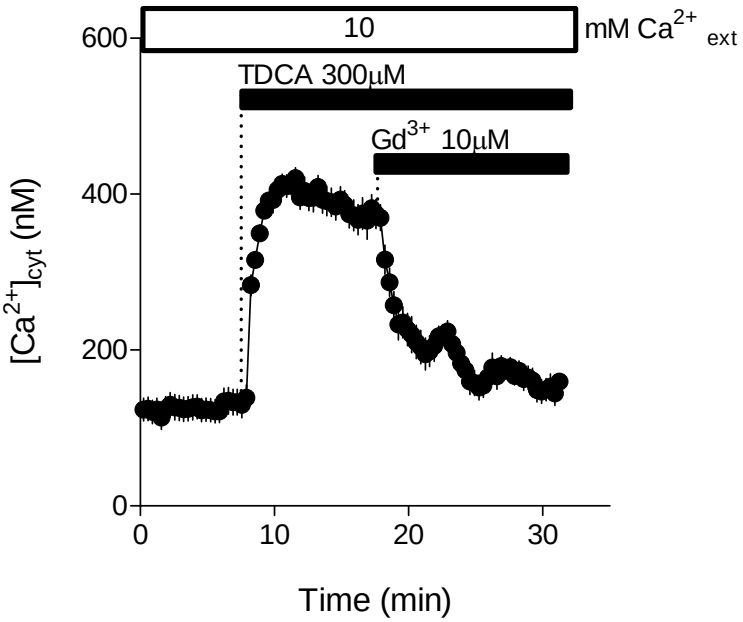

Fig. 3.8. Choleretic bile salt TDCA induces Ca^{2+} entry through SOCs in H4-IIE liver cells. The increase in $[Ca^{2+}]_{cyt}$ induced by TDCA, in 10mM Ca^{2+}_{ext}, is inhibited by 10 µM Gd^{3+}. The measurement of $[Ca^{2+}]_{cyt}$ as a function of time in cells loaded with fura-2 was conducted as described in Section 2.3. The additions to the bath are indicated by the horizontal bars. The result shown is representative (averaged for 19 cells on a coverslip) of those obtained for one of 3 experiments which each gave similar results.

To test if TDCA addition was activating only SOCs or other plasma membrane Ca^{2+} permeable channels, the Ca^{2+} entry induced by TDCA alone or in combination with thapsigargin (activator of SOCs), was investigated.

In cells incubated in the presence of 10mM Ca^{2+}_{ext}, addition of TDCA following thapsigargin did not cause a further increase in $[Ca^{2+}]_{cyt}$ (Fig. 3.9 A). In addition, the magnitude of the $[Ca^{2+}]_{cyt}$ reached following TDCA addition was not significantly different to that following thapsigargin addition (Fig. 3.9 B *cf* Fig. 3.9 A and Fig. 3.9 C). These results provide further evidence that TDCA activates the same Ca^{2+} entry pathway as that activated by SERCA inhibitor thapsigargin.

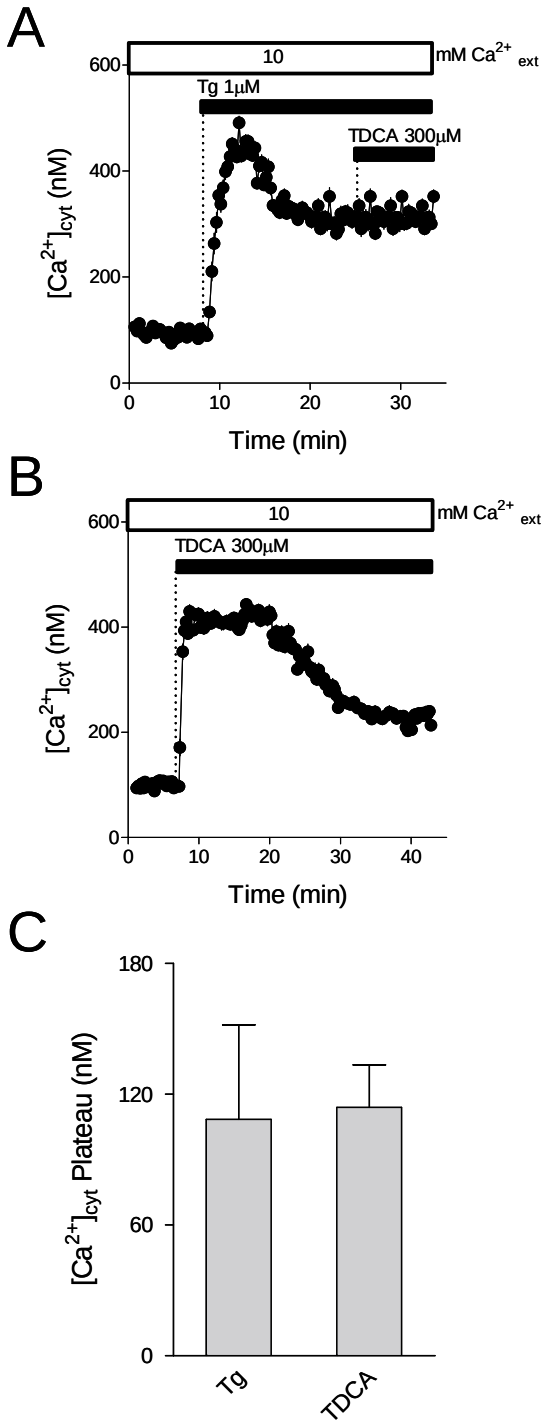

Fig. 3.9. Choleretic bile salt TDCA-induced Ca^{2+} entry is no additive to thapsigargin-induced Ca^{2+} entry in H4-IIE liver cells. (**A**) Effect of addition of TDCA following thapsigargin. (**B**) Effect of addition of TDCA. (**C**) The magnitude of the plateaus following TDCA or thapsigargin additions. $[Ca^{2+}]_{cyt}$ was measured, in 10mM Ca^{2+}_{ext}, as a function of time in H4-IIE cells loaded with fura-2, as described in Section 2.3. The additions to the bath are indicated by the horizontal bars. The results shown in **A** and **B** are representatives of those obtained for one of 3 experiments which each gave similar results. The values in **C** are the means ± SEM of 3 experiments ($P > 0.05$).

The effect of choleretic bile acid TDCA on Ca^{2+} entry through SOCs in primary cultured rat hepatocytes in primary culture was also investigated.

When added directly to the hepatocyte incubation medium, choleretic bile acid TDCA increased $[Ca^{2+}]_{cyt}$ in the presence of 10mM Ca^{2+}_{ext}, which was reverted to the basal levels when $[Ca^{2+}]_{ext}$ was reduced from 10mM to zero (Fig. 3.10 A). This increase was inhibited by 10μM Gd^{3+} (Fig. 3.10 B), similar to the results obtained with H4-IIE liver cell line.

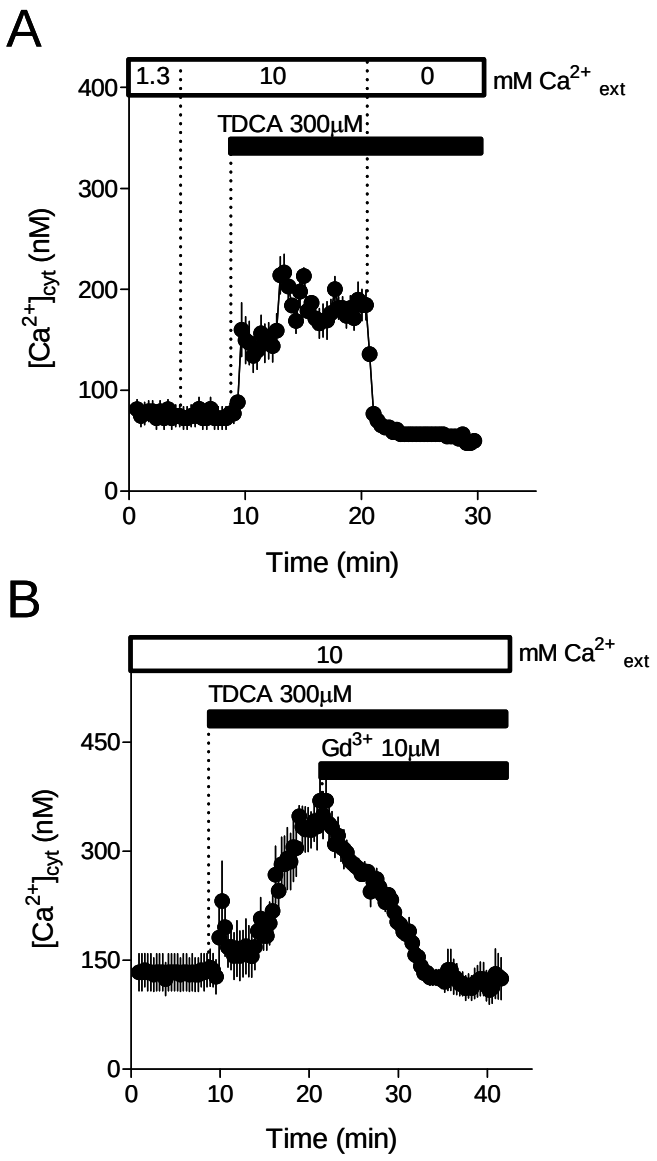

Fig. 3.10. Choleretic bile salt TDCA induces Ca^{2+} entry through SOCs in rat hepatocytes. (**A**) TDCA induces an increase in $[Ca^{2+}]_{cyt}$ in the presence of 10mM Ca^{2+}_{ext}, which is abolished when $[Ca^{2+}]_{ext}$ is reduced to zero in the presence of TDCA. (**B**) The increase in $[Ca^{2+}]_{cyt}$ induced by TDCA, in 10mM Ca^{2+}_{ext}, is inhibited by 10 µM Gd^{3+}. The measurement of $[Ca^{2+}]_{cyt}$ as a function of time in rat hepatocytes loaded with fura-2 was conducted as described in Section 2.3. The additions to the bath are indicated by the horizontal bars. The results shown in **A** and **B** are from a representative experiment, of those obtained in 3 similar experiments, in which the fluorescence of 10-20 rat hepatocytes was measured.

3.2.5. Choleretic bile acid TDCA induces the release of Ca^{2+} from intracellular stores in fura-2 loaded H4-IIE liver cells and rat hepatocytes

It has been demonstrated that the release of Ca^{2+} from intracellular stores is a pre-requisite for the activation of SOCs (Putney, 1986). To test whether the activation of Ca^{2+} entry through SOCs by choleretic bile acids is associated with the release of Ca^{2+} from intracellular stores, the effect of TDCA in $[Ca^{2+}]_{cyt}$ was evaluated in the presence of 10μM Gd^{3+} to inhibit the Ca^{2+} entry (through the SOCs) component of the TDCA response.

As illustrated in Fig 3.11, in the presence of 2.4mM Ca^{2+}_{ext} and 10μM Gd^{3+}, the addition of TDCA caused a transient increase in $[Ca^{2+}]_{cyt}$, indicative of the release of Ca^{2+} from intracellular stores. Compare this response with the sustained increases in $[Ca^{2+}]_{cyt}$ induced by TDCA in the presence of 2.4mM Ca^{2+}_{ext} and in the absence of Gd^{3+} observed in Fig 3.7 B.

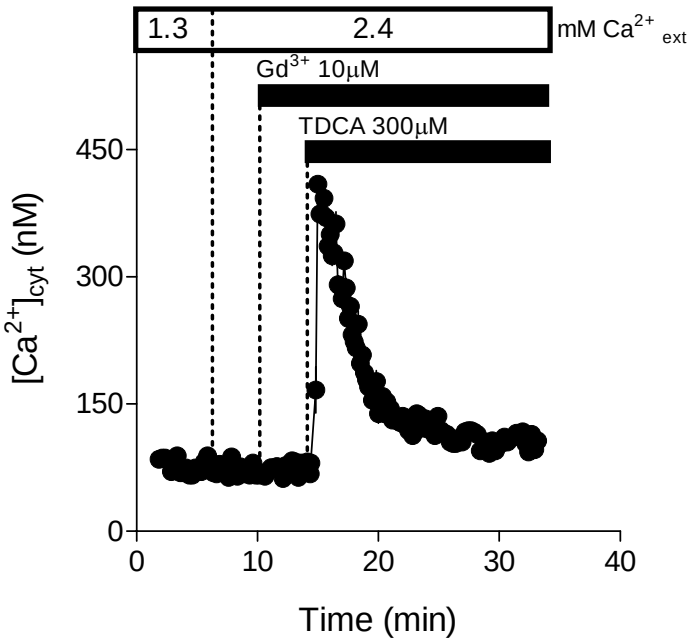

Fig. 3.11. TDCA-induced Ca^{2+} release is detected by fura-2, in the presence of 2.4mM Ca^{2+}_{ext} and 10μM Gd^{3+}. (A) In the presence of 2.4mM Ca^{2+}_{ext} and 10μM Gd^{3+} (to inhibit TDCA-induced Ca^{2+} entry through SOCs), TDCA (300μM) induces a transient increase in $[Ca^{2+}]_{cyt}$. $[Ca^{2+}]_{cyt}$ was measured as a function of time in cells loaded with fura-2, as described in Section 2.3. The additions to the bath are indicated by the horizontal bars. The result shown is from a representative experiment, of those obtained in 3 similar experiments, in which the fluorescence of 10-20 H4-IIE cells was measured.

An alternative approach to evaluate the TDCA-induced Ca^{2+} release from intracellular stores was performed, in which the changes in $[Ca^{2+}]_{cyt}$ induced by addition of TDCA, were measured with fura-2 in an incubation medium with zero mM Ca^{2+}. The zero mM Ca^{2+} incubation medium composition is described in Section 2.3.2.

Under these conditions the addition of TDCA, failed to induce a fura-2 detectable increase in $[Ca^{2+}]_{cyt}$ and subsequently, the addition of DBHQ induces a transient increase in $[Ca^{2+}]_{cyt}$ (Fig. 3.12 A). No significant differences, in the DBHQ-induced increases in $[Ca^{2+}]_{cyt}$, were observed in the absence or presence of TDCA in the incubation medium (Fig. 3.12 A, insert). Similar results were observed in rat hepatocytes in primary culture (Fig. 3.12 B).

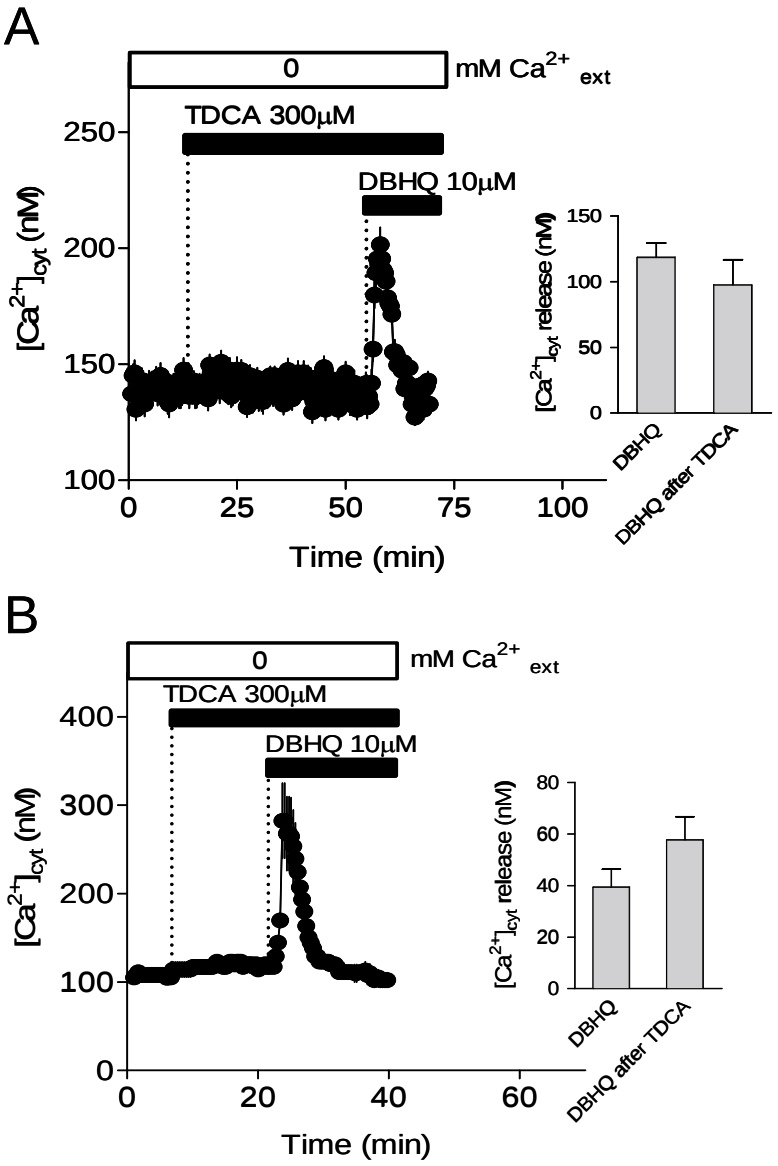

Fig. 3.12. TDCA does not induce any apparent Ca^{2+} release detected by fura-2, in the absence of Ca^{2+}_{ext}, in H4-IIE liver cells and rat hepatocytes. In the absence of Ca^{2+}_{ext}, TDCA does not induce any change in $[Ca^{2+}]_{cyt}$ and the subsequent addition of 10µM DBHQ releases intracellular Ca^{2+} either in H4-IIE liver cells (**A**) and rat hepatocytes (**B**). The inserts in **A** and **B** shown the amount of Ca^{2+} released (peak height) by DBHQ in the presence and absence of TDCA. Comparison by Student's t-test showed no significant difference ($P > 0.05$). $[Ca^{2+}]_{cyt}$ was measured as a function of time in cells loaded with fura-2, as described in Section 2.3. The additions to the bath are indicated by the horizontal bars. The results shown are from a representative experiment, of those obtained in 3 similar experiments, in which the fluorescence of 10-20 H4-IIE (**A**) cells or 9-15 rat hepatocytes (**B**) was measured.

In order to understand the lack of fura-2 detection of the TDCA-induced Ca^{2+} release from intracellular stores, observed in the absence Ca^{2+}_{ext}, the following group of experiments were performed.

It could be possible that in the absence of Ca^{2+}_{ext}, TDCA released just an small amount of Ca^{2+} from the stores, but this release can not be detected by cytoplasmic fura-2, due to a rapid clearance out of the cytoplasmic space mediated by the plasma membrane Ca^{2+} ATP-ase (PMCA) pumps. To test this theory, the activity of the PMCA pump was inhibited and the effect of TDCA on $[Ca^{2+}]_{cyt}$ was evaluated with fura-2. It has been reported that high concentrations of Gd^{3+} (1mM) efficiently block PMCA pumps (Bird and Putney, 2005).

As is shown in Fig 3.13 A, in zero Ca^{2+}_{ext}, when thapsigargin was added in the presence of 1mM Gd^{3+}, a large and sustained increase in $[Ca^{2+}]_{cyt}$ was observed. The lack of recovery of $[Ca^{2+}]_{cyt}$ to basal levels in cells pre-treated with 1mM Gd^{3+}, as compared with Gd^{3+}- untreated cells (Fig. 3.13 B), demonstrated a diminished capacity of cellular Ca^{2+} clearance through PMCA pumps.

Using this strategy to inhibit the PMCA pumps, the effect of TDCA (in zero Ca^{2+}_{ext}), in the presence of 1mM Gd^{3+}, was then tested. As shown in Fig. 3.13 C, TDCA is capable of inducing an increase in $[Ca^{2+}]_{cyt}$, in the absence of Ca^{2+}_{ext}, when added in the presence of 1mM Gd^{3+}. This result suggests that, in the absence of Ca^{2+}_{ext}, TDCA could be releasing Ca^{2+} from intracellular stores, as detected by fura-2 in cells with PMCA pumps inhibited.

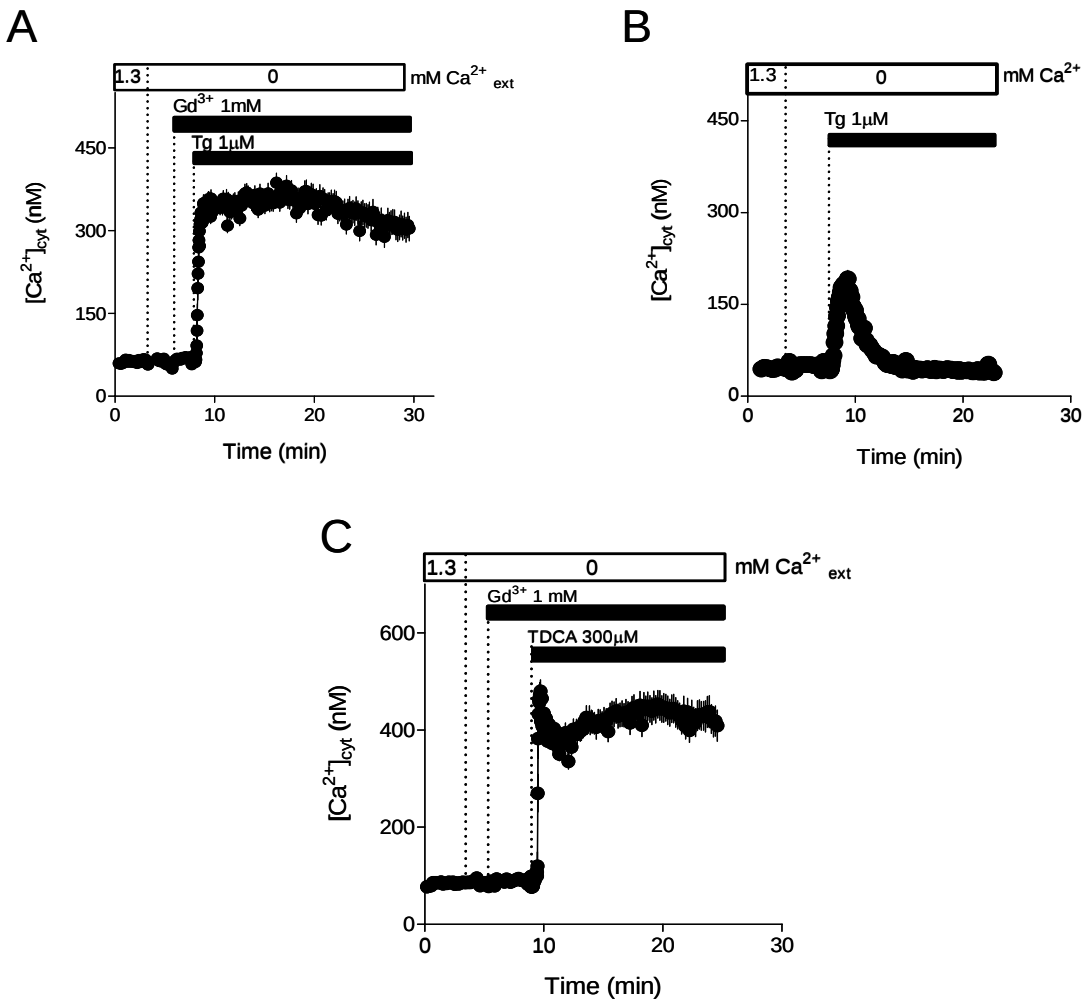

Fig. 3.13. TDCA-induced Ca^{2+} release in the absence of Ca^{2+}_{ext}, is detected by fura-2 in H4-IIE cells with PMCA pumps inhibited by Gd^{3+} 1mM. (A) In the absence of Ca^{2+}_{ext} and the presence of 1mM Gd^{3+} (to inhibit Ca^{2+} extrusion by PMCA pumps), Tg (1 µM) induces a sustained and maintained increase in $[Ca^{2+}]_{cyt}$. **(B)** In the absence of Ca^{2+}_{ext} and any added Gd^{3+}, Tg (1 µM) induces a transient increase in $[Ca^{2+}]_{cyt}$. (**C**) In the absence of Ca^{2+}_{ext} and the presence of 1mM Gd^{3+}, TDCA (300µM) induces a sustained increase in $[Ca^{2+}]_{cyt}$ in H4-IIE cells. $[Ca^{2+}]_{cyt}$ was measured as a function of time in cells loaded with fura-2, as described in Section 2.3. The additions to the bath are indicated by the horizontal bars. The results shown in **A**, **B and C** are from a representative experiment, of those obtained in 3 similar experiments, in which the fluorescence of 10-20 H4-IIE cells was measured.

3.2.6. Effect of TDCA on inducing Ca^{2+} release, in the absence of Ca^{2+}_{ext}, when measured with FFP-18

It is possible that the TDCA-induced Ca^{2+} release could escape fura-2 detection, if it is originated from an intracellular store region in the vicinity of the plasma membrane. If this was the case, the TDCA-induced Ca^{2+} release could be rapidly pumped out of the cells by the action of the PMCA pumps, escaping fura-2 detection. To test this hypothesis, the TDCA effects on the levels of Ca^{2+} beneath the plasma membrane ($(Ca^{2+})_{SPM}$) were measured using the Ca^{2+} dye FFP-18. FFP-18 has been successfully used to monitor changes in $(Ca^{2+})_{SPM}$ (Etter *et al.*, 1994; Etter *et al.*, 1996; Davies and Hallett, 1998; Graier *et al.*, 1998; Chadborn *et al.*, 2002).

As shown in Fig. 3.14 A, in the absence of Ca^{2+}_{ext}, the addition of TDCA does not induce any fura-2 detectable changes in $[Ca^{2+}]_{cyt}$ in H4-IIE cells. However, in the absence of Ca^{2+}_{ext}, TDCA caused a transient increase in FFP-18 fluorescence (Fig. 3.14 B). This TDCA-induced increase in FFP-18 fluorescence represents an increase in the $(Ca^{2+})_{SPM}$ levels originated by the release of Ca^{2+} from intracellular stores in the vicinity of the plasma membrane.

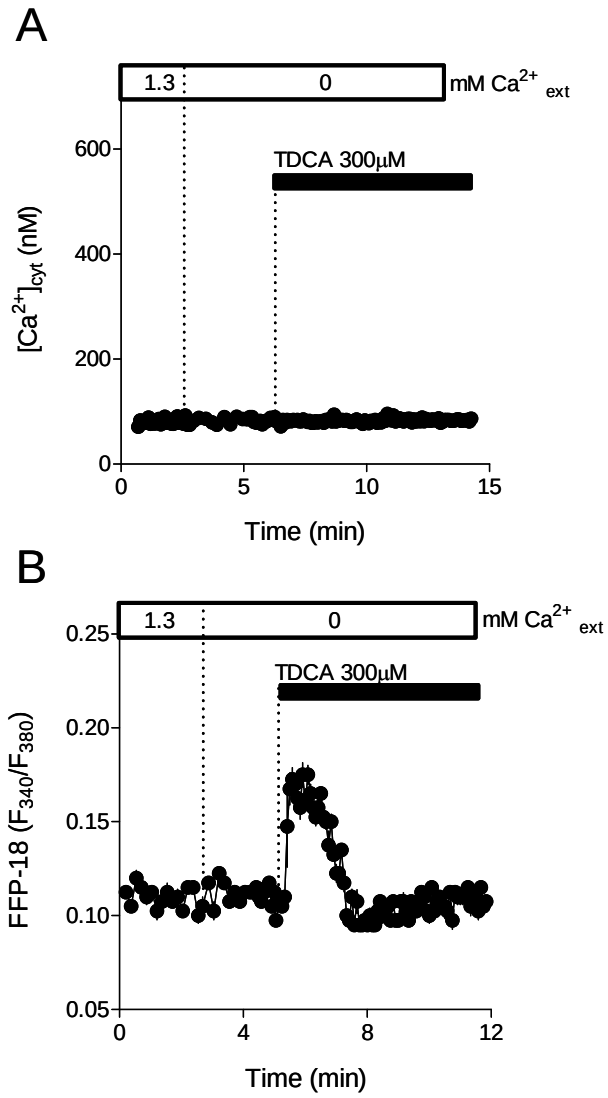

Fig. 3.14. TDCA-induced Ca^{2+} release from intracellular stores, in the absences of Ca^{2+}_{ext}, is detected by FFP-18. (A) In the absence of Ca^{2+}_{ext}, TDCA (300µM) failed to induce any change in $[Ca^{2+}]_{cyt}$ when measured using fura-2. (**B**) In the absence of Ca^{2+}_{ext}, TDCA (300µM) induces a transient increase in FFP-18 fluorescence. $[Ca^{2+}]_{cyt}$ and $[Ca^{2+}]_{SPM}$ were measured as a function of time in cells loaded with fura-2 and FFP-18 respectively, as described in Section 2.3. The additions to the bath are indicated by the horizontal bars. The results shown in **A** and **B** are from a representative experiment, of those obtained in 3 similar experiments, in which the fluorescence of 10-20 H4-IIE cells was measured.

3.3 Discussion

In this chapter evidence has been provided that 12 h pre-incubation with cholestatic bile acids cause the inhibition of the SERCA inhibitor (DBHQ)-induced Ca^{2+} release from intracellular stores (ER), and Ca^{2+} entry through SOCs in H4-IIE liver cells and rat hepatocytes. In addition, cholestatic bile acid 12 h pre-incubation induced mitochondrial depolarisation. However, the inhibition of Ca^{2+} entry through SOCs and the mitochondrial depolarisation, observed in H4-IIE cells pre-incubated with cholestatic bile acids, were counteracted by incubation with choleretic bile acid TDCA. In contrast to cholestatic bile acids effects, when the choleretic bile acid TDCA was added to H4-IIE cells (in the presence of Ca^{2+}_{ext}), an increase in $[Ca^{2+}]_{cyt}$ caused by Ca^{2+} entry through SOCs, was observed. The choleretic bile acid-induced SOCs activation involves the release of Ca^{2+} from a particular region of the intracellular stores (presumably ER), located in the vicinity of the plasma membrane.

3.3.1. Cholestatic bile acids inhibition of SOCs, is associated with inhibition of DBHQ-induced Ca^{2+} release from ER and mitochondrial depolarisation

The results of the "Ca^{2+}-add back" experiments performed in H4-IIE cells using fura-2 demonstrated that, 12 h pre-incubation with cholestatic bile acids caused the inhibition of both the initial rate and the magnitude of Ca^{2+} entry through SOCs. These results are complemented by a group of experiments undertaken by our collaborators Edoardo C. Aromataris and Grigori Y. Rychkov (Aromataris *et al.*, 2008), using whole cell patch clamp recording on H4-IIE cells. In those experiments, it was demonstrated that 12 h pre-incubation of different cholestatic bile acids caused the inhibition of I_{SOC} currents, elicited by the addition of IP_3 in the patch pipette.

It was observed that the cholestatic bile acids-induced inhibition of Ca^{2+} entry through SOCs was associated with the inhibition of Ca^{2+} release from intracellular stores. This result suggests that either the intracellular Ca^{2+} stores were depleted of Ca^{2+} before DBHQ addition, or that the interaction of cholestatic bile acids with the ER leads to disruption of the action of DBHQ on their target (SERCA pumps). While the amount of Ca^{2+} in intracellular stores was not directly measured in this study, it is considered that the most likely explanation is that pre-incubation with cholestatic bile acids, induces Ca^{2+} release from intracellular stores. This is consistent with previous findings that cholestatic bile acids inhibit SERCA pumps leading to Ca^{2+} depletion of the ER (Kim *et al.*, 2002; Lau *et al.*, 2005).

It might be expected that, if pre-incubation with cholestatic bile acids leads to depletion of the ER Ca^{2+} stores, SOCs would be constitutively activated (i.e. active in the absence SERCA inhibitor DBHQ). Hence, it is perhaps surprising that the release of Ca^{2+} from intracellular stores induced by pre-incubation with cholestatic bile acids is associated with inhibition of Ca^{2+} entry through SOCs. One possible explanation for this inhibition is that if bile acids could cause modifications of the ER structure (Payne *et al.*, 2005), an impairment of the coupling between the ER and the plasma membrane would occur. This interaction is required for SOC activation (Baba *et al.*, 2006; Peinelt *et al.*, 2006; Lewis, 2007). Another possibility is that bile acids inhibit a step in the pathway of activation of SOCs, downstream from the release of Ca^{2+} from the ER. Additionally, it is possible that inhibition of SOCs by cholestatic bile salts could be mediated by protein kinase C. It has been described that bile acids could directly or indirectly activate protein kinase C (Craven *et al.*, 1987; Huang *et al.*, 1992; Milovic *et al.*, 2002; Lau *et al.*, 2005) and in addition there are evidence suggesting that the activation of protein kinase C can inhibit Ca^{2+}

release-activated Ca^{2+} channels (Tornquist, 1993; Montero *et al.*, 1994; Parekh and Putney, 2005).

Furthermore, using TMRM as a tool to estimate the mitochondrial potential of H4-IIE cells it was demonstrated that, 12 h pre-incubation with cholestatic bile acid LCA caused mitochondrial depolarisation. This may represent an additional factor responsible for the inhibition of DBHQ-induced Ca^{2+} entry through SOCs. Consistent with this possibility is the observation that DBHQ when added to H4-IIE cells treated with FCCP (to induce mitochondrial depolarisation) failed to activate Ca^{2+} entry through SOCs. It has been proposed that polarised mitochondria located below the plasma membrane can buffer the Ca^{2+} entry through SOCs. This would bypass SOCs inhibition caused by Ca^{2+} accumulation at the channel mouth, resulting in a sustained Ca^{2+} entry through SOCs (Gilabert and Parekh, 2000b; Hoth *et al.*, 2000; Gilabert *et al.*, 2001; Glitsch *et al.*, 2002a; Malli *et al.*, 2003; Montalvo *et al.*, 2006). However, in the experiments undertaken in parallel by our collaborators Edoardo C. Aromataris and Grigori Y. Rychkov (Aromataris *et al.*, 2008); where the inhibition of SOCs by cholestatic bile acids was evaluated using patch clamp, depolarisation of mitochondria would not account for the inhibition of Ca^{2+} entry through SOCs. In those experiments, 10mM EGTA was introduced via the patch pipette in the cytoplasm of the cells, which would prevent any increase in Ca^{2+} concentration at the cytoplasmic mouth of the SOCs. However, even under those experimental conditions, IP_3 addition failed to activate SOCs.

3.3.2. Choleretic bile acid activation of Ca^{2+} entry through SOCs, is associated with the release of Ca^{2+} from a region of the intracellular stores located in the vicinity of the plasma membrane

Evidence provided in this chapter suggests that in contrast to the inhibitory effect of cholestatic bile acids on SOCs activity, the addition of choleretic bile acid TDCA, induced Ca^{2+} entry through SOCs. The evidence supporting the activation of SOCs by TDCA is provided by:

- The sensitivity of the TDCA-induced Ca^{2+} entry, to inhibition by 10μM Gd^{3+}. Similar concentrations of Gd^{3+} have been shown to inhibit Ca^{2+}-entry through SOCs in a hepatocyte cell line (Auld *et al.*, 2000; Rychkov *et al.*, 2001; Rychkov *et al.*, 2005).
- The absence of additive effect of TDCA on the thapsigargin-induced Ca^{2+} entry through SOCs.

These results are complemented by the whole cell patch clamp recording experiments, undertaken by our collaborators Edoardo C. Aromataris and Grigori Y. Rychkov (Aromataris *et al.*, 2008). In those experiments, the currents activated by different types of choleretic bile acids exhibit similarities with the currents induced by IP_3 (these include the shape of I-V plots, the time course of activation by IP_3 and the effects of Ba^{2+}, the sensitivity to 2-APB among others).

The activation of SOCs requires the release of Ca^{2+} from intracellular stores (ER) (Putney, 1986). However, TDCA-induced activation of Ca^{2+} entry through SOCs, TDCA did not cause a fura-2 detectable release of Ca^{2+} from intracellular stores, in the absence of extracellular Ca^{2+}. There is some evidence to suggest that Ca^{2+} enhances the solubility of bile acids and their ability to form micelles (Gu et al., 1992; Hofmann and Mysels, 1992). Thus, it could be possible that the absence of

Ca^{2+}_{ext} could reduce the capability of bile acids to interact with the cells. Another possibility is that TDCA could release some Ca^{2+} from a small component of ER, in an intracellular micro-domain that escapes fura-2 detection, which nevertheless, activates SOCs. An experimental observation supporting this hypothesis is the effect of TDCA (in the absence of Ca^{2+}_{ext}) on inducing a fura-2-detectable release of Ca^{2+} from intracellular stores in cells pre-treated with 1mM Gd^{3+} (to inhibit PMCA pumps action). This result suggests that, in the absence of Ca^{2+}_{ext}, TDCA could be releasing some Ca^{2+} from the stores although the cytoplasmic calcium dye fura-2 failed to detect it, due to rapid clearance out of the cell through the PMCA pumps.

Additionally, when the sub-plasma membrane Ca^{2+} dye FFP-18 was used instead of fura-2, TDCA addition (in the absence of Ca^{2+}_{ext}) induced a transient increase in FFP-18 fluorescence, reflecting Ca^{2+} release from intracellular stores. FFP-18 has been successfully used to monitor rapid changes in the sub-plasma membrane Ca^{2+} levels, in a variety of cells types (Etter *et al.*, 1994; Etter *et al.*, 1996; Davies and Hallett, 1998; Graier *et al.*, 1998; Chadborn *et al.*, 2002). Additionally there are some reports which demonstrate that FFP-18 monitor changes in $[Ca^{2+}]_{SPM}$ rather than the bulk $[Ca^{2+}]_{cyt}$ (Davies *et al.*, 1997; Paltauf-Doburzynska *et al.*, 1998; Chadborn *et al.*, 2002). The result obtained in this chapter using FFP-18, indicated the potential sub-plasma membrane location of the TDCA-induced Ca^{2+} release from intracellular stores.

Taking together these results, it can be concluded that in the absence of Ca^{2+}_{ext} the choleretic bile acid TDCA induces the release of Ca^{2+} from a region of intracellular stores (presumably ER) located in close apposition to the plasma membrane, which in turn induces the activation of SOCs at the plasma membrane of liver cells. It has previously been suggested that a small sub-component of intracellular stores is

involved in the activation of liver cell SOCs (Gregory *et al.*, 1999; Gregory *et al.*, 2004a)

3.3.3. Clinical relevance of the results

- The inhibitory effect of bile acids on SOCs activity required 12 h pre-incubation with cholestatic bile acids; short periods (up to an hour) were ineffective to cause any $[Ca^{2+}]_{cyt}$ alteration (data not shown). Considering the reported evidence that during cholestasis, bile acids accumulate in the blood, hepatocytes and possibly also in the bile canaliculus (Boyer, 2002a), this tardy effect of cholestatic bile acids action could be relevant during the progress of cholestasis and subsequent liver damage. It has been suggested that Ca^{2+} entry through SOCs is required for normal bile flow in the liver (Gregory *et al.*, 2004a). The inhibition of SOCs induced by 12 h pre-incubation of cholestatic bile acids, may represent an explanation for the further inhibition of bile flow, and the altered hepatocyte growth, apoptosis and necrosis all being consequences of cholestasis (Chieco *et al.*, 1997; Benz *et al.*, 1998; Sodeman *et al.*, 2000; Higuchi and Gores, 2003; Higuchi *et al.*, 2003; Borgognone *et al.*, 2005).

- In this chapter, it has been demonstrated that treatment with choleretic bile acid TDCA can counteract the mitochondrial depolarisation and the inhibition of SOCs caused by cholestatic bile acid 12 h pre-incubation. This evidence may contribute to explaining the beneficial pharmacological effects of choleretic bile acids on cholestasis. The pharmacological use of choleretic bile acids UDCA and TUDCA to enhance bile flow in cholestatic conditions, has been reported (Bouchard *et al.*, 1993; Jacquemin *et al.*, 1993; Azer *et al.*, 1995; van de Meeberg *et al.*, 1996; Kinbara *et al.*, 1997; Poupon *et al.*, 1997; Beuers *et al.*, 1998; Ono *et al.*, 1998;

Fabris *et al.*, 1999; Pares *et al.*, 2000; Lazaridis *et al.*, 2001). In addition, it has been shown in rat models of cholestasis, that treatment with choleretic bile acids can stimulate bile flow (Ishizaki *et al.*, 2001).

Several previous studies have shown that exposure of liver cells to bile acids induces an increase in $[Ca^{2+}]_{cyt}$ (Combettes *et al.*, 1990; Beuers *et al.*, 1993a; Gerasimenko *et al.*, 2006), which subsequently affects diverse cellular processes (Beuers *et al.*, 1993a; Alpini *et al.*, 2004; Borgognone *et al.*, 2005). However, the site(s) of action of the bile acids on cellular Ca^{2+} movements has not been clearly defined. The results presented, identify SOCs as a target for cholestatic and choleretic bile acids in liver cells.

Given that a decrease in the ER Ca^{2+} content is a necessary requirement for the activation of SOCs and considering that it is not clearly established whether this involves the whole of the ER or only a small part; the effect of Ca^{2+} release from the ER on SOCs activation in liver cells, were investigated in the next chapter using an alternative approach.

CHAPTER IV: EFFECT OF TRPV1-INDUCED Ca^{2+} RELEASE ON THE ACTIVATION OF SOCs IN LIVER CELLS

4.1 Introduction

While there is good evidence to indicate that a decrease in Ca^{2+} in the ER is a necessary requirement for the activation of SOCs, it is not clearly established whether this involves the whole ER or only a small part. The results of some studies suggest that only a small component of the ER or some other intracellular store is required for the activation of SOCs (Parekh and Penner, 1997; Hartmann and Verkhratsky, 1998; Huang and Putney, 1998; Gregory *et al.*, 1999; Parekh and Putney, 2005; Ong *et al.*, 2007b). Other studies suggest that the whole ER is involved (Hofer *et al.*, 1998; Park *et al.*, 2000; Sedova *et al.*, 2000). Previous studies from our laboratory, performed in hepatocytes, employing adenophostin A (a tight-binding agonist of IP_3 receptors) and IP_3 analogues to activate Ca^{2+} entry; suggest that only a sub-region of the ER is required for the activation of SOCs in liver cells (Gregory *et al.*, 1999; Gregory *et al.*, 2004b). Furthermore, studies with some other cell types also indicate that the activation of SOCs requires Ca^{2+} release from a small region of the ER (Parekh and Penner, 1997; Hartmann and Verkhratsky, 1998; Huang and Putney, 1998; Parekh and Putney, 2005; Ong *et al.*, 2007b). Moreover, the results of recent experiments in which two concentrations of thapsigargin (1.0nM and 1.0μM) were compared in their ability to release Ca^{2+} from the ER and activate

Ca^{2+} entry provided evidence that only a small component of the ER in close proximity to the plasma membrane is required to activate SOCs (Ong *et al.*, 2007b).

Considering the above evidence and the conclusion from the results described in chapter III, which suggests that the activation of SOCs by choleretic bile acid TDCA is associated with the release of Ca^{2+} from a small region of ER, the general aim of the present experiments was to investigate the extent and possible localisation of the ER Ca^{2+} store required for the activation of SOCs in liver cells.

The experimental strategy used to investigate this question employed ectopically expressed TRPV1 channels as a tool to induce the release Ca^{2+} from the ER. Studies with other cell types have shown that TRPV1 is localised in the PM and in intracellular membranes (presumably ER) (Olah *et al.*, 2001; Liu *et al.*, 2003; Turner *et al.*, 2003; Wisnoskey *et al.*, 2003; Karai *et al.*, 2004; Vos *et al.*, 2006; Thomas *et al.*, 2007). Furthermore, it has been reported that TRPV1 activation, promotes Ca^{2+} entry across the PM and releases Ca^{2+} from intracellular stores (Liu *et al.*, 2003; Marshall *et al.*, 2003; Turner *et al.*, 2003; Wisnoskey *et al.*, 2003; Karai *et al.*, 2004).

This chapter describes the localisation of functionally active ectopically expressed TRPV1 in the ER and the plasma membrane of H4-IIE liver cells. It is demonstrated that the release of Ca^{2+} from the bulk of the ER, via ectopically expressed TRPV1, does not activate SOCs.

4.2 Results

4.2.1. TRPV1 protein expression and distribution in H4-IIE liver cells

To test for the presence of endogenous TRPV1 proteins in H4-IIE liver cells, an immunofluorescence assay against TRPV1 was performed in normal H4-IIE cells (non-transfected cells).

The results (Fig. 4.1) indicate that TRPV1 proteins could not be detected in H4-IIE liver cells. There was no difference with control experiments in which the antibody against TRPV1 was omitted in the immunofluorescence assay. This result suggests that H4-IIE liver cells do not express endogenous TRPV1 proteins.

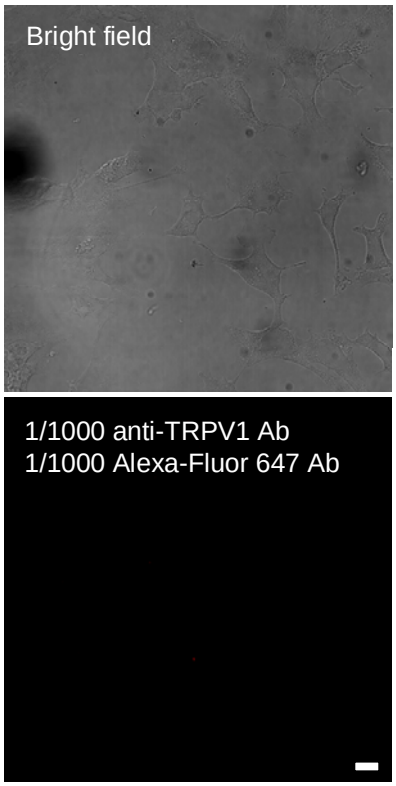

Fig. 4.1. H4-IIE cells do not express detectable endogenous TRPV1 proteins. Representative confocal images resulting from immunofluorescence against TRPV1, performed in H4-IIE, are shown. Note the lack of fluorescence corresponding to Alexa-Fluor 647 antibody (red emission). Immunofluorescence and imaging by confocal microscopy assays were performed as described in Section 2.7.1. The scale bar represents 10 μm. The results shown are representative of those obtained for one of 54 cells examined in three separate experiments.

The ectopical expression of TRPV1 proteins in H4-IIE liver cells was then performed and the cellular localisation of the expressed TRPV1 proteins was subsequently assessed by immunofluorescence using confocal microscopy.

As shown in Fig. 4.2, in H4-IIE liver cells transiently transfected with Ad-Track-CMV-TRPV1, the ectopically expressed TRPV1 proteins were found predominately in intracellular locations and at the plasma membrane. TRPV1 transfected H4-IIE cells were identified by the presence of GFP, as is shown in Fig. 4.2, top panel.

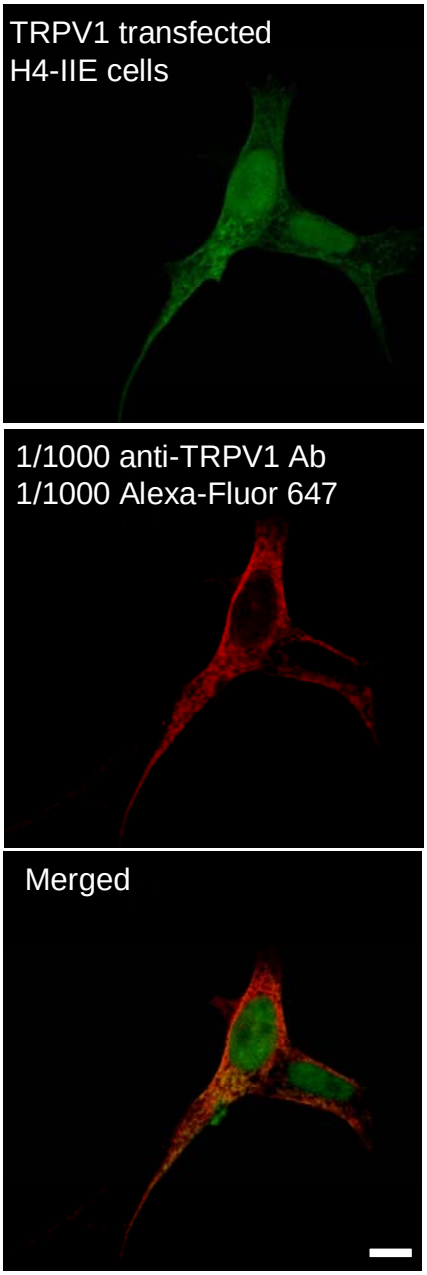

Fig. 4.2. Confocal microscopy imaging of ectopically expressed TRPV1 proteins in Ad-Track-CMV-TRPV1 transfected H4-IIE cells. Representative confocal images, of the immunofluorescence against TRPV1, performed in Ad-Track-CMV-TRPV1 transfected H4-IIE cells, are shown. Top panel shows TRPV1 transfected cells. The middle panel shows the Alexa-Fluor 647 antibody red fluorescence, illustrating the presence and localisation of TRPV1 proteins. The bottom panel represents the merged images. TRPV1(+) cells were identified by the GFP fluorescence (which is encoded in the Ad-Track-CMV-TRPV1 plasmid). Cellular transfection, immunofluorescence and imaging by confocal microscopy assays were performed as described in Sections 2.5.4 and 2.7.1. The scale bar represents 10 μm. The results shown are representative of those obtained for one of 18 TRPV1(+) cells examined in three separate experiments.

To determine if intracellular TRPV1 was ectopically expressed in the endoplasmic reticulum; a co-localisation assay was developed by co-transfection of Ad-Track-CMV-TRPV1 plasmid plus the ER marker pDsRed2-ER plasmid, followed by an immunofluorescence assay against TRPV1 proteins.

As shown in Fig. 4.3, the intracellular localisation of ectopically expressed TRPV1 (imaged by Alexa-Fluor 647 fluorescence) showed substantial co-localisation with the ER (imaged using DsRed2) indicating that TRPV1 proteins are being ectopically expressed at this intracellular site (Fig. 4.3, ER and merged).

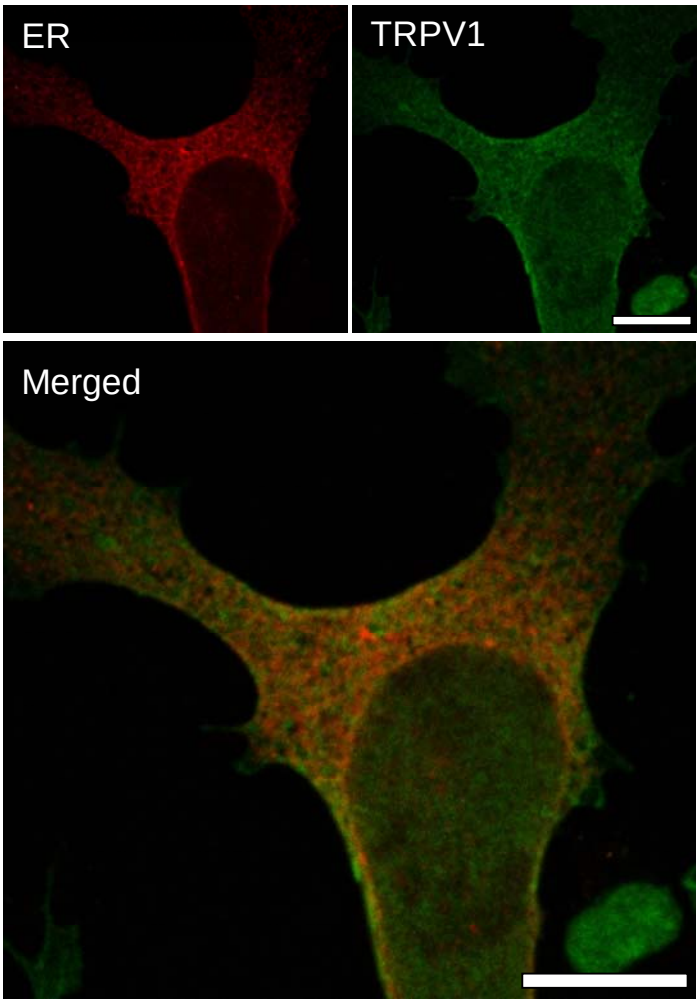

Fig. 4.3. In Ad-Track-CMV-TRPV1 transfected H4-IIE cells TRPV1 protein is distributed throughout the ER and the PM. Representative confocal image of a H4-IIE cell co-transfected with Ad-Track-CMV-TRPV1 and pDsRed2-ER plasmids is shown. The ER structure (identified by DsRed2 fluorescence, top left panel), the endogenous expressed STIM1 proteins (identified by Alexa-Fluor 647 through immunofluorescence, top right panel) and the merged images (bottom panel) are presented. Due to the near infrared emission wavelength of Alexa-Fluor 647 (675-750nm), green colour was used in the image in order to facilitate co-localisation. TRPV1 positive cells were identified by the GFP fluorescence (encoded in the Ad-Track-CMV-TRPV1 plasmid). Cellular transfection, immunofluorescence and imaging by confocal microscopy assays were performed as described in Sections 2.5.4 and 2.8.1. The scale bar represents 10 μm. The results shown are representative of those obtained for one of 12 TRPV1(+) cells examined in three separate experiments.

Immunofluorescence assays are based on the binding of the antibodies to their targets. In addition, this technique requires the fixation of cells, a process that could either affect cellular protein distribution and/or add extra noise to the images. For these reasons, a different type of approach was also performed to confirm the ER localisation of ectopically expressed TRPV1 proteins. In this case a different plasmid was used to ectopically express TRPV1, namely YFP-TRPV1 plasmid. The cellular transfection with YFP-TRPV1 plasmid induces the expression of TRPV1 proteins with an YFP fluorescent molecule directly attached; so the exact localisation of TRPV1 could be tracked by imaging the intracellular YFP fluorescence.

For this, H4-IIE liver cells were co-transfected with YFP-TRPV1 plasmid plus pDsRed2-ER plasmid. 48 h later, the fluorescent molecules expressed from both plasmids (YFP and DsRed2 respectively) were captured by confocal microscopy. After that a de-convolution of the acquired images was performed in order to improve their resolution.

The classic ER structural pattern is visualised in Fig. 4.4 A by the DsRed2 fluorescence (left panel). It can be seen, in the middle panel, that the YFP distribution exhibits an almost identical pattern to the DsRed2 fluorescence and, furthermore, the merged image (right panel) shows the high co-localisation between the two fluorescent molecules (yellow colour). This represents strong evidence of TRPV1 localisation in the ER. In addition to the ER localisation, TRPV1-YFP proteins are expressed in the PM as can be seen by the green fluorescence surrounding the periphery of the cells (arrows heads). Note that in the merged image those areas indicated by arrow heads, exhibit only green fluorescence (from TRPV1-YFP), which confirms they belong to a non ER structure (most likely PM).

To confirm TRPV1 co-localisation with ER, another ER marker, BODIPY TR-X Tg, (Engelke *et al.*, 2002; Burdyga *et al.*, 2007; Macgregor *et al.*, 2007; Rengifo *et al.*, 2007) was employed. For this H4-IIE cells were transfected with YFP-TRPV1 plasmid. 48 h later the cells were loaded with the permeant fluorescent dye BODIPY TR-X Tg and subsequently, images of both fluorescent molecules were acquired by confocal microscopy. After that a de-convolution of the images was performed in order to improve their resolution.

The typical ER structural pattern is shown in Fig. 4.4 B by the BODIPY TR-X fluorescence (left panel). The TRPV1-YFP distribution (middle panel) exhibits an almost identical pattern to the BODIPY TR-X and, furthermore, the merged image (right panel) shows a high co-localisation between the two fluorescent molecules (yellow colour), indicating the TRPV1 localisation in the ER. In addition to the ER localisation, TRPV1-YFP proteins are expressed at the PM as can be seen by the YFP fluorescence (green) surrounding the periphery of the cells (arrows heads). This represents additional evidence of TRPV1 localisation in the ER and some at the PM.

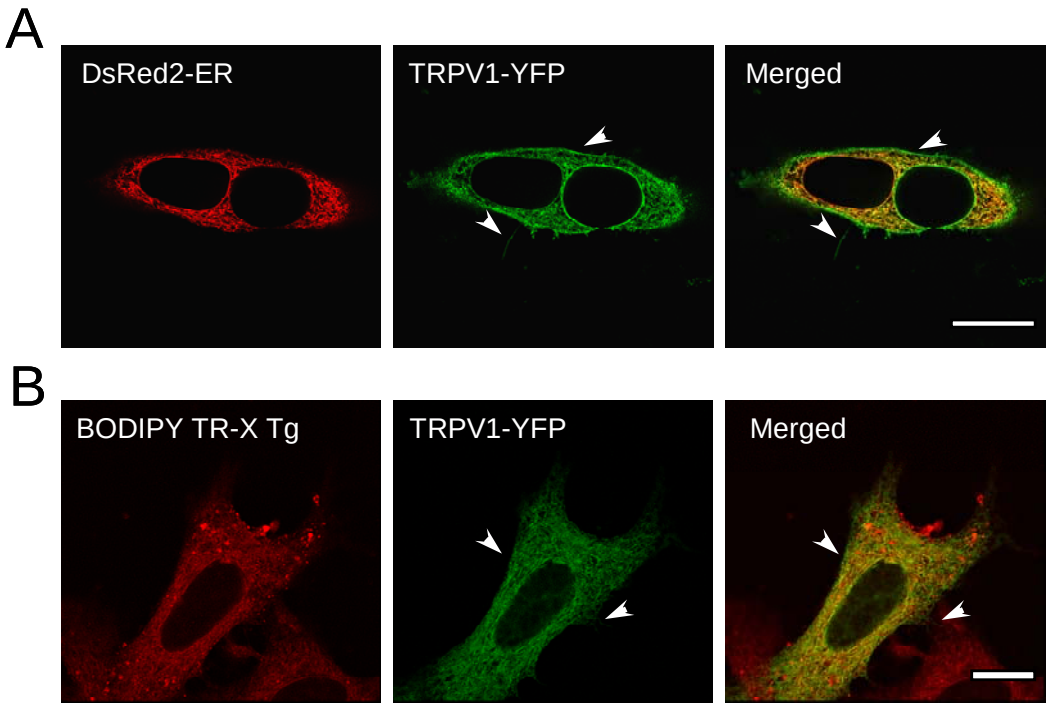

Fig. 4.4. In YFP-TRPV1 transfected H4-IIE cells, TRPV1 protein is distributed throughout the ER and the PM. (**A**) Representative de-convoluted confocal images of the DsRed2 (left panel) and YFP (right panel) fluorescence, obtained by co-expression of YFP-TRPV1 and pDsRed2-ER plasmids, in a TRPV1 positive H4-IIE cell. (**B)** Representative de-convoluted confocal images of the BODIPY TR-X (left panel) and YFP (right panel) fluorescence, obtained by expression of YFP-TRPV1 plasmid and stained with the ER marker BODIPY TR-X Tg in a TRPV1 positive H4-IIE cell. Note the high degree of co-localisation of both fluorescent molecules (yellow colour) in the merged image (right panels). The arrows head indicated a cellular area (PM) exhibiting only the YFP fluorescence. STIM1 proteins were visualised in a Z-plane section in the middle of the cell (note nucleus region excluding STIM1). TRPV1 positive cells were identified by the GFP fluorescence (encoded in the Ad-Track-CMV-TRPV1 plasmid). Cellular transfection, confocal microscopy and de-convolution of the images were performed as described in Sections 2.8.1 and 2.8.2. The scale bar represents 10 μm. The results shown are representative of those obtained for one of 6-8 TRPV1(+) cells examined in two separate experiments.

4.2.2. Effect of TRPV1 agonists on $[Ca^{2+}]_{cyt}$ in H4-IIE liver cells expressing TRPV1 channels

To test if the ectopically expressed TRPV1 channels were functionally active in H4-IIE cells, addition of TRPV1 agonist into the incubation medium was carried out in the presence or absence of extracellular Ca^{2+} and changes in $[Ca^{2+}]_{cyt}$ were measured with fura-2.

The cells transfected with the Ad-Track-CMV-TRPV1 plasmid (designated TRPV1(+) cells), were identified by GFP fluorescence, non transfected cells on the same coverslip (designated TRPV1(-) cells), were used as controls. Cells transfected with empty vector Ad-Track-CMV were used as additional controls.

As shown in Fig. 4.5 A, in the presence of Ca^{2+}_{ext}, the addition of TRPV1 agonist RTX induced a large and sustained increase in $[Ca^{2+}]_{cyt}$ in TRPV1(+) cells, but not in TRPV1(-) cells or in cells transfected with the Ad-Track-CMV plasmid (no TRPV1 cDNA) (insert). As is shown in Fig. 4.5 B, in the absence of Ca^{2+}_{ext}, the addition of RTX induced a transient increase in $[Ca^{2+}]_{cyt}$ in TRPV1(+) cells but caused no increase in $[Ca^{2+}]_{cyt}$ in TRPV1(-) cells or in cells transfected with the Ad-Track-CMV plasmid (no TRPV1 cDNA) (insert). Similar results were obtained in H4-IIE cells ectopically expressing YFP-TRPV1 and with the TRPV1 agonist capsaicin (10μM) and N-vanillylnonamide (10μM) in place of RTX (result not shown).

These results indicate that TRPV1 ectopically expressed in the ER and PM of H4-IIE liver cells is functionally active, offering a tool to release Ca^{2+} from intracellular stores (ER) via TRPV1-agonist activation in the absence of Ca^{2+}_{ext}. Since TRPV1(-) cells responded in the same way as cells transfected with the Ad-Track-CMV plasmid, TRPV1(-) cells were used as control in all subsequent experiments.

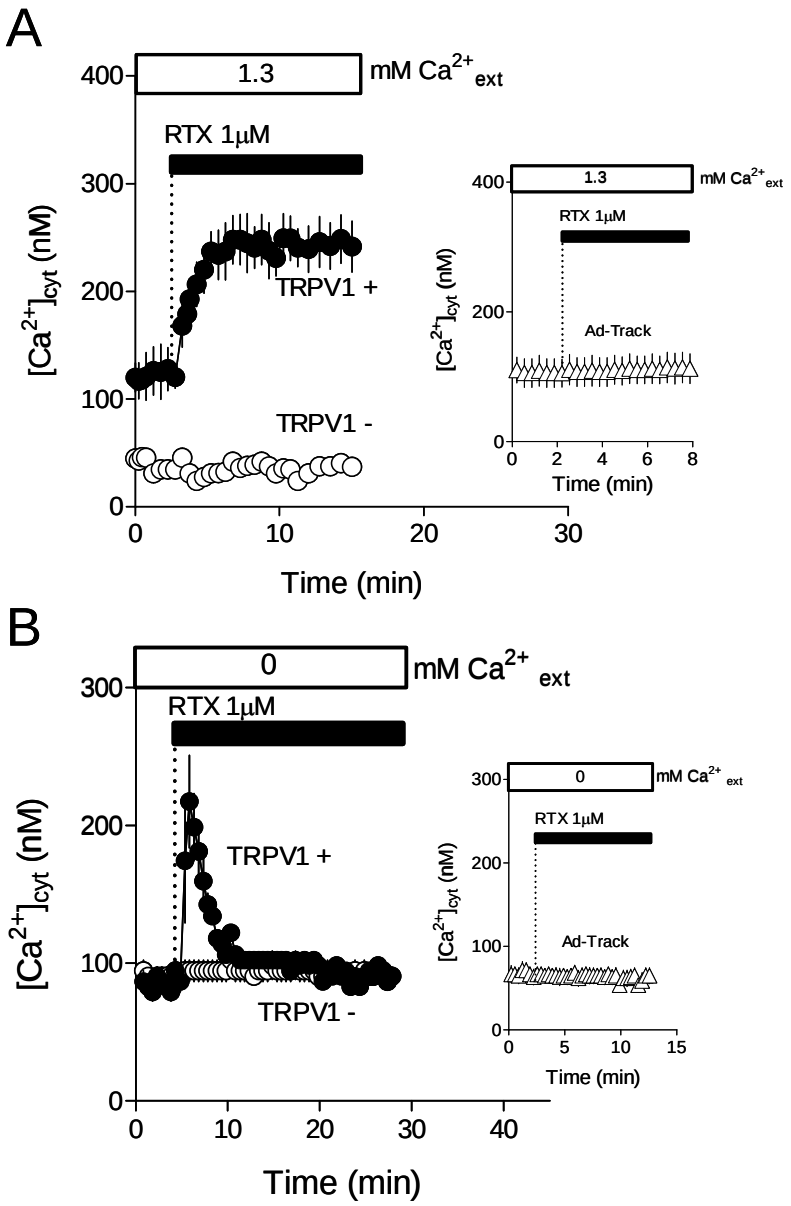

Fig. 4.5. RTX induces Ca^{2+} entry and release from intracellular stores in TRPV1-transfected cells. Representative traces are showing the effect of TRPV1 agonist RTX on $[Ca^{2+}]_{cyt}$ of TRPV1(+) and TRPV1(-) H4-IIE cells, are shown. In the presence of Ca^{2+}_{ext} (**A**), RTX (1μM) induced a sustained increase in $[Ca^{2+}]_{cyt}$ only in TRPV1(+) cells, while in the absence of Ca^{2+}_{ext} (**B**) RTX induced a transient increase in $[Ca^{2+}]_{cyt}$ only in TRPV1(+) cells. In cells transfected with Ad-Track-CMV plasmid (which does not have TRPV1), the addition of RTX, in the absence or presence of Ca^{2+}_{ext}, does not alter $[Ca^{2+}]_{cyt}$ (inserts). TRPV1 proteins were ectopically expressed by transfection with Track-CMV-TRPV1 plasmid and TRPV1(+) cells were identified by the GFP fluorescence encoded in the plasmid. Cellular transfection and $[Ca^{2+}]_{cyt}$ measurements as a function of time in cells loaded with fura-2, were performed as described in Section 2.5.4 and 2.3. The additions to the bath are indicated by the horizontal bars. The results shown are from a representative experiment, of those obtained in 3 similar experiments, in which the fluorescence of 4-7 TRPV1(+) or (-) H4-IIE cells was measured.

4.2.3. Effect of the TRPV1 antagonist ruthenium red on Ca^{2+} entry and release induced by TRPV1 agonists

In order to verify if the increases in $[Ca^{2+}]_{cyt}$ induced by the TRPV1 agonist RTX, takes place exclusively through TRPV1 channels, a group of experiments were performed with the TRPV1 channel antagonist ruthenium red (RR) (Dray *et al*., 1990).

As shown is Fig. 4.6 A, the sustained increase in $[Ca^{2+}]_{cyt}$ caused by RTX in TRPV1(+) cells was inhibited by RR. Subsequently $[Ca^{2+}]_{cyt}$ returned close to basal levels. However, in TRPV1(+) cells, the RTX-induced Ca^{2+} release from intracellular stores (in the absence of extracellular Ca^{2+}) was still apparent in the presence of this inhibitor (Fig. 4.6 B), and was not significantly different from the release induced by RTX alone (Fig. 4.6 B, insert). In addition, the presence of RR in the incubation medium caused no difference in the thapsigargin-induced Ca^{2+} release from the ER (Fig. 4.6 C, insert).

The results in Fig. 4.6 indicate that in TRPV1(+) cells, TRPV1 agonists activate Ca^{2+} entry through TRPV1 channels in the plasma membrane (sensitive to RR inhibition) and cause Ca^{2+} release from the ER (insensitive to RR inhibition). Similar results to those shown in Fig. 4.6 were obtained using the TRPV1 agonists capsaicin (10 μM) or N-vanillylnonamide (10 μM) in place of RTX (results not shown).

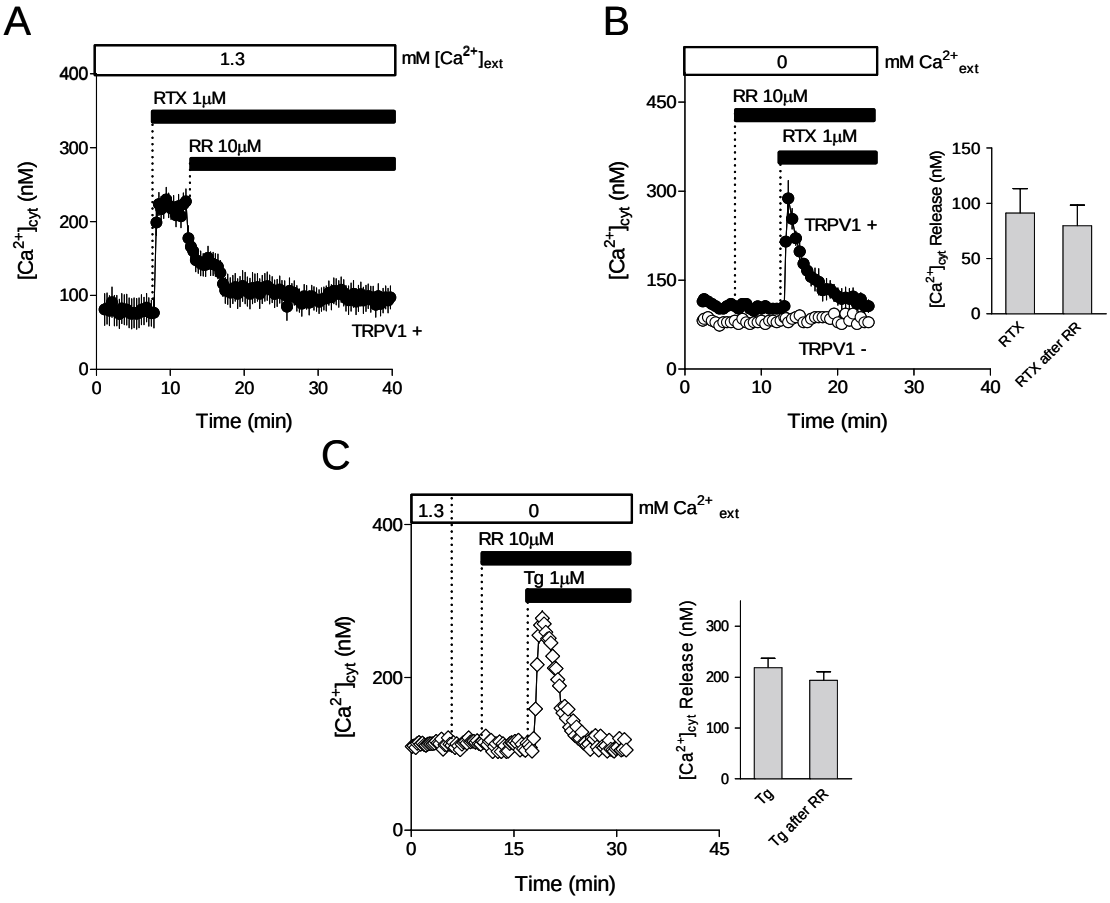

Fig. 4.6. Ruthenium red inhibits RTX-induced Ca^{2+} entry but not the Ca^{2+} release from the stores in TRPV1-transfected H4-IIE cells. (**A**) In the presences of 1.3 mM Ca^{2+}_{ext}, the RTX-induced sustained increase of $[Ca^{2+}]_{cyt}$ in TRPV1(+) cells was abolished by addition of RR (10μM). The values are the means ± SEM of those obtained in 3 experiments. (**B**) In the absence of Ca^{2+}_{ext} the RTX-induced Ca^{2+} release from intracellular stores in TRPV1(+) cells, was not affected by the presence of RR in the incubation medium (insert) ($P>0.05$). The values are the means ± SEM of those obtained in 7 and 5 experiments for RTX alone and RTX after RR, respectively, in which the fluorescence of 4-7 TRPV1(+) H4-IIE cells were measured. (**C**) RR failed to significantly inhibit the Ca^{2+} release from ER induced by the SERCA inhibitor Tg in un-transfected H4-IIE cells. The insert shows no significant difference in the magnitude of Ca^{2+} release by Tg in the absence or presence of RR ($P=1$). The values are the means ± SEM of those obtained in 9 and 4 experiments for Tg alone and Tg after RR, respectively. Cellular transfection and $[Ca^{2+}]_{cyt}$ measurements as a function of time in cells loaded with fura-2, were performed as described in Section 2.5.4 and 2.3. The additions to the bath are indicated by the horizontal bars.

4.2.4. TRPV1 agonist RTX caused Ca^{2+} depletion of much of the DBHQ sensitive stores (ER)

The extent of the TRPV1-mediated release of Ca^{2+} from intracellular stores was evaluated in H4-IIE cells transfected with Ad-Track-CMV-TRPV1 plasmid.

As illustrated in Fig. 4.7 A, RTX was added into the incubation medium in the absence of Ca^{2+}_{ext}. This led to an increase in $[Ca^{2+}]_{cyt}$ in TRPV1(+) cells, but no RTX-induced increase in $[Ca^{2+}]_{cyt}$ was observed in TRPV1(-) cells. Following RTX addition to TRPV1(+) cells, the subsequent addition of DBHQ caused no further increase in $[Ca^{2+}]_{cyt}$, whereas in TRPV1(-) cells the expected DBHQ-induced increase in $[Ca^{2+}]_{cyt}$ was observed (Fig. 4.7 A). When the order of addition of RTX and DBHQ was reversed, the addition of RTX to TRPV1(+) cells, following the addition of DBHQ caused no further increase in $[Ca^{2+}]_{cyt}$ (Fig. 4.7 B). Furthermore, the release of Ca^{2+} from intracellular stores induced by RTX or DBHQ was not significantly different in TRPV1(+) cells (Fig. 4.7 C).

These results suggest that in H4-IIE cells ectopically expressing TRPV1 the Ca^{2+} stores released by TRPV1 agonist overlap substantially with the Ca^{2+} stores released by SERCA inhibitors. Results similar to those shown in Fig. 4.7 were obtained using the TRPV1 agonists capsaicin (10 μM) or N-vanillylnonamide (10 μM) in place of RTX (results not shown).

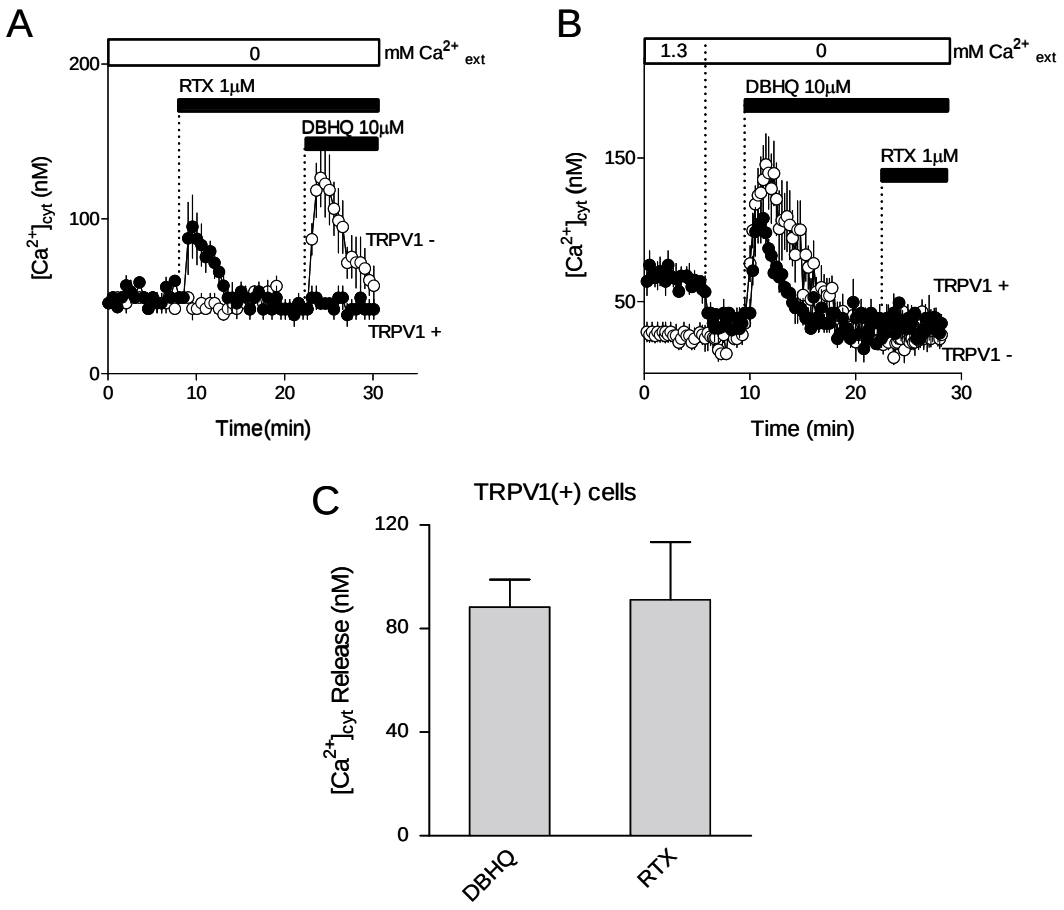

Fig. 4.7. TRPV1 agonist RTX caused Ca^{2+} depletion of much of the DBHQ sensitive stores in TRPV1-transfected H4-IIE cells. (ER) The effects of RTX addition on $[Ca^{2+}]_{cyt}$ in TRPV(+) and TRPV(-) H4-IIE cells, are shown. (**A**) In the absence of Ca^{2+}_{ext}, RTX (1μM) addition caused a transient increase on $[Ca^{2+}]_{cyt}$. The subsequent addition of DBHQ (10μM), despite inducing Ca^{2+} release in TRPV1(-) cells, failed to induce any Ca^{2+} release from intracellular stores in TRPV1 (+) cells. (**B**) When DBHQ was added the first, a transient increase of $[Ca^{2+}]_{cyt}$ was observed in both TRPV1(+) or (-) cells, but the subsequent addition of RTX (1μM) failed to induce any change in $[Ca^{2+}]_{cyt}$ in either TRPV1(+) or (-) cells. (**C**) The RTX-induced Ca^{2+} release from intracellular stores in TRPV1(+) cells, was similar to the release induced by DBHQ ($P > 0.05$**).** TRPV1 was ectopically expressed by transfection with Track-CMV-TRPV1 plasmid, and TRPV1 positive cells were identified by the GFP fluorescence (encoded in the plasmid). Cellular transfection and $[Ca^{2+}]_{cyt}$ measurements as a function of time in cells loaded with fura-2, were performed as described in Section 2.5.4 and 2.3. The additions to the bath are indicated by the horizontal bars. The results shown are from a representative experiment, of those obtained in 4 (**A**) and 3 (**B**) similar experiments, in which the fluorescence of 3-7 TRPV1(+) or(-)H4-IIE cells was measured.

The ability of RTX to induce Ca^{2+} release, from the ER, was tested in experiments performed with cells loaded with the fluorescent Ca^{2+} dye Calcium Green 5N.

This set of experiments was performed in H4-IIE cells which ectopically expressed TRPV1-GFP. Since GFP is freely diffusing in the cytoplasmic space of TRPV1 (+) cells, and the fluorescence emission of GFP overlaps with that of Calcium Green 5N, digitonin (to permeabilise the PM) was added to allow the washing out of GFP. The remaining fluorescence after the cells permeabilisation corresponds to the Calcium Green 5N dye located in the ER. Before the cellular permeabilisation the incubation medium (KRH) was changed to a "cytoplasmic" medium in which the free [Ca^{2+}] was estimated to be 100nM by using the BAD (Bound and Determined) programme (S. Brooks, Carelton University, Ottawa, Canada).

Fig. 4.8 A, shows images of Calcium Green 5N fluorescence in permeabilised control H4-IIE cells. Thapsigargin caused a decrease in Calcium Green 5N fluorescence, and the subsequent addition of the Ca^{2+} ionophore, ionomycin, caused a further decrease (Fig. 4.8 B). The decrease caused by ionomycin is most likely due to the further release of the Ca^{2+} remaining in the ER and/or by other intracellular stores like Golgi apparatus. No change in fluorescence was observed in the absence of thapsigargin and ionomycin (Fig. 4.8 B, insert). Addition of RTX to permeabilised TRPV1(+) cells loaded with Calcium Green 5N caused a decrease in Calcium Green 5N fluorescence (Fig. 4.8 C), similar in magnitude to that induced by thapsigargin in TRPV1(-) cells (Fig. 4.12 B), but with a slower time course. A further small decrease in fluorescence was caused by subsequent addition of ionomycin (Fig. 4.8 C).

These results provide additional evidence that the TRPV1 agonist RTX caused the release of Ca^{2+} from the ER to a similar extent as that caused by thapsigargin.

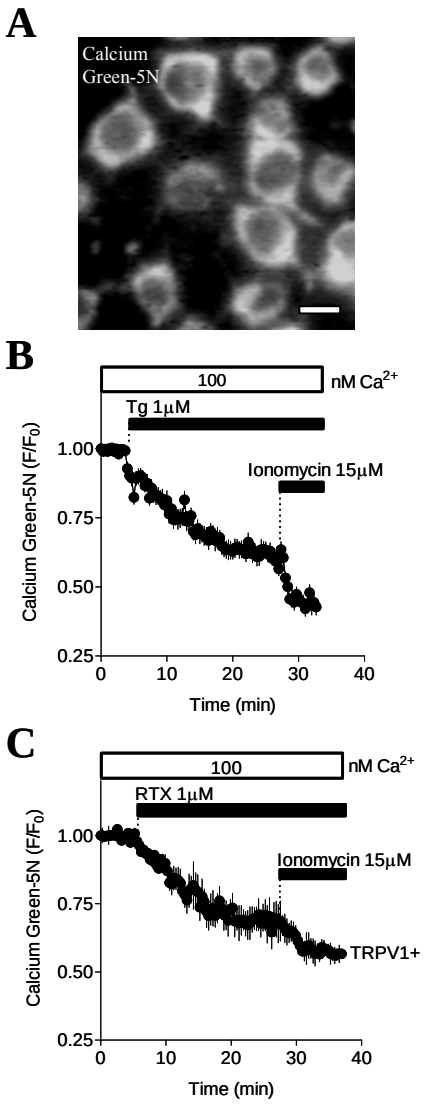

Fig. 4.8. RTX induces the release of Ca^{2+} from the ER. (**A**) A representative fluorescence image of permeabilised H4-IIE cells loaded with Calcium Green 5N. The scale bar represents 25μm. The cytoplasmic incubation medium is composed of (mM): KC1, 140; NaCl, 5; $MgSO_4$, 7; HEPES, 20; ATP, 1; EGTA, 10.2 and $CaCl_2$, 1.65, adjusted to pH 7.0. (**B**) In TRPV1(-) cells, addition of the 1μM thapsigargin (Tg), caused the decrease of Calcium Green 5N fluorescence. Subsequent addition of ionomycin (15μM) induces a further decrease in Calcium Green 5N fluorescence. (**C**) In TRPV(+) cells, RTX (1μM) addition caused a similar decrease on Calcium Green 5N fluorescence to the one caused by Tg. TRPV(+) cells were identified by the GFP fluorescence encoded in the Ad-Track-CMV-TRPV1 plasmid. To compare fluorescence values from different cells, Calcium Green 5N fluorescence data were standardised by assigning the baseline fluorescence (F_0), the value of 1. Cellular transfection was performed as described in Section 2.5.4. Additions to the bath are indicated by the horizontal bars. The results shown are from a representative experiment, of those obtained in 4 (**B**) and 7 (**C**) similar experiments, in which the fluorescence of 4-7 TRPV1(+) or (-) cells was measured.

4.2.5. Ca^{2+} release from the ER induced by TRPV1 agonists does not activate SOCs

The ability of RTX-mediated Ca^{2+} release from the ER to induce the activation of Ca^{2+} entry through SOCs was tested in H4-IIE liver cells transfected with Ad-Track-CMV-TRPV1 plasmid, loaded with fura-2.

Fig. 4.9 A shows that, in either TRPV1(+) or in TRPV1(-) cells, thapsigargin releases Ca^{2+} from the ER (in the absence of Ca^{2+}_{ext}) and activates Ca^{2+} entry through SOCs, as is indicated by the increase in $[Ca^{2+}]_{cyt}$ upon Ca^{2+}_{ext} re-addition. Nevertheless, as shown in Fig. 4.9 B, a different situation took place when RTX was used to induce the release of Ca^{2+} from intracellular stores. In TRPV1(+) cells, RTX induced an increase in $[Ca^{2+}]_{cyt}$ due to the release of Ca^{2+} from the ER (Fig. 4.9 B). However, there was no increase in $[Ca^{2+}]_{cyt}$ upon Ca^{2+}_{ext} re-addition. No RTX-induced changes in $[Ca^{2+}]_{cyt}$ were observed in TRPV1(-) cells (Fig. 4.9 B). The presence of ruthenium red in the incubation medium, in both Fig 4.9 A or B, was necessary in order to avoid Ca^{2+} entry through TRPV1 channels in the plasma membrane when Ca^{2+}_{ext} was added back.

These results indicate that, in TRPV1(+) cells, the release of Ca^{2+} from the ER induced by TRPV1 agonists acting on ectopically expressed TRPV1, does not activate Ca^{2+} entry through SOCs.

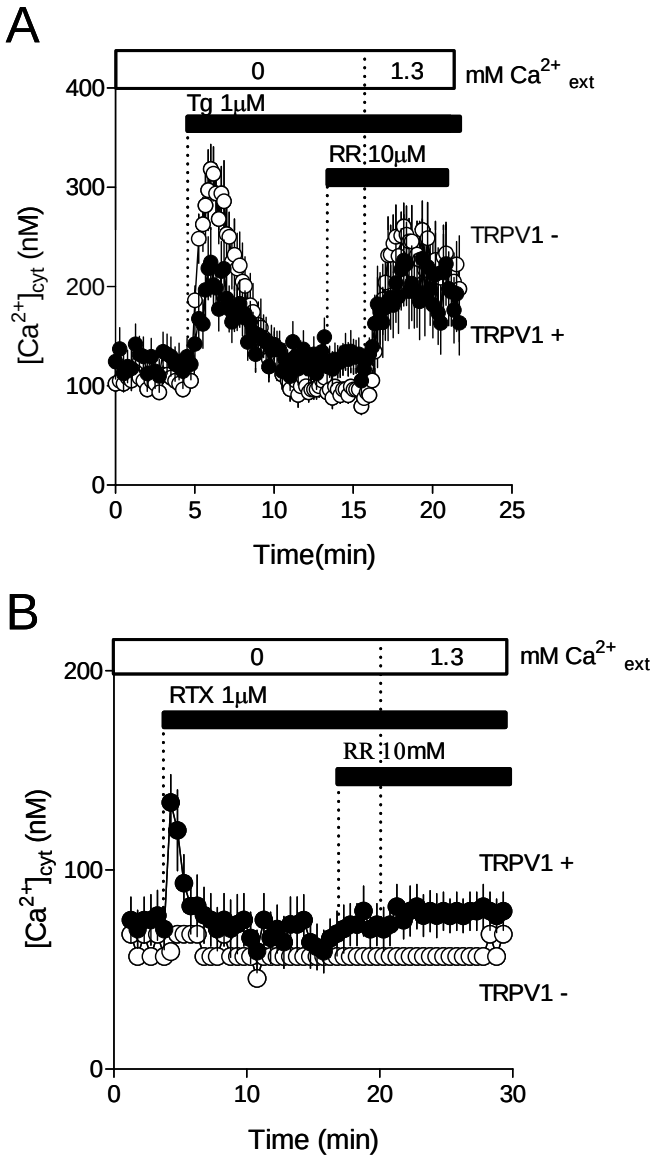

Fig. 4.9. Release of intracellular Ca^{2+} induced by RTX does not activate Ca^{2+} entry through SOCs in Ad-Track-CMV-TRPV1 transfected H4-IIE cells. (**A**) Fura-2 loaded TRPV1(+) and TRPV1(-) H4-IIE cells exposed to SERCA inhibitor thapsigargin (1µM) in the absence of Ca^{2+}_{ext} exhibits the typical release of Ca^{2+} from intracellular stores. RR (10µM) was subsequently added after Tg (to inhibit TRPV1 channels at the plasma membrane) and when Ca^{2+}_{ext} was added back to the bath, the typical increase in $[Ca^{2+}]_{cyt}$ (through the SOCs at the plasma membrane) occur in both cellular types. (**B**) RTX (1µM) addition in the absence of Ca^{2+}_{ext}, despite releasing Ca^{2+} from TRPV1 intracellular stores in TRPV1(+) cells, failed to activate Ca^{2+} entry through SOCs when Ca^{2+}_{ext} is added back in the presences of RR. Cellular transfection and $[Ca^{2+}]_{cyt}$ measurements as a function of time in cells loaded with fura-2, were performed as described in Section 2.5.4 and 2.3. The additions to the bath are indicated by the horizontal bars. The results shown are from a representative experiment, of those obtained in 4 (**A**) and 13 (**B**) similar experiments, in which the fluorescence of 4-7 TRPV1(+) or(-)H4-IIE cells was measured.

Considering the key information about the localisation of TRPV1 proteins in the ER obtained in H4-IIE cells transfected with the YFP-TRPV1 plasmid (Fig. 4.4); the ability of RTX-mediated Ca^{2+} release from the ER, to induce the activation of Ca^{2+} entry through SOCs, was tested in H4-IIE liver cells transfected with YFP-TRPV1 plasmid.

As shown in Fig. 4.10, the addition of RTX, in the absence of Ca^{2+}_{ext}, induced the release of Ca^{2+} from the ER (transient increase in $[Ca^{2+}]_{cyt}$). However, there was no Ca^{2+} entry through SOCs upon Ca^{2+}_{ext} re-addition in the presence of ruthenium red (added to avoid Ca^{2+} entry through TRPV1 channels in the plasma membrane).

This result indicates that the release of Ca^{2+} from the ER via TRPV1 channels ectopically expressed by transfection with YFP-TRPV1 plasmid, failed to activate SOCs in H4-IIE liver cells.

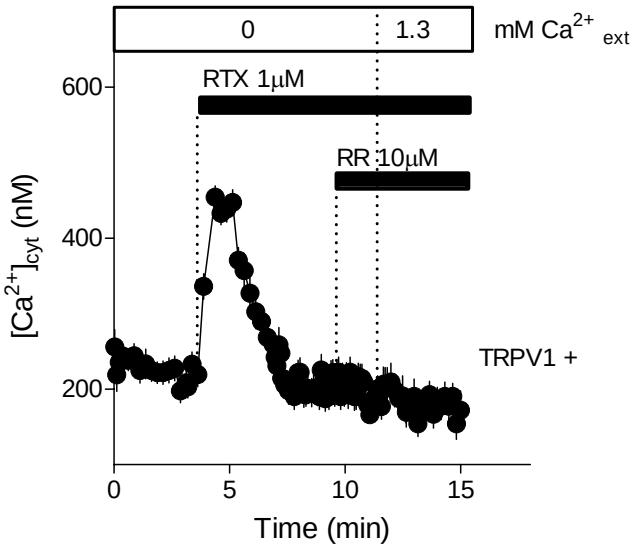

Fig. 4.10. Release of intracellular Ca^{2+} induced by RTX does not activate Ca^{2+} entry through SOCs in YFP-TRPV1 transfected H4-IIE cells. In TRPV1(+) H4-IIE cells, RTX (1μM) addition, in the absence of Ca^{2+}_{ext}, despite to release Ca^{2+} from TRPV1 intracellular stores, failed to activate Ca^{2+} entry through SOCs when Ca^{2+}_{ext} is added back in the presences of RR (to inhibit TRPV1 channels at the plasma membrane expressed by YFP-TRPV1 plasmid). H4-IIE cells transfected with YFP-TRPV1 plasmid were identified by YFP fluorescence Cellular transfection and $[Ca^{2+}]_{cyt}$ measurements as a function of time in cells loaded with fura-2, were performed as described in Section 2.5.4 and 2.3. The additions to the bath are indicated by the horizontal bars. The results shown are from a representative experiment, of those obtained in 6 similar experiments, in which the fluorescence of 4-7 TRPV1(+) H4-IIE cells was measured.

A set of control experiments was undertaken to verify that the lack of SOCs activation after RTX-mediated Ca^{2+} release was not due to the presence of RTX or RR in the incubation medium.

As is shown in Fig. 4.11, neither RTX (Fig. 4.11 B) nor RR (Fig. 4.11 C), inhibited thapsigargin-initiated Ca^{2+} entry through SOCs (Fig. 4.11 A). There was no significant difference between the initial rates of Ca^{2+} entry induced by thapsigargin and thapsigargin in the presence of RTX or RR (Fig. 4.11 D).

These results demonstrated that the presence of RTX or RR in the incubation medium did not create any artefact in the experimental protocol used in Fig. 4.9 B. Results similar to these shown in Fig. 4.11 were obtained using TRPV1 agonists capsaicin (10 μM) or N-vanillylnonamide (10 μM) in place of RTX (results not shown).

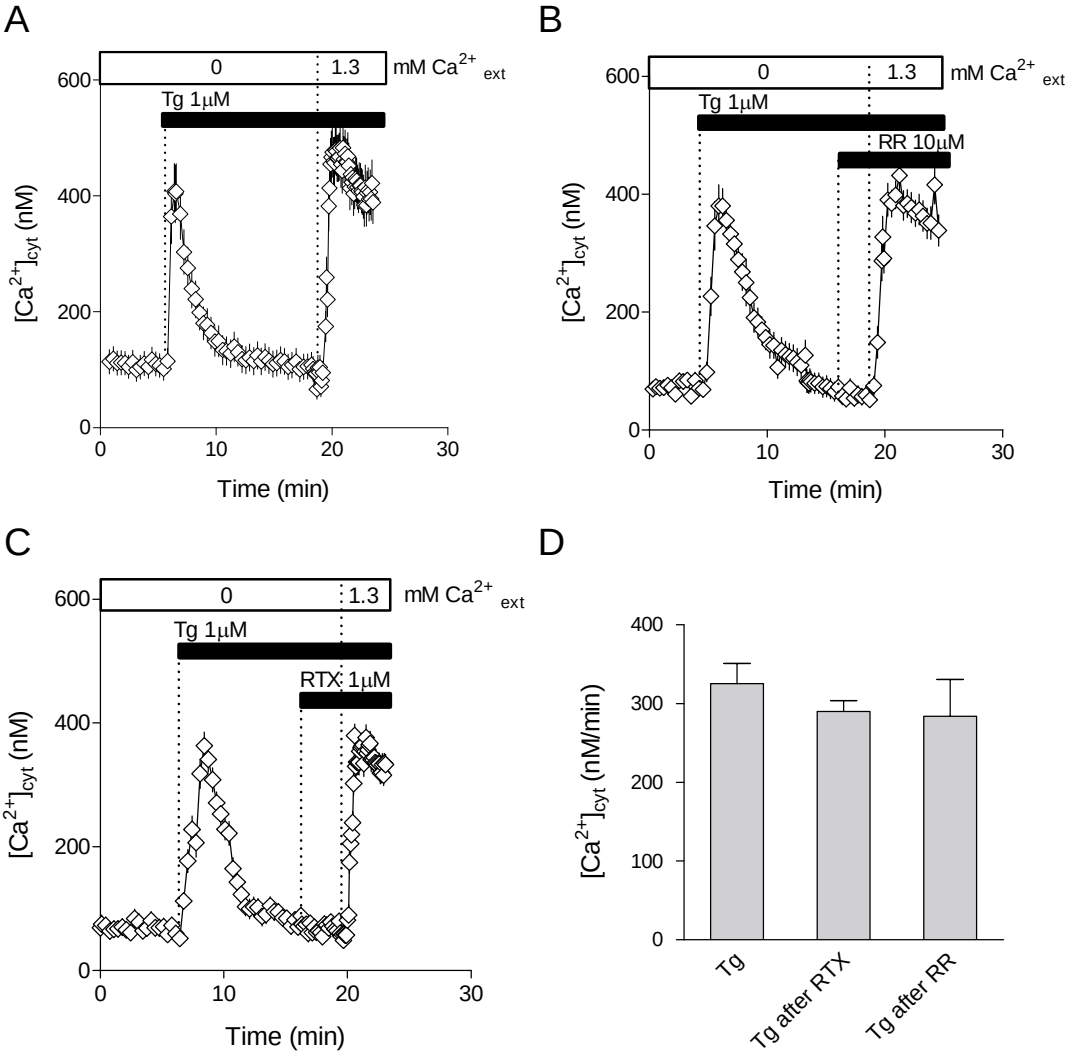

Fig. 4.11. RTX or RR do not impede thapsigargin activation of Ca^{2+} entry through SOCs. (**A**) Fura-2 loaded H4-IIE cells exposed to SERCA inhibitor thapsigargin (1μM) in the absence of Ca^{2+}_{ext}, exhibits the typical release of Ca^{2+} from intracellular stores followed by the characteristic Ca^{2+} entry through the SOCs at the plasma membrane, when Ca^{2+}_{ext} is added back to the bath. The addition of RTX (1μM) (**B**) or RR (10μM) (**C**), prior Ca^{2+}_{ext} re-addition, do not affect the typical Ca^{2+} entry through the SOCs induced by Tg. $[Ca^{2+}]_{cyt}$ measurements as a function of time in cells loaded with fura-2, were performed as described in Section 2.3. The additions to the bath are indicated by the horizontal bars. The results shown are from a representative experiment, of those obtained in 3-12 similar experiments, in which the fluorescence of 10-20 H4-IIE cells were measured. (**D**) The initial rates of Ca^{2+} entry, induced by Tg, following Ca^{2+}_{ext} re-addition into the bath (determined as described in Section 2.3), shows no significant difference with the initial rates of Ca^{2+} entry by Tg when RTX or RR were present in the incubation medium ($P > 0.05$). The values in **C** are the means ± SEM of 3-12 experiments of those in **A**, **B** and **C**.

To further investigate if the release of Ca^{2+} from the ER, via ectopically expressed TRPV1 channels, could activate SOCs, a different approach was used. In this case the additivity between the RTX-induced Ca^{2+} entry and the SERCA inhibitor (DBHQ)-induced Ca^{2+} entry was investigated.

The effects of RTX and DBHQ alone, and in combination, on Ca^{2+} entry are shown in Fig. 4.12 A. Examination of the mean values of the initial rates and the peak (maximum) values of Ca^{2+} entry after Ca^{2+}_{ext} re-addition are shown in Fig. 4.12 B. The results indicate that in the presence of RTX, DBHQ causes a large additional increase in Ca^{2+} entry, presumably due to the activation of SOCs which are not activated by the addition of RTX alone.

This result provides additional evidence about the failure of TRPV1 agonist RTX to activate SOCs in H4-IIE liver cells.

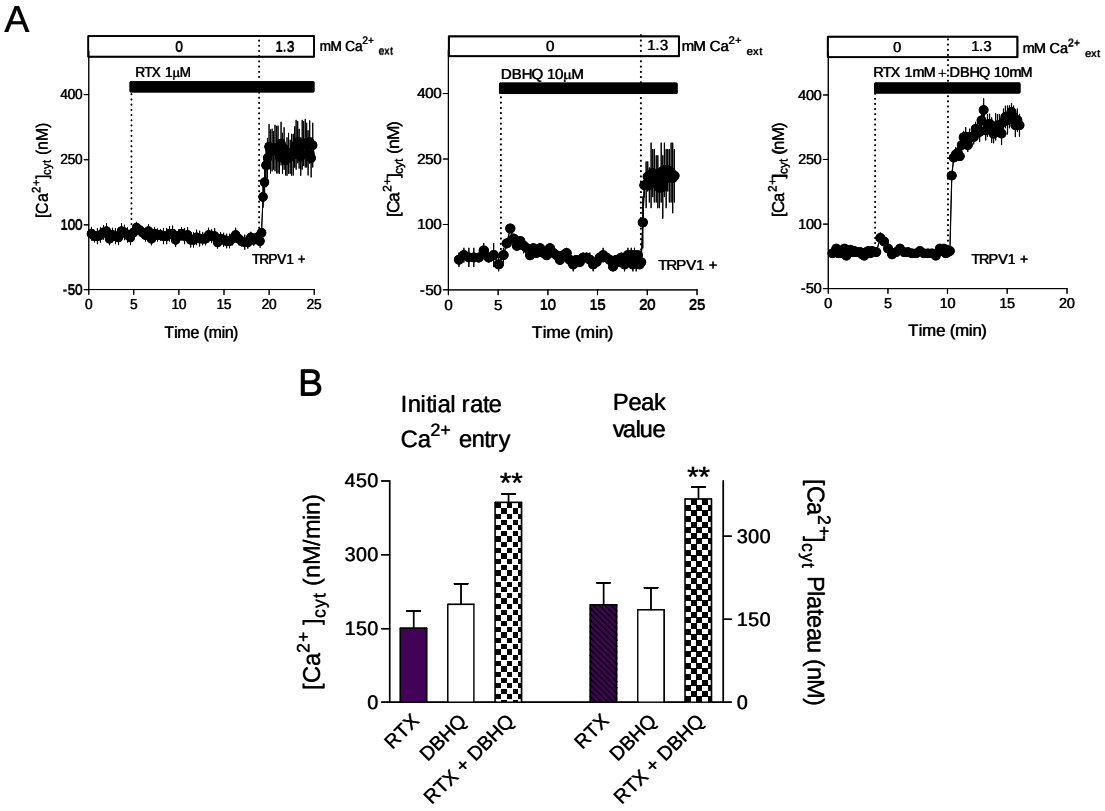

Fig. 4.12. DBHQ activates additional Ca^{2+} entry over and above that activated by RTX in cells ectopically expressing TRPV1. (**A**) The effects of RTX, DBHQ and RTX plus DBHQ, on $[Ca^{2+}]_{cyt}$ in TRPV1(+) cells. Cellular transfection and $[Ca^{2+}]_{cyt}$ measurements as a function of time in cells loaded with fura-2, were performed as described in Sections 2.5.4 and 2.3. The additions to the bath are indicated by the horizontal bars. The results shown are from a representative experiment, of those obtained in 4-6 similar experiments, in which the fluorescence of 4-8 TRPV1(+) H4-IIE cells was measured. (**B**) The initial rates of Ca^{2+} entry and peak (maximum) values of $[Ca^{2+}]_{cyt}$ following Ca^{2+}_{ext} addition (determined as described in Section 2.3), show that DBHQ activates additional Ca^{2+} entry over and above that activated by RTX. The results shown are the means $\pm$ SEM of 4-6 experiments. The degrees of significance (determined using ANOVA followed by Bonferroni *post hoc* test) for comparison of the values for initial rate and the peak of Ca^{2+} entries are: RTX *cf* DBHQ, P = 1 and RTX or DBHQ *cf* RTX plus DBHQ, ** P < 0.01.

4.2.6. Use of FFP-18 Ca^{2+} dye to determine whether the TRPV1-mediated Ca^{2+} release from the ER is originated beneath the plasma membrane

As was described in Section 3.3.9, the choleretic bile acid TDCA induced the release of Ca^{2+} from a subregion of the ER, detected by FFP-18 but not fura-2, considered to be close to the plasma membrane. This, in turn, induced the activation of Ca^{2+} entry through SOCs. Contrary to the results obtained with SERCA inhibitors or TDCA, the TRPV1-mediated Ca^{2+} release from the ER was not effective in activating SOCs as demonstrated in this chapter. Taking into account these results, it is possible that TRPV1-mediated Ca^{2+} release is originated from a different region of the ER to the one the SERCA inhibitors or TDCA mediated their Ca^{2+} release.

In order to test this hypothesis, Ca^{2+} located at sub-plasma membrane space ($(Ca^{2+})_{SPM}$) was measured using FFP-18 in H4-IIE cells previously transfected with Ad-Track-CMV-TRPV1 plasmid.

The results obtained with FFP-18 (Fig. 4.13 A) showed that, in the absence of Ca^{2+}_{ext}, RTX was unable to induce any change in $(Ca^{2+})_{SPM}$ levels in TRPV1(+) H4-IIE cells. To confirm that FFP-18 can detect an increase in Ca^{2+} near the plasma membrane, 1.3mM Ca^{2+}_{ext} was added followed RTX addition, leading to an increase in FFP-18 fluorescence due to Ca^{2+} entry through TRPV1 expressed in the plasma membrane. As shown in Fig. 4.13 B, in the absence of Ca^{2+}_{ext}, addition of the SERCA inhibitor thapsigargin induces a transient increase in $(Ca^{2+})_{SPM}$ detected by FFP-18 in TRPV1(+) cells. However, as shown previously in this chapter, the addition of RTX, in the absence of Ca^{2+}_{ext}, induced a fura-2-detectable transient increase in $[Ca^{2+}]_{cyt}$ in TRPV1(+) H4-IIE cells (Fig. 4.13 C).

These results indicate that the region of the ER from which RTX (via TRPV1) releases Ca^{2+} is further from the plasma membrane than the region (or a component of the region) from which thapsigargin releases Ca^{2+}.

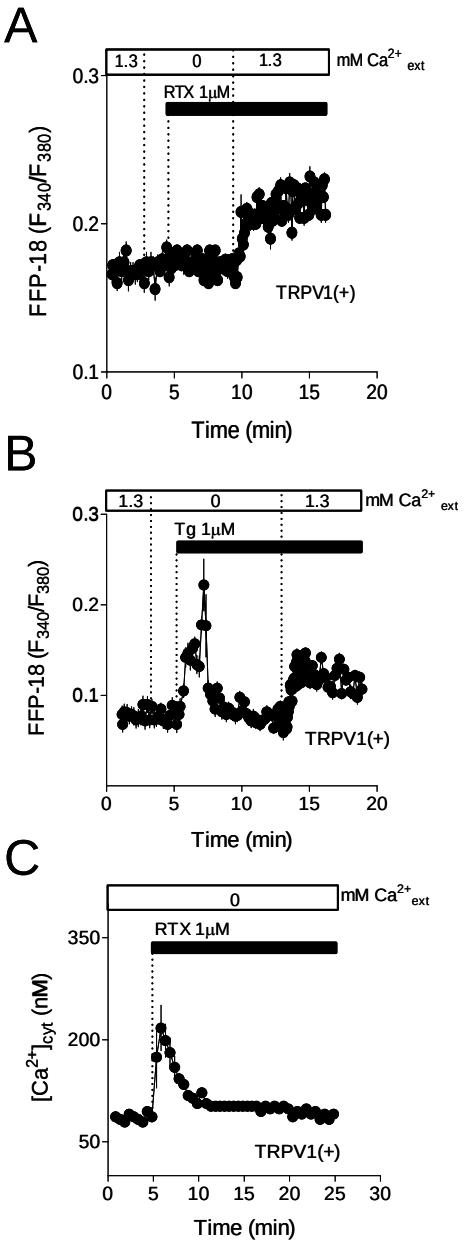

Fig. 4.13. In TRPV1(+) H4-IIE cells, the RTX-induced release of Ca^{2+} from ER detected by fura-2, is not observed using FFP-18. (**A**) In the absence of Ca^{2+}_{ext}, RTX (1μM) addition did not cause any changes in FFP-18 fluorescence in TRPV1(+). The further addition of Ca^{2+}_{ext}, in the presence of RTX, into the medium caused a sustained increase in FFP-18 fluorescence. (**B**) In cells loaded with FFP-18 and incubated in the absence of Ca^{2+}_{ext} (after prior incubation at 1.3mM Ca^{2+}_{ext}), 1μM thapsigargin (Tg) caused a transient increase in $(Ca^{2+})_{SPM}$. Subsequent addition of Ca^{2+}_{ext} caused a sustained increase in $(Ca^{2+})_{SPM}$. (**C**) In the absence of Ca^{2+}_{ext}, RTX (1μM) addition caused a fura-2 sensitive transient increase of $[Ca^{2+}]_{cyt}$ in TRPV1(+) but not TRPV1(-) H4-IIE cells. Cellular transfection, $[Ca^{2+}]_{cyt}$ and $(Ca^{2+})_{SPM}$ measurements as a function of time (in cells loaded with fura-2 and FFP-18 respectively), were performed as described in Section 2.5.4 and 2.3. The additions to the bath are indicated by the horizontal bars. The results shown are from a representative experiment, of those obtained in 3 similar experiments, in which the fluorescence of 5-7 TRPV1(+) or (-) H4-IIE cells was measured.

4.2.7. Effect of ionomycin-induced Ca^{2+} release in transfected and non-transfected TRPV1 H4-IIE liver cells

The results obtained in this chapter show that, in the presence of 1.3mM Ca^{2+}_{ext}, the initial values of $[Ca^{2+}]_{cyt}$ in TRPV1(+) cells, were higher than that in TRPV(-) cells (Figs. 4.5 A and 4.7 B). In addition, the release of Ca^{2+} induced by SERCA inhibitors DBHQ or thapsigargin was significantly smaller in TRPV1(+) cells than in TRPV1(-) cells, in the absence of Ca^{2+}_{ext} (figures 4.7 B and 4.9 A respectively). These results suggest that TRPV1 channels could have some level of constitutive activity when ectopically expressed in H4-IIE cells. In order to test this hypothesis, an experiment was designed in which, the depletion of intracellular Ca^{2+} stores was induced the by the addition of the Ca^{2+} ionophore, ionomycin in the absence of Ca^{2+}_{ext}. The resultant increases in $[Ca^{2+}]_{cyt}$ were compared in TRPV1(+) cells with respect to TRPV1(-) cells. Those values should represent the content of Ca^{2+} present in the intracellular stores.

As illustrated in Fig. 4.14, ionomycin induced the release of a large amount of Ca^{2+} from intracellular stores in TRPV1(+) cells when added to the incubation medium in zero Ca^{2+}_{ext}. However, the $[Ca^{2+}]_{cyt}$ released in TRPV1(-) cells was much higher than that induced in TRPV1(+) cells. This agrees with the possibility of a basal activity of ectopically expressed TRPV1 in H4-IIE cells.

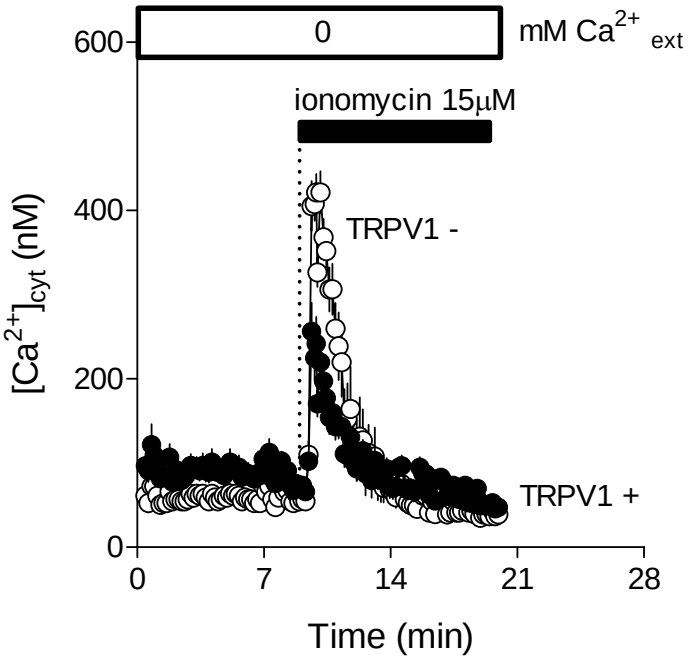

Fig. 4.14. Ionomycin-induced Ca^{2+} release in TRPV1(+) and TRPV1(-) H4-IIE liver cells. In the absence of Ca^{2+}_{ext}, ionomycin (15µM) addition caused a fura-2 sensitive transient increase on $[Ca^{2+}]_{cyt}$ in both TRPV1(-) and TRPV1(+) H4-IIE cells. The release induced by ionomycin in TRPV1(+) cells was much smaller than the one induced in TRPV1(-) cells. Cellular transfection and $[Ca^{2+}]_{cyt}$ measurements as a function of time in cells loaded with fura-2, were performed as described in Section 2.5.4 and 2.3. The additions to the bath are indicated by the horizontal bars. The result shown is from a representative experiment, of those obtained in 3 similar experiments, in which the fluorescence of 3-7 TRPV1(+) or(-)H4-IIE cells were measured.

4.3 Discussion

In this chapter evidence has been provided that when ectopically expressed in H4-IIE liver cells, TRPV1 is predominantly localised in the ER and the plasma membrane. The addition of TRPV1 agonists to TRPV1(+) cells, in the presence of Ca^{2+}_{ext}, induced Ca^{2+} entry sensitive to inhibition by the TRPV1 antagonist RR. In the absence of Ca^{2+}_{ext}, TRPV1 agonists induced the release of Ca^{2+} from intracellular stores to the extent similar to that induced by SERCA inhibitors. This Ca^{2+} release, which is insensitive to inhibition by RR, was detected by fura-2 but not FFP-18. However, in contrast to SERCA inhibitors, agonist of TRPV1 did not activate Ca^{2+} entry through SOCs in H4-IIE TRPV1(+) cells.

4.3.1. Ectopically expressed functional TRPV1 channels are distributed in the PM and the ER of H4-IIE liver cells

The results obtained by confocal microscopy using immunofluorescence and co-localisation with ER markers indicated that: in addition to the ectopical expression of TRPV1 in the plasma membrane, TRPV1 is predominately located in the ER of H4-IIE liver cells. Additional evidence indicating the ER localisation of TRPV1 channels represents the observation that TRPV1 agonists release similar amounts of intracellular Ca^{2+} to that released by the SERCA inhibitor thapsigargin. Three experimental observations indicate that TRPV1 mediates Ca^{2+} release from a large proportion of the same intracellular compartment as that which SERCA inhibitors release Ca^{2+}:

- Firstly, in TRPV1(+) cells incubated in the absence of Ca^{2+}_{ext}, SERCA inhibitors did not release any detectable additional Ca^{2+} when added after RTX. Note, the failure of SERCA inhibitors to release Ca^{2+} is unlikely to be due to RTX inhibition

of the action of the SERCA inhibitor, since it was shown that RTX does not inhibit the ability of SERCA inhibitors to release Ca^{2+} from the ER in TRPV1(-) (non-transfected) cells (see Fig. 4.7 A).

- Secondly, the amount of Ca^{2+} released by RTX in TRPV1(+) cells, incubated in the absence of Ca^{2+}_{ext}, was similar in magnitude to that released by SERCA inhibitors.

- Finally, the third evidence is given by the RTX-induced decrease in the initial (basal) fluorescence of Calcium Green 5N observed in the ER of TRPV1(+) cells. Calcium Green 5N dissociation constant for Ca^{2+} in the absence of Mg^{2+}, is ~14 μM, which means it could monitor changes in Ca^{2+} levels in intracellular stores where calcium is present at μM ranges (such as the ER) (Combettes *et al.*, 1996; Ukhanov *et al.*, 1998; Sanchez *et al.*, 2003).

The results of the experiments undertaken in TRPV1(+) cells using fura-2 and FFP-18 calcium dyes, presented some evidence about the possible cellular location of the TRPV1 agonists-induced Ca^{2+} release from the ER. FFP-18 has been successfully used to monitor rapid changes in the sub-plasma membrane Ca^{2+} levels ($(Ca^{2+})_{SPM}$), in a variety of cells types (Etter *et al.*, 1994; Etter *et al.*, 1996; Davies and Hallett, 1998; Graier *et al.*, 1998; Chadborn *et al.*, 2002). Additionally, it has been described that FFP-18 monitor changes in $[Ca^{2+}]_{SPM}$ rather than the bulk $[Ca^{2+}]_{cyt}$ (Davies *et al.*, 1997; Paltauf-Doburzynska *et al.*, 1998; Chadborn *et al.*, 2002). Using this Ca^{2+} dye, it was observed that, in the absence of Ca^{2+}_{ext}, when the TRPV1 agonist-induced Ca^{2+} release (detected with fura-2) was measured using FFP-18, RTX addition did not induce any increase in $(Ca^{2+})_{SPM}$. However FFP-18 was able to detect changes in $(Ca^{2+})_{SPM}$ induced by SERCA inhibitor thapsigargin, in the absence of Ca^{2+}_{ext}. These results indicate that the region of the ER from which RTX (via TRPV1) releases Ca^{2+}

is further from the plasma membrane than the region, or a component of the region, from which thapsigargin releases Ca^{2+}.

It has been suggested in this chapter, that ectopically expressed TRPV1 could be constitutively active in the environment of H4-IIE liver cells. The evidence supporting this observation is based on: (i) In the presence of 1.3mM Ca^{2+}_{ext}, the initial levels of $[Ca^{2+}]_{cyt}$ in TRPV1(+) cells was higher than that in TRPV1(-) cells; (ii) The amount of Ca^{2+} released by SERCA inhibitors (DBHQ and thapsigargin) from the ER of TRPV1(+) cells, was less than that released from TRPV1(-) cells; (iii) The amount of Ca^{2+} released by the Ca^{2+} ionophore ionomycin from TRPV1(+) cells was less than that released from TRPV1(-) cells. Constitutive activity of TRPV1 and some other TRP proteins has been reported previously (Chuang *et al.*, 2001; Dietrich *et al.*, 2003; Peng *et al.*, 2003; Albert *et al.*, 2006; Beech, 2007; Numaga *et al.*, 2007)). It has also been suggested that TRPV1 may be activated by endogenous signalling molecules (Caterina et al., 2000; Hwang et al., 2000).

The results described above are consistent with those obtained by others who have shown that endogenous (Olah *et al.*, 2001; Liu *et al.*, 2003; Karai *et al.*, 2004) and ectopically expressed (Turner *et al.*, 2003; Wisnoskey *et al.*, 2003; Karai *et al.*, 2004) TRPV1, are functionally localized in the ER. Although one study concluded that TRPV1 agonists released Ca^{2+} from SERCA inhibitor-insensitive stores (Liu et al., 2003). These differences may be due to the formation of heterotetrameric TRPV1 channels, in which TRPV1 is associated with other TRP polypeptides. This could produce differences in the TRPV1 proteins expressed in the host cell, which may alter the response of TRPV1 to it's agonists, and it's regulation by accessory proteins (Kedei *et al.*, 2001; Gunthorpe *et al.*, 2002).

4.3.2. TRPV1 agonist mediated Ca^{2+} release from the ER does not activate Ca^{2+} entry through SOCs in H4-IIE liver cells

The following observations provide evidence that Ca^{2+} released from the ER via TRPV1, does not activate SOCs: (i) In the presence of ruthenium red, to inhibit Ca^{2+} entry through TRPV1 in the plasma membrane, addition of TRPV1 agonists to TRPV1(+) cells did not activate Ca^{2+} entry in any of the cells tested, as assessed using fura-2 and "Ca^{2+} add-back" assay; (ii) The SERCA inhibitor DBHQ caused substantial additional Ca^{2+} entry in TRPV1(+) cells, over and above that induced by RTX; (iii) In a group of experiments undertaken in parallel by our collaborators (Edoardo C. Aromataris and Grigori Y. Rychkov) using patch clamp recording in TRPV1(+) H4-IIE cells, no inward current with the properties of the liver cell SOCs was detected, when the TRPV1 agonist N-vanillylnonamide was added to the incubation medium (see whole paper in the appendices section).

These results are consistent with the study that has showed that the release of Ca^{2+} from intracellular stores via TRPV1 does not activate SOCs (Wisnoskey *et al.*, 2003).

4.3.3. Additional observations and controls

- Using immunofluorescence assays, it was observed that H4-IIE rat liver cells do not express endogenous TRPV1 proteins. This finding was confirmed by the lack of response (increases in $[Ca^{2+}]_{cyt}$) of control cells to TRPV1 agonist. Although, the presence of TRPV1 mRNA in the HepG2 human liver cell line has been reported (Vriens et al., 2004)). Such a contradiction could be explained by the fact that even though both cell lines are derived from liver, they were obtained from the liver of different species (rat and human). In addition, it has been described that cell lines derived from the same species and tissue, can exhibit differences in mRNA levels

and subsequent expression of proteins. As is the case for the EGF receptor ligand mRNA (amphiregulin), which is abundantly expressed in the GP2d cell line but absent in GP5d cell line, despite both cell lines being derived from the same colon adenocarcinoma (Solic *et al.*, 1995).

- The failure of RR to inhibit TRPV1-mediated release of Ca^{2+} from intracellular organelles, as shown in this chapter, is most likely due to the inability of RR to reach TRPV1 at these locations. Ruthenium red binds to many proteins (Tani and Ametani, 1971; Maggi, 1991; Gunthorpe *et al.*, 2002; Smith *et al.*, 2002) and it has been suggested that it is unlikely that any ruthenium red crosses the plasma membrane to enter the cytoplasmic space (Tani and Ametani, 1971; Trudeau *et al.*, 1996).

- It is possible that, in the experiments conducted to detect TRPV1-induced Ca^{2+} entry through SOCs, the necessary presence of ruthenium red (and the TRPV1 agonist itself) could have caused the inhibition of SOCs. However, these possibilities are considered unlikely because, as shown in control experiments undertaken in this chapter, the presence of RR and TRPV1 agonist RTX in the incubation medium did not block SERCA inhibitor-initiated Ca^{2+} entry through SOCs. It has been reported that TRPV1 agonist capsaicin can inhibit cyclopiazonic acid-induced store-operated Ca^{2+} entry in neutrophils (Wang *et al.*, 2005). In another study with Jurkat cells it was observed that the TRPV1 agonist capsaicin and RTX block I_{CRAC} activated by thapsigargin (Fischer *et al.*, 2001); although, the concentration of TRPV1 agonists used in those studies ($\geq$ 100 μM and IC_{50} 32μM), were much higher to the one used in this work.

- The possibility that Ca^{2+} entry through SOCs is inhibited by a decrease in membrane potential, induced by Na^{+} entry through TRPV1 in the plasma membrane (Kagaya *et al.*, 2002), is also considered unlikely. Na^{+} entry during the Ca^{2+}-add back assay was blocked by RR. In addition it is reported that the effect of any altered membrane potential on Ca^{2+} entry through SOCs is likely to be small (Parekh and Putney, 2005).

In conclusion, the present results provide evidence that the bulk of the ER is not required for the activation of SOCs, supporting the evidence presented in chapter III, which suggested that SOCs are activated by the release of Ca^{2+} from a small ER region located in the vicinity of the plasma membrane.

Recent evidence from the literature, demonstrates that the activation of SOCs (CRAC channels) involves the release of Ca^{2+} from the ER and the movement of the Ca^{2+} sensor STIM1 (Stromal Interaction Molecule 1) within the ER, to junctional ER-PM regions, as illustrated schematically in the introductory chapter of this thesis in Fig. 1.6 (Lewis, 2007). Given this evidence, the effect of TDCA choleretic bile acid and TRPV1 agonist, on regulating STIM1 redistribution, will be investigated in the next chapter.

CHAPTER V: EFFECT OF TDCA AND TRPV1 AGONISTS ON STIM1 DISTRIBUTION WITHIN THE ER OF LIVER CELLS

5.1 Introduction

Recent studies have shown that Stromal Interaction Molecule (STIM) protein constitutes the Ca^{2+} sensor which detects the decrease in Ca^{2+} in the ER and communicates this information to SOCs in the plasma membrane. It has been demonstrated that, when Ca^{2+} decreases in the ER, STIM1 redistributes within the ER into punctate aggregates located adjacent to the plasma membrane (Liou *et al.*, 2005; Zhang *et al.*, 2005; Baba *et al.*, 2006; Mercer *et al.*, 2006; Wu *et al.*, 2006; Xu *et al.*, 2006; Liou *et al.*, 2007; Ong *et al.*, 2007a).

In the last two chapters, it was demonstrated that the choleretic bile acid TDCA induced the release of Ca^{2+} from a region of the ER located in the vicinity of the PM; while TRPV1 agonists induced the release of Ca^{2+} from the bulk of the ER. Additionally, TDCA-induced Ca^{2+} release activated SOCs, whereas the TRPV1 agonist-induced Ca^{2+} release failed to activate SOCs.

Considering that the redistribution of STIM1 within the ER region close to the PM is a necessary step in the activation of SOCs (Zhang *et al.*, 2005); the aims of the present experiments were (i) to identify the effects of TDCA bile acid and TRPV1 agonists on STIM1 distribution within the ER of H4-IIE liver cells; and (ii) to

evaluate the requirement of STIM1 proteins in the activation of Ca^{2+} entry through SOCs induced by choleretic bile acid TDCA.

This chapter demonstrates that in H4-IIE liver cells STIM1 proteins are required for the activation of thapsigargin- and TDCA-induced Ca^{2+} entry through SOCs. Additionally it is described the ability of thapsigargin and TDCA, but not TRPV1 agonists, to induce the reversible redistribution of STIM1 into punctate aggregates within the ER, in a region near to the PM.

5.2 Results

5.2.1. Effect of endogenous STIM1 proteins on SOCs activation in H4-IIE liver cells

The presence of endogenous STIM1 in H4-IIE liver cells was assessed by immunofluorescence using anti-GOK/STIM1 and Alexa-Fluor 488-conjugated antibodies. Representative images obtained from the immunofluorescence assay are shown in Fig 5.1. As shown in the middle panel, the green fluorescence (from the Alexa-Fluor 488-conjugated antibody), is distributed in the cytoplasmic space. These immunofluorescence results illustrate the endogenous STIM1 proteins expressed in H4-IIE cells.

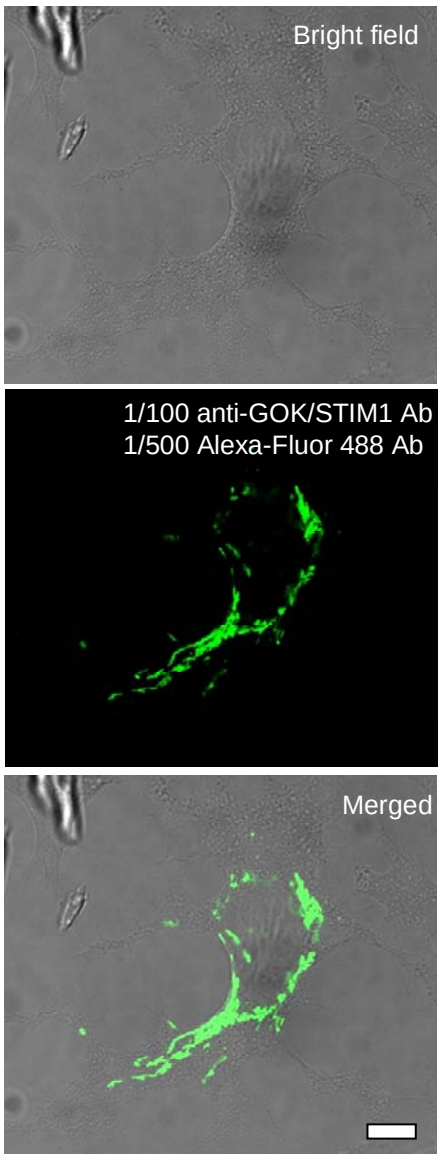

Fig. 5.1. H4-IIE cells express endogenous STIM1 proteins. A representative confocal image, of a H4-IIE cell, resulting from immunofluorescence against endogenous STIM1 is shown. The top panel shows cells in bright field, while the middle panel shows the pattern of endogenous STIM1 proteins distribution (identified by immunofluorescence using Alexa-Fluor 488-conjugated antibody). The merged image shows the distribution of endogenous expressed STIM1 proteins in a continuous intracellular structure surrounded the nucleus of H4-IIE. Immunofluorescence and imaging by confocal microscopy assays were performed as described in Section 2.7.1. The scale bar represents 10 μm. The results shown are representative of those obtained for one of 57 cells examined in 6 separate experiments.

To test if the release of Ca^{2+} from the ER could initiate the redistribution of endogenous STIM1, H4-IIE liver cells were exposed for 10 min to the SERCA inhibitor thapsigargin. After the incubation period the cells were fixed and an immunofluorescence assay, to detect STIM1 proteins, was performed. In order to determine the co-localisation of the endogenous STIM1 distribution within the ER, this experiment was performed on H4-IIE cells previously transfected with the ER marker pDsRed2-ER. The pDsRed2-ER plasmid encodes DsRed2 fluorescent proteins bearing the ER-targeting sequence KDEL (this confers exclusive ER localisation of the expressed DsRed fluorescent proteins).

The results are shown in Fig. 5.2. The green fluorescence corresponds to STIM1 proteins (identified by Alexa-Fluor 488-conjugated antibody fluorescence) and red fluorescence corresponds to the ER structure (identified by DsRed2 fluorescence expressed by DsRed2-ER plasmid). As indicated by the co-localisation of both fluorescent markers (yellow colour), endogenous STIM1 proteins are located in the ER of H4-IIE cells (Fig. 5.2, A, right panel). Additionally, thapsigargin caused the redistribution of endogenous STIM1 proteins (Fig. 5.2, A, left panel), into a punctate pattern (Fig. 5.2, B, left panel), within the ER of H4-IIE cells (Fig. 5.2, B, right panel) as indicated by the high levels of co-localisation.

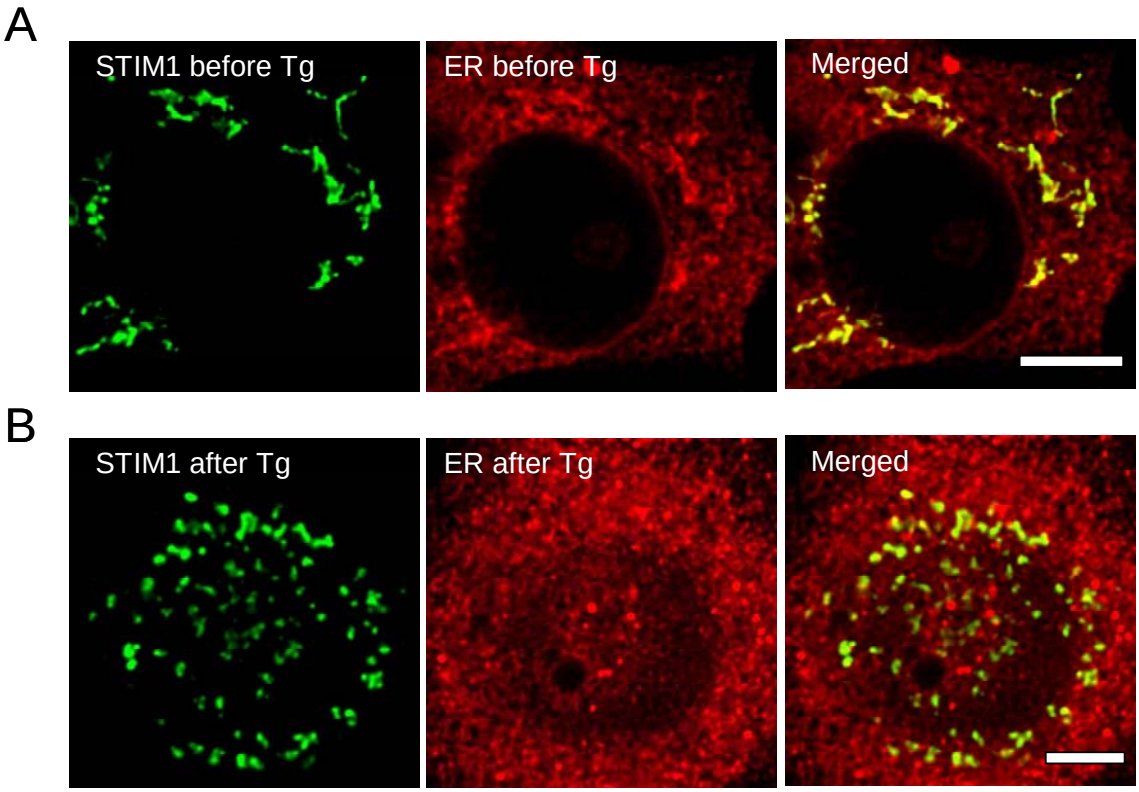

Fig. 5.2. Endogenous STIM1 redistributes throughout the ER into a punctate aggregates by thapsigargin addition. Representative confocal images of the endogenous expressed STIM1 proteins localisation (by Alexa-Fluor 488-conjugated antibody, left panels), the ER structure (DsRed2 fluorescence, middle panels), and the merged images (right panels) are presented. Before the immunofluorescence assay, the cells were treated for 10 min with either 2μL DMSO (**A**) or 1μM thapsigargin (Tg) (**B**). Treatment with Tg induced the redistribution of endogenous STIM1 proteins from a tubular like structures (top) to punctate aggregates (bottom). Note the high co-localisation (yellow colour) of both fluorescent molecules in the merged images (right panels). The ER structure was visualized by the DsRed2 fluorescent protein which is bearing the ER-targeting sequence KDEL in the pDesRed2-ER plasmid. Immunofluorescence and imaging by confocal microscopy assays were performed as described in Section 2.8.3. The scale bar represents 10 μm. The results shown are representative of those obtained for one of 30 (**A**) or 22 (**B**) cells examined in 6 separate experiments.

The requirement of endogenous STIM1 proteins in the activation of Ca^{2+} entry through the SOCs, in H4-IIE cells was then investigated. For this, the thapsigargin-induced Ca^{2+} entry through SOCs, in cells where the STIM1 protein levels were diminished by siRNA transfection, was compared with the thapsigargin-induced Ca^{2+} entry through SOCs in siRNA control transfected cells (which should have normal levels of STIM1). The initial rate and maximum peak of Ca^{2+} entry through SOCs was calculated using the "Ca^{2+}-add back" assay. The effectiveness of this siRNA against STIM1 in H4-IIE cells has been previously tested in our lab (Litjens *et al.*, 2007).

As shown in Fig. 5.3, the transfection with siRNA against STIM1 induced approximately 70% inhibition of both, the initial rate and the maximum peak values of Ca^{2+} entry through SOCs (Fig. 5.3 B and C) compared to the siRNA control transfected cells (Fig. 5.3 A). These results indicate that the presence of STIM1 in H4-IIE cells is required for the SERCA inhibitor-induced activation of Ca^{2+} entry through SOCs.

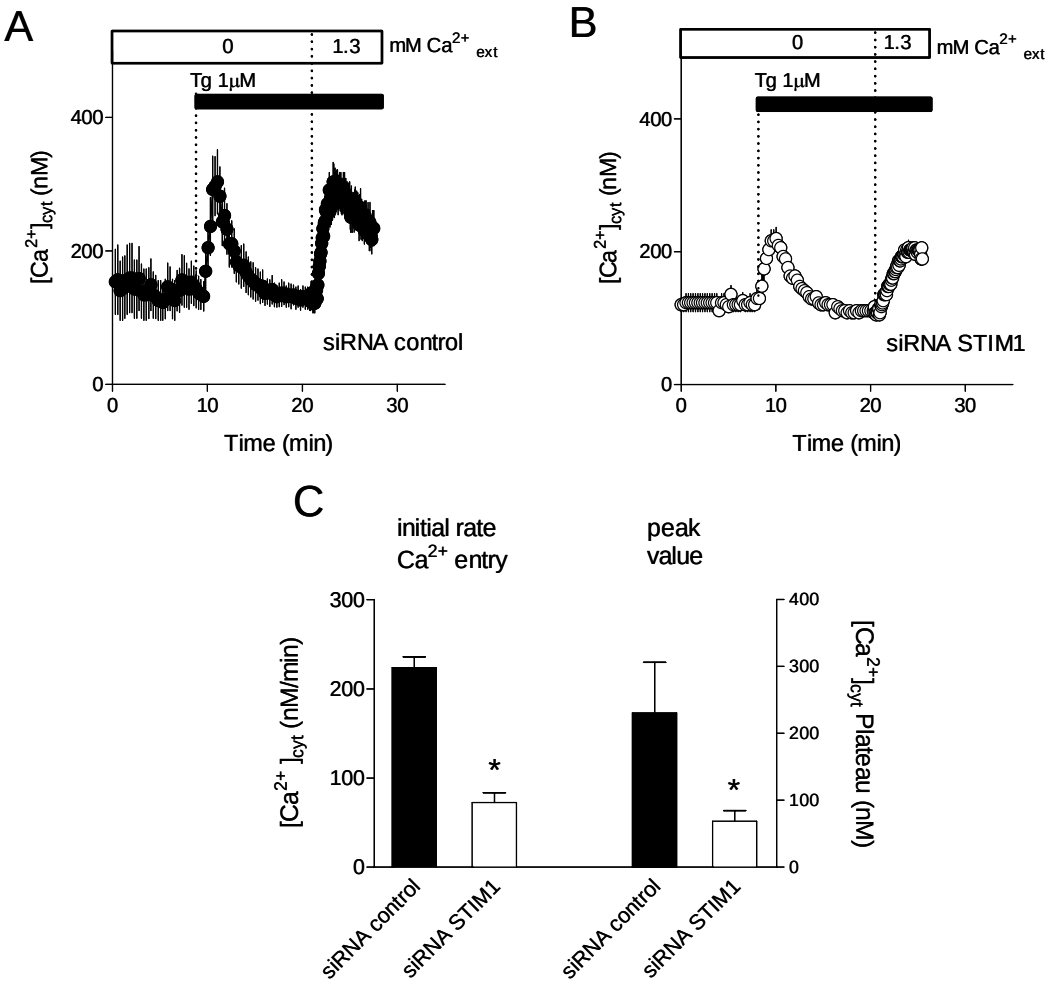

Fig. 5.3. Transfection with siRNA against STIM1 reduces the thapsigargin-induced Ca^{2+} entry through SOCs. In H4-IIE cells transfected with control siRNA (**A**) or with siRNA against STIM1 (**B**), the addition of 1μM Tg (in the absence of $Ca^{2+}{}_{ext}$) induced the release of Ca^{2+} from intracellular stores followed by the Ca^{2+} entry through the SOCs when $Ca^{2+}{}_{ext}$ is added back to the bath. Knockdown of STIM1 proteins by siRNA and $[Ca^{2+}]_{cyt}$ measurements as a function of time in cells loaded with fura-2, were performed as described in Sections 2.6 and 2.3. The additions to the bath are indicated by the horizontal bars. The results shown are from a representative experiment, of those obtained in 3 similar experiments, in which the fluorescence of 10-20 H4-IIE cells was measured. (**C**) The initial rate and the peak (maximum) of Ca^{2+} entry through SOCs (induced by Tg), in cells treated with siRNA against STIM1, were significantly smaller than the ones obtained in siRNA control treated cells ($P < 0.05$). The values in **C** are the means ± SEM of 3 experiments of those in **A** and **B**. The initial rate and the peak (maximum) of Ca^{2+} entry were determined as described in Section 2.3.

5.2.2. Distribution of ectopically expressed STIM1 proteins in H4-IIE liver cells and consequences in SOCs activity

Although the immunofluorescence experiments were useful in providing information about the presence and redistribution of endogenous STIM1 within the ER, the ectopical expression of STIM1 conjugated to a fluorescent molecule in living cells, represents a better system for monitoring the dynamics and the localisation of STIM1 redistribution. This provides the possibility of a real time study. Hence ectopical expression of STIM1 proteins via transfection with GFP-STIM1/pApuro DNA was then assessed.

A co-localisation assay was performed in order to test if ectopically expressed STIM1 proteins were located in the ER. For this, a co-transfection between of GFP-STIM1/pApuro plasmid (encoding GFP-STIM1 proteins) and pDsRed2-ER plasmid (encoding DsRed2 fluorescent proteins) was performed, and the resultant fluorescent molecules imaged by confocal microscopy.

Fig. 5.4 shows a confocal image of a H4-IIE cell co-expressing both fluorescent molecules. As illustrated in the bottom panel of this figure, STIM1 proteins are homogeneously distributed throughout the ER, as indicated by co-localisation (yellow colour) of the GFP fluorescence with the DsRed2 fluorescence. Note that the images of GFP-STIM1 fluorescence were acquired in a Z-plane near the middle of the cell (nucleus visible).

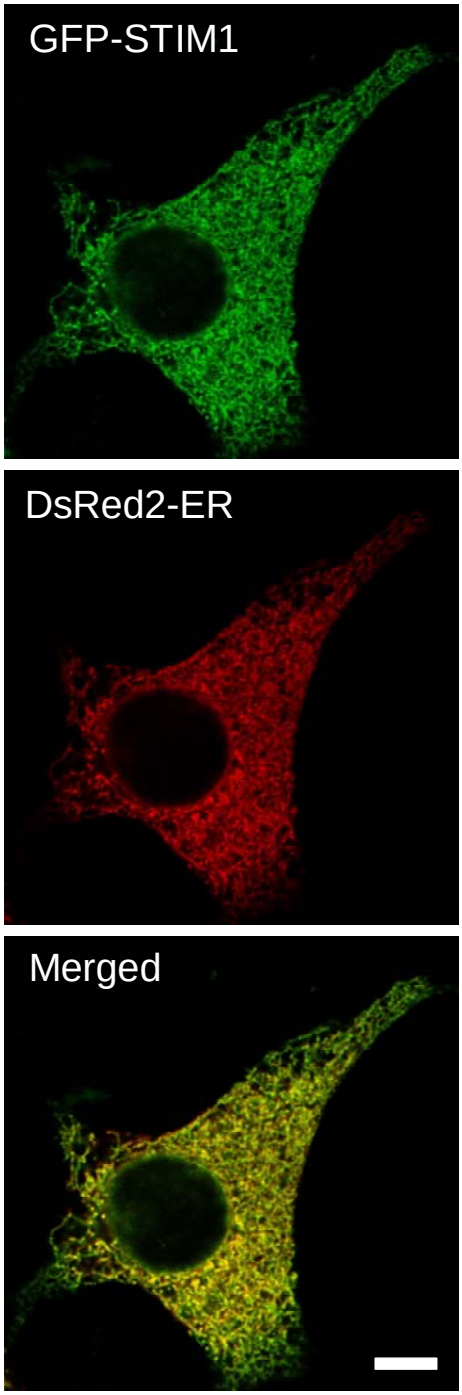

Fig. 5.4. Ectopically expressed STIM1 distributes throughout the ER in H4-IIE liver cells. Representative confocal images of ectopically expressed STIM1 proteins localisation (GFP fluorescence, top panel), the ER structure (DsRed2 fluorescence, middle panel), in the same living cell, and the merged images (bottom panels) are presented. Note in the merged image the high degree of co-localisation of both fluorescent molecules (yellow colour). STIM1 proteins were visualised in a Z-plane section in the middle of the cell (note nucleus region excluding STIM1). Cellular transfection and imaging by confocal microscopy were performed as described in Sections 2.5.4 and 2.8.4. The scale bar represents 10 μm. The results shown are representative of those obtained for one of 23 cells examined in 4 separate experiments.

To test if the release of Ca^{2+} from the ER induces the redistribution of ectopically expressed STIM1, the SERCA inhibitor thapsigargin was added to the incubation medium and the STIM1 distribution imaged by confocal microscopy. STIM1 proteins were ectopically expressed in H4-IIE cells by transfection with DNA encoding GFP-STIM1.

As shown in Fig. 5.5, the incubation with thapsigargin, in the absence of Ca^{2+}_{ext}, induced the redistribution of ectopically expressed STIM1 from a homogeneously tubular net like structure (top panel) into a punctate pattern (bottom panel) in H4-IIE cells. Note that the images of GFP-STIM1 fluorescence were acquired in a Z-plane near the plasma membrane (no nucleus visible), hence representing the STIM1 distribution close to the plasma membrane.

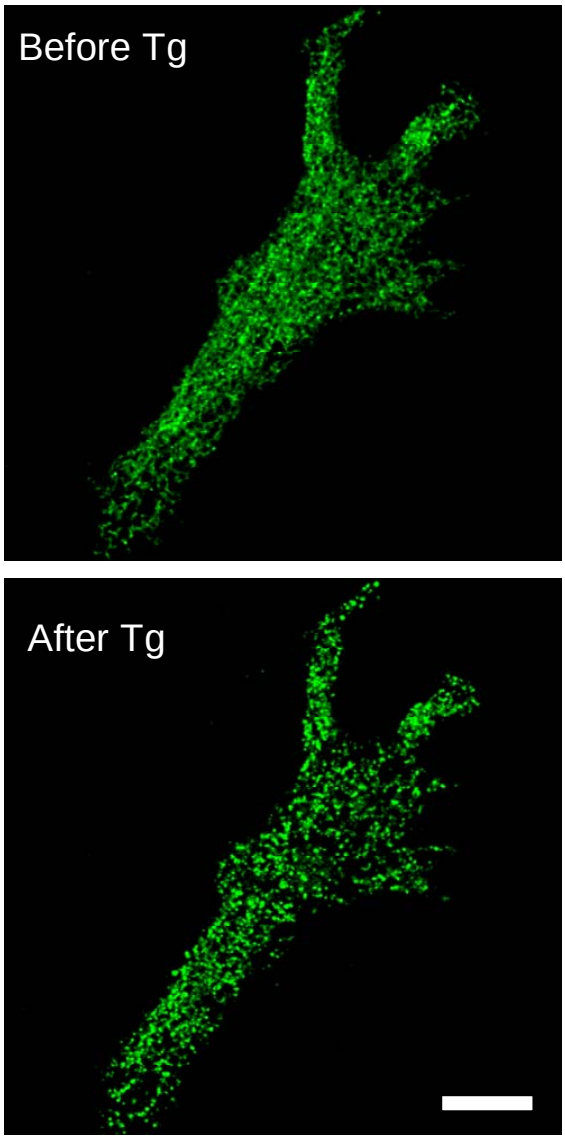

Fig. 5.5. SERCA inhibitor thapsigargin redistributes ectopically expressed STIM1 into punctate aggregates. Representative confocal images of ectopically expressed STIM1 proteins distribution before (top panel) and after 5min thapsigargin (1μM) addition (bottom panel), in the same living H4-IIE cell, are shown. Tg addition (in the absence of Ca^{2+}_{ext}) induces the redistribution of ectopically expressed STIM1 proteins from tubular net like structures (top panel) to punctate aggregates (bottom panel). STIM1 proteins were visualised in a Z-plane section close to the plasma (note the absence of nucleus), by imaging of the GFP fluorescence expressed by STIM1/pApuro plasmid. Cellular transfection and imaging by confocal microscopy were performed as described in Section 2.7.2. The scale bar represents 10 μm. The results shown are representative of those obtained for one of 32 cells examined in 4 separate experiments.

To investigate whether STIM1 ectopical expression influences the activation of Ca^{2+} entry through SOCs in H4-IIE cells; the magnitude of the thapsigargin-induced Ca^{2+} entry through SOCs, in cells where the STIM1 protein levels were augmented (by GFP-STIM1 transfection), was compared with thapsigargin-induced Ca^{2+} entry through SOCs in control transfected cells (that should have normal levels of STIM1). The rate of Ca^{2+} entry and the magnitude of the entry through SOCs were calculated using the "add-back" assay.

As shown in Fig. 5.6, the ectopical expression of STIM1 proteins caused an increase of approximately 50% in both, the initial rate and the maximum peak values of Ca^{2+} entry through SOCs (Fig. 5.6 B and C) compared to control transfected cells (Fig. 5.6 A). This result indicates that STIM1 plays an important role in the activation of Ca^{2+} entry through SOCs in H4-IIE liver cells.

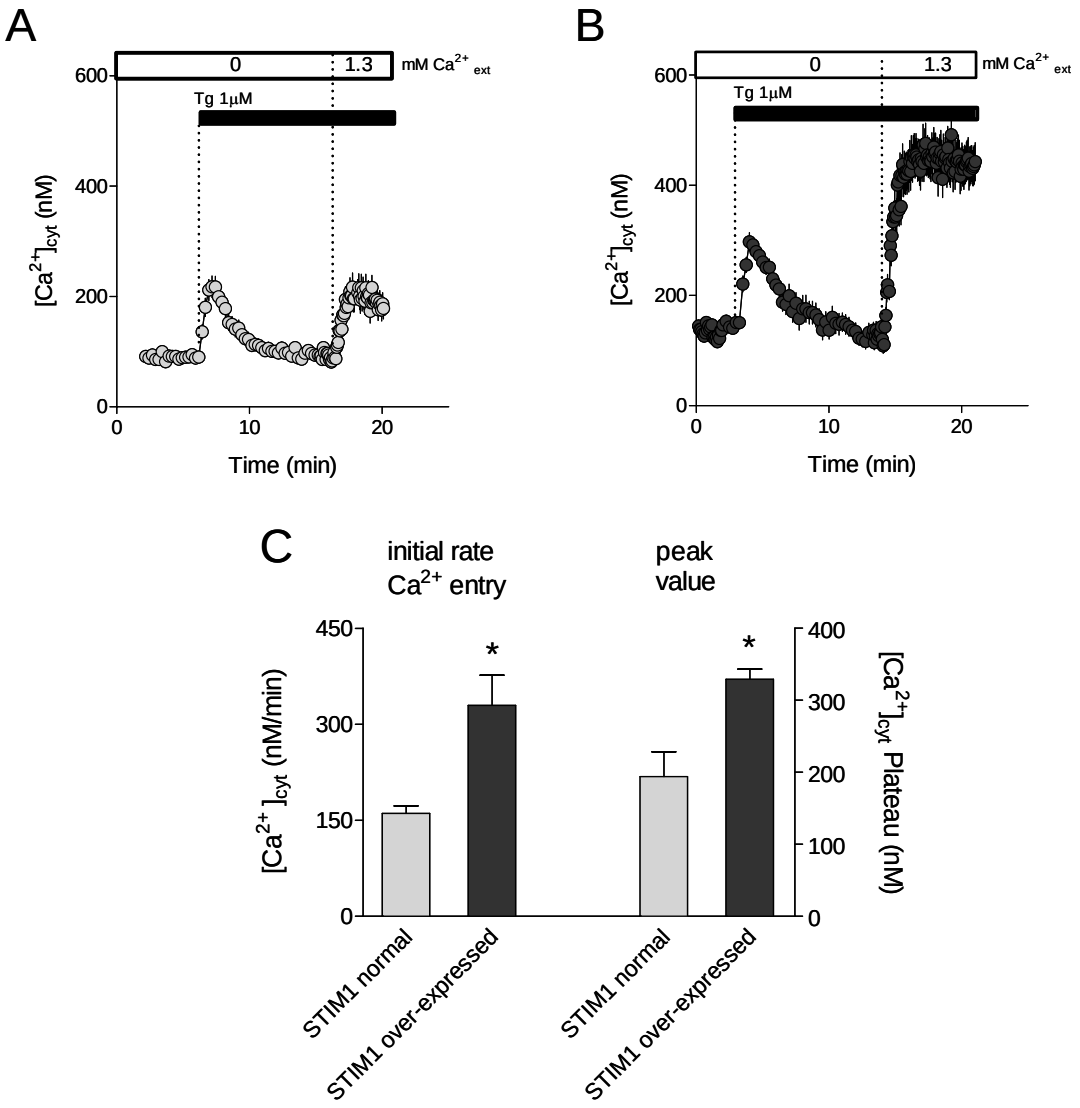

Fig. 5.6. Ectopic expression of STIM1 proteins increases thapsigargin-mediated Ca^{2+} entry through SOCs. In H4-IIE cells control transfected (**A**) or transfected with GFP-STIM1/pApuro plasmid (**B**), the addition of 1µM Tg (in the absence of Ca^{2+}_{ext}) induced the release of Ca^{2+} from intracellular stores followed by the Ca^{2+} entry through the SOCs when Ca^{2+}_{ext} is added back to the bath. Ectopic expression of STIM1 proteins by STIM1/pApuro DNA transfection and $[Ca^{2+}]_{cyt}$ measurements as a function of time in cells loaded with fura-2, were performed as described in Sections 2.5.4 and 2.3. The additions to the bath are indicated by the horizontal bars. The results shown are from a representative experiment, of those obtained in 3 similar experiments, in which the fluorescence of 10-20 H4-IIE cells was measured. (**C**) The initial rate and the peak (maximum) of Ca^{2+} entry through SOCs (induced by Tg), in cells ectopically expressing STIM1, were significantly higher than the ones obtained in control transfected cells ($P < 0.05$). The values in **C** are the means ± SEM of 3 experiments of those in **A** and **B**. The initial rate and the peak (maximum) of Ca^{2+} entry were determined as described in Section 2.3.

5.2.3. Effect of choleretic bile acid TDCA on the distribution of STIM1 in H4-IIE liver cells

In chapter III, it was demonstrated that the addition of choleretic bile acid TDCA to the incubation medium, induced activation of SOCs involving the release of Ca^{2+} from a region of the ER in the vicinity of the PM. Thus, the effect of TDCA on the distribution of endogenous STIM1 proteins was then evaluated. For this H4-IIE cells were incubated for 10 minutes with either thapsigargin (in the absence of Ca^{2+}_{ext}), TDCA (in 10mM Ca^{2+}_{ext}) or DMSO (vehicle in which thapsigargin or TDCA were dissolved). After the incubation period the cells were fixed and an immunofluorescence assay against STIM1 proteins subsequently performed using anti-GOK/STIM1 and Alexa-Fluor 488-conjugated antibodies.

The results of the immunofluorescence are shown in Fig. 5.7. As illustrated, TDCA caused a redistribution of the Alexa-Fluor 488 fluorescence (corresponding to the endogenous STIM1) from a tubular net like structure to a punctate pattern (Fig. 5.7, bottom panel), similar to that caused by thapsigargin (Fig. 5.7, middle panel), in the absence of Ca^{2+}_{ext}.

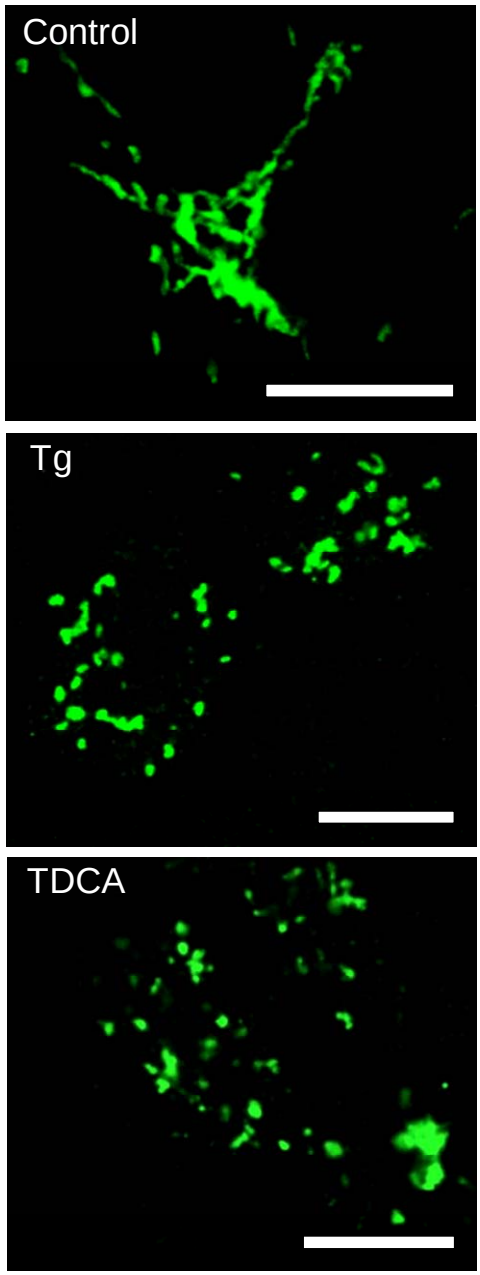

Fig. 5.7. TDCA induce the redistribution of the endogenous STIM1. Representative confocal immunofluorescence images in a Z-plane close to the plasma membrane of endogenous STIM1 in cells incubated in the absence of agonist (Control), or in the presence of 1 μM thapsigargin for 10 min in zero Ca^{2+}_{ext} (Tg), or with 300 μM TDCA for 10 min in 10 mM Ca^{2+}_{ext} (TDCA). TDCA treatment (bottom panel) induces the redistribution of endogenous STIM1 proteins to punctate aggregates in a similar to Tg manner (middle panel). Immunofluorescence and imaging by confocal microscopy assays were performed as described in Section 2.7.1. The scale bar represents 10 μm. The results shown are representative of those obtained for one of 47 cells examined in 4 separate experiments.

Additionally, the effect of TDCA on the distribution of ectopically expressed STIM1 proteins was examined. STIM1 proteins were ectopically expressed in H4-IIE cells by transfection with DNA encoding GFP-STIM1.

A series of confocal images are shown in Fig. 5.8. The images of GFP-STIM1 fluorescence were acquired in a Z-plane near the plasma membrane (no nucleus visible), hence representing the STIM1 distribution close to the plasma membrane. As shown in Fig. 5.8 B, the addition of TDCA induced the redistribution of STIM1 in a similar manner to the redistribution induced by thapsigargin (Fig. 5.8 A, bottom panel). The effect of TDCA on STIM1 redistribution was similar in the absence of Ca^{2+}_{ext} (Fig. 5.8 B, top panel) and in the presence of 10mM Ca^{2+}_{ext} (Fig. 5.8 B, bottom panel).

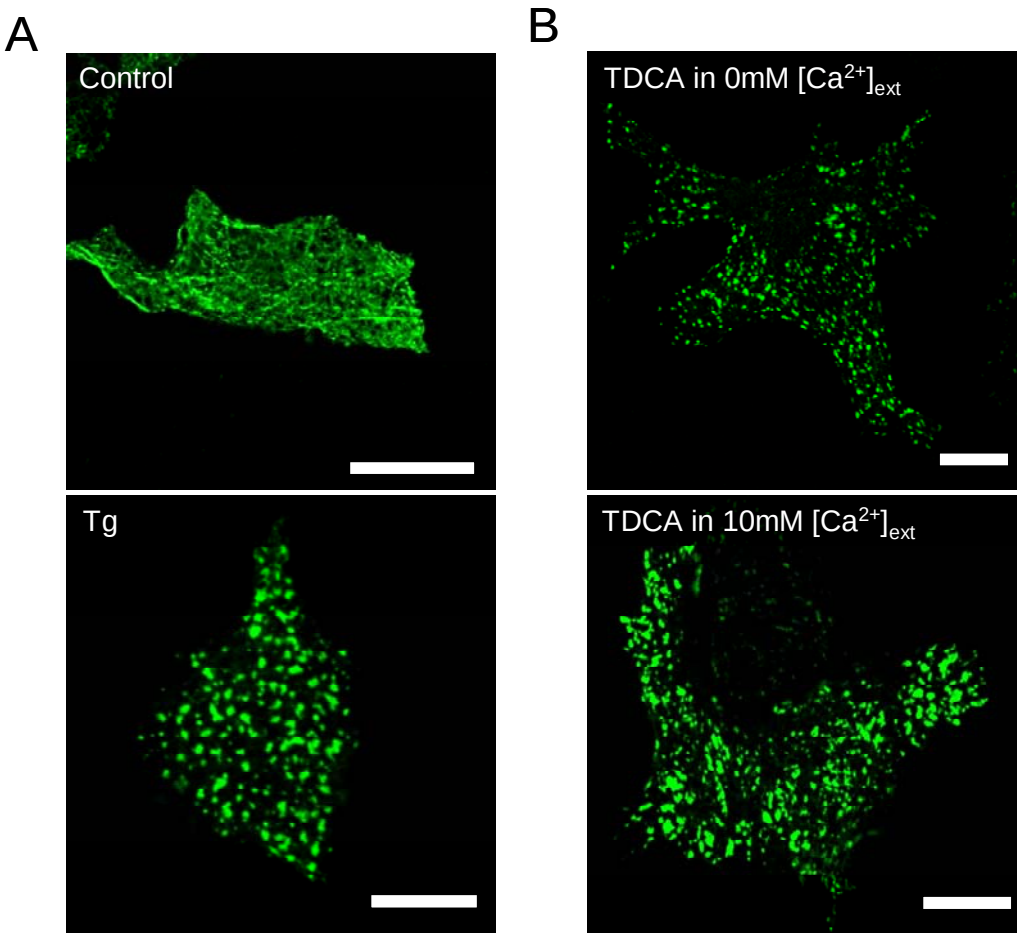

Fig. 5.8. TDCA induce the redistribution of ectopically expressed STIM1 in the presence or the absence of Ca^{2+}_{ext}. (**A**) Representative confocal images of ectopically expressed STIM1 distribution before (top panel) and after 10min thapsigargin (1μM) addition (bottom panel), of living H4-IIE cell are shown. (**B**) Representative confocal images of STIM1 distribution after 10min of TDCA (300 μM) in the absence of Ca^{2+}_{ext} (top panel) or in the presence of 10mM Ca^{2+}_{ext} (bottom panel), of living H4-IIE cell are shown. TDCA addition induces the redistribution of ectopically expressed STIM1 proteins to punctate aggregates independently of the Ca^{2+}_{ext} concentration. STIM1 proteins were visualised in a Z-plane section close to the plasma (note the absence of nucleus), by imaging of the GFP fluorescence expressed by STIM1/pApuro plasmid. Cellular transfection and imaging by confocal microscopy were performed as described in Section 2.7.2. The scale bar represents 10 μm. The results shown are representative of those obtained for one of 23 cells examined in 4 separate experiments.

The time course of redistribution of STIM1 induced by TDCA was then compared with the time course of redistribution of STIM1 caused by SERCA inhibitor thapsigargin (both in the absence of Ca^{2+}_{ext}).

As is shown in Fig. 5.9, in the absence of Ca^{2+}_{ext}, both, thapsigargin (top panels) and TDCA (bottom panels) caused the redistribution of STIM1 in H4-IIE cells, but TDCA was much slower than thapsigargin in inducing the general redistribution of STIM1 proteins.

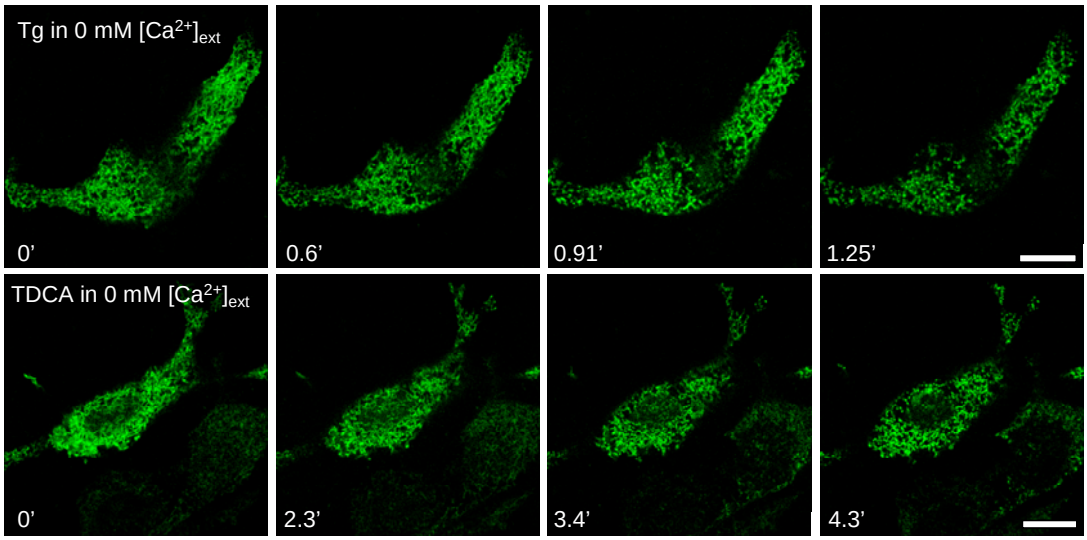

Fig. 5.9. In the absences of Ca^{2+}_{ext}, compared to thapsigargin, TDCA induces a slower redistribution of STIM1. (**A**) Representative confocal images showing the time course of redistribution of ectopically expressed STIM1 proteins induced by 1μM thapsigargin (top panel) or 300μM TDCA (bottom panel) addition are presented. In the absence of Ca^{2+}_{ext}, the time course of TDCA-induced STIM1 redistribution was approximately 3 times slower than the STIM1 redistribution induced by the SERCA inhibitor Tg. STIM1 proteins were visualized by the GFP fluorescence expressed by STIM1/pApuro plasmid in a Z-plane section close to the plasma. Cellular transfection and imaging by confocal microscopy were performed as described in Section 2.7.2. The scale bar represents 10 μm. The results shown are representative of those obtained for one of 5-7 cells examined for each condition.

To test if the STIM1 redistribution caused by TDCA is reversible, the fluorescence of the ectopically expressed STIM1-GFP was examined before the addition, in the presence, and after the wash out of TDCA in the bath.

As shown in Fig. 5.10, STIM1 redistributed homogeneously throughout the ER (top panel). When TDCA was added, STIM1 redistributed into a punctate pattern (middle panel). However, after TDCA was washed out from the incubation medium, STIM1 moved back into its original homogenous distribution throughout the ER (bottom panel), indicating the reversibility of this process.

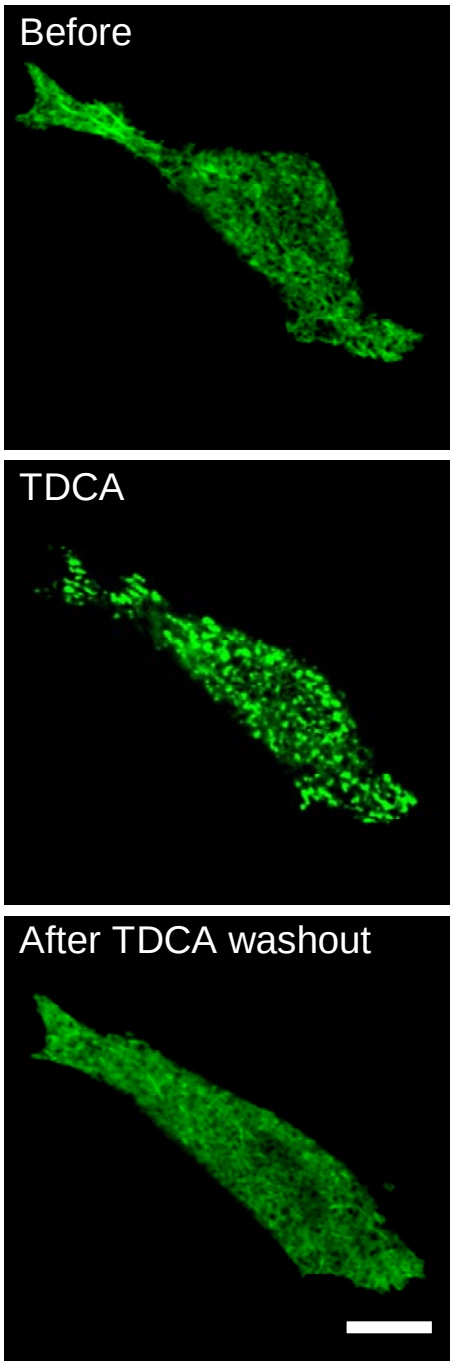

Fig. 5.10. TDCA-induced STIM1 redistribution is reversible. Representative confocal images of GFP fluorescence in a single living H4-IIE cell transfected with GFP-STIM1 before addition of TDCA (Before), after TDCA addition (TDCA), and after washing out TDCA (After TDCA washout) are shown. The images of STIM1 distribution were acquired after 5 min of each of the conditions in a medium containing 10mM Ca^{2+}_{ext}. TDCA induced redistribution of GFP-STIM1 to punctate aggregates. After the washing out of TDCA, the GFP-STIM1 moves back to the initial distribution. The images of STIM1 distribution were taken in a Z-plane section close to the plasma. Cellular transfection and imaging by confocal microscopy were performed as described in Section 2.7.2. The scale bar represents 10 μm. The results shown are representative of those obtained for one of 18 cells examined in 4 separate experiments.

In addition to the experiments shown above, a control experiment was performed in order to determine if the redistribution of STIM1 proteins, induced by TDCA or thapsigargin, could have originated from a direct effect of bile acid on the ER structure itself. To test this, H4-IIE cells were transfected with pDsRed2-ER plasmid and using confocal microscopy, the ER structure was imaged over time in cells treated with TDCA or thapsigargin.

As shown in Fig. 5.11, neither TDCA (incubated for 20min at 10mM Ca^{2+}_{ext}), nor thapsigargin (incubated for 10 min the absence of added Ca^{2+}_{ext}), caused any detectable change in the structure of the ER. This indicates that the observed redistribution of STIM1 induced by TDCA and thapsigargin is unlikely to be due to a substantial rearrangement of ER structure itself.

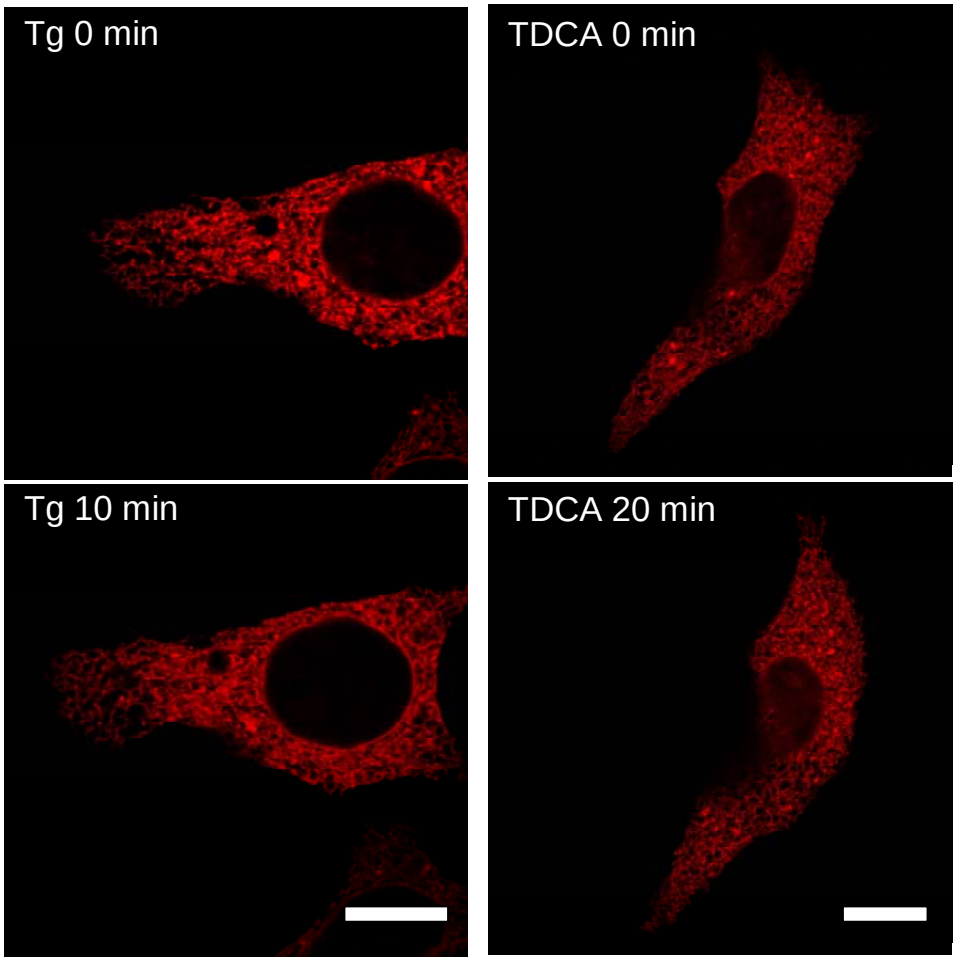

Fig. 5.11. TDCA does not cause rearrangement of ER structure. Representative confocal images of DesRed2 fluorescence in living H4-IIE cell, transfected with pDesRed2-ER plasmid, before and after the additions of Tg or TDCA are presented. 10min incubation of 1μM Tg in the absence of Ca^{2+}_{ext} (left panels) or 20min incubation of 300μM TDCA in 10mM Ca^{2+}_{ext} (right panels), failed to induce any alteration of the ER structure in the same respective cell. The ER structure was visualized by the DsRed2 fluorescent protein which is bearing the ER-targeting sequence KDEL in the pDesRed2-ER plasmid. Cellular transfection and imaging by confocal microscopy were performed as described in Section 2.5.4. The scale bar represents 10 μm. The results shown are representative of those obtained for one of 18 cells examined in 4 separate experiments.

5.2.4. The requirement of endogenous STIM1 proteins for TDCA-induced activation of Ca^{2+} entry through SOCs in H4-IIE liver cells

The requirement for endogenous STIM1 proteins for the activation of Ca^{2+} entry through SOCs induced by TDCA in H4-IIE cells (described in chapter III) was then examined. For this, TDCA-induced Ca^{2+} entry through SOCs, in cells where STIM1 proteins were diminished by siRNA transfection, was compared with the TDCA-induced Ca^{2+} entry through SOCs in siRNA control transfected cells (which should have normal levels of STIM1). The effectiveness of this siRNA against STIM1 in H4-IIE cells has been previously tested in our lab (Litjens *et al.*, 2007).

As shown in Fig. 5.12, the transfection with siRNA against STIM1 induced approximately 60% inhibition of the TDCA-induced initial rate of Ca^{2+} entry through SOCs (Fig. 5.12 B and C), compared to the siRNA control transfected cells (Fig. 5.12 A). This result suggests that in H4-IIE cells, endogenous STIM1 proteins play an important role in the TDCA-induced activation of Ca^{2+} entry through SOCs.

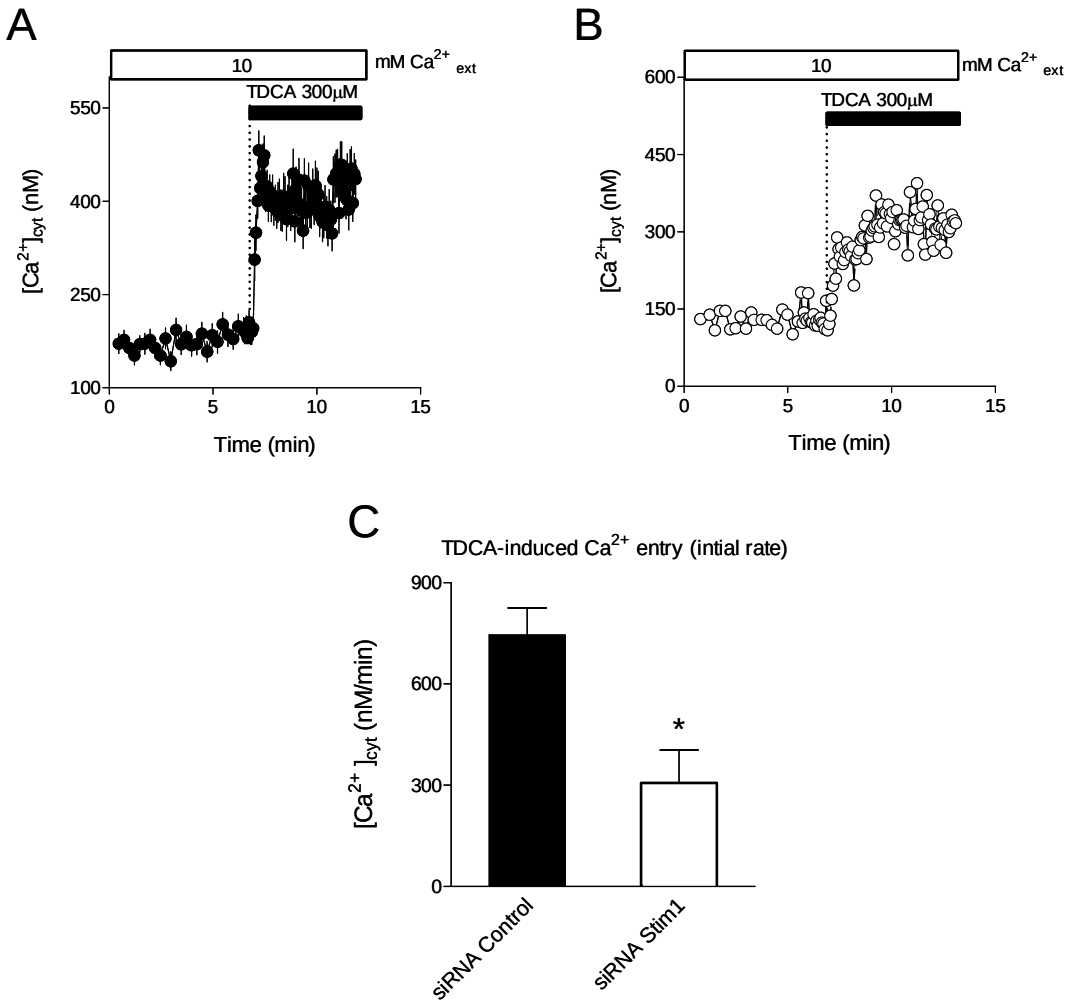

Fig. 5.12. Transfection with siRNA against STIM1 reduces the TDCA-induced Ca^{2+} entry through SOCs. In H4-IIE cells transfected with control siRNA (**A**) or with siRNA against STIM1 (**B**), the addition of 300µM TDCA (in 10mM Ca^{2+}_{ext}) induced Ca^{2+}entry through the SOCs. Knockdown of STIM1 proteins by siRNA and $[Ca^{2+}]_{cyt}$ measurements as a function of time in cells loaded with fura-2, were performed as described in Sections 2.6 and 2.3. The additions to the bath are indicated by the horizontal bars. The results shown are from a representative experiment, of those obtained in 3 similar experiments, in which the fluorescence of 10-20 H4-IIE cells was measured. (**C**) The initial rate of Ca^{2+} entry through SOCs (induced by TDCA), in cells treated with siRNA against STIM1, were significantly smaller than the ones obtained in siRNA control treated cells ($P < 0.05$). The values in **C** are the means ± SEM of 3 experiments of those in **A** and **B**. The initial rate and the peak (maximum) of Ca^{2+} entry were determined as described in Section 2.3.

5.2.5. The effect of TRPV1 channel agonist RTX on the distribution of ectopically expressed STIM1 in H4-IIE liver cells

In chapter IV, it was shown that TRPV1 agonist RTX induced the release of Ca^{2+} from the ER, as detected by fura-2 but no but FFP-18. Thus, the effect on RTX on the distribution of STIM1 proteins was then evaluated.

TRPV1 proteins were co-expressed together with GFP (encoded in Ad-Track-CMV-TRPV1 plasmid). Thus, the use of a STIM1-GFP plasmid to study the distribution of STIM1 proteins in TRPV1(+) cells is not possible, due the overlapping of both GFP molecules. To image STIM1 proteins in TRPV1(+) cells, transfection with DNA encoding Cherry-STIM1 was then performed.

First, a co-localisation assay was performed in order to test if ectopically expressed Cherry-STIM1 proteins were distributed in the ER. For this a co-transfection between the Cherry-STIM1 plasmid (encoding STIM1 conjugated to the fluorescent molecule Cherry) and YFP-ER plasmid (encoding YFP bearing the ER-targeting sequence KDEL) was performed and the resultant fluorescence imaged by confocal microscopy.

Fig. 5.13 shows a confocal image of a TRPV1(+) H4-IIE cell co-expressing both fluorescent molecules. As illustrated in the bottom panel of this figure (Merged), STIM1 proteins are distributed throughout the ER as indicated by the high level of co-localisation (yellow colour) of Cherry fluorescence with the YFP fluorescence.

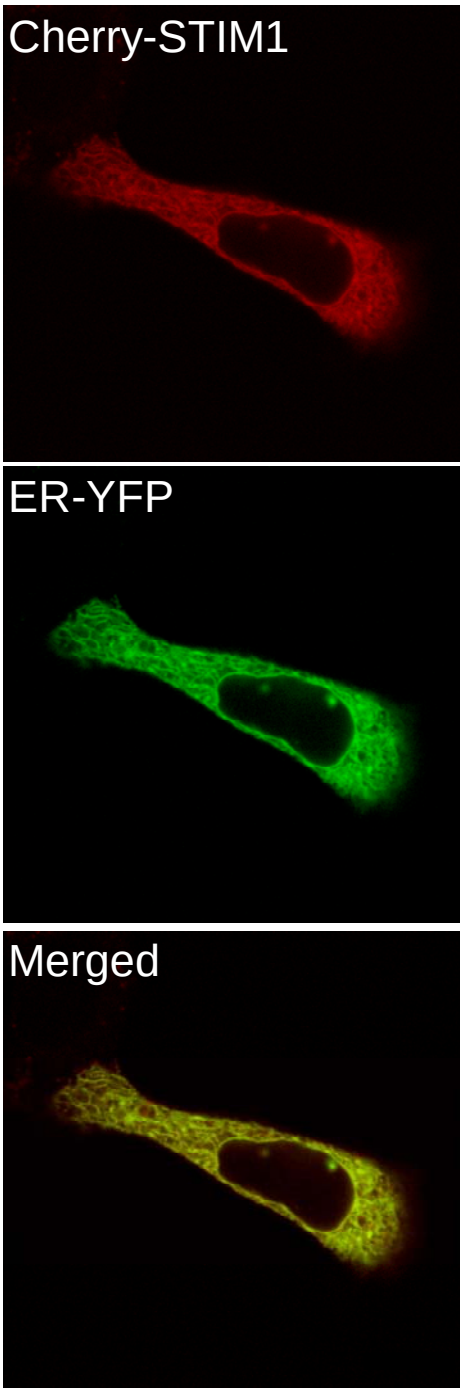

Fig. 5.13. Ectopically expressed Cherry-STIM1 proteins are distributed throughout the ER in H4-IIE liver cells. Representative confocal images of STIM1 proteins localisation (Cherry fluorescence, top panel), the ER structure (YFP fluorescence, middle panel), and the merged images (bottom panels) are presented. Note the high degree of co-localisation (yellow colour) of both fluorescent molecules observed in the merged images. Cellular transfection and imaging by confocal microscopy were performed as described in Sections 2.7.2 and 2.8.4. The scale bar represents 10 μm. The results shown are representative of those obtained for one of 12 cells examined in two separate experiments

To test if RTX addition to TRPV1(+) cells would cause the redistribution of STIM1 proteins within the ER, the following experiment was performed. H4-IIE cells were co-transfected with Ad-track-CMV-TRPV1 plasmid and Cherry-STIM1 plasmid; after 48 h the resultant Cherry fluorescence was imaged by confocal microscopy in TRPV1(+) transfected H4-IIE cells.

A series of confocal images are shown in Fig. 5.14. The images were acquired in a Z-plane near the plasma membrane (no nucleus visible), hence representing the STIM1 distribution close to the plasma membrane of TRPV1(+) transfected H4-IIE cells. The addition of the SERCA inhibitor thapsigargin induced the redistribution of STIM1 from a homogenous tubular net like structure (left top panel) into a punctate pattern (right top panel). Surprisingly, despite the intracellular Ca^{2+} releasing capacity of TRPV1 agonists (shown in chapter IV), the addition of the TRPV1 agonists RTX or N-Vanillolynamide did not cause STIM1 redistribution in the majority of the cells analysed (bottom panels). RTX and N-vanillylnonamide induced some redistribution of STIM1 in 12 and 20%, respectively, of cells examined (42 – 50 cells)).

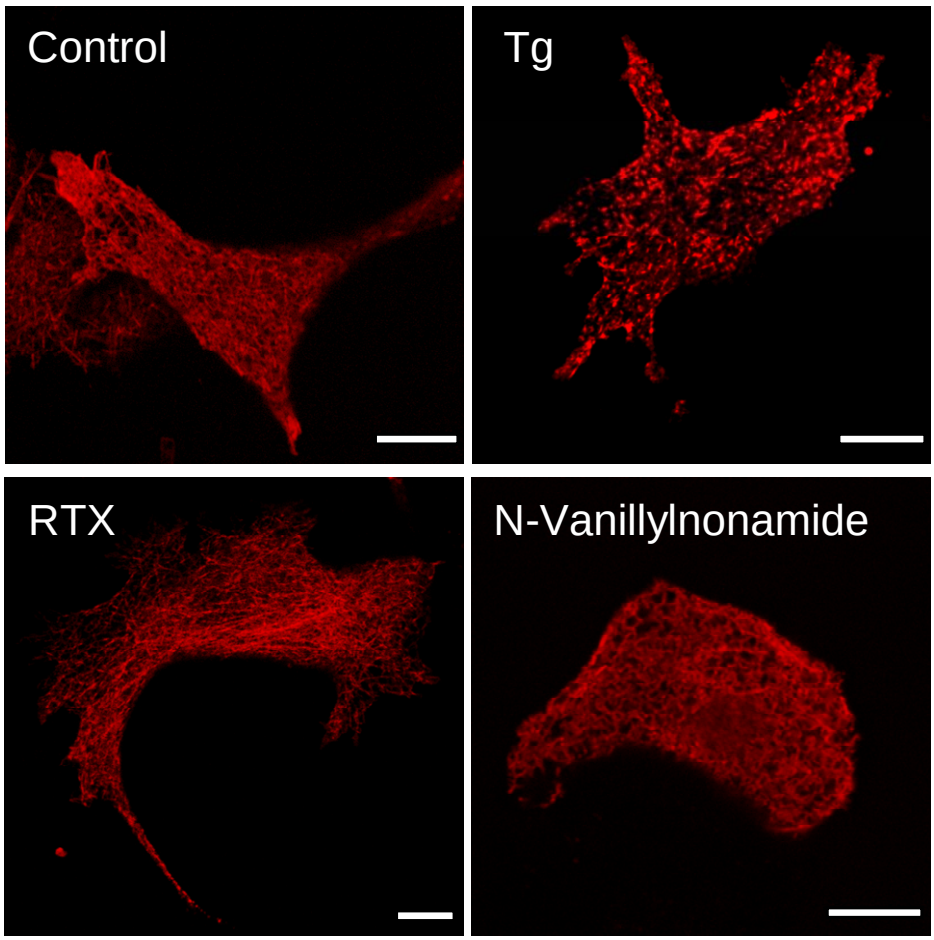

Fig. 5.14. TRPV1 agonists do not induce STIM1 redistribution in TRPV1(+) H4-IIE cells. Representative confocal images of ectopically expressed STIM1 proteins distribution before (top left) and after 10min addition of either 1μM thapsigargin (top right), 1μM RTX (bottom left) or 10μM N-Vanillylnonamide (bottom right), in living TRPV1(+) H4-IIE cells are shown. The addition of TRPV1 agonists RTX or N-Vanillylnonamide, failed to induce the redistribution of STIM1 proteins into a punctate aggregates like the SERCA inhibitor Tg does. STIM1 proteins were visualised in a Z-plane section close to the plasma (note the absence of the nucleus), by imaging of the Cherry fluorescence expressed by Cherry-STIM1 plasmid. Cellular transfection and imaging by confocal microscopy were performed as described in Section 5.2.3. The scale bar represents 10 μm. The results shown are representative of those obtained for one of 42-50 cells examined in 4 separate experiments.

5.3 Discussion

In this chapter evidence has been provided indicating that the release of Ca^{2+}, induced by SERCA inhibitor thapsigargin, causes the redistribution of endogenous or ectopically expressed STIM1 proteins, into punctate aggregates within the ER of H4-IIE liver cells. In addition it was demonstrated that STIM1 proteins are required for the activation of thapsigargin-induced Ca^{2+} entry through SOCs. Furthermore, it was found that the addition of choleretic bile acid TDCA, induced the reversible redistribution of STIM1, similar to that caused by the SERCA inhibitor thapsigargin. However, the addition of TRPV1 agonists (despite their ability to release Ca^{2+} from the ER, as demonstrated in Chapter IV) failed to redistribute STIM1 in the majority of the cells studied.

5.3.1. STIM1 proteins expressed in the ER of H4-IIE liver cells are required for SERCA inhibitor-induced Ca^{2+} entry through SOCs

The results obtained by confocal microscopy using immunofluorescence and co-localisation, indicate that endogenous and ectopically expressed STIM1 proteins are homogeneously distributed in the ER of H4-IIE liver cells. It was demonstrated, in this chapter, that STIM1 proteins in H4-IIE liver cells are required for the SERCA inhibitor-induced Ca^{2+} entry through SOCs. Two experimental observations indicate that STIM1 is required for the activation of Ca^{2+} entry through SOCs in liver cells:

- Firstly, the thapsigargin-induced Ca^{2+} entry through SOCs in H4-IIE cells, was significantly reduced (~ 70% less) when the level of STIM1 proteins were diminished by siRNA transfection.

- Second, the thapsigargin-induced Ca^{2+} entry through SOCs in H4-IIE cells was significantly enhanced (~ 50% more) when the level of STIM1 proteins were augmented (by transfection of cDNA plasmids encoding STIM1).

This result confirms the previously defined role of this intracellular protein as a calcium sensor that links the ER to the activation of SOCs in lymphocytes, mast cells, and other cell types (Liou *et al.*, 2005; Zhang *et al.*, 2005; Baba *et al.*, 2006; Luik *et al.*, 2006; Mercer *et al.*, 2006; Soboloff *et al.*, 2006a; Wu *et al.*, 2006; Xu *et al.*, 2006) including liver cells (Litjens *et al.*, 2007).

5.3.2. TDCA but not TRPV1 agonists caused the redistribution of STIM1 into punctate aggregates, within the ER, similar to that caused by thapsigargin

The evidence presented in this chapter (using confocal microscopy to visualize immunofluorescence and GFP-STIM1 and Cherry-STIM1 plasmids expression) indicates that the addition of the SERCA inhibitor thapsigargin induced the redistribution of endogenous or ectopically expressed STIM1 proteins into punctate aggregates within the ER.

It was observed that the addition of choleretic bile acid TDCA (in the presence or absence of Ca^{2+}_{ext}), induced the redistribution of endogenous or ectopically expressed STIM1, similar to that caused by the SERCA inhibitor thapsigargin. Furthermore, the redistribution of STIM1 caused by TDCA was reversible, indicating that TDCA does not act by inducing the covalent modification of a protein, or act as a tight-binding inhibitor.

In contrast to the effect of TDCA on the redistribution of STIM1, TRPV1 agonists did not induce the redistribution of STIM1 in a majority of cells studied (88 and 80% by RTX and N-vanillylnonamide, respectively), whereas thapsigargin induced

STIM1 redistribution in all cells examined. Since the images of STIM1 redistribution assays were acquired in a Z-plane near the plasma membrane (where no nucleus was visible), the results obtained represent STIM1 distributed in the vicinity of the plasma membrane (presumably "junctional ER"). As suggested in chapter IV, the addition of TRPV1 agonist induced the release of Ca^{2+} from the bulk of the ER. Hence, it could be possible that TRPV1 agonist-induced Ca^{2+} release is not effective in causing STIM1 redistribution in the ER regions at the vicinity of the PM.

These results confirm the reported evidence, which demonstrated that the release of Ca^{2+} from the ER induced the redistribution of STIM1 protein within the ER, into punctate aggregates located adjacent to the plasma membrane (Liou *et al.*, 2005; Zhang *et al.*, 2005; Baba *et al.*, 2006; Mercer *et al.*, 2006; Wu *et al.*, 2006; Xu *et al.*, 2006; Liou *et al.*, 2007; Ong *et al.*, 2007a).

5.3.3. Additional observations and controls

- As shown in chapter IV, the addition of choleretic bile acid TDCA to the incubation medium induced the activation of Ca^{2+} entry through SOCs in H4-IIE liver cells. Evidence shown in this chapter indicates that endogenous STIM1 proteins are required for the TDCA-induced activation of Ca^{2+} entry through SOCs. This is demonstrated by the experimental finding that shows that the TDCA-induced Ca^{2+} entry through SOCs in H4-IIE cells, was significantly reduced (~ 60% less) when the level of STIM1 proteins were diminished by siRNA transfection.
- In this chapter it has also been shown that in the absence of Ca^{2+}_{ext}, it takes longer for TDCA to induce redistribution of STIM1 than for thapsigargin. This observation may be explained by the reported effect of extracellular Ca^{2+} on enhancing the solubility of bile acids and their ability to form micelles (Gu *et al.*,

1992; Hofmann and Mysels, 1992). Thus, it could be possible that the absence of Ca^{2+}_{ext} in the incubation medium could reduce the capability of bile acids to interact with the cells, hence affecting the normal time course of STIM1 redistribution.

- It is possible that the observed redistribution of STIM1 proteins within the ER, induced by choleretic bile acid TDCA, could be an artifactual consequence of an effect of bile acid on the ER structure itself. There is evidence which indicates that bile acids (deoxycholate), as part of their cytotoxic effects, could induce ER stress (dilatation of the ER) causing the re-organisation of the ER structure (Payne *et al.*, 2005). However, the possibility that TDCA could induce ER structure changes is unlikely, as when the ER structure of H4-IIE living cells was imaged by confocal microscopy with the pDsRed2-ER marker; TDCA was ineffective in inducing any detectable alteration on the ER structure under the experimental conditions employed.

Since the redistribution of STIM1 is a pre-requisite for the activation of SOCs and given the effects of TDCA, but not TRPV1 agonist, on causing the redistribution of STIM1 within the ER regions located in the vecinity of the PM; these results give additional evidence for the conclusion postulated throughout this work, that release of Ca^{2+} (which causes STIM1 redistribution) from only a small region of the ER, close to the plasma membrane, is required for the activation of SOCs.

The integration of all the evidence supported in these three consecutive results chapters will be analysed and discussed together in the next chapter.

CHAPTER VI: GENERAL DISCUSSION AND CONCLUSION

The work described in this thesis has determined that choleretic and cholestatic bile acids activate and inhibit, respectively, the previously well-characterised Ca^{2+}-selective channels, SOCs. Using ectopically expressed TRPV1 channels, TRPV1 agonists and the choleretic bile acid TDCA to release Ca^{2+} from different regions of the ER; it was demonstrated that the activation of SOCs in liver cells requires the release of Ca^{2+} from- and the redistribution of STIM1 within- a region of the ER adjacent to the PM.

The aim of this chapter is to discuss and integrate the experimental findings obtained in this study. Additionally, the possible cellular and physiological implications of these findings will be considered. The themes discussed are: (i) the possible cellular mechanism(s) of bile acid-mediated regulation of SOCs in liver cells; (ii) the potential clinical relevance of bile acid-mediated regulation of SOCs; (iii) the requirement of a sub-region of the ER for the activation of SOCs; and (iv) the analysis of future strategies and experiments which could be employed and finally, overall conclusions for this study.

6.1 Possible mechanism(s) of bile acids regulation of liver cells SOCs

The present study provides evidence that a 12 h pre-incubation with cholestatic bile acids inhibits Ca^{2+} entry through SOCs in H4-IIE liver cells and hepatocytes in

primary culture. In contrast to the inhibitory effect of cholestatic bile acids on SOCs activity, the choleretic bile acid TDCA, when added directly to the cells, induced Ca^{2+} entry through SOCs.

6.1.1 Possible mechanism(s) of cholestatic bile acids regulation of SOCs

As mentioned above in this study, it was found that pre-incubation with cholestatic bile acids is associated with the inhibition of Ca^{2+} entry through SOCs. It was observed that this inhibition involves the release of Ca^{2+} from the ER. It might be expected that if cholestatic bile acids leads to depletion of the ER Ca^{2+} stores, SOCs would be constitutively activated. Hence, it is perhaps surprising that the release of Ca^{2+} from intracellular stores, induced by the pre-incubation with cholestatic bile acids, is associated with inhibition of Ca^{2+} entry through SOCs. A possible explanation for this contradictory cause/effect phenomenon is based in the kinetics of cholestatic bile acid-mediated Ca^{2+} release. It was observed that short exposure (5-10 min) of this bile acid did not cause the release of Ca^{2+} from the ER, or affect Ca^{2+} entry through SOCs. In fact, a 12 h pre-incubation period with this bile acid was necessary to cause the release of Ca^{2+} and the inhibition of Ca^{2+} entry through SOCs.

Another possibility, as schematically sown in Fig. 6.1, is that cholestatic bile acid inhibits a step in the pathway of the activation of SOCs downstream from the release of Ca^{2+} from the ER and the redistribution of STIM1 (Varnai *et al.*, 2007). In this regard, cholestatic bile acids could: affect the movement of Orai1 in the plasma membrane towards junctional ER sites; or increase the open probability of Orai1. Additionally, it is possible that cholestatic bile acids could alter the fine structure of the junctional ER, or the C-terminal coiled-coil motif of Orai1; this would consequently affect the interaction between STIM1 and Orai1. It is known that the C-

terminal coiled-coil motif of Orai1, represents a key domain for dynamic coupling to STIM1 (Muik *et al.*, 2008).

Furthermore, the inhibition of the Ca^{2+} entry through SOCs caused by cholestatic bile acids could be mediated by protein kinase C (schematically shown in Fig. 6.1). Bile acids have been shown to directly or indirectly activate protein kinase C (Craven *et al.*, 1987; Huang *et al.*, 1992; Milovic *et al.*, 2002; Lau *et al.*, 2005). Additionally, it has been described that the activation of protein kinase C can inhibit Ca^{2+} release-activated Ca^{2+} channels (Tornquist, 1993; Montero *et al.*, 1994; Parekh and Putney, 2005).

Finally, it was observed in this thesis that the SOC inhibition induced by cholestatic bile acids, involves mitochondrial depolarisation (schematically sown in Fig. 6.1). This may represent an additional factor responsible for cholestatic bile acid-induced inhibition of Ca^{2+} entry through SOCs. Evidence demonstrating that polarised mitochondria are required for the maintenance of sustained Ca^{2+} entry through SOCs channels can be summarised as follows:

It has been described that the rise in $[Ca^{2+}]_{cyt}$ induced by the release of Ca^{2+} from the ER (via IP3 receptors), triggers the Ca^{2+}-dependent inactivation of the IP_3 receptors (Bezprozvanny *et al.*, 1991; Finch *et al.*, 1991; Taylor and Traynor, 1995). However, mitochondria located adjacent to the IP_3-sensitive Ca^{2+} stores (< 20 nm apart) (Csordas *et al.*, 2006) can sense, and buffer, local Ca^{2+} micro-domains located in the vicinity of open IP3 receptors. This leads to an extensive Ca^{2+} release from the ER and subsequently sustained SOCs activation (Rizzuto *et al.*, 1993; Rizzuto *et al.*, 1998; Moreau *et al.*, 2006). Using whole cells patch clamping recording in mast cells, it has been described, that an increase in the cytoplasmic levels of IP_3 (either

via direct dialysis or by receptor stimulation), fails to activate I_{crac}, unless mitochondria are maintained in an energized or hyperpolarized state (Gilabert and Parekh, 2000a; Glitsch *et al.*, 2002b).

Additionally, it has been described that Ca^{2+} entry through SOCs generates high $[Ca^{2+}]_{cyt}$ micro-domains at the mouth of the channel, which induces a Ca^{2+}-dependent inactivation of the channel. However, under physiological conditions of intracellular Ca^{2+} buffering (weak buffering), polarised mitochondria located below the plasma membrane, can buffer Ca^{2+} entry through SOCs and subsequently contributing to maintenance of Ca^{2+} entry through the channel (Gilabert and Parekh, 2000b; Hoth *et al.*, 2000; Gilabert *et al.*, 2001; Glitsch *et al.*, 2002a; Malli *et al.*, 2003; Montalvo *et al.*, 2006).

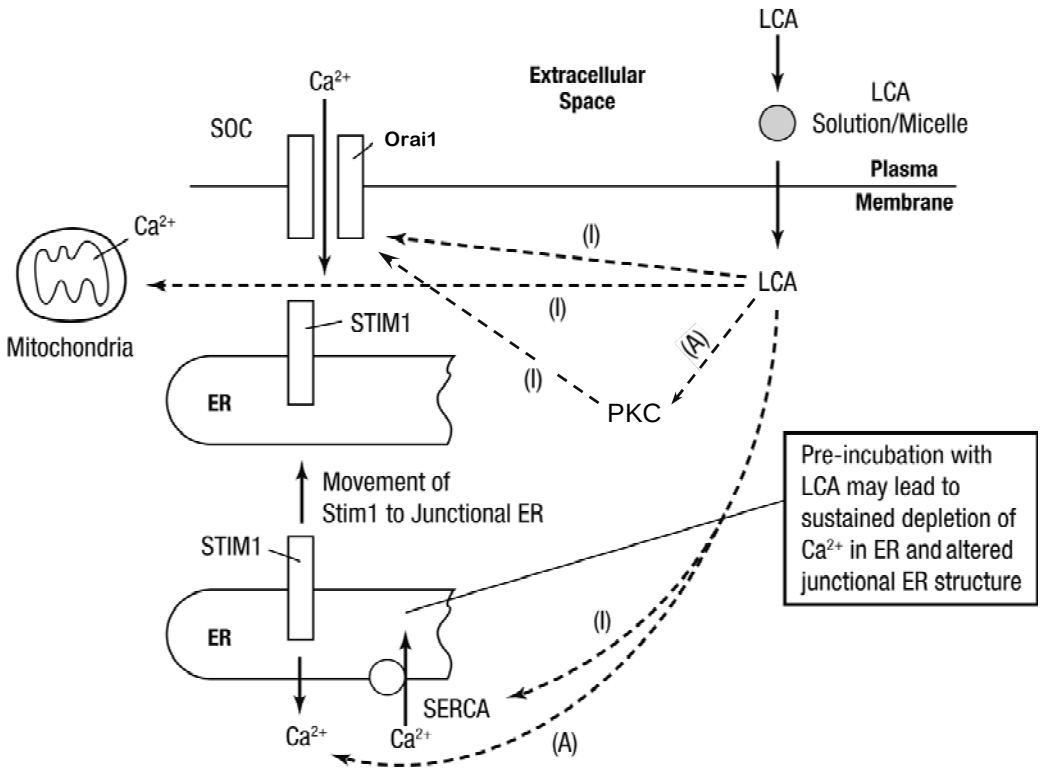

Fig. 6.1. A schematic representation of the proposed mechanisms of regulation of SOCs by cholestatic bile acids in liver cells. It is proposed that pre-incubation with LCA causes a sustained release of Ca^{2+} from the ER, and could alter the fine structure of the junctional ER and/or inhibition of movement of Orai1 in the plasma membrane so there is no activation of SOCs. Cholestatic bile acid can activate protein kinase C, leading to SOCs inhibition. Activation (A) and inhibition (I) are indicated by the broken lines.

6.1.2 Possible mechanism(s) for the modulation of SOCs by choleretic bile acids

In this thesis, evidence has been presented describing the mechanism(s) of activation of SOCs by choleretic bile acids. It is proposed, that choleretic bile acid TDCA induces the release of Ca^{2+} from the ER and causes the reversible redistribution of STIM1 proteins to punctate aggregates within the ER of liver cells (schematically shown in Fig. 6.2). It has been demonstrated recently, in different cellular types (including hepatocytes), that the activation of SOCs requires the release of Ca^{2+} from the ER, which would induce the redistribution of STIM1 proteins (the "Ca^{2+} sensor") into punctate aggregates within the ER (Liou *et al.*, 2005; Zhang *et al.*, 2005; Baba *et al.*, 2006; Luik *et al.*, 2006; Mercer *et al.*, 2006; Soboloff *et al.*, 2006a; Wu *et al.*, 2006; Xu *et al.*, 2006; Litjens *et al.*, 2007).

As described in this work, choleretic bile acid partially counteracts cholestatic bile acids-induced SOCs inhibition. However, both types of bile acids release Ca^{2+} from the ER, so it may be possible that the effects of the bile acids are not only restricted to the depletion of Ca^{2+} from the intracellular stores. There must be some other component(s) of SOCs entry that is affected by cholestatic and choleretic bile acids in opposite ways. Some possibilities are discussed as follows:

- One possible explanation, as schematically shown in Fig. 6.2, is that cholestatic bile acid inhibits, while choleretic bile acid facilitates, a step in the pathway of the activation of SOCs, downstream from the release of Ca^{2+} from the ER and redistribution of STIM1 (Craven *et al.*, 1987). Cholestatic and choleretic bile acids may have differential effects on: the movement of Orai1 in the plasma membrane towards ER junctional ER sites; the interaction between STIM1 and Orai1; and/or the open probability of Orai1 (compare Fig. 6.1 with Fig. 6.2).

- It has been shown previously that impairment of hepatobiliary exocytosis and bile flow caused by cholestatic bile acid TLCA, is associated with the activation of phosphatidylinositiol 3-kinase and the translocation of protein kinase Cε to the plasma membrane (Huang *et al.*, 1992). It has been also described, that choleretic bile acid TUDCA inhibits the activity of phosphatidylinositiol 3-kinase-dependant protein kinase B and the membrane binding of protein kinase Cε, thus reversing the effects of TLCA (Huang *et al.*, 1992). So, it could be possible, that differential regulation of protein kinase Cε and phosphatidylinositiol 3-kinase by TUDCA and TLCA, underlines their opposite effects on Ca^{2+} entry through SOCs. However, this is yet to be investigated.

The inhibition or activation of Ca^{2+} entry through SOCs caused by cholestatic or choleretic bile acids respectively, would initiate the disruption of intracellular Ca^{2+} homeostasis and downstream Ca^{2+} signalling pathways, leading to diverse consequences. In the next section some possible implications of the actions of bile acids will be discussed.

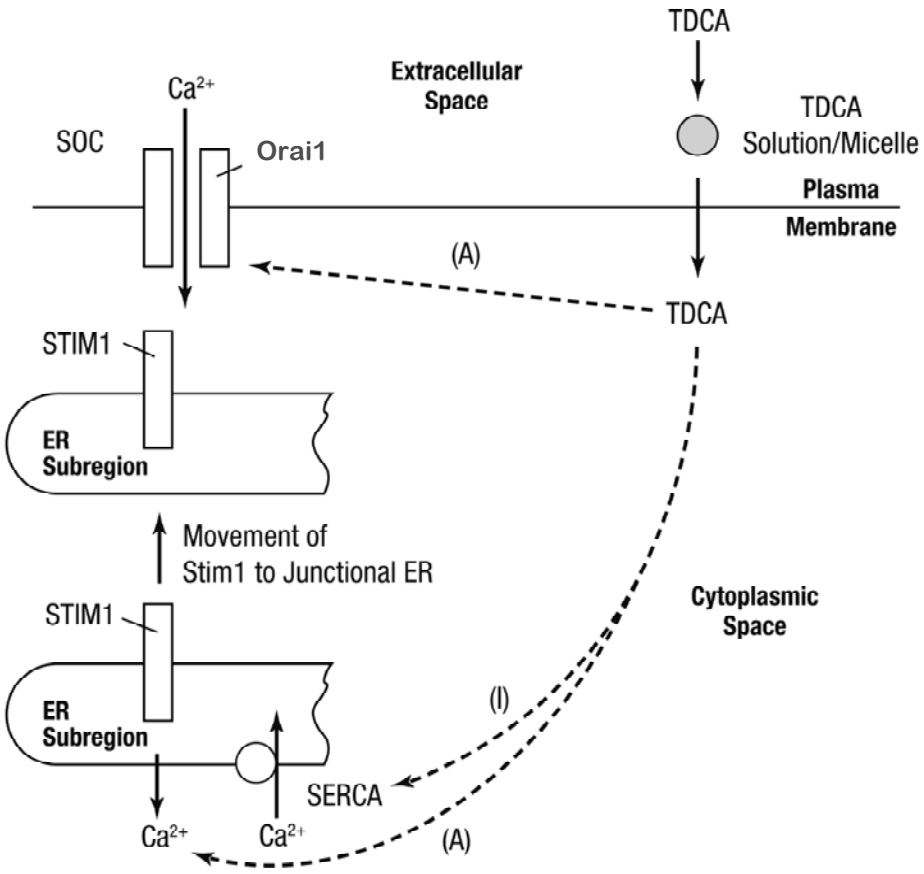

Fig. 6.2. A schematic representation of the proposed mechanisms of regulation of SOCs by choleretic bile acids in liver cells. It is proposed that TDCA induces the release of Ca^{2+} from the ER by enhancing Ca^{2+} outflow (Combettes *et al.*, 1988a, b; Beuers *et al.*, 1993a) or by inhibiting SERCA (Kim *et al.*, 2002; Lau *et al.*, 2005). This, in turn, leads to the movement of STIM1 to the junctional ER close to the plasma membrane and the subsequent activation of SOCs. Activation (A) and inhibition (I) are indicated by the broken lines.

6.2 Potential clinical relevance of bile acids-mediated regulation of SOCs

As described in the introductory chapter, the accumulation of cholestatic bile acids during cholestasis (in the blood, hepatocytes and possibly in the bile canaliculus), can induce bile flow inhibition and liver injury leading to hepatocyte apoptosis and necrosis (Chieco *et al.*, 1997; Benz *et al.*, 1998; Sodeman *et al.*, 2000; Boyer, 2002a; Higuchi and Gores, 2003; Higuchi *et al.*, 2003; Borgognone *et al.*, 2005). Considering the evidence that Ca^{2+} entry through SOCs is required for the normal bile flow in liver (Gregory *et al.*, 2004a), the inhibition of SOCs induced by cholestatic bile acids (described in this thesis) may represent an explanation for the further inhibition of bile flow, the altered hepatocyte growth and apoptosis and necrosis (Chieco *et al.*, 1997; Benz *et al.*, 1998; Sodeman *et al.*, 2000; Higuchi and Gores, 2003; Higuchi *et al.*, 2003; Borgognone *et al.*, 2005).

In this study, evidence has been provided suggesting that addition of choleretic bile acid TDCA is able to counteract the inhibition of SOCs and the mitochondrial depolarisation caused by 12 h pre-incubation with cholestatic bile acid. Choleretic bile acids are used at pharmacological doses to treat different liver pathologies such as: cholestasis (Bouchard *et al.*, 1993; Jacquemin *et al.*, 1993; Azer *et al.*, 1995; van de Meeberg *et al.*, 1996; Kinbara *et al.*, 1997; Poupon *et al.*, 1997; Beuers *et al.*, 1998; Ono *et al.*, 1998; Fabris *et al.*, 1999; Pares *et al.*, 2000; Lazaridis *et al.*, 2001; Boyer, 2002a) and liver dysfunction in patients with acute and chronic intrahepatic cholestatic disorders (Friman and Svanvik, 1994; Fabris *et al.*, 1999). Moreover, it has been shown in rat models of cholestasis, that treatment with choleretic bile acids can stimulate bile flow (Ishizaki *et al.*, 2001).

The results presented identify SOCs as a target for cholestatic and choleretic bile acids in liver cells. These results may have implications for: understanding the progression of cholestasis and subsequent hepatocyte damage, as well as the treatment of cholestasis. Inhibition of Ca^{2+} entry through SOCs induced by cholestatic bile acids may be responsible for enhancing the cholestatic condition; and activation of Ca^{2+} entry through SOCs may contribute to explain the beneficial pharmacological effects of choleretic bile acids on cholestasis.

6.3 Evaluation of the requirement of a small sub-region of the ER for activation of SOCs in liver cells

The results obtained in this study using the choleretic bile salt TDCA, TRPV1 channels and TRPV1 agonists suggest that a small sub-region of the ER is required for the activation of SOCs. As schematically shown in Fig. 6.3:

It is proposed that TDCA-mediated activation of SOCs involves the release of Ca^{2+} (detected by FFP-18 but not by fura-2); and the reversible redistribution of STIM1 proteins into punctate aggregates, from a small sub-region of the ER (coloured in orange) located close to the plasma membrane.

In a separate group of experiments undertaken with TRPV1 channels ectopically expressed in liver cells it was found that the addition of TRPV1 agonists release Ca^{2+} from an intracellular Ca^{2+} store that overlaps substantially with the SERCA inhibitor-sensitive store. The release of Ca^{2+} induced by TRPV1 agonists was detected by fura-2, but not by FFP-18, while the Ca^{2+} release induced by SERCA inhibitor thapsigargin was detected by both, FFP-18 and fura-2 (schematically represented in Fig. 6.3). Contrary to the effects of choleretic bile acid TDCA or SERCA inhibitors, TRPV1 agonists were unable to redistribute STIM1 within the ER region close to the

plasma membrane and failed to activate SOCs (schematically represented in Fig. 6.3). These experimental results suggest that the release of Ca^{2+} induced by TRPV1 agonists, originates from a region of the ER (Fig. 6.3, region in grey) far from where FFP-18 is distributed in the plasma membrane.

In conclusion, it is proposed that the region of the intracellular Ca^{2+} store required for activation of SOCs is a small sub-region of the ER (Fig. 6.3, region in orange) that does not express TRPV1 proteins (in TRPV1(+) cells). An additional implication of these results is that free Ca^{2+} within the lumen of the ER sub-region, required for SOC activation, exchanges slowly with the bulk of the ER Ca^{2+} store (pink arrow).

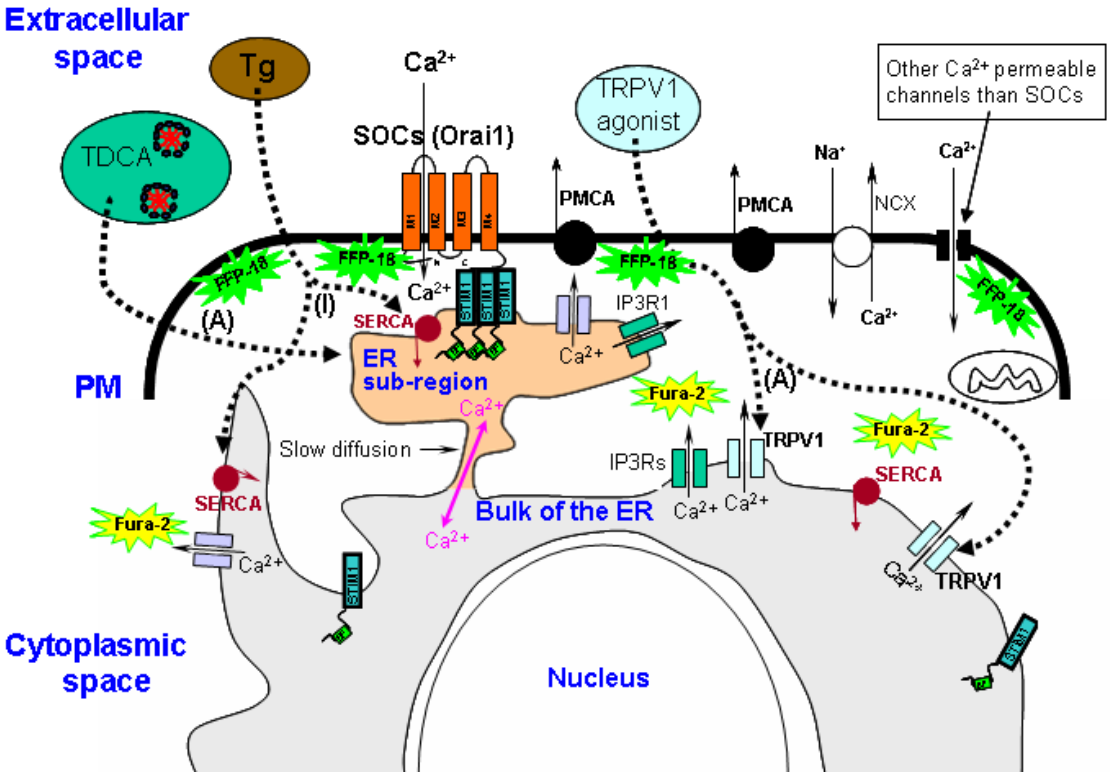

Fig. 6.3. A schematic representation of the possible ER region require for SOCs activation in liver cells. It is proposed that TDCA induces the release of Ca^{2+} from a ER sub-region (orange) beneath the PM detected by FFP-18, while TRPV1 induced the release of Ca^{2+} from the bulk of the ER (grey) which detected by fura-2 in the cytoplasmic space. The SERCA inhibitor thapsigargin (Tg) induce the release of Ca2+ from both ER regions and is detected by both FFP-18 and fura-2. The release of Ca^{2+} induced by TDCA, or SERCA inhibitor Tg (but not TRPV1 agonist in TRPV1(+) cells), leads to the movement of STIM1 to the ER sub-region close to the plasma membrane. Activation (A) and inhibition (I) are indicated by the broken lines.

6.4 Future experiments

The findings in this investigation stimulate ideas for future studies. In this section, some of these ideas are discussed:

6.4.1 Future experiments to investigate the localisation of the ER sub-region responsible for SOCs activation

The results obtained in this study suggest that in liver cells expressing TRPV1 ectopically, the region of the ER which activates SOCs does not express TRPV1 channels. To attempt to resolve the particular ER sub-region, high resolution confocal microscopy, examining the area of the ER in apposition to the PM, could be undertaken. Additionally to this, a further de-convolution analysis of the confocal images (acquired in different Z-planes), followed by a 3D reconstruction would be necessary in order to maximize the resolution and interpretation of the images acquired.

Another possibility is to perform scanning electron microscopy of cells labelled with immuno-gold antibodies against TRPV1 proteins. Gold particles may be conjugated to primary antibodies but are usually employed as secondary antibody/protein labels. So, it could be possible to make a custom gold anti-TRPV1 antibody (or a gold secondary antibody against a primary anti-TRPV1 antibody) and perform an immunofluorescence in cells ectopically expressing TRPV1. With the scanning electron microscope a resolution of ~ 10 nm can be achieved (Slayter, 1997). This would allow the identification of the ER sub-region devoid of TRPV1 proteins, suggested to be the responsible region in the activation of SOCs.

6.4.2 Additional experiments to investigate the redistribution of STIM1 associated to the ER sub-region responsible for SOCs activation:

Considering the distinct effects of bile acid TDCA- and TRPV1 agonist-mediated Ca^{2+} release, on STIM1 redistribution within the ER; future studies concerning the redistribution of STIM1 would represent a useful tool to investigate the possible sub-region of the ER required for SOCs activation. Some possible experiments:

- The distance between the plasma membrane and the TDCA-induced STIM1 aggregates, could be assessed by the use of Total Internal Reflection Fluorescence (TIRF) and the Fluorescence resonance energy transfer (FRET) techniques. These techniques would not report the exact localisation of the ER sub-region, but nevertheless they represent a useful tool to evaluate how close the ER sub-region, responsible for SOCs activation, is to the PM.
- It could be assessed whether the release of Ca^{2+} induced by TDCA (from that particular ER sub-region) can originate the redistribution of STIM1 in other regions of the ER far from the plasma membrane.
- The redistribution of STIM1 can be analysed in studies in which Ca^{2+} could be released from specific areas of the ER. For this, as is described in the introductory chapter of this thesis, different types of IP3 analogues (with different affinities for IP3 receptors) can be used.

6.4.3 Future experiments to investigate the intraluminal ER Ca^{2+} diffusion:

The results obtained suggested that Ca^{2+} diffuses slowly from the ER sub-region (located close to the PM), towards the bulk the ER. To further test this possibility, studies employing Fluorescence Recovery After Photo-bleaching (FRAP) technique, could be undertaken. The idea is to load the ER with a fluorescent dye that can diffuse freely throughout the ER, such as MagFluo-4 (reviewed in (Petersen *et al.*,

2001)). Then by the use of a laser, the dye located in specific areas of the ER (for example close to the nucleus or close to the PM), could be bleached. Subsequently, the diffusion kinetics of the dye could be examined in those particular regions.

6.4.4 Future experiments to investigate the possible beneficial role of choleretic bile acid-mediated regulation of SOCs during cholestasis

To evaluate the possible beneficial role of choleretic bile acids- mediated regulation of SOCs during cholestasis, studies in animal models can be performed. Cholestasis can be initiated in rats by surgical bile duct ligation. After 24 h of bile duct ligation, the rat liver can be perfused with (i) control perfusion medium; (ii) perfusion medium containing choleretic bile acid (for example TDCA or TUDCA); or (iii) perfusion medium containing choleretic bile acid plus SOCs inhibitors (like Gd^{3+} or 2-APB). During liver perfusion, under the different conditions mentioned above, bile flow could be measured via collection of bile fluid samples over the time. This offers a quantitative parameter of cholestasis-induced liver damage. Additionally, other markers indicative of liver damage can be determined, for example: liver enzymes functional markers (LDH, bilirubin, etc) and integrity of cellular structure using histochemistry techniques.

6.5 Conclusions

The presents results provide evidence that SOCs and STIM1 are important targets for the actions of bile acids on hepatocytes. The studies performed with choleretic bile acid TDCA and TRPV1 agonist suggests that in liver cells, only a small sub-region of the ER, in the proximity of the plasma membrane, is require for the redistribution of STIM1 and the activation of SOCs.

APPENDICES

I. Articles published in referred journals as a result of Ph.D. studies

Castro, J., Rychkov, G.Y. and Barritt, G. A small component of the endoplasmic reticulum is required for Store-Operated-Ca^{2+} channels activation in liver cells: evidence from studies using TRPV1 and Taurodeoxycholic acid. *Journal of Biological Chemistry* (*JBC)*. Submitted 15 April 2008 (See the whole text below).

Aromatis, E.*, Castro, J. *, Barritt, G. and Rychkov, G.Y. Store-operated Ca^{2+} channels and stromal interaction factor1 (Stim1) are targets for the actions of bile acids on liver cells. *Biochimica et Biophysica Acta (BBA) Molecular cell*. 1783, 874-885. (2008). (* Each author contributed equally to the work).

Litjens, T., Nguyen, T. Castro, J., Aromataris, E. C, Jones, L., Barritt, G.J. and Rychkov, G.Y. Phospholipase cγ1 is required for the activation of store-operated Ca^{2+} channels in liver cells. *Biochemical Journal.* 405 (2), 269-276. (2007).

II. Presentations in scientific congresses as a result of Ph.D. studies

Barritt, G.J., Litjens, T.L., Castro, J., Aromataris, E., Rychkov, G.Y. Store-Operated Ca^{2+} Channels and Microdomains of Ca^{2+} in Liver Cells. *Australian Physiological Society 2007 meeting. AuPS/ABS*. Symposium Calcium channels, Microdomains and muscle function. Page 5 (2007).

Castro, J., Aromataris, E., Rychkov, G.Y., Barritt, G.J. Bile Acids Induce a Redistribution of the Store-Operated Ca^{2+} Sensor Stim1 in Rat Liver Cells. *ComBio2007 Combined Conference. ASBMB, ANZSCDB and ASPS annual Meeting*. POS-TUE-037 page 136 (2007).

Barritt, G.J., Litjens, T.L., Nguyen, T., Jones, L., Castro, J., Aromataris, E., Roberts, M., and Rychkov, G. Y. Store Operated Ca^{2+} Channels in Liver Cells. *ComBio2007 Combined Conference. ASBMB, ANZSCDB and ASPS annual Meeting*. SYM-06-03 page 34 (2007)

Castro, J., Aromataris, E., Rychkov, G.Y., Barritt, G.J. Bile acids affect calcium homeostasis in liver cells by modulation of Store-Operated Ca^{2+}channels. *ASMR annual Meeting*. POS-12 page 52 (2007).

Castro, J., Aromataris, E., Rychkov, G.Y., Barritt, G.J. Studies of the role of the endoplasmic reticulum in the activation Store-Operated Ca^{2+}Channels in liver cells using ectopically expressed TRPV1. *6th Congress of Federation of Asian and Oceanic Physiological societies (FAOPS) in Seoul, Korea*. POS-94 (2006).

Aromataris, E. Castro, J., Roberts, M., Barritt, G. J and Rychkov, G.Y. Store-Operated Ca^{2+} Channels are the target for the Choleretic and Cholestatic action of bile acid in liver cells. *6th Congress of Federation of Asian and Oceanic Physiological societies (FAOPS) in Seoul, Korea*. POS-81 (2006).

Castro, J., Aromataris, E., Rychkov, G.Y., Barritt, G.J. Evidence that the bulk of the endoplasmic reticulum is not required for the activation of Store-Operated Ca^{2+} Channels in liver cells. *ComBio2006 Combined Conference. ASBMB, ANZSCDB and ASPS annual Meeting*. POS-MON-070 (2006).

Litjens, T., Nguyen, T., Castro, J., Aromataris, E., Roberts, M., Barritt, G.J. and Ryckov, G.Y. Phospholipase Cy 1 is required for the activation of store-operated Ca^{2+} channels in H4-IIE in liver cells. *ComBio2006 Combined Conference. ASBMB, ANZSCDB and ASPS annual Meeting*. POS-MON-057 (2006).

Aromataris, E. Castro, J., Roberts, M., Barritt, G. and Rychkov, G.Y. Bile Salts Modulate the Hepatocyte Store-Operated Ca^{2+} Channel. *ComBio2005 Combined Conference. ASBMB, ANZSCDB and ASPS annual Meeting*. POS-MON-054. P96 (2005).

III. Awards during Ph.D.

Flinders University Overseas Field Trip Grant (2006). Flinders University scholarship to support research undertaken at Centro de Estudios Científicos (CECS), Valdivia, Chile.

Endeavour International Postgraduate Scholarship (IPRS) (2005). Australian Government scholarship to support Ph.D. studies at Flinders University, Adelaide, Australia.

IV. Full text of the article submitted to the Journal of Biological Chemistry

A SMALL COMPONENT OF THE ENDOPLASMIC RETICULUM IS REQUIRED FOR STORE-OPERATED Ca^{2+} CHANNEL ACTIVATION IN LIVER CELLS: EVIDENCE FROM STUDIES USING TRPV1 AND TAURODEOXYCHOLIC ACID

Joel Castro[1], Edoardo C. Aromataris[2], Grigori Y. Rychkov[2], Greg J. Barritt[1]*

[1]Department of Medical Biochemistry, School of Medicine, Flinders University, Adelaide, South Australia, 5001, Australia; [2]School of Molecular and Biomedical Science, University of Adelaide, Adelaide, South Australia, 5005, Australia;

Running Title: ER and SOC Activation

Key words: store-operated calcium entry, calcium release, TRPV1, endoplasmic reticulum, STIM1, bile acids

*To whom correspondence should be addressed: Professor Greg J. Barritt, Department of Medical Biochemistry, School of Medicine, Flinders University, GPO Box 2100, Adelaide SA 5001, Australia. Ph: +61 8 8204 4260 / 8204 4419, FAX: +61 8 8374 0139, Email: Greg.Barritt@flinders.edu.au

It has not been clearly established whether the activation of store-operated Ca^{2+} channels (SOCs) requires the whole or only a small component of the endoplasmic reticulum (ER). This question was investigated using ectopically-expressed TRPV1, a non-selective cation channel, and taurodeoxycholic acid (TDCA), an activator of SOCs, to release Ca^{2+} from different regions of the ER in liver cells. TRPV1 was expressed in the ER and in the plasma membrane. The amount of Ca^{2+} released from the ER by a TRPV1 agonist, measured using fura-2, was the same as that released by a SERCA (ER (Ca^{2+} + Mg^{2+})ATP-ase) inhibitor, indicating that TRPV1 agonist-sensitive stores substantially overlap with SERCA inhibitor-sensitive stores. However, in contrast to SERCA inhibitors, TRPV1 agonists did not activate Ca^{2+} entry. These findings were confirmed by patch clamp recording. Using FFP-18, which detects increases in $[Ca^{2+}]_{cyt}$ beneath the plasma membrane, it was shown that SERCA inhibitors release Ca^{2+} from a region of the ER located closer to the plasma membrane than the region from which TRPV1 agonists release Ca^{2+}. In contrast to SERCA inhibitors, TRPV1 agonists did not induce a redistribution of Stromal interaction factor 1 (STIM1). TDCA caused the release of Ca^{2+} from the ER, which was detected by FFP-18 but not by fura-2, and in non-transfected cells incubated in zero extracellular Ca^{2+} caused a redistribution of STIM1 to puncta similar to that caused by SERCA inhibitors. It is concluded that Ca^{2+} release from a small component of the ER which is located near the plasma membrane, and does not express ectopic TRPV1, is required to induce STIM1 redistribution and SOC activation.

INTRODUCTION

Hormone-induced increases in the concentration of Ca^{2+} in the cytoplasmic space ($[Ca^{2+}]_{cyt}$) play a central role in intracellular signalling in animal cells (1). In liver cells, one of the first types of animal cell in which oscillations in $[Ca^{2+}]_{cyt}$ were observed (2), hormone-induced oscillations in $[Ca^{2+}]_{cyt}$ regulate pathways of intermediary and xenobiotic metabolism, bile acid secretion, cell proliferation and apoptosis and necrosis (3). There is some evidence to indicate that the maintenance of hormone-induced Ca^{2+} oscillations in liver cells requires the replenishment of the ER Ca^{2+} stores by Ca^{2+} entering the cell through SOCs (4,5). The question of which Ca^{2+} entry pathway(s) is responsible for refilling the ER during hormone-induced Ca^{2+} signalling in animal cells is not fully resolved (6). Rat liver cells express only one type of SOC with a high selectivity for Ca^{2+} and properties essentially indistinguishable from those of Ca^{2+} release-activated Ca^{2+} (CRAC) channels in mast cells and lymphocytes (7-9). The pore of the Ca^{2+}-selective SOC is composed of a member of the Orai (CRACM) polypeptide family (reviewed in (10,11) while the Ca^{2+} sensor in the ER is composed of STIM1 or another member of the STIM family (reviewed in (11)). It is proposed that the activation of SOCs involves the movement of Orai1 and STIM1 to the junctional ER at the plasma membrane, and the direct or indirect interaction of STIM1 with Orai1 (11). We have recently shown that STIM1 redistribution is necessary for SOC activation in liver cells (12).

Integrity of the endoplasmic reticulum (ER) is required for the generation of hormone-induced Ca^{2+} oscillations and for the regulation of Ca^{2+} entry through SOCs. In polarised liver cells, type 2 inositol 1,4,5-trisphosphate receptors (IP_3R) located near the bile canaliculus initiate many hormone-induced oscillations in $[Ca^{2+}]_{cyt}$ (13). There is some evidence that, in liver cells, a small region of the ER, enriched in type 1 IP_3R, is required for the activation of SOCs (3,14,15), an idea that is compatible with observations of restricted movement of Ca^{2+} through the ER (16,17). However, the results of some studies with other cell types indicate that the whole of the ER is required for SOC activation, and show that Ca^{2+} can fully diffuse through the lumen of the whole ER (18-22). Taken together, these results suggest that different types of animal cells may have evolved different solutions to the question of how the ER is involved in Ca^{2+} entry through SOCs.

The aim of the experiments reported in this paper was to investigate whether all, or only a subregion, of the ER is required for SOC activation in liver cells. This question was investigated using ectopically expressed TRPV1, a non-selective cation channel of the TRP (transient receptor protein) family, and the choleretic bile acid taurodeoxycholic acid (TDCA) to release Ca^{2+} from different regions

of the ER. TRPV1 is localised in the ER as well as the plasma membrane and, in some cell types, TRPV1 agonists release Ca^{2+} from much of the ER but do not activate SOCs (23,24). In liver cells, TDCA induces the release of Ca^{2+} from the ER (25) and activates liver cell SOCs (26). The present results indicate that, in cells ectopically expressing TRPV1, Ca^{2+} released from the ER by TRPV1 agonists can be detected using the Ca^{2+}-sensitive fluorescent dye fura-2 but not by FFP-18, which report changes in $[Ca^{2+}]_{cyt}$ in the whole cytoplasmic space and in close proximity to the plasma membrane, respectively (27,28). The amount of Ca^{2+} released from intracellular stores by TRPV1 agonists is similar to that released by SERCA inhibitors. However, in contrast to SERCA inhibitors, TRPV1 agonists do not activate Ca^{2+} entry through SOCs and do not cause the redistribution of STIM1. Ca^{2+} released by TDCA could be detected using FFP-18 but not fura-2. TDCA caused a redistribution of STIM1 and activation of SOCs. The results indicate that only a small region of the ER, which does not express ectopic TRPV1, is required for the activation of SOCs.

EXPERIMENTAL PROCEDURES

Materials - Dulbecco's Modified Eagle's Medium (DMEM), fura-2 and FFP-18 (acetoxymethylesters), goat anti-rabbit Alexa-Fluor 647 antibody, Calcium Green 5N, pluronic acid F-127 and BODIPY TR-X thapsigargin were obtained from Invitrogen Australia, Mt Waverley, Victoria; D-myo-inositol 1, 4, 5-trisphosphate (IP_3), ruthenium red, ionomycin and taurodeoxycholic acid (TDCA) from Sigma Australia; thapsigargin and DBHQ from Sapphire Bioscience, NSW, Australia; capsaicin, resiniferatoxin (RTX), and N-vanillylnonamide from Alexis Biochemical Co, Lausem, Switzerland; FuGENE 6 from Roche Pharmaceutical, Nutley, NJ, USA; the pDsRed2-ER plasmid from Clontech, Mountain View, CA, USA; and glass coverslips from Menzel-Glaser GmbH and Co., Braunschweig, Germany. Ad-Track-CMV-TRPV1, prepared by ligating DNA encoding TRPV1, cloned from mouse nodose ganglia, into the Ad-Track-CMV plasmid, was kindly provided by Drs Lei Zhang and S Brookes, Department of Physiology, Flinders University, Adelaide. The Cherry-STIM1 plasmid (HRP-STIM1), constructed by inserting mCherry after the signal sequence of hSTIM1 then inserting this construct into HRP (29), was kindly provided by Dr Rich Lewis, Stanford University, CA, USA. The YFP-TRPV1 plasmid, constructed by inserting YFP into the Xba1 and Apa I sites of pcDNA3 vector (Invitrogen) followed by C-terminal fusion of rat TRPV1 with the FLAG epitope of the YFP, was kindly provided by Dr. Michael Schaefer, Charite University, Berlin, Germany.

Cell Culture - H4-IIE rat liver cells were plated on No. 1 glass coverslips (12, 22 and 30 mm diameter for immunofluorescence, fura-2 and live cell confocal imaging experiments, respectively) and cultured for 24-72 h in DMEM supplemented with 10% (v/v) fetal bovine serum, penicillin (100 U/ml), streptomycin (0.1 mg/ml) and 10 mM HEPES in 5% (v/v) CO_2 at 37°C, as described previously (7,8).

Cell Transfection, Immunochemistry, and Fluorescence Microscopy - For Ca^{2+} imaging and patch clamp experiments, H4-IIE cells were transfected with Ad-Track-CMV-TRPV1 or Ad-Track-CMV (1 μg) using FuGENE 6, according to the manufacturers instructions, and incubated at 37° C for 24 – 48 h. The Ad-Track-CMV-TRPV1 plasmid expresses TRPV1 and GFP as separate proteins each under the control of the CMV promoter. Cells transfected with the Ad-Track-CMV-TRPV1 plasmid, designated TRPV1(+) cells, were identified by GFP fluorescence. Untransfected cells on the same coverslips, designated TRPV1(-) cells, were used as controls. Cells transfected with empty vector (Ad-Track-CMV) were used as additional controls in some experiments.

For studies of intracellular protein localisation, H4-IIE cells were co-transfected (3 μg DNA) with pDsRed2-ER and Ad-Track-CMV-TRPV1; pDsRed2-ER and YFP-TRPV1; or Cherry-STIM1 and Ad-Track-CMV-TRPV1 using FuGENE6, and incubated at 37° C for 24 – 48 h. For cells transfected with the Ad-Track-CMV-TRPV1 plasmid, the transfection efficiency (proportion of cells expressing TRPV1) was approximately 10%. For co-localisation studies employing pDsRed2-ER and BODIPY TR-X thapsigargin, cells transfected with the pDsRed2-ER plasmid were incubated with 1

μM BODIPY TR-X thapsigargin for 10 min at room temperature, then washed twice with Krebs-Ringer-HEPES buffer (KRH). The fluorescence of GFP, YFP, pDsRed2, Cherry, and BODIPY TR-X thapsigargin was measured using a Leica SP5 laser-scanning confocal microscope. The excitation/emission wavelengths were: 488/500-550 nm for GFP; 514/520-550 for YFP; and 561/600-650 nm for pDsRed2 Cherry and BODIPY TR-X thapsigargin.

To detect TRPV1 by immunofluorescence, cells were fixed for 15 min in 4% (v/v) paraformaldehyde in PBS and permeabilised in 0.2% (v/v) Triton X-100 in PBS at room temperature. Fixed cells were blocked for 2 h in 10% (v/v) normal fetal bovine serum in PBS at room temperature, then washed and incubated overnight at 4°C with a polyclonal anti-TRPV1 antibody raised in rabbits (Chemicon International) (1/1000) in 1% (v/v) fetal bovine serum in PBS. The cells were then washed in PBS, and incubated 2 h at room temperature with Alexa-Fluor 647 labelled polyclonal anti-rabbit antibody made in goat (Molecular Probes) (1/1000), washed 5 times with PBS and mounted on glass slides in IMMU-Mount medium (Theomo Shandon, Pittsburg, PA, USA). Fluorescence was measured at 633/675-750 nm excitation/emission by confocal microscopy. Control samples were prepared by omitting the primary antibody. Control images consistently showed low fluorescence (due to non-specific binding of the secondary antibody) compared with the samples containing both primary and secondary antibodies. Routinely, the fluorescence of control samples was set to zero.

For the further resolution of YFP-TRPV1, pDsRed2-ER, and BODIPY TR-X thapsigargin confocal images, de-convolution analysis was performed. A series of images (4-9 in total) of the Z plane were captured in the confocal microscope using the 63x water immersion objective (1.2 numeric aperture). The sizes of the images were (μm): 0.045, 0.045, and 0.200 in X, Y, and Z axis respectively. The images were imported into the AutoDeblur 7.5 software (Auto Quant Imaging Inc., Watervliet, NY, USA) and a "3D blind de-convolution" analysis was performed.

Measurement of Ca^{2+} Concentrations in the Cytoplasmic Space and Endoplasmic Reticulum - To measure $[Ca^{2+}]_{cyt}$ using fura-2, H4-IIE cells attached to glass coverslips were incubated for 30 min at room temperature with 5 μM fura-2 acetoxymethylester in KRH containing 0.02% (v/v) pluronic acid. Loading of H4-IIE cells with FFP-18 was achieved by incubation with 5 μM FFP-18 acetoxymethylester in KRH containing 0.02% (v/v) pluronic acid supplemented with 10% (w/v) bovine serum albumin (27). The KRH solution contained (mM): NaCl, 136; KCl, 4.7; $CaCl_2$, 1.3; $MgCl_2$, 1.25; glucose, 10; and HEPES, 10; adjusted to pH 7.4 with NaOH. For measurement of the fluorescence of fura-2 and FFP-18, cells were incubated in KRH (1.3 mM $CaCl_2$) unless indicated otherwise. Where incubations at zero Ca^{2+}_{ext} were employed, cells were initially incubated in the presence of 1.3 mM Ca^{2+}_{ext} then the medium was changed to KRH in which Ca^{2+} was omitted and 0.5 mM EGTA included. The fluorescence of fura-2 and FFP-18 was measured at room temperature using a Nikon TE300 Eclipse microscope in conjunction with a Sutter DG-4/OF wavelength switcher, Omega XF04 filter set for fura-2, Photonic Science ISIS-3 ICCD camera and UIC Metafluor software. Fluorescence images at 340 nm and 380 nm excitation were obtained every 20 s using a 40x objective. FFP-18 is inserted into the plasma membrane (27,30). To determine the proportion of dye facing the cytoplasmic space, fluorescence was quenched with 1 mM Ni^{2+} (30). The results indicate that more than 95% of the FFP-18 is located on the cytoplasmic face of the plasma membrane.

Values of fluorescence ratio (340 nm:380 nm) were converted to $[Ca]_{cyt}$ using the equation derived by Grynkiewicz et al (31), a Kd of 224 nM for binding of fura-2 to Ca^{2+}, and ionomycin and EGTA to determine R_{max} and R_{min}, respectively. Initial rates of Ca^{2+} entry were determined using a Ca^{2+} "add-back" protocol in which cells were initially incubated in the absence of added Ca^{2+}_{ext}, treated with agonist to activate the Ca^{2+} entry pathway, then 1.3 mM Ca^{2+}_{ext} added, and the increase in $[Ca^{2+}]_{cyt}$ measured as a function of time. The initial rate of increase in $[Ca^{2+}]_{cyt}$ was determined by linear regression. Values for the peak (maximum) $[Ca^{2+}]_{cyt}$ were determined by calculating the difference between the maximum $[Ca^{2+}]_{cyt}$ after Ca^{2+}_{ext} re-addition and the value of $[Ca^{2+}]_{cyt}$ obtained immediately

before Ca^{2+}_{ext} re-addition. Amounts of Ca^{2+} released by DBHQ were determined by measuring the height of the peak of the DBHQ- or TRPV1 agonist-induced increase in $[Ca^{2+}]_{cyt}$.

For the measurement of $[Ca^{2+}]_{er}$ using Calcium Green 5N, H4-IIE cells grown on glass coverslips were incubated at 37°C with 5 μM Calcium Green 5N acetoxymethylester in KRH containing 0.02% (v/v) pluronic acid for 1 h, washed twice with KRH, then incubated for a further period of 30 min at room temperature to allow de-esterification of the acetoxymethylester. The incubation medium was then changed to a "cytoplasmic" medium composed of (mM): KC1, 140; NaCl, 5; MgSO4, 7; HEPES, 20; ATP, 1; EGTA, 10.2 and $CaCl_2$, 1.65, adjusted to pH 7.0. The free $[Ca^{2+}]$ was estimated to be 100 nM using the BAD (Bound and Determined) programme (S. Brooks, Carelton University, Ottawa, Canada). Since GFP is expressed in TRPV1(+) cells, and the fluorescence emission of GFP overlaps with that of Calcium Green 5N, an image of the cells was taken to identify the TRPV1(+) cells. Digitonin (50 μM) was then added to allow the washing out of GFP and Calcium Green 5N in the cytoplasmic space. The remaining fluorescence, which corresponds to Calcium Green 5N in the ER, was imaged in real time using a Nikon TE300 epifluorescence microscope, a 40X objective lens and a band pass emission Endow GFP filter block (Chroma Technology Corp., Rockingham, VT., USA) (excitation 470/40 nm and emission 525-550 nm and a 495 LP dichroic mirror). In order to compare fluorescence values from different cells, data were standardised by assigning the baseline fluorescence (F_o) the value of 1.

Electrophysiology - Whole-cell patch clamping was performed at room temperature using a computer-based patch clamp amplifier (EPC-9 HEKA Electronics, Germany) and PULSE software (HEKA Electronics) (32). The bath solution contained (mM): NaCl, 140; CsCl, 4; $CaCl_2$, 10; $MgCl_2$, 2; glucose, 10; and HEPES, 10; adjusted to pH 7.4 with NaOH. The internal solution contained (mM): caesium glutamate, 120; $CaCl_2$, 5; $MgCl_2$, 5; MgATP, 1; EGTA, 10; and HEPES, 10; adjusted to pH 7.2 with NaOH. SOC activation was initiated by addition of 20 μM IP_3 (D-myo-inositol 1,4,5-triphosphate hexapotassium salt) to the internal solution. Patch pipettes were pulled from borosilicate glass and fire-polished; pipette resistance ranged between 2-4 MΩ. In order to record the SOC (I_{SOC}) and TRPV1 currents, voltage ramps between −138 and +102 mV were applied every 2 s, starting immediately after achieving the whole-cell configuration. All voltages shown have been corrected for the liquid junction potential of -18 mV between the bath and electrode solutions (estimated by JPCalc (33)). The holding potential was -18 mV throughout. Cell capacitance was compensated automatically by the EPC9 amplifier.

Statistical Analysis - Results obtained for $[Ca^{2+}]_{cyt}$ and ER Ca^{2+} concentrations are expressed as means ± SEM (between 10 and 20 cells for each experiment). Statistical significance was assessed using ANOVA followed by the Bonferroni *post hoc* test and Student's t-test (two tailed). Differences between means were considered significant at $P \leq 0.05$.

RESULTS

Ectopically-Expressed TRPV1 Co-Localises with the Endoplasmic Reticulum and Plasma Membrane – To determine the intracellular localisation of ectopically-expressed TRPV1, H4-IIE liver cells were transfected with DNA encoding TRPV1-YFP. TRPV1-YFP was principally located intracellularly with some at the plasma membrane (Fig. 1A). Substantial co-localisation of TRPV1-YFP with the ER, labelled using DsRed2-ER, was observed (Fig. 1A). Similar results, indicating co-localisation of most of the ectopically-expressed TRPV1 with the ER were obtained using BODIPY TR-X thapsigargin to label the ER (Fig. 1B). The results obtained using TRPV1-YFP were confirmed using immunofluorescence to localise ectopically-expressed TRPV1, and DsRed2-ER to identify the ER (results not shown). No endogenous TRPV1 was detected in non-transfected cells using immunofluorescence (results not shown) (*cf* the detection of TRPV1 mRNA in the HepG2 human liver cell line (34)).

In Cells Ectopically Expressing TRPV1, the Intracellular Ca^{2+} Store Released by RTX Overlaps Substantially with the SERCA Inhibitor-Releasable Store – To determine

whether TRPV1 facilitates the release of Ca^{2+} from intracellular stores, the TRPV1 agonist RTX was added in the absence of Ca^{2+}_{ext}. RTX induced an increase in $[Ca^{2+}]_{cyt}$ in cells expressing TRPV1 (TRPV1(+) cells), but no RTX-induced increase in $[Ca^{2+}]_{cyt}$ was observed in non-transfected (TRPV1(-)) cells (Fig. 2A), or in cells transfected with the Ad-Track CMV plasmid (no TRPV1 DNA) (not shown). Following RTX addition to TRPV1(+) cells, the subsequent addition of DBHQ caused no further increase in $[Ca^{2+}]_{cyt}$, whereas in TRPV1(-) cells the expected DBHQ-induced increase in $[Ca^{2+}]_{cyt}$ was observed (Fig. 2A). When the order of addition of RTX and DBHQ was reversed, the addition of RTX to TRPV1(+) cells following the addition of DBHQ caused no further increase in $[Ca^{2+}]_{cyt}$ (Fig. 2B). For TRPV1(+) cells there was no significant difference between the increase in $[Ca^{2+}]_{cyt}$ induced by RTX and that induced by DBHQ (Fig. 2C). The results shown in Fig. 2B indicate that the amount of Ca^{2+} released by DBHQ from TRPV1(+) cells was less than that released from TRPV1(-) cells. When ionomycin was employed in an alternative strategy to release Ca^{2+} from intracellular stores, the amount released in TRPV1(+) cells was also found to be less than that released in TRPV1(-) cells (Fig. 2D). Taken together, these results indicate that, in cells ectopically expressing TRPV1, the stores from which TRPV1 agonists release Ca^{2+} overlap substantially with those from which SERCA inhibitors release Ca^{2+}, and that in TRPV1(+) cells there is less Ca^{2+} in the ER than in TRPV1(-) cells.

The difference in the amount of SERCA inhibitor-releasable Ca^{2+} in the ER of TRPV1(+) and TRPV1(-) cells is likely due to the constitutive activity of TRPV1 in the ER membrane resulting in a lower steady state concentration of Ca^{2+} in the ER of TRPV1(+) cells compared with that in TRPV1(-) cells. Thus it has previously been reported that in some other cell types ectopically-expressed TRPV1 is constitutively active (35-40). This may be due, in part, to the activation of TRPV1 by endogenous signalling molecules (41,42).

The ability of RTX to induce Ca^{2+} release from the ER was tested directly in experiments performed with cells in which the ER was loaded with the fluorescent Ca^{2+} reporter Calcium Green 5N. After incubation with the acetoxymethylester of Calcium Green 5N, the cells were subsequently permeabilised to release any dye located outside the ER in the cytoplasmic space. Fig. 3A shows images of Calcium Green 5N fluorescence in permeabilised control cells. Thapsigargin caused a decrease in Calcium Green 5N fluorescence, and the subsequent addition of ionomycin caused a further decrease (Fig. 3B). The decrease caused by ionomycin may be due to the further release of Ca^{2+} remaining in the ER after thapsigargin treatment, since the time-course for the release of Ca^{2+} from the ER is quite slow (43) and/or to Ca^{2+} release from other intracellular stores. No change in fluorescence as a function of time was observed in cells incubated in the absence of thapsigargin and ionomycin (results not shown). The addition of RTX to permeabilised TRPV1(+) cells loaded with Calcium Green 5N caused a decrease in fluorescence (Fig. 3C) slightly less in magnitude compared with that induced by thapsigargin in TRPV1(-) cells, and with a similar time course. A further small decrease in fluorescence was caused by subsequent addition of ionomycin (Fig. 3C).

Ca^{2+} Release from the ER Mediated by Ectopically-Expressed TRPV1 Does Not Activate Ca^{2+} Entry Through Store-Operated Ca^{2+} Channels – In order to test whether the release of Ca^{2+} from the ER induced by TRPV1 agonists can activate SOCs, it was necessary to conduct the experiment in the presence of ruthenium red, a membrane-impermeant inhibitor of TRPV1 channels (44-46), to inhibit Ca^{2+} entry through TRPV1 located in the plasma membrane. Therefore we first tested whether ruthenium red effectively inhibits Ca^{2+} entry through TRPV1 without inhibiting TRPV1 agonist-induced release of Ca^{2+} from the ER. To confirm that the activation of TRPV1 initiates Ca^{2+} entry through TRPV1 channels in the plasma membrane of TRPV1(+) cells, RTX was added to cells in the presence of Ca^{2+}_{ext}. RTX (1 μM) induced a substantial and sustained increase in $[Ca^{2+}]_{cyt}$ in TRPV1(+) cells (Fig. 4A) but caused no increase in $[Ca^{2+}]_{cyt}$ in TRPV1(-) cells (Fig. 4A), or in cells transfected with the Ad-Track-CMV plasmid (results not shown). (The higher initial (basal) value of $[Ca^{2+}]_{cyt}$ observed in the presence of 1.3 mM Ca^{2+}_{ext} but not in the absence of Ca^{2+}_{ext} is likely to be due

to constitutive activity of TRPV1 in the plasma membrane.) Since TRPV1(-) cells responded in the same way as cells transfected with the Ad-Track-CMV plasmid, TRPV1(-) cells were used as controls in all subsequent experiments.

Ruthenium red caused a substantial decrease in $[Ca^{2+}]_{cyt}$ (Fig. 4B), indicating that ruthenium red inhibits Ca^{2+} entry in TRPV1(+) cells. Ruthenium red did not inhibit the ability of RTX to release Ca^{2+} from the ER (Fig. 4C). There was no significant difference between the increase in $[Ca^{2+}]_{cyt}$ induced by RTX in TRPV1(+) cells in the presence of ruthenium red and that induced by RTX in the absence of inhibitor. The amounts of Ca^{2+} released (peak height) by RTX and by RTX in the presence of ruthenium red were 91 ± 22 and 80 ± 19 nM, respectively (means ± SEM, n = 5). Results similar to those shown in Fig. 4 were obtained using capsaicin (10 μM) or N-vanillylnonamide (10 μM) in place of RTX, and with TRPV1-YFP in place of TRPV1 (results not shown). These results indicate that, in TRPV1(+) cells, Ca^{2+} entry through TRPV1 channels in the plasma membrane is inhibited by ruthenium red, but ruthenium red does not inhibit RTX-induced release of Ca^{2+} from the ER.

It was also necessary to test whether either ruthenium red or RTX inhibits Ca^{2+} entry through SOCs induced by a SERCA inhibitor, and whether ruthenium red inhibits SERCA inhibitor-induced release of Ca^{2+} from the ER. These experiments were conducted using TRPV1(-) cells. Neither ruthenium red (Fig. 5B *cf* Fig. 5A) nor RTX (Fig. 5C *cf* Fig. 5A) inhibited thapsigargin-initiated Ca^{2+} entry, assessed by comparison of the initial rates of increase in $[Ca^{2+}]_{cyt}$ following Ca^{2+}_{ext} addition. The initial rates of Ca^{2+} entry for thapsigargin, thapsigargin in the presence of ruthenium red, and thapsigargin in the presence of RTX were 199 ± 14, 180 ± 47 and 160 ± 14 nM/min (means ± SEM, n = 4-5), respectively (no significant difference between any of the groups, P = 1). Ruthenium red did not inhibit the ability of thapsigargin to induce Ca^{2+} release (Fig. 5D and inset). Results similar to those shown in Fig. 5 were obtained using capsaicin (10 μM) or N-vanillylnonamide (10 μM) in place of RTX and with TRPV1-YFP in place of TRPV1 (not shown).

To test whether the release of Ca^{2+} from the ER induced by the action of RTX on TRPV1 in the ER can activate Ca^{2+} entry through SOCs, TRPV1(+) cells were initially incubated in the absence of Ca^{2+}_{ext}. RTX was added to induce Ca^{2+} release from the ER through TRPV1, ruthenium red to block Ca^{2+} entry through TRPV1 in the plasma membrane, then Ca^{2+}_{ext} to activate Ca^{2+} entry. Ca^{2+}_{ext} addition did not lead to an increase $[Ca^{2+}]_{cyt}$ (Fig. 6A) (61 cells analysed in 13 separate experiments). No RTX-induced changes in $[Ca^{2+}]_{cyt}$ were observed in cells which did not express TRPV1 (TRPV(-) cells) (Fig. 6A). Results similar to these shown in Fig. 6A were obtained using capsaicin (10 μM) or N-vanillylnonamide (10 μM) in place of RTX, and with TRPV1-YFP in place of TRPV1 (not shown). As a control, we showed that thapsigargin can activate Ca^{2+} entry in TRPV1(+) cells. In these experiments, ruthenium red was added before the addition of Ca^{2+}_{ext} in order to block Ca^{2+} entry through TRPV1 in the plasma membrane. In TRPV1(+) cells, thapsigargin caused a transient increase in $[Ca^{2+}]_{cyt}$ in the absence of Ca^{2+}_{ext}, and the subsequent addition of 1.3 mM Ca^{2+}_{ext} caused an increase in $[Ca^{2+}]_{cyt}$ (Fig. 6B). Similar results were obtained with TRPV1(-) cells. In confirmation of the results with DBHQ and ionomycin described above, the amount of Ca^{2+} released by thapsigargin in TRPV1(-) cells was greater than that released in TRPV1(+) cells (Fig. 6B). The amount of Ca^{2+} released (peak height) by thapsigargin (1 μM) was 84 ± 6 and 161 ± 30 nM for TRPV(+) and TRPV(-) cells, respectively (means ± SEM for three independent experiments similar to the one shown in Fig. 6B). Taken together, these results indicate that, in TRPV1(+) cells, release of Ca^{2+} from the ER induced by TRPV1 agonists acting on ectopically-expressed TRPV1 does not activate Ca^{2+} entry through SOCs (*cf* (23,24)).

To further investigate the ability of Ca^{2+} release from the ER via ectopically expressed TRPV1 channels to activate SOCs, the effects of RTX and DBHQ alone, and in combination, on Ca^{2+}_{ext}-dependent Ca^{2+} entry (the Ca^{2+}_{ext}-dependent increase in $[Ca^{2+}]_{cyt}$) were measured. Examination of the mean values for the initial rates of the Ca^{2+}_{ext}-dependent increase in $[Ca^{2+}]_{cyt}$ and the peak value of $[Ca^{2+}]_{cyt}$ (Fig. 7) indicates that, in the presence of RTX, DBHQ causes a large additional

increase in Ca^{2+} entry, presumably due to the activation of SOCs which are not activated by the addition of RTX alone.

Patch clamp recording was used to confirm that TRPV1-mediated release of Ca^{2+} from the ER activates SOCs. Since RTX cannot readily be removed by washing cells, the experiments were conducted using N-vanillylnonamide as the TRPV1 agonist. Addition of N-vanillylnonamide (10 μM) to TRPV1(+) cells induced a large outwardly rectifying current (Fig. 8A, B). When N-vanillylnonamide was washed out, the amplitude of the inward current returned exactly to the baseline value recorded before agonist addition (Fig. 8A, C, D). The current-voltage plots and the currents recorded in response to -138 mV steps obtained before and after the application of N-vanillylnonamide overlap each other, suggesting there is no activation of I_{SOC} during depletion of the intracellular Ca^{2+} stores caused by the application of N-vanillylnonamide (Fig. 8C, D). In contrast, depletion of the intracellular Ca^{2+} stores in cells ectopically expressing TRPV1 by application of IP_3 through the patch pipette activated a current, I_{SOC} (Fig. 8E, F), typical of that previously described in untransfected liver cells (9,12). Current activated by IP_3 showed Ca^{2+} dependent inactivation at -138 mV (Fig. 8F) typical of I_{SOC} in H4-IIE cells and hepatocytes (8,9), while the current remaining after the washout of N-vanillylnonamide showed no inactivation (Fig. 8D).

SERCA Inhibitors Release Ca^{2+} from Stores Located Closer to the Plasma Membrane Than Those Released by RTX in Cells Ectopically Expressing TRPV1 – Since we observed that RTX releases a substantial amount of Ca^{2+} from the ER of TRPV1(+) cells but that this does not activate SOCs, we investigated whether there was any difference in the spatial location of the RTX- and SERCA inhibitor-releasable Ca^{2+} stores using FFP-18. This fluorescent Ca^{2+} reporter detects rapid changes in $[Ca^{2+}]_{cyt}$ close to the plasma membrane (27,28). Ca^{2+} release profiles obtained using FFP-18 were compared with those obtained using fura-2. In TRPV1(+) cells incubated in the absence of Ca^{2+}_{ext}, no RTX-induced increase in $[Ca^{2+}]_{cyt}$ could be detected by FFP-18 (Fig. 9A) in contrast to the RTX-induced increase in $[Ca^{2+}]_{cyt}$ detected using fura-2 (eg Fig. 2A). A transient thapsigargin-induced increase in $[Ca^{2+}]_{cyt}$ was observed with FFP-18 in TRPV1(+) cells (Fig. 9B) (*cf* the transient thapsigargin-induced increase in $[Ca^{2+}]_{cyt}$ detected by fura-2 (eg Fig. 6A)). To confirm that FFP-18 can detect an increase in $[Ca^{2+}]_{cyt}$ near the plasma membrane, 1.3 mM Ca^{2+}_{ext} was added, leading to an increase in FFP-18 fluorescence for cells incubated with RTX (Fig. 9A) and also with thapsigargin (Fig. 9B). These results indicate that the region of the ER from which RTX (via TRPV1) releases Ca^{2+} is further from the plasma membrane than the region from which thapsigargin principally releases Ca^{2+}.

Ca^{2+} Release Mediated by Ectopically-Expressed TRPV1 Does Not Cause a Redistribution of STIM1 – It has previously been shown that STIM1 is expressed in liver cells and is required for the activation of SOCs (12). Studies with other cell types have shown that the release of Ca^{2+} from the ER induced by SERCA inhibitors is associated with a re-localisation of some STIM1 to ER-plasma membrane junctions (47-53). This redistribution of STIM1 is a necessary step in the activation of SOCs (11,54). We investigated whether RTX would induce a redistribution of STIM1 in TRPV1(+) cells. Since cells transfected with TRPV1 also express GFP, the experiments were conducted by co-transfecting the cells with Cherry-STIM1 to monitor the distribution of STIM1. We first investigated the distribution of STIM1 in relation to the ER. In cells co-transfected with DNA encoding Cherry-STIM1 and pEYFP-ER (encoding EYFP targeted to the ER by the KDEL sequence), Cherry-STIM1 co-localised with ER-targeted EYFP as indicated by the merged image (Fig. 10A). This figure shows a confocal image of a cell taken in a Z-plane at the middle of the cell. The outline of the nucleus, which does not contain ER or STIM1, is evident. These results indicate that STIM1 is principally located in the ER

The ability of RTX to induce a redistribution of STIM1 in TRPV(+) cells was compared with that of thapsigargin. Thapsigargin induced a redistribution of STIM1 to a punctate pattern in essentially all TRPV1(+) cells examined (Fig. 10B, Tg *cf* Control) as shown previously for other cell types (47-53). Figure 10B shows a confocal image of a cell in a Z-plane near the plasma

membrane (no outline of the nucleus visible) and hence shows STIM1 distribution close to the plasma membrane. Neither RTX nor N-vanillylnonamide caused a redistribution of STIM1 in the majority of cells examined (Fig. 10B, RTX, N-vanillylnonamide). STIM1 redistribution was observed in 12% (42 cells examined) and 20% (50 cells examined) of cells treated with RTX and N-vanillylnonamide, respectively.

The Choleretic Bile Acid, Taurodeoxycholic Acid (TDCA), Causes a Redistribution of STIM1 with Little Detectable Release of Ca^{2+} from Intracellular Stores – We have previously shown that the choleretic bile acid taurodeoxycholic acid (TDCA) activates Ca^{2+} entry through Ca^{2+}-selective SOCs in liver cells (26). The SOCs activated by TDCA were characterised by patch clamp recording and shown to be identical to the liver cell Ca^{2+}-selective SOCs activated by thapsigargin, IP_3 and agonists such as ATP. We also previously showed that TDCA induces the release of Ca^{2+} from intracellular stores, monitored using fura-2, in the presence of 2.4 mM Ca^{2+}_{ext} and 10 μM Gd^{3+} (added to inhibit Ca^{2+} entry). However, in the absence of Gd^{3+} and at zero Ca^{2+}_{ext} no TDCA-induced release of Ca^{2+} from intracellular stores could be detected (26). This observation was confirmed in the present study by adding TDCA to cells loaded with fura-2 and incubated in the absence of added Ca^{2+}_{ext} (Fig. 11A). The subsequent addition of DBHQ (in the absence of Ca^{2+}_{ext}) increased $[Ca^{2+}]_{cyt}$ (Fig. 11A). TDCA did not substantially reduce the amount of Ca^{2+} released by DBHQ (Fig. 11A inset). Taken together with the previous observations that TDCA activates Ca^{2+} entry through SOCs (26), these results indicate that the ability of TDCA to activate SOCs is not associated with a detectable release of Ca^{2+} from SERCA inhibitor-releasable intracellular Ca^{2+} stores in fura-2-loaded cells.

The actions of TDCA at zero Ca^{2+}_{ext} were investigated further by conducting the following experiments. In the absence of Ca^{2+}_{ext}, TDCA caused a redistribution of STIM1 to give a punctate pattern similar to that induced by thapsigargin (Fig. 12). While the effect of TDCA was slower in onset than that caused by thapsigargin, the resulting pattern of STIM1 localisation was similar to that induced by thapsigargin (Fig. 12). Since a redistribution of STIM1 is thought to be caused by Ca^{2+} release from the ER (11,12), the results shown in Fig. 12 indicate that, in the absence of Ca^{2+}_{ext}, TDCA induces the release of some Ca^{2+} from the ER, even though this cannot be detected by fura-2 as indicated in the experiment in Fig. 11A. We therefore tested whether any Ca^{2+} release from the ER induced by TDCA in the absence of Ca^{2+}_{ext} could be detected using FFP-18, which should detect an increase in $[Ca^{2+}]_{cyt}$ close to the plasma membrane (27,28). In cells incubated in the absence of Ca^{2+}_{ext}, a transient increase in $[Ca^{2+}]_{cyt}$ was observed using FFP-18 (Fig. 11B). Taken together these results suggest that TDCA induces Ca^{2+} release from a small region of the ER near the plasma membrane, and this is necessary and sufficient to activate SOCs.

DISCUSSION

The main new findings reported here can be summarized as follows. In cells ectopically expressing TRPV1, the amount of Ca^{2+} released from the ER by TRPV1 agonists was the same as that released by SERCA inhibitors, indicating that the Ca^{2+} stores released by TRPV1 agonists and SERCA inhibitors substantially overlap. However, in contrast to the actions of SERCA inhibitors, TRPV1 agonists did not activate SOCs or cause a redistribution of STIM1. Moreover, SERCA inhibitors released Ca^{2+} from a region of the ER closer to the plasma membrane than the region of the ER from which TRPV1 agonists released Ca^{2+}, as indicated by the results obtained using FFP-18. Using TDCA, an activator of SOCs, and zero Ca^{2+}_{ext} it was possible to release Ca^{2+} from a region of the ER close to the plasma membrane without releasing Ca^{2+} from the bulk of the ER. These actions of TDCA were associated with a redistribution of STIM1. In addition, it was found that the amount of Ca^{2+} stored in the ER of cells ectopically expressing TRPV1 was less than that in control cells. These results provide evidence that the activation of SOCs in liver cells requires Ca^{2+} release from a small region of the ER close to the plasma membrane, and that Ca^{2+} release from the bulk of the ER is not necessary for SOC activation.

The results obtained using TRPV1-YFP and immunofluorescence together with confocal fluorescence microscopy indicate

that, while some ectopically-expressed TRPV1 is at the plasma membrane, the TRPV1 is predominately found in the ER. The observations that, when expressed ectopically in liver cells, TRPV1-YFP facilitates Ca^{2+} movement across the plasma and ER membranes in a manner similar to TRPV1, indicate that TRPV1-YFP functions in the same way as TRPV1 in liver cells, and is likely to be localised to the same sites as TRPV1. Further evidence for a predominately ER localization of TRPV1 comes from the observation that TRPV1 agonists release the same amount of intracellular Ca^{2+} as that released by SERCA inhibitors. Two observations indicate that TRPV1 mediates Ca^{2+} release from the same intracellular compartment from which SERCA inhibitors release Ca^{2+}. Firstly, in TRPV1(+) cells incubated in the absence of added Ca^{2+}_{ext}, SERCA inhibitors did not release any detectable additional Ca^{2+} when added after RTX. The failure of SERCA inhibitors to release Ca^{2+} in this experiment is unlikely to be due to the inhibition by RTX of the action of the SERCA inhibitor, since it was shown that RTX does not inhibit the ability of SERCA inhibitors to release Ca^{2+} from the ER in control (non-transfected) cells. Secondly, as indicated above, the amount of Ca^{2+} released by TRPV1 agonists in TRPV1(+) cells incubated in the absence of Ca^{2+}_{ext} was similar to that released by SERCA inhibitors.

The following observations provide evidence that Ca^{2+} release from intracellular stores mediated by TRPV1 does not activate SOCs. (i) In the presence of ruthenium red to inhibit Ca^{2+} entry through TRPV1 in the plasma membrane, addition of TRPV1 agonists to TRPV1(+) cells did not activate Ca^{2+} entry, assessed using fura-2 and the Ca^{2+} add-back assay. In control experiments, neither ruthenium red nor RTX blocked SERCA inhibitor-activated Ca^{2+} entry through SOCs. (ii) The SERCA inhibitor DBHQ caused substantial additional Ca^{2+} entry in TRPV1(+) cells (assessed using the fura-2 and Ca^{2+} add-back assay), over and above that induced by RTX. (iii) In patch clamp recording experiments with TRPV1(+) cells no inward current with the properties of the liver cell SOC could be detected following addition of the TRPV1 agonist N-vanillylnonamide. (iv) In TRPV1(+) cells, TRPV1 agonists did not induce the redistribution of STIM1 whereas SERCA inhibitors induced a redistribution of STIM1 similar to that observed in other cell types. Moreover, it has previously been shown that the redistribution of STIM1 induced by SERCA inhibition is a necessary step in the activation of SOCs in several types of cells including liver cells (11,12).

The amount of Ca^{2+} in the ER in TRPV1(+) cells was less than that in the ER of TRPV1(-) cells, most likely due to constitutive activity of TRPV1 in the ER membrane (35-42). There was no evidence from either fura-2 or patch clamp experiments that the lower ER Ca^{2+} in TRPV1(+) cells caused a constitutive activation of SOCs. Moreover, it was possible to activate Ca^{2+} entry through SOCs with SERCA inhibitors in TRPV1(+) cells, in a manner similar to that for TRPV1(-) cells.

In TRPV1(+) cells, TRPV1 agonists released Ca^{2+} from an intracellular Ca^{2+} store which overlaps substantially with the SERCA inhibitor-sensitive store. However, TRPV1 agonists did not activate SOCs or induce a redistribution of STIM1. These observations indicate that the intracellular Ca^{2+} store required for activation of SOCs is a small component of the ER, and does not contain TRPV1. Some indication of the nature of the ER subcomponent responsible for SOC activation was obtained from the results of experiments conducted with TDCA. We showed previously that in liver cells TDCA activates SOCs which are identical to those activated by IP_3 and thapsigargin (26). In cells incubated in the absence of Ca^{2+}_{ext} we could not detect, using fura-2, a TDCA-induced release of Ca^{2+} from the ER, yet under these conditions TDCA did cause a redistribution of STIM1 similar to that caused by SERCA inhibitors. This last result suggests that TDCA does cause Ca^{2+} release from the ER, but fura-2 failed to detect it. Thus TDCA may release Ca^{2+} from a small subregion of the ER required for SOC activation.

These ideas are consistent with results obtained using FFP-18. In TRPV1(+) cells, the release of Ca^{2+} induced by TRPV1 agonists was detected by fura-2, but not by FFP-18, which detects Ca^{2+} near the plasma membrane (27,28,30). By contrast, Ca^{2+} release induced by TDCA could be detected by FFP-18 but not by fura-2 while both FFP-18 and fura-2

detected Ca^{2+} release induced by SERCA inhibitors. These results suggest that the putative subregion of the ER from which TDCA releases Ca^{2+} is near the plasma membrane, whereas the region of ER from which TRPV1 agonists release Ca^{2+} (in TRPV1(+) cells) is located further from the plasma membrane. An additional implication is that luminal Ca^{2+} in the ER subregion responsible for SOC activation exchanges slowly with luminal Ca^{2+} in the rest of the ER.

The idea that a small region of the ER (or another intracellular organelle) is required for the activation of the SOCs in liver cells is consistent with conclusions reached from previous studies with rat hepatocytes which employed adenophostin A, an IP_3 receptor agonist with high affinity for IP_3R, and IP_3 agonists with different affinities for type 1 and type 2 IP_3R (14,15). Studies with some other cell types also provide evidence that Ca^{2+} release from a small region of the ER is sufficient for SOC activation (6,55-57). A recent study in human salivary gland cells compared the abilities of two concentrations of thapsigargin (1.0 nM and 1.0 μM) to release Ca^{2+} from the ER and activate Ca^{2+} entry. The results provide evidence that only a small component of the thapsigargin-sensitive intracellular Ca^{2+} store is required to activate SOCs in this cell type, and that this ER component is in close proximity to the plasma membrane (51). The results of other recent experiments conducted with DT40B lymphocytes and ectopically-expressed STIM1-GFP indicate that, while the bulk of STIM1 is located in the ER, some is localised in a sub-compartment, possibly comprised of mobile vesicles. When Ca^{2+} stores are depleted these vesicles accumulate just below the plasma membrane and are responsible for activation of SOCs (47). Moreover, there is evidence to suggest that the critical movement of STIM1 in the ER during the activation of Orai1 in the plasma membrane takes place in close proximity to the plasma membrane at the ER-plasma membrane junctions (48,52,58)

In conclusion, the present results provide evidence that Ca^{2+} release from only a small sub-region of the ER is required to initiate the redistribution of STIM1 and the activation of SOCs. This ER sub-region may correspond to ER located at ER-plasma membrane junctions. Further experiments are required to investigate the nature of the ER sub-region, its communication with the bulk of the ER, and whether the release of Ca^{2+} from this ER sub-region can affect STIM1 redistribution in other regions of the ER.

Acknowledgements – We would like to thank Dr Rich Lewis, Stanford University, Ca, for providing Cherry-STIM1, Drs. Lei Zhang and S. Brooks for providing the Ad-Track-CMV-TRPV1 plasmid, Dr. Michael Schaefer, Charite University, Berlin, for providing YFP-TRPV1, and Ms Karen Jennings for preparation of the manuscript. This work was supported by grants from the Australian Research Council and the Flinders Medical Centre Foundation, South Australia.

ABBREVIATIONS

*ER, endoplasmic reticulum; SERCA, endoplasmic reticulum (Ca^{2+} + Mg^{2+})ATP-ase; IP_3, inositol 1,4,5-trisphosphate; IP_3R, inositol 1,4,5-trisphosphate receptor; SOC, store-operated Ca^{2+} channel; I_{SOC}, the Ca^{2+} current through liver cell SOCs; $[Ca^{2+}]_{cyt}$, cytoplasmic free Ca^{2+} concentration; $Ca^{2+}{}_{ext}$, extracellular Ca^{2+}; RTX, resiniferatoxin; KRH, Krebs-Ringer-Hepes buffer; Tg, thapsigargin; DBHQ, 2,5-di-(*tert*)-butyl)-1,4-benzohydro-quinone; DMEM, Dulbecco's Modified Eagles Medium; PBS, phosphate buffered saline; TDCA, taurodeoxycholic acid.

REFERENCES

1. Berridge, M. J., Bootman, M. D., and Roderick, H. L. (2003) *Nature Reviews Molecular Cell Biology* **4**, 517-529
2. Woods, N. M., Cuthbertson, K. S., and Cobbold, P. H. (1986) *Nature* **319**, 600-602
3. Barritt, G. J., Chen, J., and Rychkov, G. (2008) *Biochimica et Biophysica Acta*, doi:10.1016/j.bbamcr.2008.01.016
4. Gregory, R. B., and Barritt, G. J. (2003) *Biochemical Journal* **370**, 695-702
5. Gregory, R. B., Sykiotis, D., and Barritt, G. J. (2003) *Cell Calcium* **34**, 241-251
6. Parekh, A. B., and Putney, J. W., Jr. (2005) *Physiological Reviews* **85**, 757-810
7. Rychkov, G., Brereton, H. M., Harland, M. L., and Barritt, G. J. (2001) *Hepatology* **33**, 938-947
8. Rychkov, G. Y., Litjens, T., Roberts, M. L., and Barritt, G. J. (2005) *Cell Calcium* **37**, 183-191
9. Litjens, T., Harland, M. L., Roberts, M. L., Barritt, G. J., and Rychkov, G. Y. (2004) *Journal of Physiology* **558**, 85-97
10. Lis, A., Peinelt, C., Beck, A., Parvez, S., Monteilh-Zoller, M., Fleig, A., and Penner, R. (2007) *Current Biology* **17**, 1-7
11. Lewis, R. S. (2007) *Nature* **446**, 284-287
12. Litjens, T., Nguyen, T., Castro, J., Aromataris, E. C., Jones, L., Barritt, G. J., and Rychkov, G. Y. (2007) *Biochemical Journal* **405**, 269-276
13. Nagata, J., Guerra, M. T., Shugrue, C. A., Gomes, D. A., Nagata, N., and Nathanson, M. H. (2007) *Gastroenterology* **133**, 256-267
14. Gregory, R. B., Hughes, R., Riley, A. M., Potter, B. V., Wilcox, R. A., and Barritt, G. J. (2004) *Biochemical Journal* **381**, 519-526
15. Gregory, R. B., Wilcox, R. A., Berven, L. A., van Straten, N. C., van der Marel, G. A., van Boom, J. H., and Barritt, G. J. (1999) *Biochemical Journal* **341**, 401-408
16. Golovina, V. A., and Blaustein, M. P. (1997) *Science* **275**, 1643-1648
17. Horne, J. H., and Meyer, T. (1997) *Science* **276**, 1690-1693
18. Subramanian, K., and Meyer, T. (1997) *Cell* **89**, 963-971
19. Mogami, H., Nakano, K., Tepikin, A. V., and Petersen, O. H. (1997) *Cell* **88**, 49-55
20. Park, M. K., Petersen, O. H., and Tepikin, A. V. (2000) *EMBO Journal* **19**, 5729-5739
21. Hofer, A. M., Fasolato, C., and Pozzan, T. (1998) *Journal of Cell Biology* **140**, 325-334
22. Sedova, M., Klishin, A., Huser, J., and Blatter, L. A. (2000) *Journal of Physiology* **523**, 549-559
23. Turner, H., Fleig, A., Stokes, A., Kinet, J. P., and Penner, R. (2003) *Biochemical Journal* **371**, 341-350
24. Wisnoskey, B. J., Sinkins, W. G., and Schilling, W. P. (2003) *Biochemical Journal* **372**, 517-528
25. Combettes, L., Berthon, B., Doucet, E., Erlinger, S., and Claret, M. (1990) *European Journal of Biochemistry* **190**, 619-623
26. Aromataris, E. C., Castro, J., Rychkov, G., and Barritt, G. J. (2008) *Biochimica et Biophysica Acta*, doi:10.1016/j.bbamcr.2008.02.011
27. Golovina, V. A. (2005) *Journal of Physiology* **564**, 737-749
28. Vorndran, C., Minta, A., and Poenie, M. (1995) *Biophysical Journal* **69**, 2112-2124
29. Luik, R. M., Wu, M. M., Buchanan, J., and Lewis, R. S. (2006) *Journal of Cell Biology* **174**, 815-825
30. Davies, E. V., Blanchfield, H., and Hallett, M. B. (1997) *Cell Biology International* **21**, 655-663
31. Grynkiewicz, G., Poenie, M., and Tsien, R. Y. (1985) *Journal of Biological Chemistry* **260**, 3440-3450
32. Aromataris, E. C., Roberts, M. L., Barritt, G. J., and Rychkov, G. Y. (2006) *Journal of Physiology* **573**, 611-625
33. Barry, P. H. (1994) *Journal of Neuroscience Methods* **51**, 107-116
34. Vriens, J., Janssens, A., Prenen, J., Nilius, B., and Wondergem, R. (2004) *Cell Calcium* **36**, 19-28
35. Albert, A. P., Pucovsky, V., Prestwich, S. A., and Large, W. A. (2006) *Journal of Physiology* **571**, 361-369
36. Beech, D. J. (2007) *Handbook of Experimental Pharmacology* **179**, 109-123

37. Chuang, H. H., Prescott, E. D., Kong, H., Shields, S., Jordt, S. E., Basbaum, A. I., Chao, M. V., and Julius, D. (2001) *Nature* **411**, 957-962
38. Dietrich, A., Mederos y Schnitzler, M., Emmel, J., Kalwa, H., Hofmann, T., and Gudermann, T. (2003) *Journal of Biological Chemistry* **278**, 47842-47852
39. Numaga, T., Wakamori, M., and Mori, Y. (2007) *Handbook of Experimental Pharmacology* **179**, 143-151
40. Peng, J. B., Brown, E. M., and Hediger, M. A. (2003) *Journal of Physiology* **551**, 729-740
41. Caterina, M. J., Leffler, A., Malmberg, A. B., Martin, W. J., Trafton, J., Petersen-Zeitz, K. R., Koltzenburg, M., Basbaum, A. I., and Julius, D. (2000) *Science* **288**, 306-313
42. Hwang, S. W., Cho, H., Kwak, J., Lee, S. Y., Kang, C. J., Jung, J., Cho, S., Min, K. H., Suh, Y. G., Kim, D., and Oh, U. (2000) *Proceedings of the National Academy of Sciences USA* **97**, 6155-6160
43. Barrero, M. J., Montero, M., and Alvarez, J. (1997) *Journal of Biological Chemistry* **272**, 27694-27699
44. Dray, A., Forbes, C. A., and Burgess, G. M. (1990) *Neuroscience Letters* **110**, 52-59
45. Tani, E., and Ametani, T. (1971) *Journal of Ultrastructure Research* **34**, 1-14
46. Trudeau, L. E., Doyle, R. T., Emery, D. G., and Haydon, P. G. (1996) *Journal of Neuroscience* **16**, 46-54
47. Baba, Y., Hayashi, K., Fujii, Y., Mizushima, A., Watarai, H., Wakamori, M., Numaga, T., Mori, Y., Iino, M., Hikida, M., and Kurosaki, T. (2006) *Proceedings of the National Academy of Sciences USA* **103**, 16704-16709
48. Liou, J., Fivaz, M., Inoue, T., and Meyer, T. (2007) *Proceedings of the National Academy of Sciences USA* **104**, 9301-9306
49. Liou, J., Kim, M. L., Heo, W. D., Jones, J. T., Myers, J. W., Ferrell, J. E., Jr., and Meyer, T. (2005) *Current Biology* **15**, 1235-1241
50. Mercer, J. C., Dehaven, W. I., Smyth, J. T., Wedel, B., Boyles, R. R., Bird, G. S., and Putney, J. W., Jr. (2006) *Journal of Biological Chemistry* **281**, 24979-24990
51. Ong, H. L., Liu, X., Tsaneva-Atanasova, K., Singh, B. B., Bandyopadhyay, B. C., Swaim, W. D., Russell, J. T., Hegde, R. S., Sherman, A., and Ambudkar, I. S. (2007) *Journal of Biological Chemistry* **282**, 12176-12185
52. Wu, M. M., Buchanan, J., Luik, R. M., and Lewis, R. S. (2006) *Journal of Cell Biology* **174**, 803-813
53. Xu, P., Lu, J., Li, Z., Yu, X., Chen, L., and Xu, T. (2006) *Biochemical & Biophysical Research Communications* **350**, 969-976
54. Taylor, C. W. (2006) *Trends in Biochemical Sciences* **31**, 597-601
55. Hartmann, J., and Verkhratsky, A. (1998) *Journal of Physiology* **513**, 411-424
56. Huang, Y., and Putney, J. W., Jr. (1998) *Journal of Biological Chemistry* **273**, 19554-19559
57. Parekh, A. B., and Penner, R. (1997) *Physiological Reviews* **77**, 901-930
58. Varnai, P., Toth, B., Toth, D. J., Hunyady, L., and Balla, T. (2007) *Journal of Biological Chemistry*, **282**, 29678-29690

LEGENDS TO FIGURES

FIGURE 1. **Ectopically-expressed TRPV1 is principally located in the endoplasmic reticulum and plasma membrane.** Images of the localisation of TRPV1, identified using TRPV1-YFP (*TRPV1*), and the ER (*ER*), identified using DsRed2-ER (*A*) or BODIPY thapsigargin (*B*) and the merged images (*Merged*). H4-IIE liver cells were co-transfected with TRPV1-YFP and pDsRed2-ER, or were transfected with TRPV1-YFP and subsequently incubated with BODIPY TR-X thapsigargin, fluorescence was imaged by confocal microscopy, and images deconvoluted as described in Experimental Procedures. The scale bar represents 10 μm. The results shown are representative of those obtained for one of 16 (DsRed2-ER) or 10 (BODIPY TR-X thapsigarin) cells examined in 3 separate experiments.

FIGURE 2. **RTX-sensitive stores overlap substantially with SERCA inhibitor-releasable stores in cells ectopically expressing TRPV1.** *A.* In the absence of Ca^{2+}_{ext}, RTX induces the release of Ca^{2+} from the ER in TRPV1(+) but not TRPV1(-) cells. Subsequent addition of DBHQ releases no further Ca^{2+} in TRPV1(+) cells but does release Ca^{2+} in the TRPV1(-) cells. *B.* In the absence of Ca^{2+}_{ext} (following incubation in the presence of 1.3 mM Ca^{2+}_{ext}) DBHQ releases Ca^{2+} from TRPV1(+) and TRPV1(-) cells. Subsequent addition of RTX does not release any Ca^{2+}. *C.* Comparison of the amounts of Ca^{2+} released (height of the $[Ca^{2+}]_{cyt}$ peak) in TRPV1(+) cells by DBHQ and RTX. The values are the means ± SEM of those obtained in 8 and 5 experiments, respectively. There was no significant difference between any of the peak heights, assessed by the ANNOVA test (DBHQ *cf* RTX, P = 1). *D.* Ionomycin induces the release of Ca^{2+} from intracellular stores in TRPV1(+) and TRPV1(-) cells incubated in the absence of Ca^{2+}_{ext}, with greater release observed in TRPV1(-) cells. H4-IIE liver cells were loaded with fura-2, and $[Ca^{2+}]_{cyt}$ measured as described in Experimental Procedures. The times of addition of reagents are indicated by the horizontal bars. The results shown in each of *A, B* and *C* are those obtained in one experiment which is representative of 3-8 separate experiments which each gave similar results.

FIGURE 3. **RTX induces a decrease in the concentration of Ca^{2+} in the lumen of the endoplasmic reticulum, monitored by measuring the fluorescence of Calcium Green 5N, in permeabilised cells ectopically expressing TRPV1.** *A.* A representative fluorescence image of permeabilised H4-IIE cells loaded with Calcium Green 5N. The scale bar represents 25 μm. *B.* Effects of addition of thapsigargin and ionomycin on Calcium Green 5N fluorescence in TRPV1(-) cells. *C.* Effect of addition of RTX on Calcium Green 5N fluorescence in TRPV(+) cells. The loading of cells with Calcium Green 5N and measurement of fluorescence were conducted as described in Experimental Procedures. The times of addition of reagents are indicated by the horizontal bars. The results shown in *B* and *C* are representative of one of 4 and 7, respectively, separate experiments which each gave similar results.

FIGURE 4. **Ruthenium red blocks RTX-initiated Ca^{2+} entry but not RTX-initiated Ca^{2+} release in cells ectopically expressing TRPV1.** *A.* Effect of RTX on $[Ca^{2+}]_{cyt}$ in TRPV1(+) and TRPV1(-) cells incubated in the presence of 1.3 mM Ca^{2+}_{ext}. *B.* Inhibition by ruthenium red of the RTX-induced increase in $[Ca^{2+}]_{cyt}$ in TRPV1(+) cells. *C.* Ruthenium red does not inhibit RTX-induced release of Ca^{2+} from intracellular stores. H4-IIE liver cells were loaded with fura-2 and $[Ca^{2+}]_{cyt}$ was measured as described in Experimental Procedures. The times of addition of reagents are indicated by the horizontal bars. The results shown are those obtained in one experiment which is representative of 5 separate experiments which each gave similar results.

FIGURE 5. **Ruthenium red does not inhibit thapsigargin-initiated Ca^{2+} entry or Ca^{2+} release, and RTX does not inhibit thapsigargin-initiated Ca^{2+} release.** *A,B,C.* Control experiments showing that neither ruthenium red (RR) nor RTX inhibits SERCA inhibitor-activated Ca^{2+} entry. Effect of thapsigargin addition on $[Ca^{2+}]_{cyt}$ in non-transfected cells incubated initially in the absence of Ca^{2+}_{ext} followed by the subsequent addition of Ca^{2+}_{ext} in the absence of TRPV1 inhibitor or activator (*A*) and in the presence of ruthenium red (*B*) or RTX (*C*). *D.* A control experiment showing that ruthenium red does not inhibit thapsigargin-induced release of Ca^{2+} from intracellular stores. Effect of thapsigargin addition in non-transfected cells in the presence of ruthenium red. The inset shows comparison of the amount of Ca^{2+} released (height of the $[Ca^{2+}]_{cyt}$ peak) by thapsigargin in the absence and presence of ruthenium red. The values are the means ± SEM of those obtained for 9 and 4 experiments, respectively. There was no significant difference between the peak heights, assessed by Student's t-test (P = 0.4). H4-IIE liver cells were loaded with fura-2 and $[Ca^{2+}]_{cyt}$ measured as described in Experimental Procedures. The times of addition of reagents are indicated by the horizontal bars. The results shown in each panel are the means ± SEM of those obtained in one of 3 or more experiments which each gave similar results.

FIGURE 6. **RTX-induced Ca^{2+} release from the ER does not activate Ca^{2+} entry through SOCs in cells ectopically expressing TRPV1.** *A.* Effect of RTX addition on $[Ca^{2+}]_{cyt}$ in TRPV1(+) and TRPV1(-) cells incubated initially in the absence of Ca^{2+}_{ext}, followed by the subsequent addition of Ca^{2+}_{ext} in the presence of ruthenium red. *B.* Effect of thapsigargin addition on $[Ca^{2+}]_{cyt}$ in TRPV1(+) and TRPV1(-) cells incubated initially in the absence of Ca^{2+}_{ext}, followed by the subsequent addition of Ca^{2+}_{ext} in the presence of ruthenium red. H4-IIE liver cells were loaded with fura-2 and $[Ca^{2+}]_{cyt}$ meausred as described in Experimental Procedures. The times of addition of reagents are indicated by horizontal bars. The results shown in *A* are representative of one of 13 (a total of 61 TRPV1(+) cells) and 4, respectively, separate experiments which each gave similar results.

FIGURE 7. **Ca^{2+} entry induced by RTX and a SERCA inhibitor is additive in cells ectopically expressing TRPV1.** Cells were initially incubated in the absence of added Ca^{2+}_{ext}. DBHQ (10 μM), RTX (1 μM) or DBHQ plus RTX were added to induce Ca^{2+} release from the ER, then 1.3 mM Ca^{2+}_{ext} was added to initiate Ca^{2+} entry. H4-IIE cells were loaded with fura-2, and changes in $[Ca^{2+}]_{cyt}$ were measured as described in Experimental Procedures. Initial rates of Ca^{2+} entry and peak (maximum) values of $[Ca^{2+}]_{cyt}$ following Ca^{2+}_{ext} addition, determined as described in Experimental Procedures. The results shown are the means ± SEM of 4-6 experiments. The degrees of significance for comparison of the values for initial rate are: RTX *cf* DBHQ, P = 1; RTX *cf* RTX plus DBHQ, *P = 0.006; DBHQ *cf* RTX plus DBHQ, *P = 0.002. The degrees of significance for comparison of the values for the peak are: RTX *cf* DBHQ, P = 1; RTX *cf* RTX plus DBHQ, *P = 0.002; DBHQ *cf* RTX plus DBHQ, *P = 0.003.

FIGURE 8. **N-vanillylnonamide does not activate Ca^{2+} entry through SOCs in cells ectopically expressing TRPV1 as monitored by patch clamp recording.** *A.* The inward (measured at -118 mV) and outward (measured at 82 mV) currents recorded in response to voltage ramps and induced by the addition of 10 μM N-vanillylnonamide (indicated by the horizontal bar) to TRPV(+) cells. Voltage ramps were not applied at the peak of the response to N-vanillylnonamide to limit Ca^{2+} entry into the cell. The arrows (1 and 2) represent the basal value of the inward current before (1) and after (2) N-vanillylnonamide addition, and the locations of the current-voltage plots in panel C. *B.* TRPV1 current-voltage plot obtained at the peak of the response to N-vanillylnonamide. *C.* Current-voltage plots obtained in response to a voltage ramp recorded before (arrow 1 in panel A) and after (arrow 2 in panel A) N-vanillylnonamide addition in TRPV1(+) cells. *D.* Current recorded in response to -132 mV steps in TRPV1(+) cells before the addition and after the washout of N-vanillylnonamide. *E.* The time course of the I_{SOC} development in TRPV1(+) cells. I_{SOC} was activated by 20 μM IP_3 in the pipette solution. *F.* Currents recorded in response to -138 mV steps in TRPV1(+) cells before (trace 1) and

after (trace 2) depletion of intracellular Ca^{2+} stores by IP_3. Leakage was not subtracted in any of the panels. The results shown are representative of those obtained in one of 3 or more experiments which gave similar results.

FIGURE 9. **The increase in $[Ca^{2+}]_{cyt}$ induced by RTX is not detected by FFP-18 at the plasma membrane in cells ectopically expressing TRPV1.** *A.* In cells loaded with FFP-18 and incubated in the absence of Ca^{2+}_{ext} (after prior incubation at 1.3 mM Ca^{2+}_{ext}), RTX does not cause a detectable increase in $[Ca^{2+}]_{cyt}$. Subsequent addition of Ca^{2+}_{ext} does lead to an increase in $[Ca^{2+}]_{cyt}$. *B.* In cells loaded with FFP-18 and incubated in the absence of Ca^{2+}_{ext} (after prior incubation at 1.3 mM Ca^{2+}_{ext}), thapsigargin causes a transient increase in $[Ca^{2+}]_{cyt}$. Subsequent addition of Ca^{2+}_{ext} causes a sustained increase in $[Ca^{2+}]_{cyt}$. H4-IIE liver cells were loaded with FFP-18 and $[Ca^{2+}]_{cyt}$ measured as described in Experimental Procedures. The times of addition of reagents are indicated by the horizontal bars. The results shown are those obtained in one experiment which is representative of 3 separate experiments which each gave similar results.

FIGURE 10. **In contrast to thapsigargin, RTX does not induce a redistribution of STIM1 in cells ectopically expressing TRPV1.** *A.* Images of the distribution of STIM1, observed using Cherry-STIM1 (*STIM1*) and the ER (*ER*), observed using DsRed2-ER, in the same cell, and the merged image (*Merged*). *B.* TRPV1(+) cells expressing Cherry-STIM1 treated with vehicle (*Control*), 1 μM thapsigargin for 10 min (*Tg*), 1 μM RTX for 10 min (*RTX*), and 10 μM N-vanillylnonamide for 10 min (*N-vanillylnonamide*). Co-transfection of H4-IIE liver cells with DNA encoding Cherry-STIM1 and DsRed2-ER, or encoding TRPV1 and Cherry-STIM1, and confocal microscopy were performed as described in Experimental Procedures. The scale bars represent 10 μm. The results shown in each panel are representative of those obtained for 42-50 cells examined.

FIGURE 11. **The increase in $[Ca^{2+}]_{cyt}$ induced by the choleretic bile acid taurodeoxycholic acid (TDCA) is detected by FFP-18 at the plasma membrane but not by fura-2.** *A.* In cells loaded with fura-2 incubated in the absence of Ca^{2+}_{ext}, TDCA (300 μM) does not induce any detectable increase in $[Ca^{2+}]_{cyt}$, while the subsequent addition of 10 μM DBHQ causes a substantial transient increase in $[Ca^{2+}]_{cyt}$. The inset shows the amount of Ca^{2+} released by DBHQ (peak height) in the presence and absence of TDCA. (Comparison by Student's t-test showed no significant difference with and without TDCA.) *B.* In cells loaded with FFP-18 incubated in the absence of Ca^{2+}_{ext}, TDCA induces a detectable increase in $[Ca^{2+}]_{cyt}$. H4-IIE cells were loaded with fura-2 or FFP-18 and $[Ca^{2+}]_{cyt}$ measured as described in Experimental Procedures. The times of addition of reagents are indicated by the horizontal bars. The results shown are those obtained in one experiment which is representative of 3 separate experiments which each gave similar results.

FIGURE 12. **Taurodeoxycholic acid (TDCA) induces a redistribution of STIM1 under conditions where no increase in $[Ca^{2+}]_{cyt}$ is detected with fura-2.** TRPV1(+) cells expressing Cherry-STIM1 were treated with TDCA (*TDCA*) or thapsigargin (*thapsigargin*). The time elapsed (seconds) after addition of agonist is shown at the bottom of each frame. The scale bars represent 10 μM. Cell transfection and confocal microscopy were performed as described in the legend of Fig. 10 and Experimental Procedures. The results shown in each panel are representative of those obtained in separate experiments for 5 and 7 cells examined for thapsigargin and TDCA, respectively.

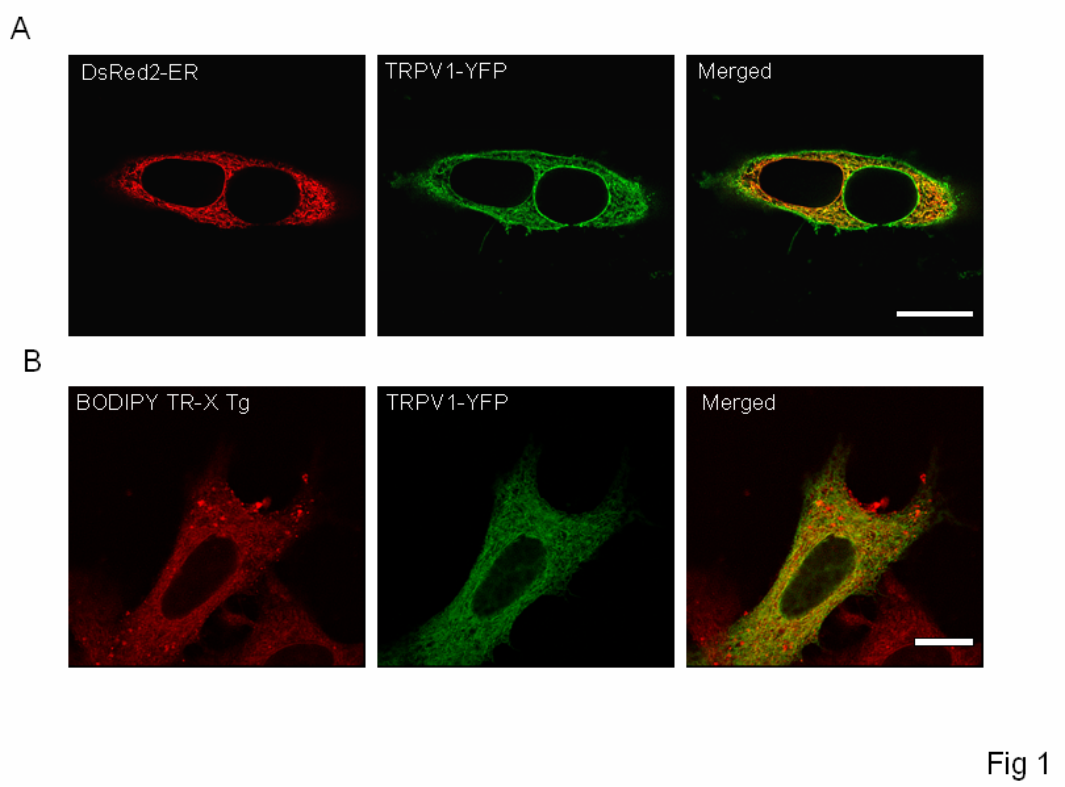
A
DsRed2-ER
TRPV1-YFP
Merged
B
BODIPY TR-X Tg
TRPV1-YFP
Merged

Fig 1

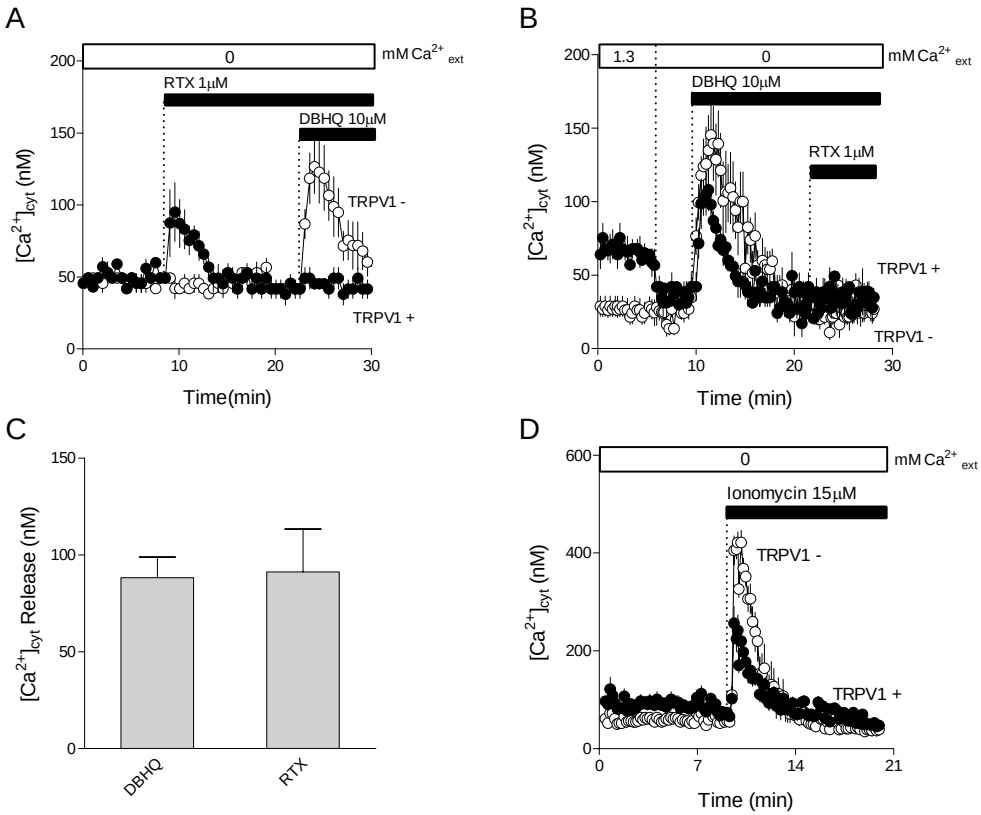
A
0
mM Ca2+ ext
RTX 1μM
DBHQ 10μM
TRPV1 -
TRPV1 +
[Ca2+]cyt (nM)
Time(min)
B
1.3
0
mM Ca2+ ext
DBHQ 10μM
RTX 1μM
TRPV1 +
TRPV1 -
[Ca2+]cyt (nM)
Time (min)
C
[Ca2+]cyt Release (nM)
DBHQ
RTX
D
0
mM Ca2+ ext
Ionomycin 15μM
TRPV1 -
TRPV1 +
[Ca2+]cyt (nM)
Time (min)

Fig 2

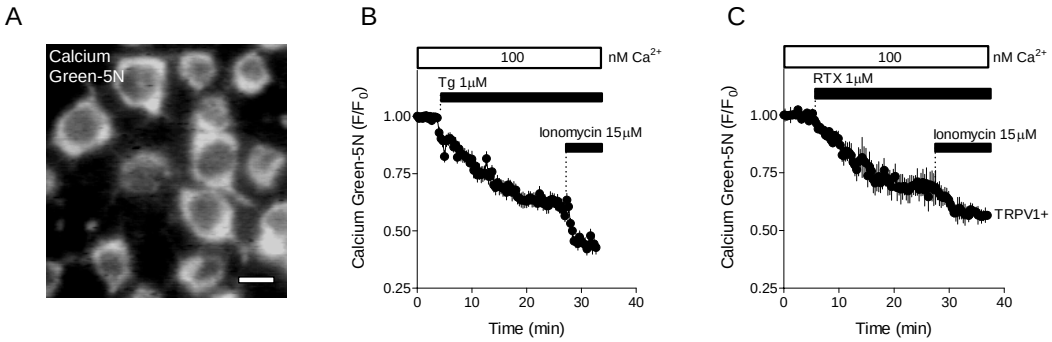
A
Calcium
Green-5N
B
100
nM Ca2+
Tg 1μM
Ionomycin 15μM
Calcium Green-5N (F/F0)
Time (min)
C
100
nM Ca2+
RTX 1μM
Ionomycin 15μM
TRPV1+
Calcium Green-5N (F/F0)
Time (min)

Fig 3

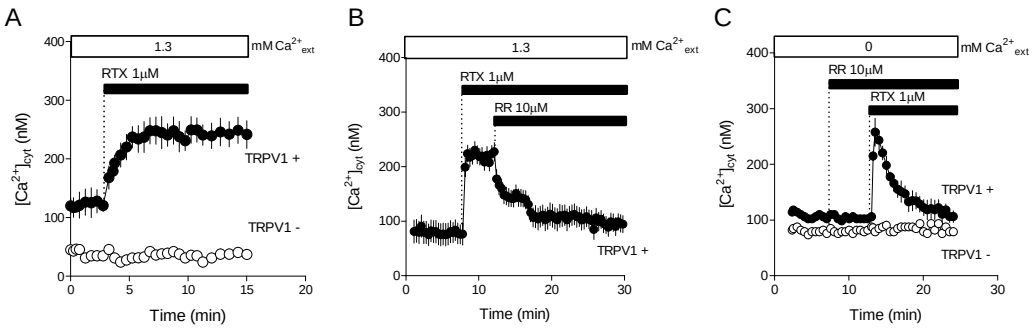
A
1.3
mM Ca2+ext
RTX 1μM
TRPV1 +
TRPV1 -
[Ca2+]cyt (nM)
Time (min)
B
1.3
mM Ca2+ext
RTX 1μM
RR 10μM
TRPV1 +
[Ca2+]cyt (nM)
Time (min)
C
0
mM Ca2+ext
RR 10μM
RTX 1μM
TRPV1 +
TRPV1 -
[Ca2+]cyt (nM)
Time (min)

Fig 4

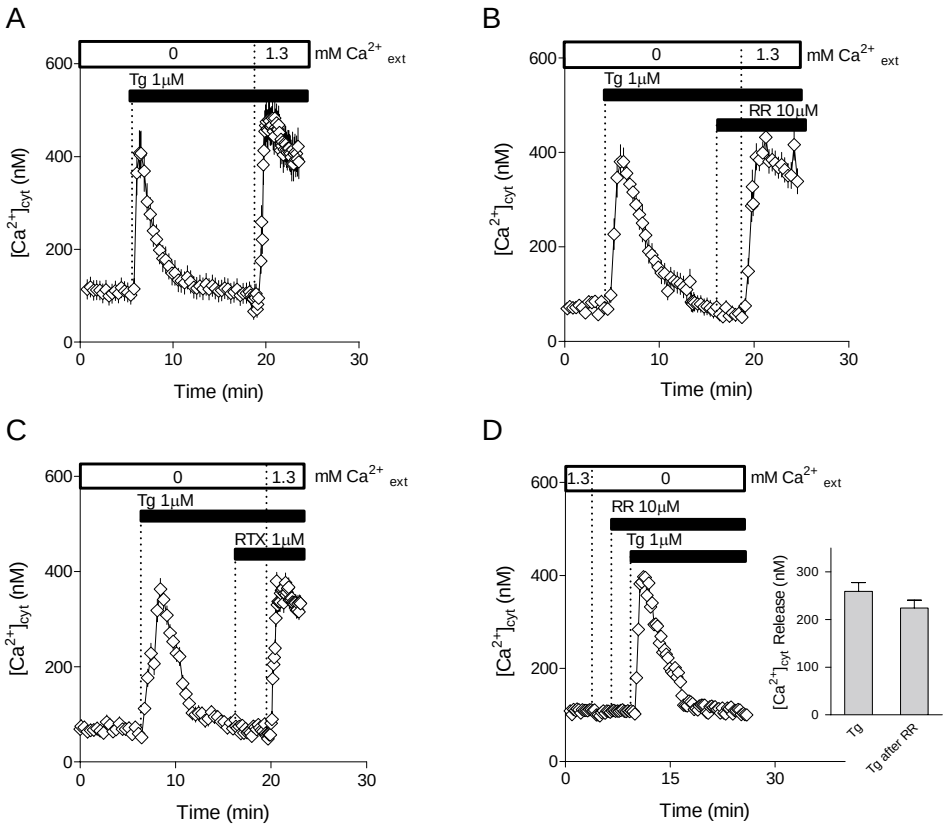
A
B
C
D
0
1.3
mM Ca2+ ext
Tg 1μM
RR 10μM
RTX 1μM
[Ca2+]cyt (nM)
Time (min)
[Ca2+]cyt Release (nM)
Tg
Tg after RR

Fig 5

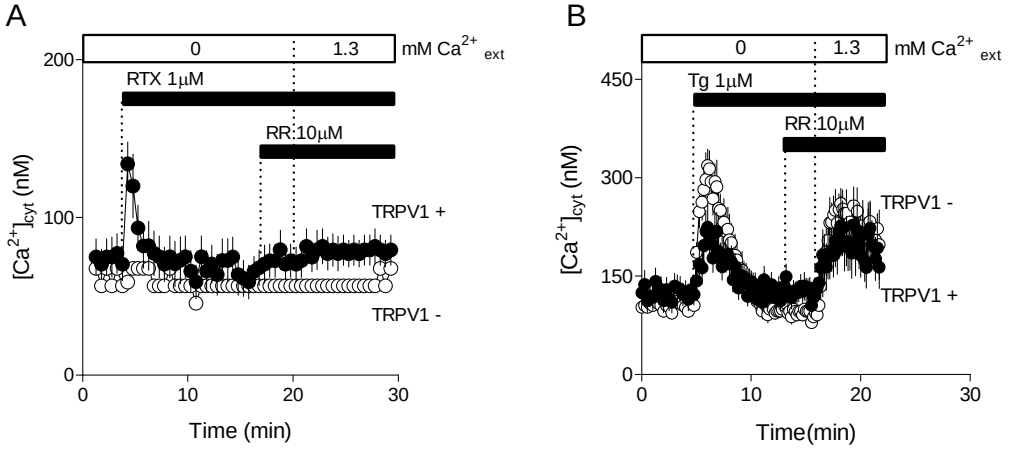
A
B
0
1.3
mM Ca2+ ext
RTX 1μM
RR 10μM
Tg 1μM
TRPV1 +
TRPV1 -
[Ca2+]cyt (nM)
Time (min)
Time(min)

Fig 6

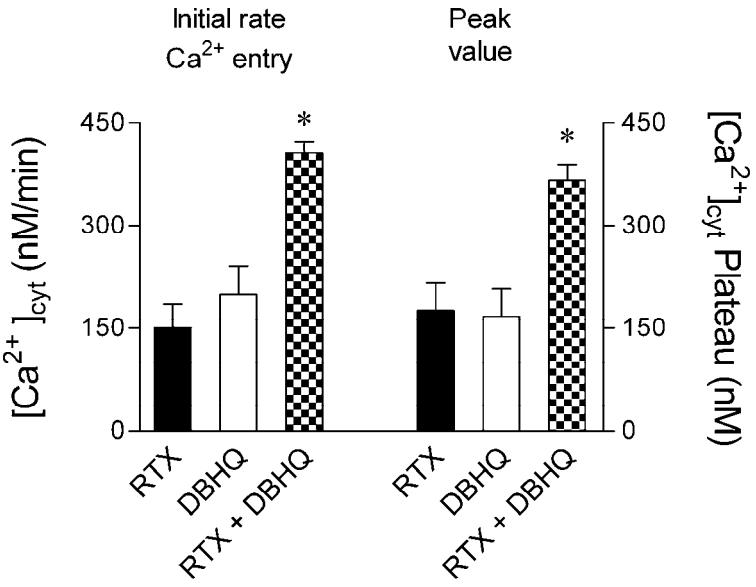
Initial rate
Ca2+ entry
Peak
value
[Ca2+]cyt (nM/min)
[Ca2+]cyt Plateau (nM)
450
300
150
0
*
RTX
DBHQ
RTX + DBHQ

Fig 7

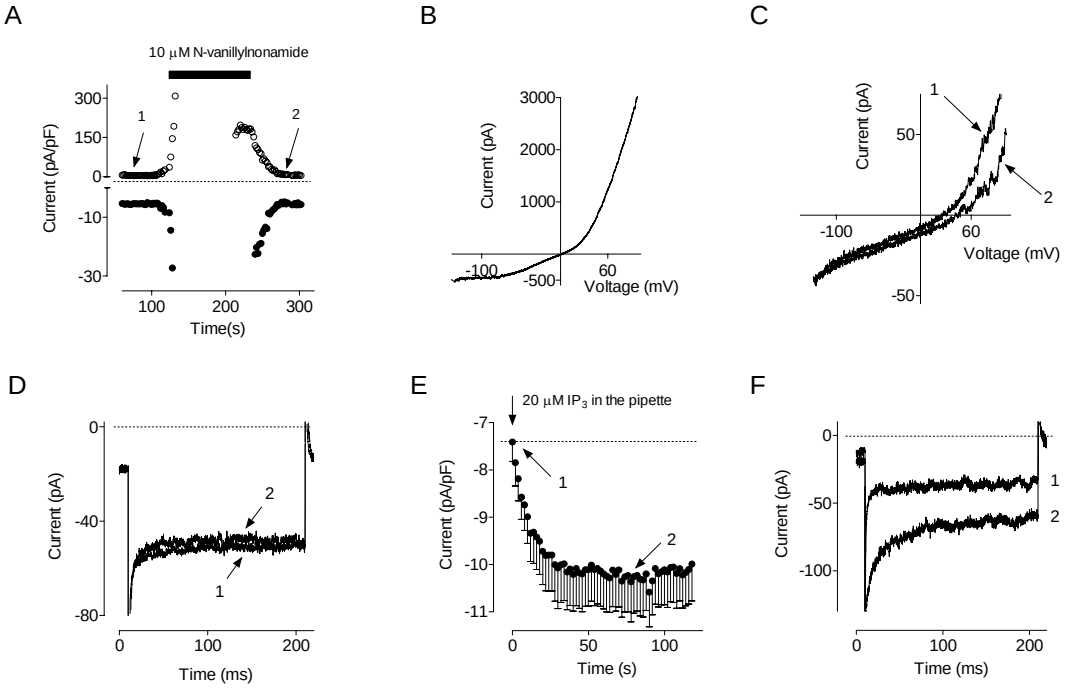
A
10 µM N-vanillylnonamide
Current (pA/pF)
Time(s)
B
Current (pA)
Voltage (mV)
C
Current (pA)
Voltage (mV)
D
Current (pA)
Time (ms)
E
20 µM IP3 in the pipette
Current (pA/pF)
Time (s)
F
Current (pA)
Time (ms)

Fig 8

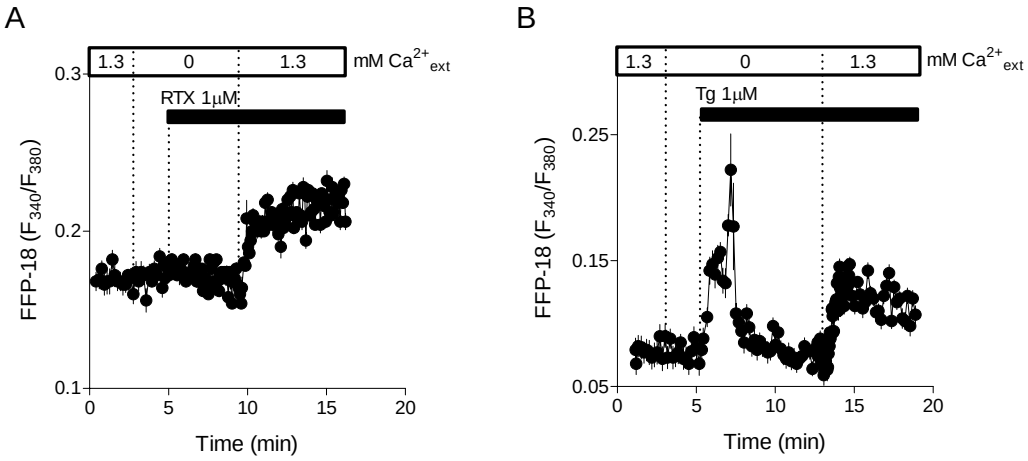
A
1.3
0
1.3
mM Ca2+ext
RTX 1μM
FFP-18 (F340/F380)
0.3
0.2
0.1
0
5
10
15
20
Time (min)
B
1.3
0
1.3
mM Ca2+ext
Tg 1μM
FFP-18 (F340/F380)
0.25
0.15
0.05
0
5
10
15
20
Time (min)

Fig 9

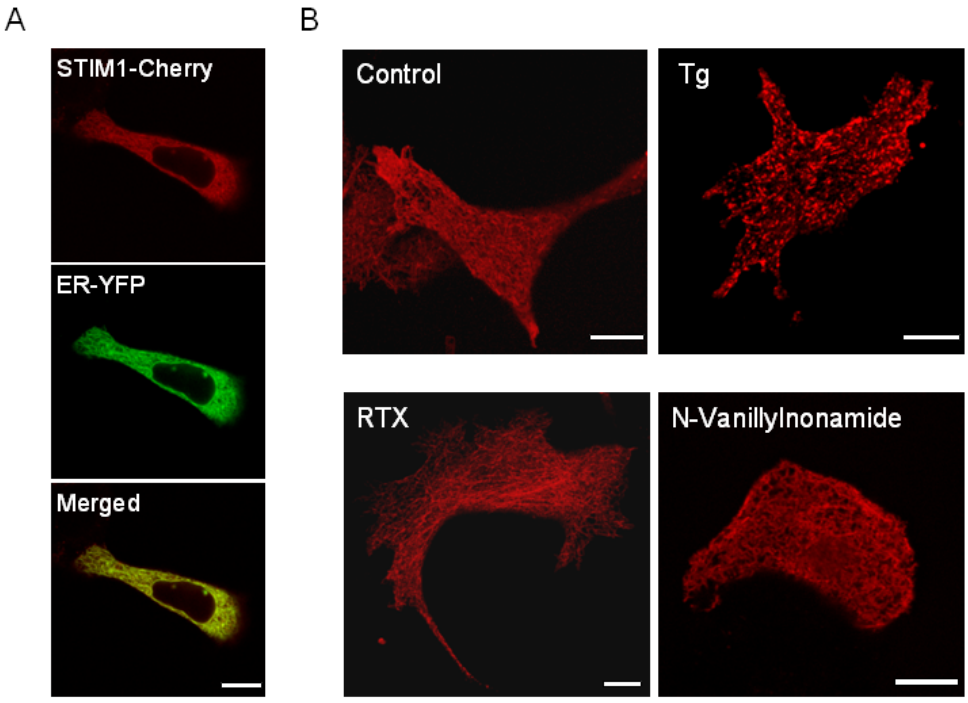
A
STIM1-Cherry
ER-YFP
Merged
B
Control
Tg
RTX
N-VanillylInonamide

Fig 10

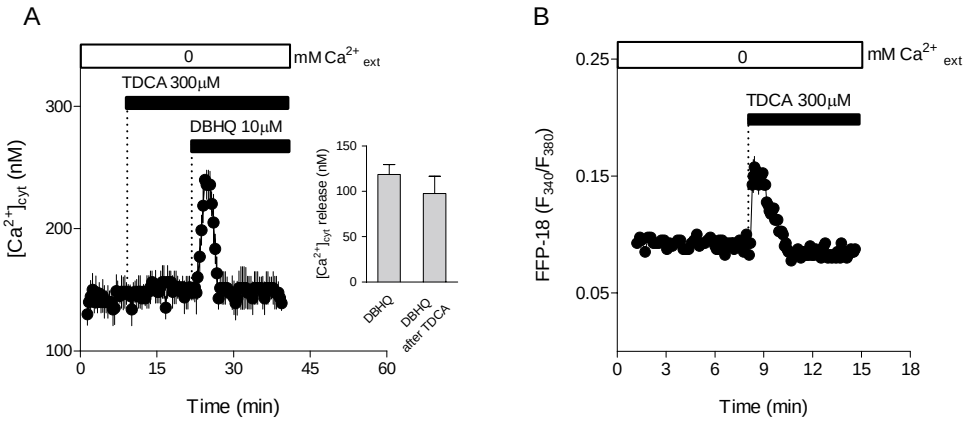
A
0
mM Ca2+ ext
TDCA 300µM
DBHQ 10µM
[Ca2+]cyt (nM)
300
200
100
0
15
30
45
60
Time (min)
[Ca2+]cyt release (nM)
150
100
50
0
DBHQ
DBHQ after TDCA
B
0
mM Ca2+ ext
TDCA 300µM
FFP-18 (F340/F380)
0.25
0.15
0.05
0
3
6
9
12
15
18
Time (min)

Fig 11

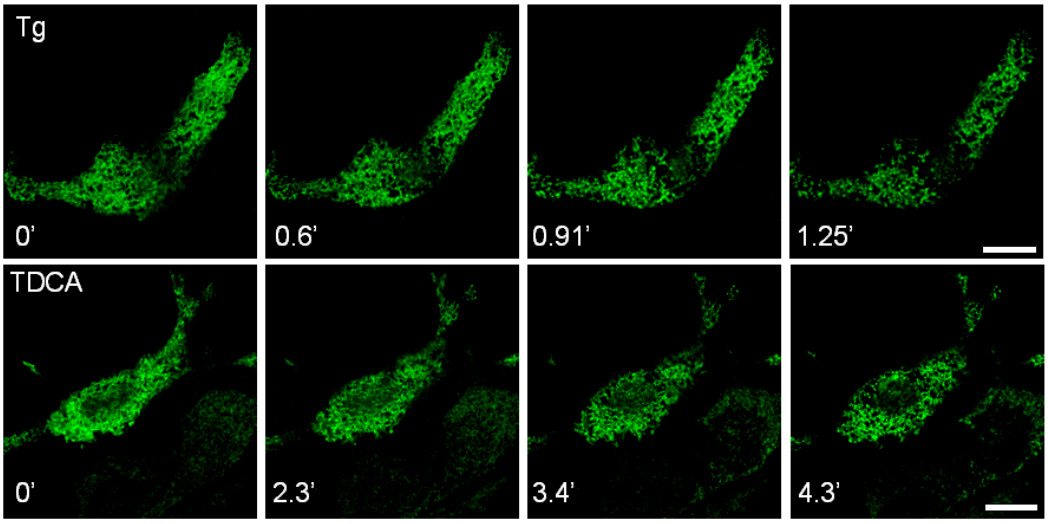
Tg
0'
0.6'
0.91'
1.25'
TDCA
0'
2.3'
3.4'
4.3'

Fig 12

REFERENCES

Albert, A.P., Pucovsky, V., Prestwich, S.A., and Large, W.A. (2006). TRPC3 properties of a native constitutively active Ca2+-permeable cation channel in rabbit ear artery myocytes. Journal of Physiology *571*, 361-369.

Alpini, G., Kanno, N., Phinizy, J.L., Glaser, S., Francis, H., Taffetani, S., and LeSage, G. (2004). Tauroursodeoxycholate inhibits human cholangiocarcinoma growth via Ca2+-, PKC-, and MAPK-dependent pathways. American Journal of Physiology - Gastrointestinal & Liver Physiology *286*, G973-982.

Aromataris, E.C., Castro, J., Rychkov, G.Y., and Barritt, G.J. (2008). Store-operated Ca(2+) channels and Stromal Interaction Molecule 1 (STIM1) are targets for the actions of bile acids on liver cells. Biochimica et biophysica acta *1783*, 874-885.

Aromataris, E.C., Roberts, M.L., Barritt, G.J., and Rychkov, G.Y. (2006). Glucagon activates Ca2+ and Cl- channels in rat hepatocytes. Journal of Physiology *573*, 611-625.

Artalejo, A.R., Ellory, J.C., and Parekh, A.B. (1998). Ca2+-dependent capacitance increases in rat basophilic leukemia cells following activation of store-operated Ca2+ entry and dialysis with high-Ca2+-containing intracellular solution. Pflugers Arch *436*, 934-939.

Auld, A., Chen, J., Brereton, H.M., Wang, Y.J., Gregory, R.B., and Barritt, G.J. (2000). Store-operated Ca(2+) inflow in Reuber hepatoma cells is inhibited by voltage-operated Ca(2+) channel antagonists and, in contrast to freshly isolated hepatocytes, does not require a pertussis toxin-sensitive trimeric GTP-binding protein. Biochimica et biophysica acta *1497*, 11-26.

Azer, S.A., Canfield, P.J., and Stacey, N.H. (1995). Hepatoprotection in ethinylestradiol-treated rats is provided by tauroursodeoxycholic acid, but not by ursodeoxycholic acid. Journal of Gastroenterology & Hepatology *10*, 261-269.

Baba, Y., Hayashi, K., Fujii, Y., Mizushima, A., Watarai, H., Wakamori, M., Numaga, T., Mori, Y., Iino, M., Hikida, M., and Kurosaki, T. (2006). Coupling of STIM1 to store-operated Ca2+ entry through its constitutive and inducible movement in the endoplasmic reticulum. Proceedings of the National Academy of Sciences of the United States of America *103*, 16704-16709.

Bakowski, D., Glitsch, M.D., and Parekh, A.B. (2001). An examination of the secretion-like coupling model for the activation of the Ca2+ release-activated Ca2+ current I(CRAC) in RBL-1 cells. J Physiol *532*, 55-71.

Bakowski, D., and Parekh, A.B. (2000). Voltage-dependent conductance changes in the store-operated Ca2+ current ICRAC in rat basophilic leukaemia cells. J Physiol *529 Pt 2*, 295-306.

Bakowski, D., and Parekh, A.B. (2002). Monovalent cation permeability and Ca(2+) block of the store-operated Ca(2+) current I(CRAC)in rat basophilic leukemia cells. Pflugers Arch *443*, 892-902.

Barritt, G.J. (1999). Receptor-activated Ca2+ inflow in animal cells: a variety of pathways tailored to meet different intracellular Ca2+ signalling requirements. Biochem J *337 (Pt 2)*, 153-169.

Barritt, G.J., Chen, J., and Rychkov, G.Y. (2008). Ca(2+)-permeable channels in the hepatocyte plasma membrane and their roles in hepatocyte physiology. Biochimica et biophysica acta.

Barritt, G.J., Pochet, R., Donato, R., Haiech, J., Heizmann, C.W., and Gerke, V. (2000). Calcium: the molecular basis of calcium action in biology and medicine. Kluwer Academic Publishers

Barros, L.F., Stutzin, A., Calixto, A., Catalan, M., Castro, J., Hetz, C., and Hermosilla, T. (2001). Nonselective cation channels as effectors of free radical-induced rat liver cell necrosis. Hepatology (Baltimore, Md *33*, 114-122.

Bear, C.E. (1990). A nonselective cation channel in rat liver cells is activated by membrane stretch. The American journal of physiology *258*, C421-428.

Bear, C.E., and Li, C.H. (1991). Calcium-permeable channels in rat hepatoma cells are activated by extracellular nucleotides. The American journal of physiology *261*, C1018-1024.

Beech, D.J. (2007). Canonical transient receptor potential 5. Handbook of Experimental Pharmacology, 109-123.

Benz, C., Angermuller, S., Tox, U., Kloters-Plachky, P., Riedel, H.D., Sauer, P., Stremmel, W., and Stiehl, A. (1998). Effect of tauroursodeoxycholic acid on bile-acid-induced apoptosis and cytolysis in rat hepatocytes. Journal of Hepatology *28*, 99-106.

Berridge, M.J. (1993). Inositol trisphosphate and calcium signalling. Nature *361*, 315-325.

Berry, M.N., Edwards, A.M., and Barritt, G.J. (1991). Isolated hepatocytes — preparation, properties and applications. Elsevier

Beuers, U., Boyer, J.L., and Paumgartner, G. (1998). Ursodeoxycholic acid in cholestasis: potential mechanisms of action and therapeutic applications. Hepatology (Baltimore, Md *28*, 1449-1453.

Beuers, U., Nathanson, M.H., and Boyer, J.L. (1993a). Effects of tauroursodeoxycholic acid on cytosolic Ca2+ signals in isolated rat hepatocytes. Gastroenterology *104*, 604-612.

Beuers, U., Nathanson, M.H., Isales, C.M., and Boyer, J.L. (1993b). Tauroursodeoxycholic acid stimulates hepatocellular exocytosis and mobilizes extracellular Ca++ mechanisms defective in cholestasis. Journal of Clinical Investigation *92*, 2984-2993.

Beuers, U., Probst, I., Soroka, C., Boyer, J.L., Kullak-Ublick, G.A., and Paumgartner, G. (1999). Modulation of protein kinase C by taurolithocholic acid in isolated rat hepatocytes. Hepatology (Baltimore, Md *29*, 477-482.

Bezprozvanny, I., Watras, J., and Ehrlich, B.E. (1991). Bell-shaped calcium-response curves of Ins(1,4,5)P3- and calcium-gated channels from endoplasmic reticulum of cerebellum. Nature *351*, 751-754.

Bird, G.S., and Putney, J.W., Jr. (2005). Capacitative calcium entry supports calcium oscillations in human embryonic kidney cells.[see comment]. Journal of Physiology *562*, 697-706.

Bohan, A., and Boyer, J.L. (2002). Mechanisms of hepatic transport of drugs: implications for cholestatic drug reactions. Seminars in liver disease *22*, 123-136.

Borgognone, M., Perez, L.M., Basiglio, C.L., Ochoa, J.E., and Roma, M.G. (2005). Signaling modulation of bile salt-induced necrosis in isolated rat hepatocytes. Toxicological Sciences *83*, 114-125.

Bouchard, G., Yousef, I.M., and Tuchweber, B. (1993). Influence of oral treatment with ursodeoxycholic and tauroursodeoxycholic acids on estrogen-induced cholestasis in rats: effects on bile formation and liver plasma membranes. Liver *13*, 193-202.

Bouscarel, B., Fromm, H., and Nussbaum, R. (1993). Ursodeoxycholate mobilizes intracellular Ca2+ and activates phosphorylase a in isolated hepatocytes. American journal of physiology *264*, G243-251.

Boyer, J.L. (2001). Molecular pathophysiology of membrane transport function in cholestasis. The liver: biology and pathobiology, 663-677.

Boyer, J.L. (2002a). Bile formation and cholestasis. In: Schiffs diseases of the liver, vol. 1, Philadelphia Lippincott, Williams & Wilkins, 135-165.

Boyer, J.L. (2002b). Schiffs diseases of the liver. Lippincott, Williams & Wilkins: Philadelphia

Braun, A.P., and Schulman, H. (1995). A non-selective cation current activated via the multifunctional Ca(2+)-calmodulin-dependent protein kinase in human epithelial cells. J Physiol *488 (Pt 1)*, 37-55.

Broad, L.M., Cannon, T.R., Short, A.D., and Taylor, C.W. (1999). Receptors linked to polyphosphoinositide hydrolysis stimulate Ca2+ extrusion by a phospholipase C-independent mechanism. Biochem J *342 (Pt 1)*, 199-206.

Brown, M.S., and Goldstein, J.L. (1999). A proteolytic pathway that controls the cholesterol content of membranes, cells, and blood. Proc Natl Acad Sci U S A *96*, 11041-11048.

Burdyga, T., Wray, S., and Noble, K. (2007). In situ calcium signaling: no calcium sparks detected in rat myometrium. Annals of the New York Academy of Sciences *1101*, 85-96.

Capiod, T. (1998). ATP-activated cation currents in single guinea-pig hepatocytes. J Physiol *507 (Pt 3)*, 795-805.

Carafoli, E. (2002). Calcium signaling: a tale for all seasons. Proc Natl Acad Sci U S A *99*, 1115-1122.

Castro, J., Bittner, C.X., Humeres, A., Montecinos, V.P., Vera, J.C., and Barros, L.F. (2004). A cytosolic source of calcium unveiled by hydrogen peroxide with relevance for epithelial cell death. Cell Death & Differentiation *11*, 468-478.

Caterina, M.J., Leffler, A., Malmberg, A.B., Martin, W.J., Trafton, J., Petersen-Zeitz, K.R., Koltzenburg, M., Basbaum, A.I., and Julius, D. (2000). Impaired nociception and pain sensation in mice lacking the capsaicin receptor.[see comment]. Science *288*, 306-313.

Caterina, M.J., Schumacher, M.A., Tominaga, M., Rosen, T.A., Levine, J.D., and Julius, D. (1997). The capsaicin receptor: a heat-activated ion channel in the pain pathway. Nature *389*, 816-824.

Chadborn, N., Eickholt, B., Doherty, P., and Bolsover, S. (2002). Direct measurement of local raised subplasmalemmal calcium concentrations in growth cones advancing on an N-cadherin substrate. Eur J Neurosci *15*, 1891-1898.

Chan, C., Harland, M.L., Webb, S.E., Chen, J., Miller, A.L., and Barritt, G.J. (2004). Evaluation, using targeted aequorins, of the roles of the endoplasmic reticulum and its (Ca2++Mg2+)ATP-ases in the activation of store-operated Ca2+ channels in liver cells. Cell Calcium *35*, 317-331.

Chieco, P., Romagnoli, E., Aicardi, G., Suozzi, A., Forti, G.C., and Roda, A. (1997). Apoptosis induced in rat hepatocytes by in vivo exposure to taurochenodeoxycholate. Histochemical Journal *29*, 875-883.

Chuang, H.H., Prescott, E.D., Kong, H., Shields, S., Jordt, S.E., Basbaum, A.I., Chao, M.V., and Julius, D. (2001). Bradykinin and nerve growth factor release the capsaicin receptor from PtdIns(4,5)P2-mediated inhibition. Nature *411*, 957-962.

Clapham, D.E. (1995). Calcium signaling. Cell *80*, 259-268.

Combettes, L., Berthon, B., Doucet, E., Erlinger, S., and Claret, M. (1990). Bile acids mobilise internal Ca2+ independently of external Ca2+ in rat hepatocytes. European Journal of Biochemistry *190*, 619-623.

Combettes, L., Cheek, T.R., and Taylor, C.W. (1996). Regulation of inositol trisphosphate receptors by luminal Ca2+ contributes to quantal Ca2+ mobilization. The EMBO journal *15*, 2086-2093.

Combettes, L., Dumont, M., Berthon, B., Erlinger, S., and Claret, M. (1988a). Effect of the bile acid taurolithocholate on cell calcium in saponin-treated rat hepatocytes. FEBS letters *227*, 161-166.

Combettes, L., Dumont, M., Berthon, B., Erlinger, S., and Claret, M. (1988b). Release of calcium from the endoplasmic reticulum by bile acids in rat liver cells. Journal of Biological Chemistry *263*, 2299-2303.

Cooper, D.M., Karpen, J.W., Fagan, K.A., and Mons, N.E. (1998). Ca(2+)-sensitive adenylyl cyclases. Advances in second messenger and phosphoprotein research *32*, 23-51.

Craven, P.A., Pfanstiel, J., and DeRubertis, F.R. (1987). Role of activation of protein kinase C in the stimulation of colonic epithelial proliferation and reactive oxygen formation by bile acids. Journal of Clinical Investigation *79*, 532-541.

Criddle, D.N., Raraty, M.G., Neoptolemos, J.P., Tepikin, A.V., Petersen, O.H., and Sutton, R. (2004). Ethanol toxicity in pancreatic acinar cells: mediation by nonoxidative fatty acid metabolites. Proceedings of the National Academy of Sciences of the United States of America *101*, 10738-10743.

Csordas, G., Renken, C., Varnai, P., Walter, L., Weaver, D., Buttle, K.F., Balla, T., Mannella, C.A., and Hajnoczky, G. (2006). Structural and functional features and significance of the physical linkage between ER and mitochondria. J Cell Biol *174*, 915-921.

Cui, M., Honore, P., Zhong, C., Gauvin, D., Mikusa, J., Hernandez, G., Chandran, P., Gomtsyan, A., Brown, B., Bayburt, E.K., Marsh, K., Bianchi, B., McDonald, H., Niforatos, W., Neelands, T.R., Moreland, R.B., Decker, M.W., Lee, C.H., Sullivan, J.P., and Faltynek, C.R. (2006). TRPV1 receptors in the CNS play a key role in broad-spectrum analgesia of TRPV1 antagonists. J Neurosci *26*, 9385-9393.

Darlington, G.J. (1987). Liver cell lines. Methods in Enzymology *151*, 19-38.

Davies, E.V., Blanchfield, H., and Hallett, M.B. (1997). Use of fluorescent dyes for measurement and localization of organelles associated with Ca2+ store release in human neutrophils. Cell Biol Int *21*, 655-663.

Davies, E.V., and Hallett, M.B. (1998). High micromolar Ca2+ beneath the plasma membrane in stimulated neutrophils. Biochem Biophys Res Commun *248*, 679-683.

Dawson, J.L., and Tan, K.C. (1992). In Wright's liver and biliary diseases, pathophysiology, diagnosis and management. (Eds, Millward-Sadler, G. H., Wright, R. and Arthur, M. S. P.), WB Saunders: London.

Delgado-Coello, B., Santiago-Garcia, J., Zarain-Herzberg, A., and Mas-Oliva, J. (2003). Plasma membrane Ca2+-ATPase mRNA expression in murine hepatocarcinoma and regenerating liver cells. Molecular and cellular biochemistry *247*, 177-184.

Delgado-Coello, B., Trejo, R., and Mas-Oliva, J. (2006). Is there a specific role for the plasma membrane Ca2+ -ATPase in the hepatocyte? Molecular and cellular biochemistry *285*, 1-15.

Delmas, P., and Brown, D.A. (2002). Junctional signaling microdomains: bridging the gap between the neuronal cell surface and Ca2+ stores. Neuron *36*, 787-790.

Dietrich, A., Mederos y Schnitzler, M., Emmel, J., Kalwa, H., Hofmann, T., and Gudermann, T. (2003). N-linked protein glycosylation is a major determinant for basal TRPC3 and TRPC6 channel activity. Journal of Biological Chemistry *278*, 47842-47852.

Dixon, C.J., White, P.J., Hall, J.F., Kingston, S., and Boarder, M.R. (2005). Regulation of human hepatocytes by P2Y receptors: control of glycogen phosphorylase, Ca2+, and mitogen-activated protein kinases. The Journal of pharmacology and experimental therapeutics *313*, 1305-1313.

Dray, A., Forbes, C.A., and Burgess, G.M. (1990). Ruthenium red blocks the capsaicin-induced increase in intracellular calcium and activation of membrane currents in sensory neurones as well as the activation of peripheral nociceptors in vitro. Neuroscience Letters *110*, 52-59.

Elferink, R.O., and Groen, A.K. (2002). Genetic defects in hepatobiliary transport. Biochimica et biophysica acta *1586*, 129-145.

Enfissi, A., Prigent, S., Colosetti, P., and Capiod, T. (2004). The blocking of capacitative calcium entry by 2-aminoethyl diphenylborate (2-APB) and

carboxyamidotriazole (CAI) inhibits proliferation in Hep G2 and Huh-7 human hepatoma cells. Cell Calcium *36*, 459-467.

Engelke, M., Friedrich, O., Budde, P., Schafer, C., Niemann, U., Zitt, C., Jungling, E., Rocks, O., Luckhoff, A., and Frey, J. (2002). Structural domains required for channel function of the mouse transient receptor potential protein homologue TRP1beta. FEBS letters *523*, 193-199.

Etter, E.F., Kuhn, M.A., and Fay, F.S. (1994). Detection of changes in near-membrane Ca2+ concentration using a novel membrane-associated Ca2+ indicator. J Biol Chem *269*, 10141-10149.

Etter, E.F., Minta, A., Poenie, M., and Fay, F.S. (1996). Near-membrane [Ca2+] transients resolved using the Ca2+ indicator FFP18. Proc Natl Acad Sci U S A *93*, 5368-5373.

Fabris, P., Tositti, G., Mazzella, G., Zanetti, A.R., Nicolin, R., Pellizzer, G., Benedetti, P., and de Lalla, F. (1999). Effect of ursodeoxycholic acid administration in patients with acute viral hepatitis: a pilot study. Alimentary Pharmacology & Therapeutics *13*, 1187-1193.

Fagan, K.A., Mons, N., and Cooper, D.M. (1998). Dependence of the Ca2+-inhibitable adenylyl cyclase of C6-2B glioma cells on capacitative Ca2+ entry. J Biol Chem *273*, 9297-9305.

Fanger, C.M., Hoth, M., Crabtree, G.R., and Lewis, R.S. (1995). Characterization of T cell mutants with defects in capacitative calcium entry: genetic evidence for the physiological roles of CRAC channels. J Cell Biol *131*, 655-667.

Ferri, K.F., and Kroemer, G. (2001). Organelle-specific initiation of cell death pathways. Nature cell biology *3*, E255-263.

Feske, S., Gwack, Y., Prakriya, M., Srikanth, S., Puppel, S.H., Tanasa, B., Hogan, P.G., Lewis, R.S., Daly, M., and Rao, A. (2006). A mutation in Orai1 causes immune deficiency by abrogating CRAC channel function. Nature *441*, 179-185.

Fierro, L., and Parekh, A.B. (1999). Fast calcium-dependent inactivation of calcium release-activated calcium current (CRAC) in RBL-1 cells. The Journal of membrane biology *168*, 9-17.

Finch, E.A., Turner, T.J., and Goldin, S.M. (1991). Calcium as a coagonist of inositol 1,4,5-trisphosphate-induced calcium release. Science (New York, N.Y *252*, 443-446.

Fischer, B.S., Qin, D., Kim, K., and McDonald, T.V. (2001). Capsaicin inhibits Jurkat T-cell activation by blocking calcium entry current I(CRAC). The Journal of pharmacology and experimental therapeutics *299*, 238-246.

Fomina, A.F., and Nowycky, M.C. (1999). A current activated on depletion of intracellular Ca2+ stores can regulate exocytosis in adrenal chromaffin cells. J Neurosci *19*, 3711-3722.

Friman, S., and Svanvik, J. (1994). A possible role of ursodeoxycholic acid in liver transplantation. Scandinavian Journal of Gastroenterology - Supplement *204*, 62-64.

Gasbarrini, A., Borle, A.B., and Van Thiel, D.H. (1993). Ca2+ antagonists do not protect isolated perfused rat hepatocytes from anoxic injury. Biochimica et biophysica acta *1177*, 1-7.

Gaspers, L.D., and Thomas, A.P. (2005). Calcium signaling in liver. Cell Calcium *38*, 329-342.

Gerasimenko, J.V., Flowerdew, S.E., Voronina, S.G., Sukhomlin, T.K., Tepikin, A.V., Petersen, O.H., and Gerasimenko, O.V. (2006). Bile acids induce Ca2+ release from both the endoplasmic reticulum and acidic intracellular calcium stores through activation of inositol trisphosphate receptors and ryanodine receptors. Journal of Biological Chemistry *281*, 40154-40163.

Gilabert, J.A., Bakowski, D., and Parekh, A.B. (2001). Energized mitochondria increase the dynamic range over which inositol 1,4,5-trisphosphate activates store-operated calcium influx. EMBO Journal *20*, 2672-2679.

Gilabert, J.A., and Parekh, A.B. (2000a). Respiring mitochondria determine the pattern of activation and inactivation of the store-operated Ca(2+) current I(CRAC). The EMBO journal *19*, 6401-6407.

Gilabert, J.A., and Parekh, A.B. (2000b). Respiring mitochondria determine the pattern of activation and inactivation of the store-operated Ca(2+) current I(CRAC). EMBO Journal *19*, 6401-6407.

Glitsch, M.D., Bakowski, D., and Parekh, A.B. (2002a). Effects of inhibitors of the lipo-oxygenase family of enzymes on the store-operated calcium current I(CRAC) in rat basophilic leukaemia cells. Journal of Physiology *539*, 93-106.

Glitsch, M.D., Bakowski, D., and Parekh, A.B. (2002b). Store-operated Ca2+ entry depends on mitochondrial Ca2+ uptake. The EMBO journal *21*, 6744-6754.

Golovina, V.A. (2005). Visualization of localized store-operated calcium entry in mouse astrocytes. Close proximity to the endoplasmic reticulum. J Physiol *564*, 737-749.

Golovina, V.A., and Blaustein, M.P. (1997). Spatially and functionally distinct Ca2+ stores in sarcoplasmic and endoplasmic reticulum. Science *275*, 1643-1648.

Gorelick, F.S., and Shugrue, C. (2001). Exiting the endoplasmic reticulum. Molecular and cellular endocrinology *177*, 13-18.

Graier, W.F., Paltauf-Doburzynska, J., Hill, B.J., Fleischhacker, E., Hoebel, B.G., Kostner, G.M., and Sturek, M. (1998). Submaximal stimulation of porcine endothelial cells causes focal Ca2+ elevation beneath the cell membrane. J Physiol *506 (Pt 1)*, 109-125.

Gregory, R.B., and Barritt, G.J. (2003). Evidence that Ca2+-release-activated Ca2+ channels in rat hepatocytes are required for the maintenance of hormone-induced Ca2+ oscillations. Biochemical Journal *370*, 695-702.

Gregory, R.B., Hughes, R., and Barritt, G.J. (2004a). Induction of cholestasis in the perfused rat liver by 2-aminoethyl diphenylborate, an inhibitor of the hepatocyte plasma membrane Ca2+ channels. Journal of Gastroenterology & Hepatology *19*, 1128-1134.

Gregory, R.B., Hughes, R., Riley, A.M., Potter, B.V., Wilcox, R.A., and Barritt, G.J. (2004b). Inositol trisphosphate analogues selective for types I and II inositol trisphosphate receptors exert differential effects on vasopressin-stimulated Ca2+ inflow and Ca2+ release from intracellular stores in rat hepatocytes. Biochemical Journal *381*, 519-526.

Gregory, R.B., Wilcox, R.A., Berven, L.A., van Straten, N.C., van der Marel, G.A., van Boom, J.H., and Barritt, G.J. (1999). Evidence for the involvement of a small subregion of the endoplasmic reticulum in the inositol trisphosphate receptor-induced activation of Ca2+ inflow in rat hepatocytes. Biochemical Journal *341*, 401-408.

Grynkiewicz, G., Poenie, M., and Tsien, R.Y. (1985). A new generation of Ca2+ indicators with greatly improved fluorescence properties. Journal of Biological Chemistry *260*, 3440-3450.

Gu, C., and Cooper, D.M. (2000). Ca(2+), Sr(2+), and Ba(2+) identify distinct regulatory sites on adenylyl cyclase (AC) types VI and VIII and consolidate the apposition of capacitative cation entry channels and Ca(2+)-sensitive ACs. J Biol Chem *275*, 6980-6986.

Gu, J.J., Hofmann, A.F., Ton-Nu, H.T., Schteingart, C.D., and Mysels, K.J. (1992). Solubility of calcium salts of unconjugated and conjugated natural bile acids. J Lipid Res *33*, 635-646.

Guillemette, G., Balla, T., Baukal, A.J., and Catt, K.J. (1988). Characterization of inositol 1,4,5-trisphosphate receptors and calcium mobilization in a hepatic plasma membrane fraction. J Biol Chem *263*, 4541-4548.

Gunthorpe, M.J., Benham, C.D., Randall, A., and Davis, J.B. (2002). The diversity in the vanilloid (TRPV) receptor family of ion channels. Trends in Pharmacological Sciences *23*, 183-191.

Hartmann, J., and Verkhratsky, A. (1998). Relations between intracellular Ca2+ stores and store-operated Ca2+ entry in primary cultured human glioblastoma cells. Journal of Physiology *513*, 411-424.

Hellwig, N., Albrecht, N., Harteneck, C., Schultz, G., and Schaefer, M. (2005). Homo- and heteromeric assembly of TRPV channel subunits. J Cell Sci *118*, 917-928.

Henkart, M., Landis, D.M., and Reese, T.S. (1976). Similarity of junctions between plasma membranes and endoplasmic reticulum in muscle and neurons. J Cell Biol *70*, 338-347.

Hernandez, E., Leite, M.F., Guerra, M.T., Kruglov, E.A., Bruna-Romero, O., Rodrigues, M.A., Gomes, D.A., Giordano, F.J., Dranoff, J.A., and Nathanson, M.H. (2007). The spatial distribution of inositol 1,4,5-trisphosphate receptor isoforms shapes Ca2+ waves. J Biol Chem *282*, 10057-10067.

Higuchi, H., and Gores, G.J. (2003). Bile acid regulation of hepatic physiology: IV. Bile acids and death receptors. American Journal of Physiology - Gastrointestinal & Liver Physiology *284*, G734-738.

Higuchi, H., Yoon, J.H., Grambihler, A., Werneburg, N., Bronk, S.F., and Gores, G.J. (2003). Bile acids stimulate cFLIP phosphorylation enhancing TRAIL-mediated apoptosis. Journal of Biological Chemistry *278*, 454-461.

Hirata, K., Pusl, T., O'Neill, A.F., Dranoff, J.A., and Nathanson, M.H. (2002). The type II inositol 1,4,5-trisphosphate receptor can trigger Ca2+ waves in rat hepatocytes. Gastroenterology *122*, 1088-1100.

Hofer, A.M., Fasolato, C., and Pozzan, T. (1998). Capacitative Ca2+ entry is closely linked to the filling state of internal Ca2+ stores: a study using simultaneous measurements of ICRAC and intraluminal [Ca2+]. Journal of Cell Biology *140*, 325-334.

Hofmann, A.F., and Mysels, K.J. (1992). Bile acid solubility and precipitation in vitro and in vivo: the role of conjugation, pH, and Ca2+ ions. J Lipid Res *33*, 617-626.

Horne, J.H., and Meyer, T. (1997). Elementary calcium-release units induced by inositol trisphosphate. Science *276*, 1690-1693.

Hoth, M., Button, D.C., and Lewis, R.S. (2000). Mitochondrial control of calcium-channel gating: a mechanism for sustained signaling and transcriptional activation in T lymphocytes. Proceedings of the National Academy of Sciences of the United States of America *97*, 10607-10612.

Hoth, M., and Penner, R. (1992). Depletion of intracellular calcium stores activates a calcium current in mast cells. Nature *355*, 353-356.

Hoth, M., and Penner, R. (1993). Calcium release-activated calcium current in rat mast cells. J Physiol *465*, 359-386.

Howard, A., Barley, N.F., Legon, S., and Walters, J.R. (1994). Plasma-membrane calcium-pump isoforms in human and rat liver. Biochem J *303 (Pt 1)*, 275-279.

Huang, S.M., Bisogno, T., Trevisani, M., Al-Hayani, A., De Petrocellis, L., Fezza, F., Tognetto, M., Petros, T.J., Krey, J.F., Chu, C.J., Miller, J.D., Davies, S.N., Geppetti, P., Walker, J.M., and Di Marzo, V. (2002). An endogenous capsaicin-like substance with high potency at recombinant and native vanilloid VR1 receptors. Proc Natl Acad Sci U S A *99*, 8400-8405.

Huang, X.P., Fan, X.T., Desjeux, J.F., and Castagna, M. (1992). Bile acids, non-phorbol-ester-type tumor promoters, stimulate the phosphorylation of protein kinase C substrates in human platelets and colon cell line HT29. International Journal of Cancer *52*, 444-450.

Huang, Y., and Putney, J.W., Jr. (1998). Relationship between intracellular calcium store depletion and calcium release-activated calcium current in a mast cell line (RBL-1). Journal of Biological Chemistry *273*, 19554-19559.

Huang, Y.T., Hsu, Y.C., Chen, C.J., Liu, C.T., and Wei, Y.H. (2003). Oxidative-stress-related changes in the livers of bile-duct-ligated rats. Journal of Biomedical Science *10*, 170-178.

Hubbard, A.L., Barr, V.A., and Scott, L.J. (1994). The Liver: Biology and pathobiology. Raven Press Ltd: New York

Hwang, S.W., Cho, H., Kwak, J., Lee, S.Y., Kang, C.J., Jung, J., Cho, S., Min, K.H., Suh, Y.G., Kim, D., and Oh, U. (2000). Direct activation of capsaicin receptors by products of lipoxygenases: endogenous capsaicin-like substances. Proceedings of the National Academy of Sciences of the United States of America *97*, 6155-6160.

Ishikawa, J., Ohga, K., Yoshino, T., Takezawa, R., Ichikawa, A., Kubota, H., and Yamada, T. (2003). A pyrazole derivative, YM-58483, potently inhibits store-operated sustained Ca2+ influx and IL-2 production in T lymphocytes. J Immunol *170*, 4441-4449.

Ishizaki, K., Kinbara, S., Hirabayashi, N., Uchiyama, K., and Maeda, M. (2001). Effect of sodium tauroursodeoxycholate on phalloidin-induced cholestasis in rats. European Journal of Pharmacology *421*, 55-60.

Jacquemin, E., Dumont, M., Mallet, A., and Erlinger, S. (1993). Ursodeoxycholic acid improves ethinyl estradiol-induced cholestasis in the rat. European Journal of Clinical Investigation *23*, 794-802.

Jansen, P.L., Muller, M., and Sturm, E. (2001). Genes and cholestasis. Hepatology (Baltimore, Md *34*, 1067-1074.

Kagaya, M., Lamb, J., Robbins, J., Page, C.P., and Spina, D. (2002). Characterization of the anandamide induced depolarization of guinea-pig isolated vagus nerve. British journal of pharmacology *137*, 39-48.

Karai, L.J., Russell, J.T., Iadarola, M.J., and Olah, Z. (2004). Vanilloid receptor 1 regulates multiple calcium compartments and contributes to Ca2+-induced Ca2+ release in sensory neurons. Journal of Biological Chemistry *279*, 16377-16387.

Kaufman, R.J. (1999). Stress signaling from the lumen of the endoplasmic reticulum: coordination of gene transcriptional and translational controls. Genes & development *13*, 1211-1233.

Kedei, N., Szabo, T., Lile, J.D., Treanor, J.J., Olah, Z., Iadarola, M.J., and Blumberg, P.M. (2001). Analysis of the native quaternary structure of vanilloid receptor 1. Journal of Biological Chemistry *276*, 28613-28619.

Kim, J.Y., Kim, K.H., Lee, J.A., Namkung, W., Sun, A.Q., Ananthanarayanan, M., Suchy, F.J., Shin, D.M., Muallem, S., and Lee, M.G. (2002). Transporter-mediated bile acid uptake causes Ca2+-dependent cell death in rat pancreatic acinar cells.[see comment]. Gastroenterology *122*, 1941-1953.

Kinbara, S., Ishizaki, K., Sakakura, H., Hirabayashi, N., Kasai, H., and Araki, T. (1997). Improvement of estradiol-17 beta-D-glucuronide-induced cholestasis by sodium tauroursodeoxycholate therapy in rats. Scandinavian Journal of Gastroenterology *32*, 947-952.

Kunzelmann-Marche, C., Freyssinet, J.M., and Martinez, M.C. (2001). Regulation of phosphatidylserine transbilayer redistribution by store-operated Ca2+ entry: role of actin cytoskeleton. J Biol Chem *276*, 5134-5139.

Lau, B.W., Colella, M., Ruder, W.C., Ranieri, M., Curci, S., and Hofer, A.M. (2005). Deoxycholic acid activates protein kinase C and phospholipase C via increased Ca2+ entry at plasma membrane. Gastroenterology *128*, 695-707.

Lazaridis, K.N., Gores, G.J., and Lindor, K.D. (2001). Ursodeoxycholic acid 'mechanisms of action and clinical use in hepatobiliary disorders'. Journal of Hepatology *35*, 134-146.

Lee, J., and Boyer, J.L. (2000). Molecular alterations in hepatocyte transport mechanisms in acquired cholestatic liver disorders. Seminars in liver disease *20*, 373-384.

Leite, M.F., and Nathanson, M.H. (2001). The Liver Biology and Pathobiology. Lippincott, Williams & Wilkins: Philadelphia

Lewis, R.S. (1999). Store-operated calcium channels. Advances in second messenger and phosphoprotein research *33*, 279-307.

Lewis, R.S. (2007). The molecular choreography of a store-operated calcium channel. Nature *446*, 284-287.

Lievremont, J.P., Hill, A.M., Hilly, M., and Mauger, J.P. (1994). The inositol 1,4,5-trisphosphate receptor is localized on specialized sub-regions of the endoplasmic reticulum in rat liver. Biochem J *300 (Pt 2)*, 419-427.

Lievremont, J.P., Hill, A.M., Tran, D., Coquil, J.F., Stelly, N., and Mauger, J.P. (1996). Intracellular calcium stores and inositol 1,4,5-trisphosphate receptor in rat liver cells. Biochem J *314 (Pt 1)*, 189-197.

Lin, S., Fagan, K.A., Li, K.X., Shaul, P.W., Cooper, D.M., and Rodman, D.M. (2000). Sustained endothelial nitric-oxide synthase activation requires capacitative Ca2+ entry. J Biol Chem *275*, 17979-17985.

Liou, J., Fivaz, M., Inoue, T., and Meyer, T. (2007). Live-cell imaging reveals sequential oligomerization and local plasma membrane targeting of stromal interaction molecule 1 after Ca2+ store depletion. Proceedings of the National Academy of Sciences of the United States of America *104*, 9301-9306.

Liou, J., Kim, M.L., Heo, W.D., Jones, J.T., Myers, J.W., Ferrell, J.E., Jr., and Meyer, T. (2005). STIM is a Ca2+ sensor essential for Ca2+-store-depletion-triggered Ca2+ influx. Current Biology *15*, 1235-1241.

Lippincoott-Schwartz, J. (1994). The liver biology and pathology: The endoplasmic reticulum-Golgi membrane system. (Arias I. M., Boyer, J. L., Fausto, N., Jakoby, W. B., Schachter, D. A., and Shafritz, D. A.) Raven Press: New York.

Litjens, T., Harland, M.L., Roberts, M.L., Barritt, G.J., and Rychkov, G.Y. (2004). Fast Ca(2+)-dependent inactivation of the store-operated Ca2+ current (ISOC) in liver cells: a role for calmodulin. Journal of Physiology *558*, 85-97.

Litjens, T., Nguyen, T., Castro, J., Aromataris, E.C., Jones, L., Barritt, G.J., and Rychkov, G.Y. (2007). Phospholipase C-gamma1 is required for the activation of store-operated Ca2+ channels in liver cells. Biochemical Journal *405*, 269-276.

Liu, M., Liu, M.C., Magoulas, C., Priestley, J.V., and Willmott, N.J. (2003). Versatile regulation of cytosolic Ca2+ by vanilloid receptor I in rat dorsal root ganglion neurons. Journal of Biological Chemistry *278*, 5462-5472.

Locke, E.G., Bonilla, M., Liang, L., Takita, Y., and Cunningham, K.W. (2000). A homolog of voltage-gated Ca(2+) channels stimulated by depletion of secretory Ca(2+) in yeast. Molecular and cellular biology *20*, 6686-6694.

Luik, R.M., Wu, M.M., Buchanan, J., and Lewis, R.S. (2006). The elementary unit of store-operated Ca2+ entry: local activation of CRAC channels by STIM1 at ER-plasma membrane junctions. Journal of Cell Biology *174*, 815-825.

Ma, H.T., Patterson, R.L., van Rossum, D.B., Birnbaumer, L., Mikoshiba, K., and Gill, D.L. (2000). Requirement of the inositol trisphosphate receptor for activation of store-operated Ca2+ channels. Science (New York, N.Y *287*, 1647-1651.

Macgregor, A., Yamasaki, M., Rakovic, S., Sanders, L., Parkesh, R., Churchill, G.C., Galione, A., and Terrar, D.A. (2007). NAADP controls cross-talk between distinct Ca2+ stores in the heart. J Biol Chem *282*, 15302-15311.

Maddrey, W.C. (2002). The cholestasis disorders. In: Schiffs diseases of the liver, vol. 1, Philadelphia: Lippincott, Williams & Wilkins, 647-649.

Maggi, C.A. (1991). Capsaicin and primary afferent neurons: from basic science to human therapy? Journal of the Autonomic Nervous System *33*, 1-14.

Malli, R., Frieden, M., Osibow, K., and Graier, W.F. (2003). Mitochondria efficiently buffer subplasmalemmal Ca2+ elevation during agonist stimulation. Journal of Biological Chemistry *278*, 10807-10815.

Marshall, I.C., Owen, D.E., Cripps, T.V., Davis, J.B., McNulty, S., and Smart, D. (2003). Activation of vanilloid receptor 1 by resiniferatoxin mobilizes calcium from inositol 1,4,5-trisphosphate-sensitive stores. British Journal of Pharmacology *138*, 172-176.

Martinez, M.C., Martin, S., Toti, F., Fressinaud, E., Dachary-Prigent, J., Meyer, D., and Freyssinet, J.M. (1999). Significance of capacitative Ca2+ entry in the regulation of phosphatidylserine expression at the surface of stimulated cells. Biochemistry *38*, 10092-10098.

Mercer, J.C., Dehaven, W.I., Smyth, J.T., Wedel, B., Boyles, R.R., Bird, G.S., and Putney, J.W., Jr. (2006). Large store-operated calcium selective currents due to co-expression of Orai1 or Orai2 with the intracellular calcium sensor, Stim1. Journal of Biological Chemistry *281*, 24979-24990.

Miayai, K. (1991). Hepatotoxicology. (Eds, meeks, R. G., Harrison, S. D. and Bull, R. J.) CRC Press, Bola, Raton.

Milovic, V., Teller, I.C., Faust, D., Caspary, W.F., and Stein, J. (2002). Effects of deoxycholate on human colon cancer cells: apoptosis or proliferation. European Journal of Clinical Investigation *32*, 29-34.

Mogami, H., Nakano, K., Tepikin, A.V., and Petersen, O.H. (1997). Ca2+ flow via tunnels in polarized cells: recharging of apical Ca2+ stores by focal Ca2+ entry through basal membrane patch. Cell *88*, 49-55.

Mohammed, F.F., and Khokha, R. (2005). Thinking outside the cell: proteases regulate hepatocyte division. Trends in cell biology *15*, 555-563.

Montalvo, G.B., Artalejo, A.R., and Gilabert, J.A. (2006). ATP from subplasmalemmal mitochondria controls Ca2+-dependent inactivation of CRAC channels. Journal of Biological Chemistry *281*, 35616-35623.

Montero, M., Garcia-Sancho, J., and Alvarez, J. (1994). Phosphorylation down-regulates the store-operated Ca2+ entry pathway of human neutrophils. Journal of Biological Chemistry *269*, 3963-3967.

Moreau, B., Nelson, C., and Parekh, A.B. (2006). Biphasic regulation of mitochondrial Ca2+ uptake by cytosolic Ca2+ concentration. Curr Biol *16*, 1672-1677.

Morgan, A.J., and Jacob, R. (1994). Ionomycin enhances Ca2+ influx by stimulating store-regulated cation entry and not by a direct action at the plasma membrane. Biochem J *300 (Pt 3)*, 665-672.

Muik, M., Frischauf, I., Derler, I., Fahrner, M., Bergsmann, J., Eder, P., Schindl, R., Hesch, C., Polzinger, B., Fritsch, R., Kahr, H., Madl, J., Gruber, H., Groschner, K., and Romanin, C. (2008). Dynamic Coupling of the Putative Coiled-coil Domain of ORAI1 with STIM1 Mediates ORAI1 Channel Activation. J Biol Chem *283*, 8014-8022.

Nathanson, M.H., and Boyer, J.L. (1991). Mechanisms and regulation of bile secretion. Hepatology (Baltimore, Md *14*, 551-566.

Neher, E., and Sakmann, B. (1976). Single-channel currents recorded from membrane of denervated frog muscle fibres. Nature *260*, 799-802.

Nieuwenhuijs, V.B., De Bruijn, M.T., Padbury, R.T., and Barritt, G.J. (2006). Hepatic ischemia-reperfusion injury: roles of Ca2+ and other intracellular mediators of impaired bile flow and hepatocyte damage. Digestive diseases and sciences *51*, 1087-1102.

Numaga, T., Wakamori, M., and Mori, Y. (2007). Trpc7. Handbook of Experimental Pharmacology, 143-151.

O'Brien, E.M., Gomes, D.A., Sehgal, S., and Nathanson, M.H. (2007). Hormonal regulation of nuclear permeability. J Biol Chem *282*, 4210-4217.

O'Leary, J.G., and Pratt, D.S. (2007). Cholestasis and cholestatic syndromes. Curr Opin Gastroenterology *23*, 232-236.

Olah, Z., Szabo, T., Karai, L., Hough, C., Fields, R.D., Caudle, R.M., Blumberg, P.M., and Iadarola, M.J. (2001). Ligand-induced dynamic membrane changes and cell deletion conferred by vanilloid receptor 1. Journal of Biological Chemistry *276*, 11021-11030.

Ong, H.L., Liu, X., Tsaneva-Atanasova, K., Singh, B.B., Bandyopadhyay, B.C., Swaim, W.D., Russell, J.T., Hegde, R.S., Sherman, A., and Ambudkar, I.S. (2007a). Relocalization of stim1 for activation of store-operated Ca2+ entry is determined by the depletion of subplasma membrane endoplasmic reticulum Ca2+ store Journal of Biological Chemistry *282*, 12176-12185.

Ong, H.L., Liu, X., Tsaneva-Atanasova, K., Singh, B.B., Bandyopadhyay, B.C., Swaim, W.D., Russell, J.T., Hegde, R.S., Sherman, A., and Ambudkar, I.S. (2007b). Relocalization of Stim1 for activation of store operated Ca2+ entry is determined by the depletion of subplasma membrane endoplasmic reticuluum Ca2+ store. Journal of Biological Chemistry *282*, 12176-12185.

Ono, T., Imai, K., Kohno, H., Uchida, M., Takemoto, Y., Dhar, D.K., and Nagasue, N. (1998). Tauroursodeoxycholic acid protects cholestasis in rat reperfused livers: its roles in hepatic calcium mobilization. Digestive Diseases & Sciences *43*, 2201-2210.

Paltauf-Doburzynska, J., Posch, K., Paltauf, G., and Graier, W.F. (1998). Stealth ryanodine-sensitive Ca2+ release contributes to activity of capacitative Ca2+ entry and nitric oxide synthase in bovine endothelial cells. J Physiol *513 (Pt 2)*, 369-379.

Parekh, A.B., and Penner, R. (1995). Activation of store-operated calcium influx at resting InsP3 levels by sensitization of the InsP3 receptor in rat basophilic leukaemia cells. J Physiol *489 (Pt 2)*, 377-382.

Parekh, A.B., and Penner, R. (1997). Store depletion and calcium influx. Physiological reviews *77*, 901-930.

Parekh, A.B., and Putney, J.W., Jr. (2005). Store-operated calcium channels. Physiological Reviews *85*, 757-810.

Pares, A., Caballeria, L., Rodes, J., Bruguera, M., Rodrigo, L., Garcia-Plaza, A., Berenguer, J., Rodriguez-Martinez, D., Mercader, J., and Velicia, R. (2000). Long-term effects of ursodeoxycholic acid in primary biliary cirrhosis: results of a double-blind controlled multicentric trial. UDCA-Cooperative Group from the Spanish Association for the Study of the Liver.[see comment]. Journal of Hepatology *32*, 561-566.

Park, M.K., Petersen, O.H., and Tepikin, A.V. (2000). The endoplasmic reticulum as one continuous Ca(2+) pool: visualization of rapid Ca(2+) movements and equilibration. EMBO Journal *19*, 5729-5739.

Partiseti, M., Le Deist, F., Hivroz, C., Fischer, A., Korn, H., and Choquet, D. (1994). The calcium current activated by T cell receptor and store depletion in human lymphocytes is absent in a primary immunodeficiency. J Biol Chem *269*, 32327-32335.

Patterson, R.L., van Rossum, D.B., and Gill, D.L. (1999). Store-operated Ca2+ entry: evidence for a secretion-like coupling model. Cell *98*, 487-499.

Pauli-Magnus, C., Stieger, B., Meier, Y., Kullak-Ublick, G.A., and Meier, P.J. (2005). Enterohepatic transport of bile salts and genetics of cholestasis. Journal of Hepatology *43*, 342-357.

Payne, C.M., Crowley-Weber, C.L., Dvorak, K., Bernstein, C., Bernstein, H., Holubec, H., Crowley, C., and Garewal, H. (2005). Mitochondrial perturbation attenuates bile acid-induced cytotoxicity. Cell Biology & Toxicology *21*, 215-231.

Peinelt, C., Vig, M., Koomoa, D.L., Beck, A., Nadler, M.J., Koblan-Huberson, M., Lis, A., Fleig, A., Penner, R., and Kinet, J.P. (2006). Amplification of CRAC current by STIM1 and CRACM1 (Orai1).[see comment]. Nature cell biology *8*, 771-773.

Peng, J.B., Brown, E.M., and Hediger, M.A. (2003). Epithelial Ca2+ entry channels: transcellular Ca2+ transport and beyond. Journal of Physiology *551*, 729-740.

Petersen, O.H., Tepikin, A., and Park, M.K. (2001). The endoplasmic reticulum: one continuous or several separate Ca(2+) stores? Trends in neurosciences *24*, 271-276.

Pettit, E.J., and Hallett, M.B. (1995). Early Ca2+ signalling events in neutrophils detected by rapid confocal laser scanning. Biochem J *310 (Pt 2)*, 445-448.

Pichler, H., Gaigg, B., Hrastnik, C., Achleitner, G., Kohlwein, S.D., Zellnig, G., Perktold, A., and Daum, G. (2001). A subfraction of the yeast endoplasmic reticulum associates with the plasma membrane and has a high capacity to synthesize lipids. European journal of biochemistry / FEBS *268*, 2351-2361.

Pierobon, N., Renard-Rooney, D.C., Gaspers, L.D., and Thomas, A.P. (2006). Ryanodine receptors in liver. J Biol Chem *281*, 34086-34095.

Poupon, R.E., Lindor, K.D., Cauch-Dudek, K., Dickson, E.R., Poupon, R., and Heathcote, E.J. (1997). Combined analysis of randomized controlled trials of ursodeoxycholic acid in primary biliary cirrhosis. Gastroenterology *113*, 884-890.

Pozzan, T., Rizzuto, R., Volpe, P., and Meldolesi, J. (1994). Molecular and cellular physiology of intracellular calcium stores. Physiological reviews *74*, 595-636.

Prakriya, M., Feske, S., Gwack, Y., Srikanth, S., Rao, A., and Hogan, P.G. (2006). Orai1 is an essential pore subunit of the CRAC channel. Nature *443*, 230-233.

Prakriya, M., and Lewis, R.S. (2001). Potentiation and inhibition of Ca(2+) release-activated Ca(2+) channels by 2-aminoethyldiphenyl borate (2-APB) occurs independently of IP(3) receptors. J Physiol *536*, 3-19.

Putney, J.W., Jr. (1986). A model for receptor-regulated calcium entry. Cell Calcium *7*, 1-12.

Rengifo, J., Gibson, C.J., Winkler, E., Collin, T., and Ehrlich, B.E. (2007). Regulation of the inositol 1,4,5-trisphosphate receptor type I by O-GlcNAc glycosylation. J Neurosci *27*, 13813-13821.

Ribeiro, C.M., and Putney, J.W. (1996). Differential effects of protein kinase C activation on calcium storage and capacitative calcium entry in NIH 3T3 cells. J Biol Chem *271*, 21522-21528.

Rizzuto, R., Brini, M., Murgia, M., and Pozzan, T. (1993). Microdomains with high Ca2+ close to IP3-sensitive channels that are sensed by neighboring mitochondria. Science (New York, N.Y *262*, 744-747.

Rizzuto, R., Pinton, P., Carrington, W., Fay, F.S., Fogarty, K.E., Lifshitz, L.M., Tuft, R.A., and Pozzan, T. (1998). Close contacts with the endoplasmic reticulum as determinants of mitochondrial Ca2+ responses. Science (New York, N.Y *280*, 1763-1766.

Rolo, A.P., Oliveira, P.J., Moreno, A.J., and Palmeira, C.M. (2000). Bile acids affect liver mitochondrial bioenergetics: possible relevance for cholestasis therapy. Toxicological Sciences *57*, 177-185.

Rooney, T.A., Sass, E.J., and Thomas, A.P. (1989). Characterization of cytosolic calcium oscillations induced by phenylephrine and vasopressin in single fura-2-loaded hepatocytes. J Biol Chem *264*, 17131-17141.

Rooney, T.A., Sass, E.J., and Thomas, A.P. (1990). Agonist-induced cytosolic calcium oscillations originate from a specific locus in single hepatocytes. J Biol Chem *265*, 10792-10796.

Roos, J., DiGregorio, P.J., Yeromin, A.V., Ohlsen, K., Lioudyno, M., Zhang, S., Safrina, O., Kozak, J.A., Wagner, S.L., Cahalan, M.D., Velicelebi, G., and

Stauderman, K.A. (2005). STIM1, an essential and conserved component of store-operated Ca2+ channel function. J Cell Biol *169*, 435-445.

Rosado, J.A., Jenner, S., and Sage, S.O. (2000). A role for the actin cytoskeleton in the initiation and maintenance of store-mediated calcium entry in human platelets. Evidence for conformational coupling. J Biol Chem *275*, 7527-7533.

Rossier, M.F., Bird, G.S., and Putney, J.W., Jr. (1991). Subcellular distribution of the calcium-storing inositol 1,4,5-trisphosphate-sensitive organelle in rat liver. Possible linkage to the plasma membrane through the actin microfilaments. Biochem J *274 (Pt 3)*, 643-650.

Rychkov, G., Brereton, H.M., Harland, M.L., and Barritt, G.J. (2001). Plasma membrane Ca2+ release-activated Ca2+ channels with a high selectivity for Ca2+ identified by patch-clamp recording in rat liver cells. Hepatology (Baltimore, Md *33*, 938-947.

Rychkov, G.Y., Litjens, T., Roberts, M.L., and Barritt, G.J. (2005). ATP and vasopressin activate a single type of store-operated Ca2+ channel, identified by patch-clamp recording, in rat hepatocytes. Cell Calcium *37*, 183-191.

Sanchez, G., Hidalgo, C., and Donoso, P. (2003). Kinetic studies of calcium-induced calcium release in cardiac sarcoplasmic reticulum vesicles. Biophysical journal *84*, 2319-2330.

Saunders, C.M., Larman, M.G., Parrington, J., Cox, L.J., Royse, J., Blayney, L.M., Swann, K., and Lai, F.A. (2002). PLC zeta: a sperm-specific trigger of Ca(2+) oscillations in eggs and embryo development. Development (Cambridge, England) *129*, 3533-3544.

Scaduto, R.C., Jr., and Grotyohann, L.W. (1999). Measurement of mitochondrial membrane potential using fluorescent rhodamine derivatives. Biophysical journal *76*, 469-477.

Sedova, M., Klishin, A., Huser, J., and Blatter, L.A. (2000). Capacitative Ca2+ entry is graded with degree of intracellular Ca2+ store depletion in bovine vascular endothelial cells. Journal of Physiology *523 Pt 3*, 549-559.

Slayter, E.M. (1997). Electron Microscope. In: Grolier multimedia Encyclopedia: Electronic publishing.

Smith, G.D., Gunthorpe, M.J., Kelsell, R.E., Hayes, P.D., Reilly, P., Facer, P., Wright, J.E., Jerman, J.C., Walhin, J.P., Ooi, L., Egerton, J., Charles, K.J., Smart, D., Randall, A.D., Anand, P., and Davis, J.B. (2002). TRPV3 is a temperature-sensitive vanilloid receptor-like protein. Nature *418*, 186-190.

Soboloff, J., Spassova, M.A., Hewavitharana, T., He, L.P., Xu, W., Johnstone, L.S., Dziadek, M.A., and Gill, D.L. (2006a). STIM2 is an inhibitor of STIM1-mediated store-operated Ca2+ Entry. Curr Biol *16*, 1465-1470.

Soboloff, J., Spassova, M.A., Tang, X.D., Hewavitharana, T., Xu, W., and Gill, D.L. (2006b). Orai1 and STIM reconstitute store-operated calcium channel function. J Biol Chem *281*, 20661-20665.

Sodeman, T., Bronk, S.F., Roberts, P.J., Miyoshi, H., and Gores, G.J. (2000). Bile salts mediate hepatocyte apoptosis by increasing cell surface trafficking of Fas.

American Journal of Physiology - Gastrointestinal & Liver Physiology *278*, G992-999.

Solic, N., Collins, J.E., Richter, A., Holt, S.J., Campbell, I., Alexander, P., and Davies, D.E. (1995). Two newly established cell lines derived from the same colonic adenocarcinoma exhibit differences in EGF-receptor ligand and adhesion molecule expression. Int J Cancer *62*, 48-57.

Sorrentino, V., and Rizzuto, R. (2001). Molecular genetics of Ca(2+) stores and intracellular Ca(2+) signalling. Trends in pharmacological sciences *22*, 459-464.

Spassova, M.A., Soboloff, J., He, L.P., Xu, W., Dziadek, M.A., and Gill, D.L. (2006). STIM1 has a plasma membrane role in the activation of store-operated Ca(2+) channels. Proc Natl Acad Sci U S A *103*, 4040-4045.

Studer, R.K., and Borle, A.B. (1992). Na(+)-Ca2+ antiporter activity of rat hepatocytes. Effect of adrenalectomy on Ca2+ uptake and release from plasma membrane vesicles. Biochimica et biophysica acta *1134*, 7-16.

Subramanian, K., and Meyer, T. (1997). Calcium-induced restructuring of nuclear envelope and endoplasmic reticulum calcium stores. Cell *89*, 963-971.

Sweeney, M., Yu, Y., Platoshyn, O., Zhang, S., McDaniel, S.S., and Yuan, J.X. (2002). Inhibition of endogenous TRP1 decreases capacitative Ca2+ entry and attenuates pulmonary artery smooth muscle cell proliferation. American journal of physiology *283*, L144-155.

Szallasi, A., and Blumberg, P.M. (1999). Vanilloid (Capsaicin) receptors and mechanisms. Pharmacological reviews *51*, 159-212.

Tani, E., and Ametani, T. (1971). Extracellular distribution of ruthenium red-positive substance in the cerebral cortex. Journal of Ultrastructure Research *34*, 1-14.

Taylor, C.W. (2006). Store-operated Ca2+ entry: A STIMulating stOrai. Trends in Biochemical Sciences *31*, 597-601.

Taylor, C.W., and Traynor, D. (1995). Calcium and inositol trisphosphate receptors. The Journal of membrane biology *145*, 109-118.

Thomas, A.P., Renard, D.C., and Rooney, T.A. (1991). Spatial and temporal organization of calcium signalling in hepatocytes. Cell Calcium *12*, 111-126.

Thomas, K.C., Sabnis, A.S., Johansen, M.E., Lanza, D.L., Moos, P.J., Yost, G.S., and Reilly, C.A. (2007). Transient receptor potential vanilloid 1 agonists cause endoplasmic reticulum stress and cell death in human lung cells. Journal of Pharmacology & Experimental Therapeutics *321*, 830-838.

Tornquist, K. (1993). Modulatory effect of protein kinase C on thapsigargin-induced calcium entry in thyroid FRTL-5 cells. Biochemical Journal *290*, 443-447.

Trudeau, L.E., Doyle, R.T., Emery, D.G., and Haydon, P.G. (1996). Calcium-independent activation of the secretory apparatus by ruthenium red in hippocampal neurons: a new tool to assess modulation of presynaptic function. Journal of Neuroscience *16*, 46-54.

Tsien, R.Y. (1980). New calcium indicators and buffers with high selectivity against magnesium and protons: design, synthesis, and properties of prototype structures. Biochemistry *19*, 2396-2404.

Tsien, R.Y. (1981). A non-disruptive technique for loading calcium buffers and indicators into cells. Nature *290*, 527-528.

Turner, H., Fleig, A., Stokes, A., Kinet, J.P., and Penner, R. (2003). Discrimination of intracellular calcium store subcompartments using TRPV1 (transient receptor potential channel, vanilloid subfamily member 1) release channel activity. Biochemical Journal *371*, 341-350.

Ukhanov, K., Ukhanova, M., Taylor, C.W., and Payne, R. (1998). Putative inositol 1,4,5-trisphosphate receptor localized to endoplasmic reticulum in Limulus photoreceptors. Neuroscience *86*, 23-28.

van Breemen, C., Chen, Q., and Laher, I. (1995). Superficial buffer barrier function of smooth muscle sarcoplasmic reticulum. Trends in pharmacological sciences *16*, 98-105.

van de Meeberg, P.C., Wolfhagen, F.H., Van Berge-Henegouwen, G.P., Salemans, J.M., Tangerman, A., van Buuren, H.R., van Hattum, J., and van Erpecum, K.J. (1996). Single or multiple dose ursodeoxycholic acid for cholestatic liver disease: biliary enrichment and biochemical response. Journal of Hepatology *25*, 887-894.

Varnai, P., Toth, B., Toth, D.J., Hunyady, L., and Balla, T. (2007). Visualization and manipulation of plasma membrane-endoplasmic reticulum contact sites indicates the presence of additional molecular components within the STIM1-Orai1 Complex. Journal of Biological Chemistry *282*, 29678-29690.

Venkatachalam, K., van Rossum, D.B., Patterson, R.L., Ma, H.T., and Gill, D.L. (2002). The cellular and molecular basis of store-operated calcium entry. Nature cell biology *4*, E263-272.

Vig, M., Peinelt, C., Beck, A., Koomoa, D.L., Rabah, D., Koblan-Huberson, M., Kraft, S., Turner, H., Fleig, A., Penner, R., and Kinet, J.P. (2006). CRACM1 is a plasma membrane protein essential for store-operated Ca2+ entry. Science (New York, N.Y *312*, 1220-1223.

Voets, T., Prenen, J., Fleig, A., Vennekens, R., Watanabe, H., Hoenderop, J.G., Bindels, R.J., Droogmans, G., Penner, R., and Nilius, B. (2001). CaT1 and the calcium release-activated calcium channel manifest distinct pore properties. J Biol Chem *276*, 47767-47770.

Vorndran, C., Minta, A., and Poenie, M. (1995). New fluorescent calcium indicators designed for cytosolic retention or measuring calcium near membranes. Biophysical journal *69*, 2112-2124.

Voronina, S.G., Barrow, S.L., Gerasimenko, O.V., Petersen, O.H., and Tepikin, A.V. (2004). Effects of secretagogues and bile acids on mitochondrial membrane potential of pancreatic acinar cells: comparison of different modes of evaluating DeltaPsim. Journal of Biological Chemistry *279*, 27327-27338.

Vos, M.H., Neelands, T.R., McDonald, H.A., Choi, W., Kroeger, P.E., Puttfarcken, P.S., Faltynek, C.R., Moreland, R.B., and Han, P. (2006). TRPV1b overexpression negatively regulates TRPV1 responsiveness to capsaicin, heat and low pH in HEK293 cells. Journal of Neurochemistry *99*, 1088-1102.

Vriens, J., Janssens, A., Prenen, J., Nilius, B., and Wondergem, R. (2004). TRPV channels and modulation by hepatocyte growth factor/scatter factor in human hepatoblastoma (HepG2) cells. Cell Calcium *36*, 19-28.

Wakabayashi, Y., Kipp, H., and Arias, I.M. (2006). Transporters on demand: intracellular reservoirs and cycling of bile canalicular ABC transporters. J Biol Chem *281*, 27669-27673.

Wang, J.P., Tseng, C.S., Sun, S.P., Chen, Y.S., Tsai, C.R., and Hsu, M.F. (2005). Capsaicin stimulates the non-store-operated Ca2+ entry but inhibits the store-operated Ca2+ entry in neutrophils. Toxicology and applied pharmacology *209*, 134-144.

Wang, Y.J., Gregory, R.B., and Barritt, G.J. (2000). Regulation of F-actin and endoplasmic reticulum organization by the trimeric G-protein Gi2 in rat hepatocytes. Implication for the activation of store-operated Ca2+ inflow. J Biol Chem *275*, 22229-22237.

Watanabe, H., and Burnstock, G. (1976). Junctional subsurface organs in frog sympathetic ganglion cells. Journal of neurocytology *5*, 125-136.

Watanabe, S., and Phillips, M.J. (1984). Ca2+ causes active contraction of bile canaliculi: direct evidence from microinjection studies. Proceedings of the National Academy of Sciences of the United States of America *81*, 6164-6168.

Williams, R.T., Manji, S.S., Parker, N.J., Hancock, M.S., Van Stekelenburg, L., Eid, J.P., Senior, P.V., Kazenwadel, J.S., Shandala, T., Saint, R., Smith, P.J., and Dziadek, M.A. (2001). Identification and characterization of the STIM (stromal interaction molecule) gene family: coding for a novel class of transmembrane proteins. Biochem J *357*, 673-685.

Wisnoskey, B.J., Sinkins, W.G., and Schilling, W.P. (2003). Activation of vanilloid receptor type I in the endoplasmic reticulum fails to activate store-operated Ca2+ entry. Biochemical Journal *372*, 517-528.

Wojcikiewicz, R.J. (1995). Type I, II, and III inositol 1,4,5-trisphosphate receptors are unequally susceptible to down-regulation and are expressed in markedly different proportions in different cell types. J Biol Chem *270*, 11678-11683.

Woods, N.M., Cuthbertson, K.S., and Cobbold, P.H. (1986). Repetitive transient rises in cytoplasmic free calcium in hormone-stimulated hepatocytes. Nature *319*, 600-602.

Woods, N.M., Cuthbertson, K.S., and Cobbold, P.H. (1987). Agonist-induced oscillations in cytoplasmic free calcium concentration in single rat hepatocytes. Cell Calcium *8*, 79-100.

Wu, M.M., Buchanan, J., Luik, R.M., and Lewis, R.S. (2006). Ca2+ store depletion causes STIM1 to accumulate in ER regions closely associated with the plasma membrane. Journal of Cell Biology *174*, 803-813.

Xu, P., Lu, J., Li, Z., Yu, X., Chen, L., and Xu, T. (2006). Aggregation of STIM1 underneath the plasma membrane induces clustering of Orai1. Biochemical & Biophysical Research Communications *350*, 969-976.

Yao, Y., Ferrer-Montiel, A.V., Montal, M., and Tsien, R.Y. (1999). Activation of store-operated Ca2+ current in Xenopus oocytes requires SNAP-25 but not a diffusible messenger. Cell *98*, 475-485.

Yeromin, A.V., Zhang, S.L., Jiang, W., Yu, Y., Safrina, O., and Cahalan, M.D. (2006). Molecular identification of the CRAC channel by altered ion selectivity in a mutant of Orai. Nature *443*, 226-229.

Yoshida, M., Ishikawa, M., Izumi, H., De Santis, R., and Morisawa, M. (2003). Store-operated calcium channel regulates the chemotactic behavior of ascidian sperm. Proc Natl Acad Sci U S A *100*, 149-154.

Young, B., and J.W. (2000). Heath, Wheater's Functional Histology: Churchill Livingstone, Edinburgh.

Zegers, M.M., and Hoekstra, D. (1998). Mechanisms and functional features of polarized membrane traffic in epithelial and hepatic cells. Biochem J *336 (Pt 2)*, 257-269.

Zhang, S.L., Yeromin, A.V., Zhang, X.H., Yu, Y., Safrina, O., Penna, A., Roos, J., Stauderman, K.A., and Cahalan, M.D. (2006). Genome-wide RNAi screen of Ca(2+) influx identifies genes that regulate Ca(2+) release-activated Ca(2+) channel activity. Proc Natl Acad Sci U S A *103*, 9357-9362.

Zhang, S.L., Yu, Y., Roos, J., Kozak, J.A., Deerinck, T.J., Ellisman, M.H., Stauderman, K.A., and Cahalan, M.D. (2005). STIM1 is a Ca2+ sensor that activates CRAC channels and migrates from the Ca2+ store to the plasma membrane. Nature *437*, 902-905.

Zweifach, A., and Lewis, R.S. (1993). Mitogen-regulated Ca2+ current of T lymphocytes is activated by depletion of intracellular Ca2+ stores. Proc Natl Acad Sci U S A *90*, 6295-6299.

Zweifach, A., and Lewis, R.S. (1995). Rapid inactivation of depletion-activated calcium current (ICRAC) due to local calcium feedback. The Journal of general physiology *105*, 209-226.